Paleontología de Vertebrados

Ornithischia

Sergio Soto Acuña
Paleontólogo de Vertebrados

Ornithischia

Definición: Todos los dinosaurios más cercanamente emparentados a *Triceratops horridus* que a *Passer domesticus* o *Saltasaurus loricatus* (Butler et al., 2008).

Rango Temporal: Jurásico Inferior-Cretácico Superior.

Sinapomorfías (sensu Boyd 2015 y otros autores)

- Ligera emarginación bucal en el maxilar.
- Desarrollo de un proceso coronoides distintivo en la mandíbula.
- Contribución del dentario a la porción anterior del proceso coronoides.
- Presencia de hueso predentario.
- Presencia de hueso palpebral.
- Región anterior a primer diente premaxilar desdentada (2 t).
- Proceso preacetabular del íleon se extiende anterior al pedúnculo púbico.
- Pubis posteroventralmente orientado.
- Cuarto trocánter sobresaliente.
- Presencia de prepubis.

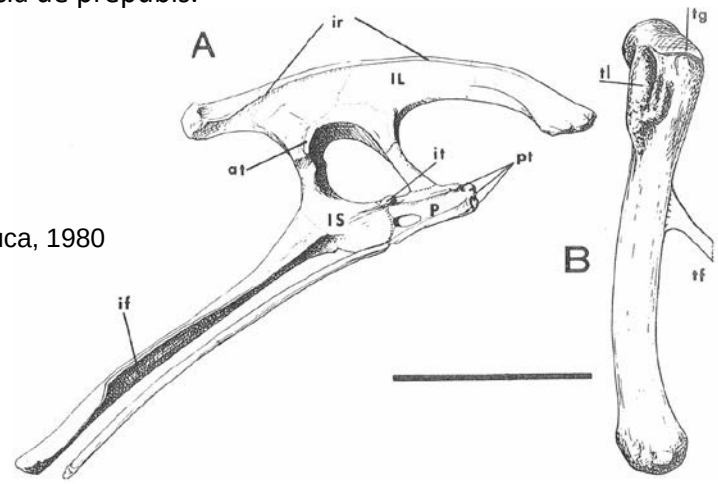

Fig. 18. *H. tucki*. A. Right pelvis, lateral view. B. Left femur, lateral view. Scale = 5 cm.

Santa Luca, 1980

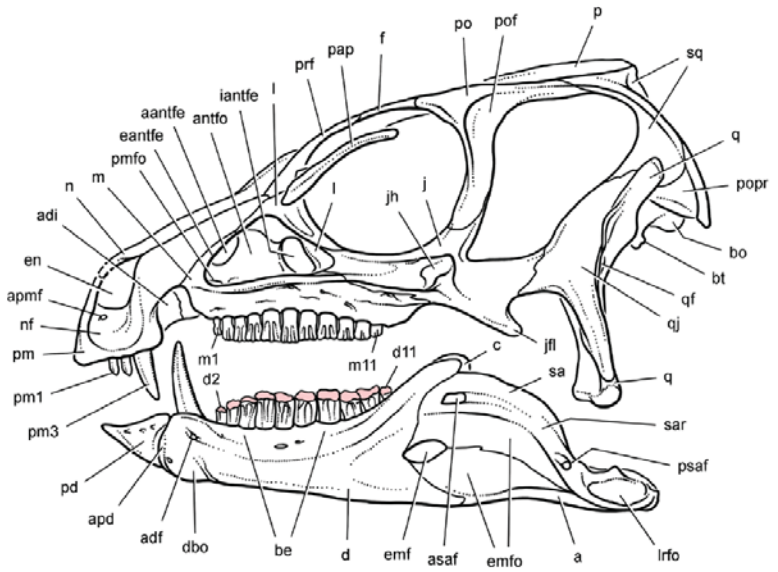

Figure 59. Skull of *Heterodontosaurus tucki* from the Lower Jurassic Upper Elliot and Clarens formations of South Africa. New skull reconstruction in lateral view showing the dentition with intermediate wear (scleral ring not shown). Pink tone indicates wear facets. Abbreviations: ***a*** angular ***aantfe*** accessory antorbital fenestra ***adf*** anterior dentary foramen ***adi*** arched diastema ***antfo*** antorbital fossa ***apd*** articular surface for the predentary ***apmf*** anterior premaxillary foramen ***asaf*** anterior surangular foramen ***be*** buccal emargination ***bo*** basioccipital ***bt*** basal tubera ***c*** coronoid ***d*** dentary ***d2***, ***d11*** dentary tooth 2, 11 ***dbo*** dentary boss ***eantfe*** external antorbital fenestra ***emf*** external mandibular fenestra ***emfo*** external mandibular fossa ***en*** external naris ***f*** frontal ***iantfe*** internal antorbital fenestra ***j*** jugal ***jfl*** jugal flange ***jh*** jugal horn ***l*** lacrimal ***lrfo*** lateral retroarticular fossa ***m*** maxilla ***m1***, ***11*** maxillary tooth 1, 11 ***n*** nasal ***nf*** narial fossa ***p*** parietal ***pap*** palpebral ***pd*** predentary ***pm*** premaxilla ***pm1***, ***3*** premaxillary tooth 1, 3 ***pmfo*** promaxillary fossa ***po*** postorbital ***pof*** postorbital fossa ***popr*** paroccipital process ***prf*** prefrontal ***psaf*** posterior surangular foramen ***q*** quadrate ***qf*** quadrate foramen ***qj*** quadratojugal ***sa*** surangular ***sar*** surangular ridge ***sq*** squamosal.

Sereno, 2012

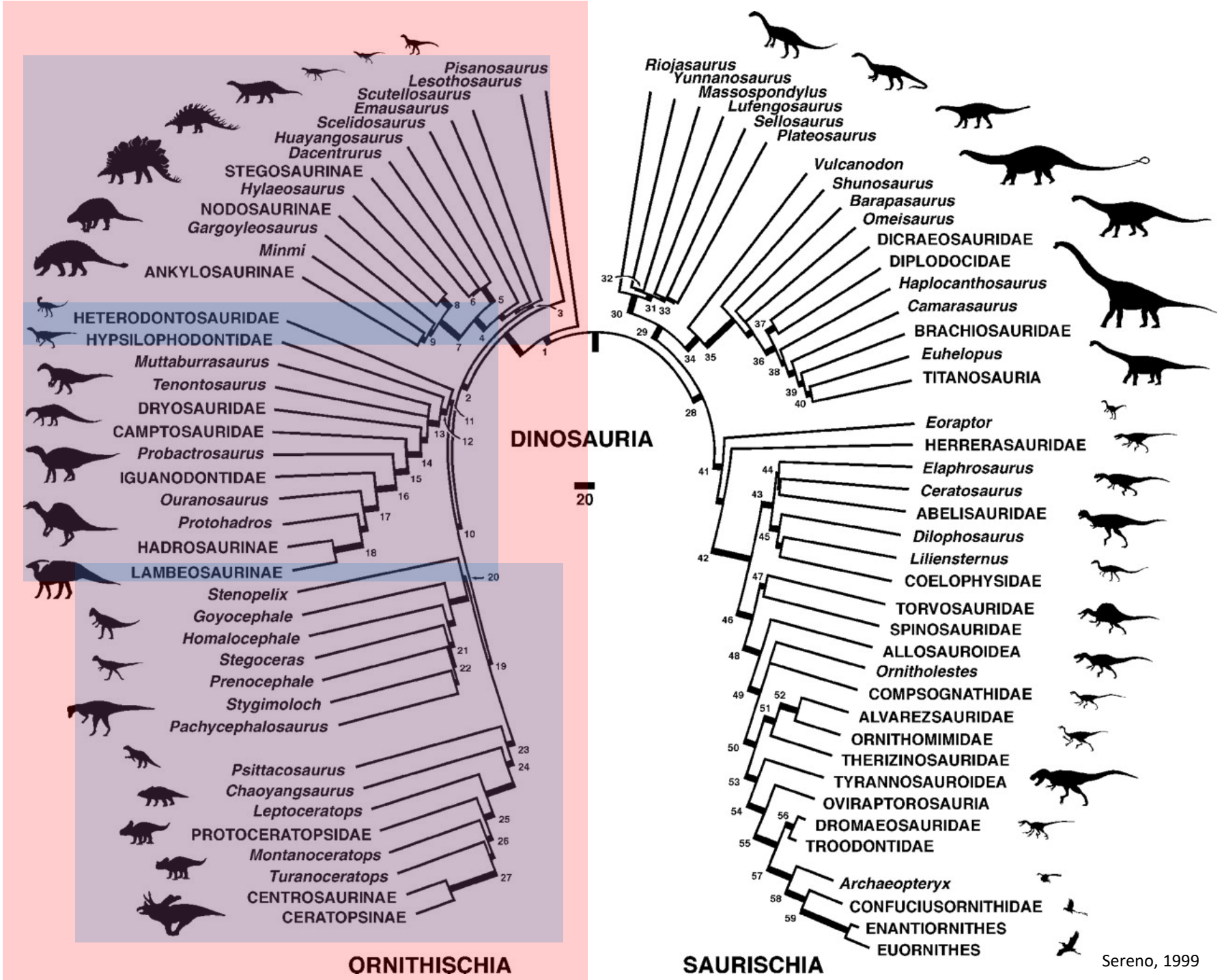
Pisanosaurus
Lesothosaurus
Scutellosaurus
Emausaurus
Scelidosaurus
Huayangosaurus
Dacentrurus
STEGOSAURINAE
Hylaeosaurus
NODOSAURINAE
Gargoyleosaurus
Minmi
ANKYLOSAURINAE
HETERODONTOSAURIDAE
HYPSILOPHODONTIDAE
Muttaburrasaurus
Tenontosaurus
DRYOSAURIDAE
CAMPTOSAURIDAE
Probactrosaurus
IGUANODONTIDAE
Ouranosaurus
Protohadros
HADROSAURINAE
LAMBEOSAURINAE
Stenopelix
Goyocephale
Homalocephale
Stegoceras
Prenocephale
Stygimoloch
Pachycephalosaurus
Psittacosaurus
Chaoyangsaurus
Leptoceratops
PROTOCERATOPSIDAE
Montanoceratops
Turanoceratops
CENTROSAURINAE
CERATOPSINAE
ORNITHISCHIA
Riojasaurus
Yunnanosaurus
Massospondylus
Lufengosaurus
Sellosaurus
Plateosaurus
Vulcanodon
Shunosaurus
Barapasaurus
Omeisaurus
DICRAEOSAURIDAE
DIPLODOCIDAE
Haplocanthosaurus
Camarasaurus
BRACHIOSAURIDAE
Euhelopus
TITANOSAURIA
DINOSAURIA
20
Eoraptor
HERRERASAURIDAE
Elaphrosaurus
Ceratosaurus
ABELISAURIDAE
Dilophosaurus
Liliensternus
COELOPHYSIDAE
TORVOSAURIDAE
SPINOSAURIDAE
ALLOSAUROIDEA
Ornitholestes
COMPSOGNATHIDAE
ALVAREZSAURIDAE
ORNITHOMIMIDAE
THERIZINOSAURIDAE
TYRANNOSAUROIDEA
OVIRAPTOROSAURIA
DROMAEOSAURIDAE
TROODONTIDAE
Archaeopteryx
CONFUCIUSORNITHIDAE
ENANTIORNITHES
EUORNITHES
SAURISCHIA

Sereno, 1999

Interpretaciones alternativas: Ornithoscelida

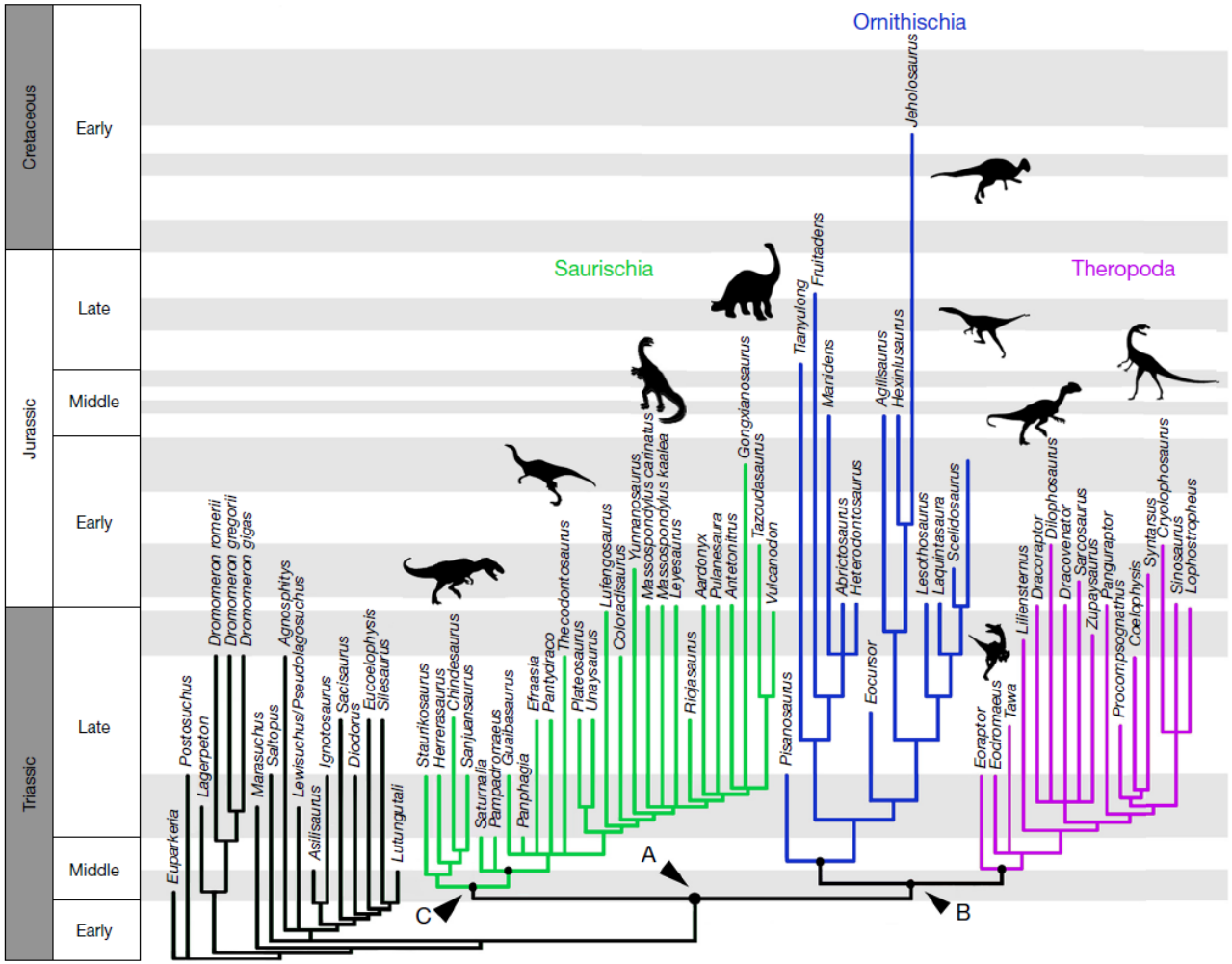

Figure 1 | Phylogenetic relationships of early dinosaurs. Time-calibrated strict consensus of 94 trees from an analysis with 73 taxa and 457 characters (see Supplementary Information). A, the least inclusive clade that includes *Passer domesticus*, *Triceratops horridus* and *Diplodocus carnegii*—Dinosauria, as newly defined. B, the least inclusive clade that includes *P. domesticus* and *T. horridus*—Ornithoscelida, as defined. C, the most inclusive clade that contains *D. carnegii*, but not *T. horridus*—Saurischia, as newly defined. For further information on definitions see Table 1. All subdivisions of the time periods (white and grey bands) are scaled according to their relative lengths with the exception of the Olenekian (Early Triassic), which has been expanded relative to the other subdivisions to better show the resolution within Silesauridae and among other non-dinosaurian dinosauromorphs.

Baron et al 2017

Origen temprano de Ornithoscelida?

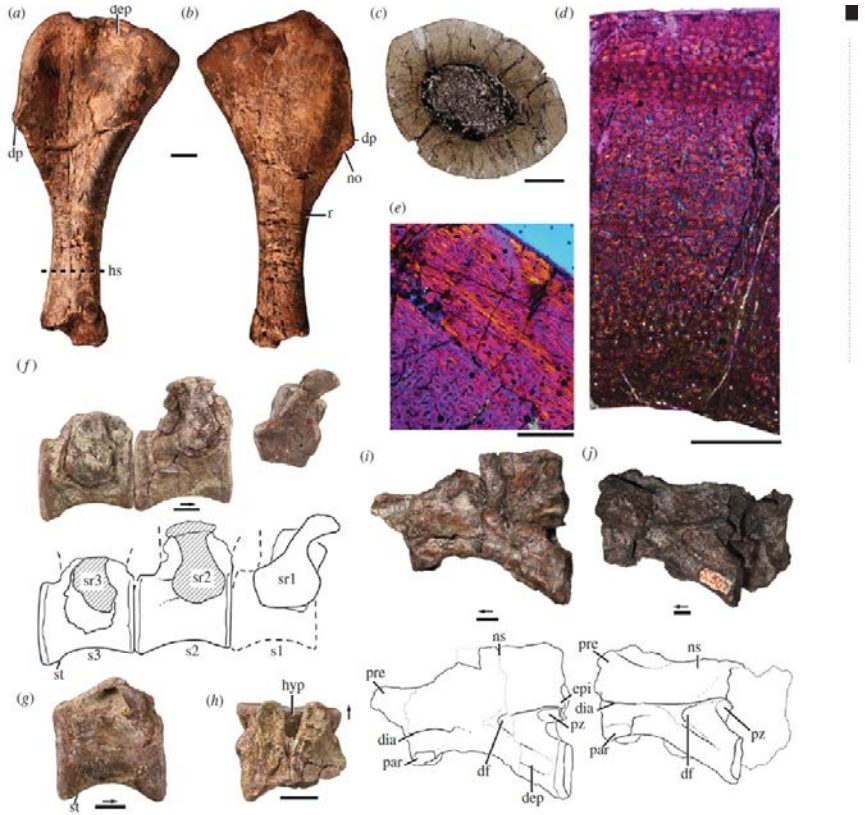

Figure 1. Holotype (*a–h*; NHMUK R6856) and referred (*i–j*; SAM-PK-K10654) specimens of *Nyasasaurus parringtoni* gen. et sp. nov. Right humerus in (*a*) anterior and (*b*) posterior views. Histological section of humerus in (*c*) complete cross-section in transmitted light, (*d*) cross-section through the entire cortex in crossed Nicols, and (*e*) cross-section through the outer portion of cortex in crossed Nicols. (*f*) Rearticulated sacrum in right lateral view with interpretive drawing (below). (*g*) Posterior presacral vertebra in right lateral view. (*h*) Partial posterior presacral vertebra in dorsal view. (*i*) Anterior cervical vertebra in left lateral view with interpretive drawing (below). (*j*) Anterior cervical vertebra in left lateral view with interpretive drawing (below). Arrows point anteriorly. Scale bars, (*a*,*b*,*f–j*) 1 cm, (*c*) 4 mm, (*d*) 1 mm, (*e*) 500 nm. Dep, depression; df, deep fossa; dia, diapophysis; dp, deltopectoral crest; epi, epipophysis; hs, histology section; hyp, hypantrum; no, notch; ns, neural spine; par, parapophysis; pre, prezygapophysis; pz, postzygapophysis; r, ridge; s1–3, sacral vertebra number; sr1–3, sacral rib number; st, striations.

Nesbitt et al 2012

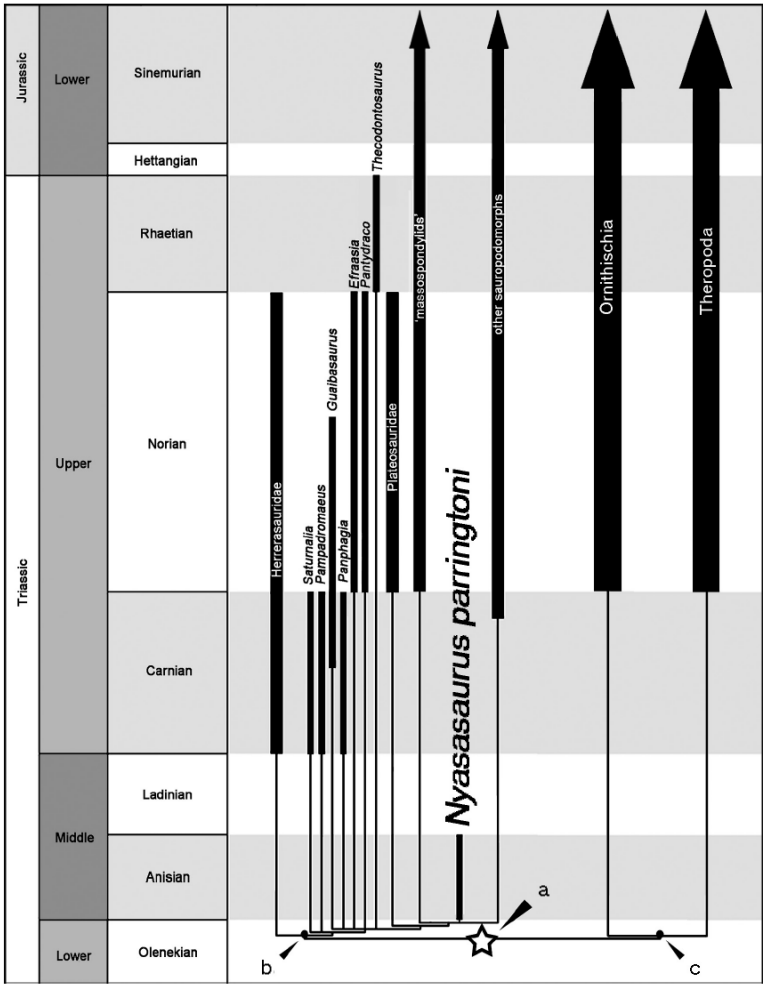

Extended Data Figure 5 | Strict consensus tree set against the geological timescale, showing the predicted Early Triassic divergence dates of Dinosauria (star) and of the major dinosaurian lineages when the potential 'massospondylid' sauropodomorph *Nyasasaurus parringtoni* is included in the analysis. a, Origin of Dinosauria (new definition) when *Nyasasaurus* is considered. **b**, Origin of Saurischia (new definition) when *Nyasasaurus* is considered. **c**, Origin of Ornithoscelida when *Nyasasaurus* is considered. For further details on the additional analyses that were carried out as part of this study, see the Supplementary Information.

Baron et al 2017

Re-análisis de hipótesis Ornithoscelida

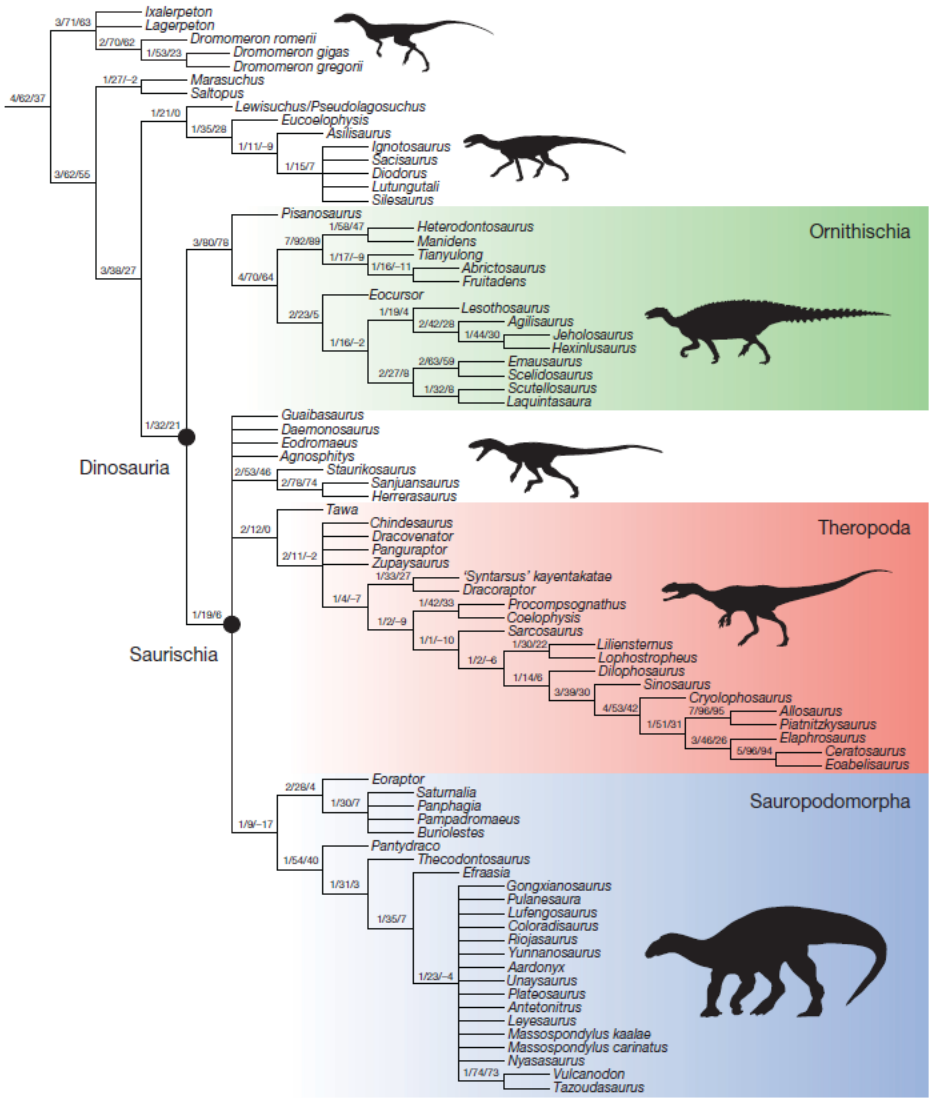

Figure 1 | Results of the reanalysis of a revised dataset on early dinosaur relationships. Strict consensus of the most parsimonious trees found in the analysis of the rescored dataset of Baron *et al.*[5] with additional taxa, showing a monophyletic traditional Saurischia. Bremer support values (left) and bootstrap values (absolute (middle) and 'group present/ contradicted' (right)) are shown for each clade.

Langer et al 2017

Contraataque de hipótesis Ornithoscelida

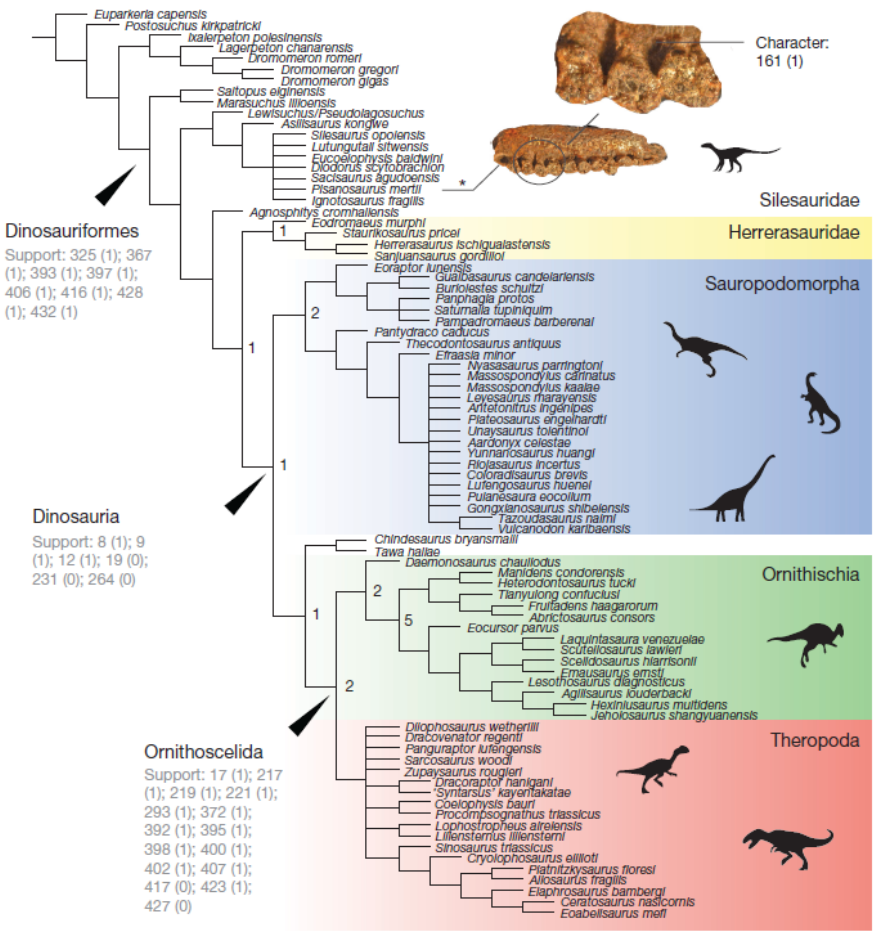

Figure 1 | Results of the phylogenetic analysis of the dataset following the re-scoring of *Pisanosaurus mertii*. Strict consensus tree of the 427 most parsimonious trees (length = 1,923) found in the re-analysis of the early dinosaur dataset following the re-scoring of Langer *et al.*[2] and our own re-scoring of *Pisanosaurus mertii* alone (indicated by an asterisk). Analyses were carried out using the new technology search function in TNT[10], following the original protocol[1] and using tree bisection reconnection (TBR) branch swapping; by applying a second round of TBR branch swapping, following the protocol of Langer *et al.*[2], we recover a polytomy within Dinosauria and note that a monophyletic Saurischia is not recovered. Although this is not conclusive evidence in favour of either hypothesis, we stress that this result follows corrections to only a single taxon in the revised matrix provided by Langer *et al.*[2]. This suggests that their result hinges on the scorings of one or two key early taxa. It also suggests that additional changes, where justified, may further support the results of our original study.

Baron et al 2017

Chilesaurus podría ser la clave…

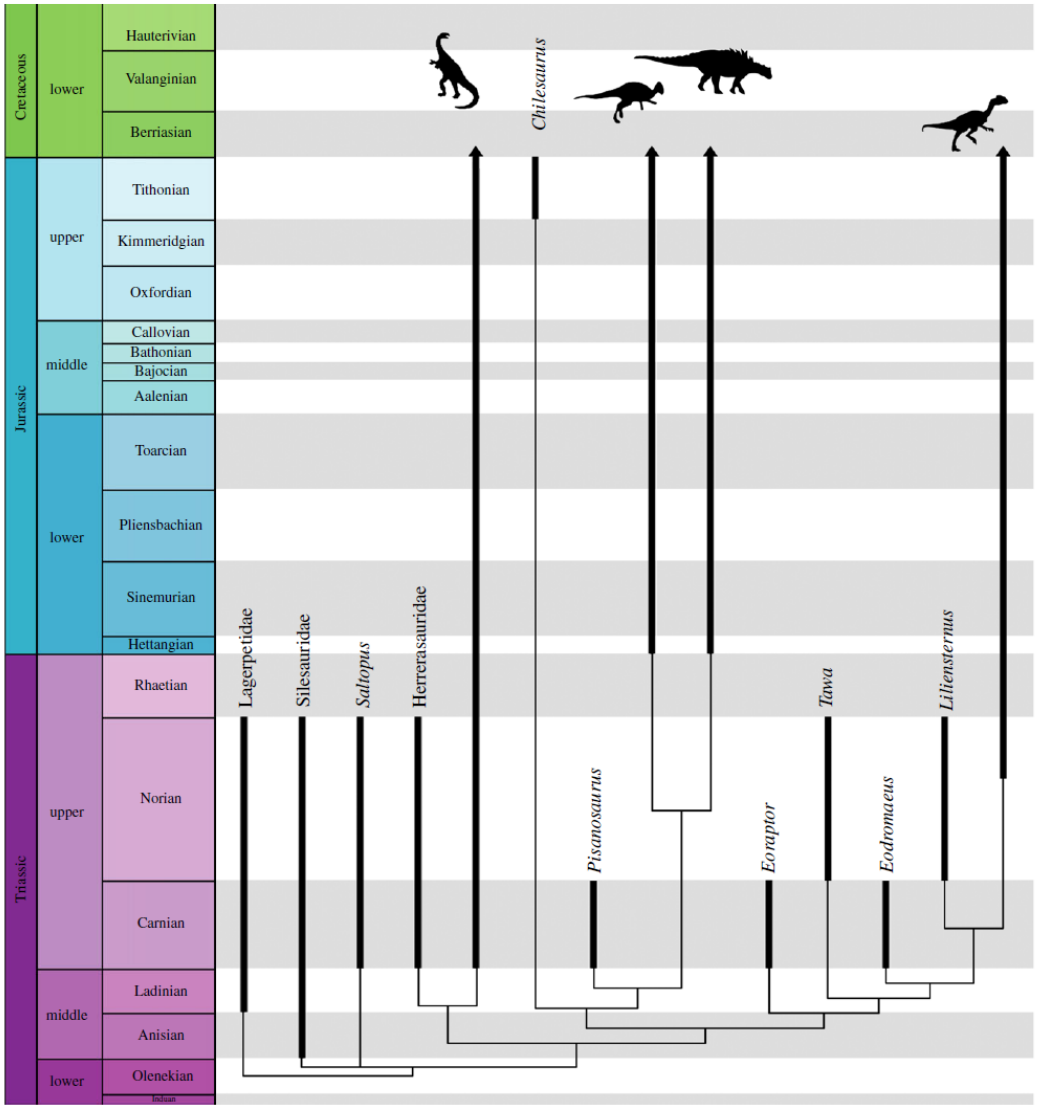

Figure 1. Simplified time-calibrated strict consensus tree in which *Chilesaurus* is recovered within Ornithischia. Silhouettes represent supraspecific taxa—from left to right: Sauropodomorpha, Heterodontosauridae, Genasauria and Neotheropoda.

Baron & Barrett 2018

Chilesaurus podría ser la clave…

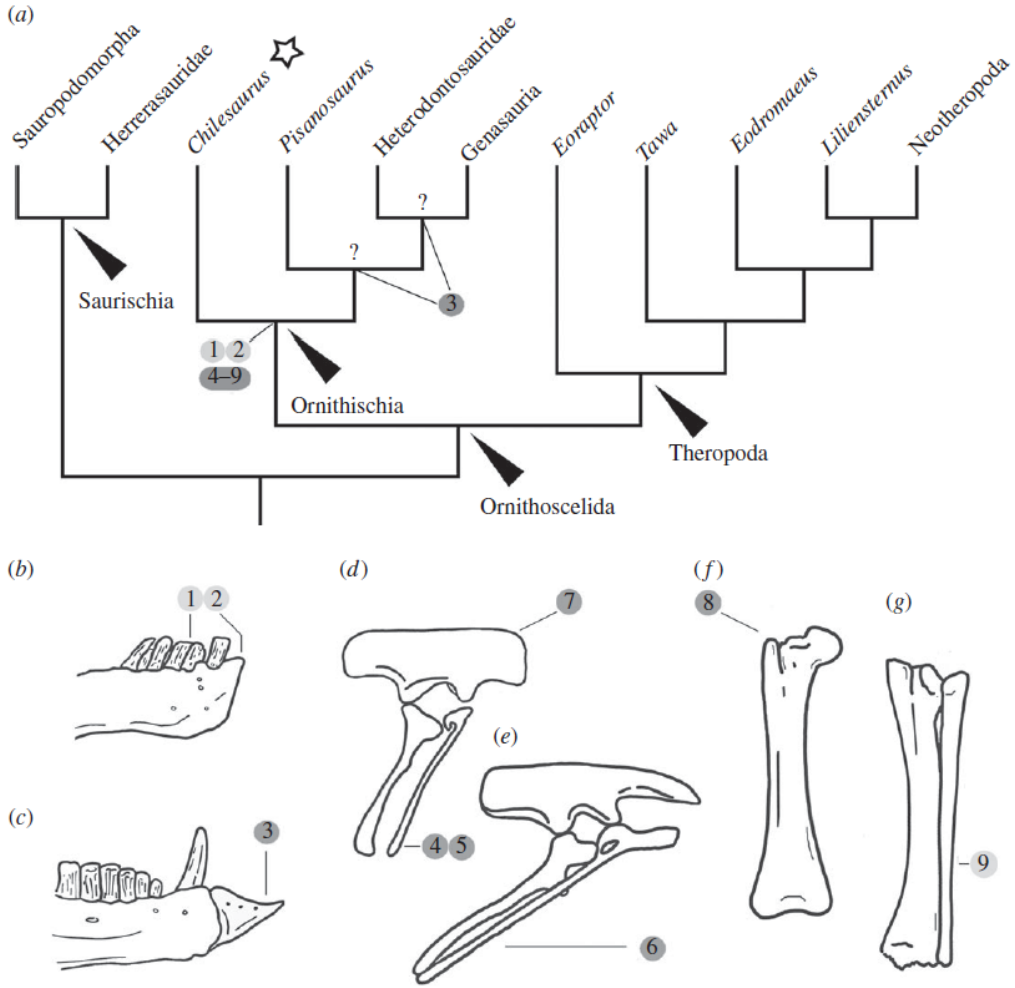

Figure 2. Ornithischian features of *Chilesaurus*. (*a*) Simplified tree with key acquisitions marked on; (*b*) right dentary of *Chilesaurus* (SNGM-1935) in lateral view; (*c*) right dentary of *Heterodontosaurus* (SAM-PK-K1332) in lateral view; (*d*) pelvic girdle of *Chilesaurus* SNGM-1936 in lateral view; (*e*) pelvic girdle of *Agilisaurus* (ZDM T6011) in lateral view; (*f*) right femur of *Chilesaurus* (SNGM-1935) in anterior view; (*g*) right tibia and fibula of *Chilesaurus* (SNGM-1935) in posterior view. Numbers indicate the acquisition of key ornithischian synapomorphies within the clade: 1, complete loss of recurvature in maxillary and dentary teeth; 2, edentulous anterior end of the dentary; 3, predentary bone at the anterior end of the lower jaw; 4, retroversion of the pubis; 5, rod-like pubic shaft; 6, pubic symphysis restricted to the distal end; 7, anteriorly elongate preacetabular process; 8, broadened, wing-like anterior trochanter; 9, fibula less than half the width of the tibia at midshaft. Dark grey circles denote unknown in *Pisanosaurus*.

Baron & Barrett 2018

Filogenia de Ornithischia

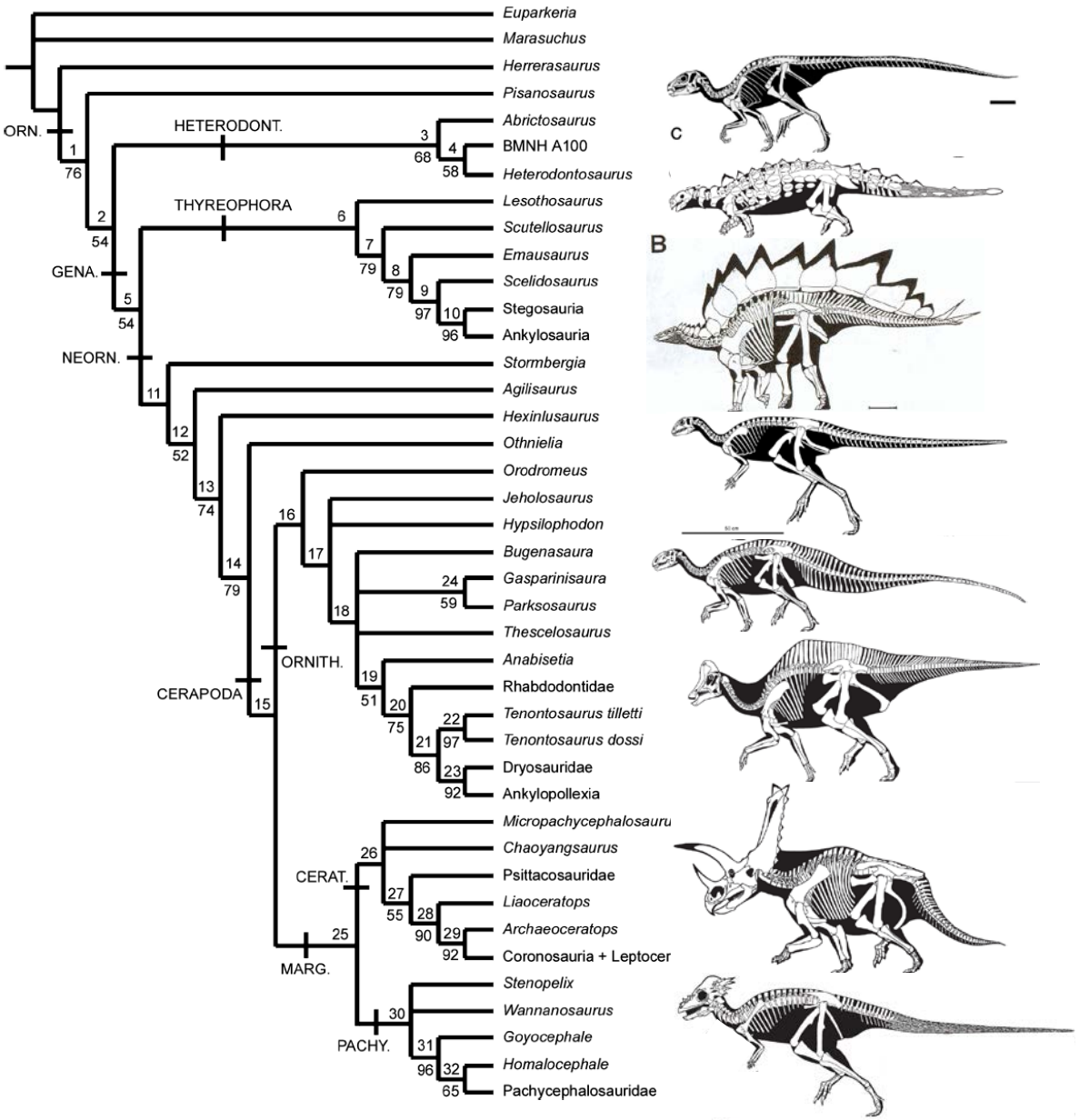

Figure 4 Derivative strict reduced consensus tree derived by *a posteriori* pruning of five unstable taxa (*Echinodon*, *Lycorhinus*, *Zephyrosaurus*, *Talenkauen* and *Yandusaurus*) from the set of 756 most parsimonious trees (MPTs) generated by the full analysis. The number above each node is a unique identifier used in the tree description (see Appendix 4). The number beneath a node represents the bootstrap proportion for that node (taken from the reduced bootstrap analysis). Note the increased levels of bootstrap support for a number of nodes when compared to Fig. 2. Abbreviations: ORN., Ornithischia; HETERODONT., Heterodontosauridae; GENA., Genasauria; NEORN., Neornithischia; ORNITH., Ornithopoda; MARG., Marginocephalia; CERAT., Ceratopsia; PACHY., Pachycephalosauria.

Butler et al 2008

Nuevas filogenias de Ornithischia

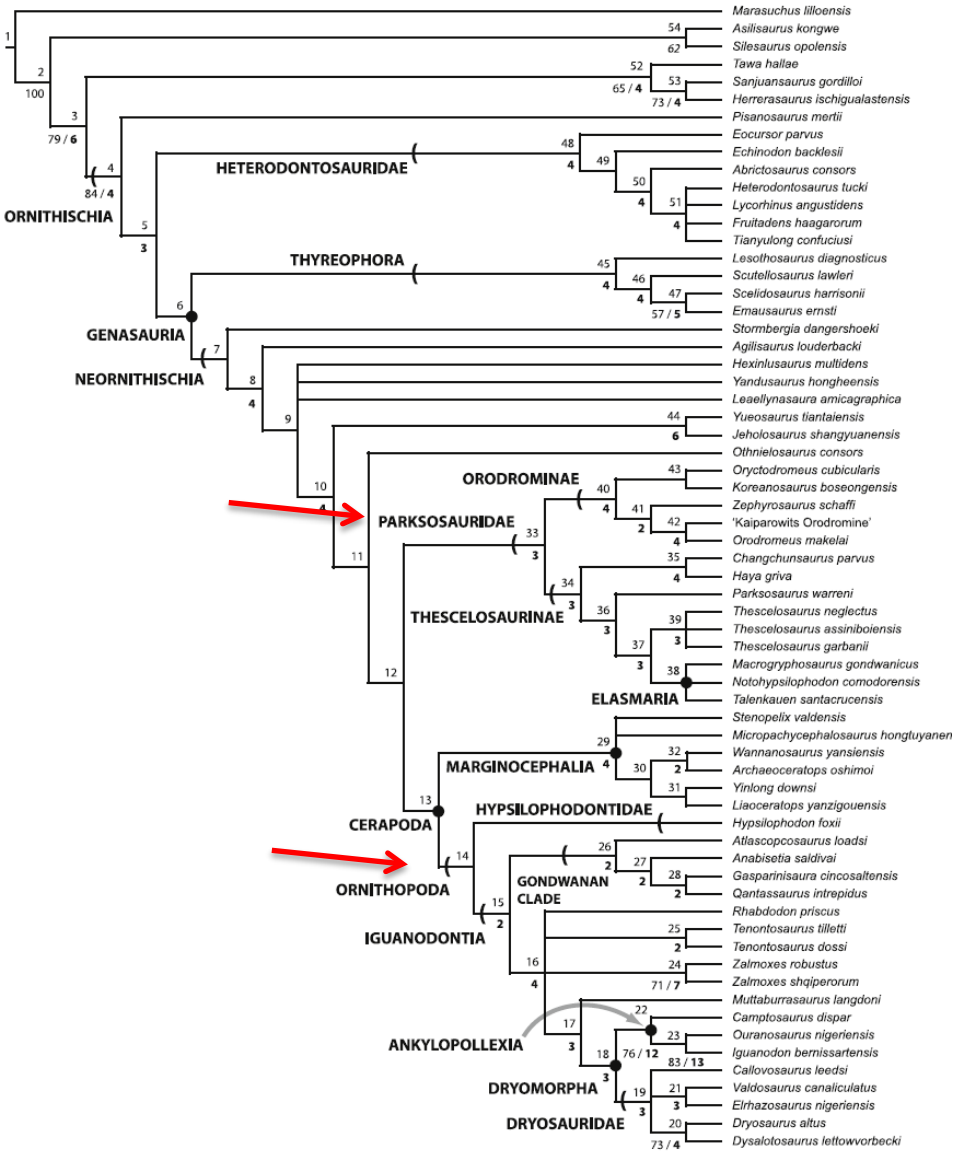

Figure 2 **Strict consensus of the 36 most parsimonious trees recovered by this study.** Major ornithischian subclades are labeled either along branches (stem-based definitions) or at nodes (node-based definitions). See Table 1 for phylogenetic definitions. Numbers above nodes refer to the list of unambiguous character changes reported for each node in Table S4. Bold numbers beneath nodes are Bremer support numbers >1, while non-bold numbers beneath nodes are bootstrap support values >50%.

Boyd, 2015

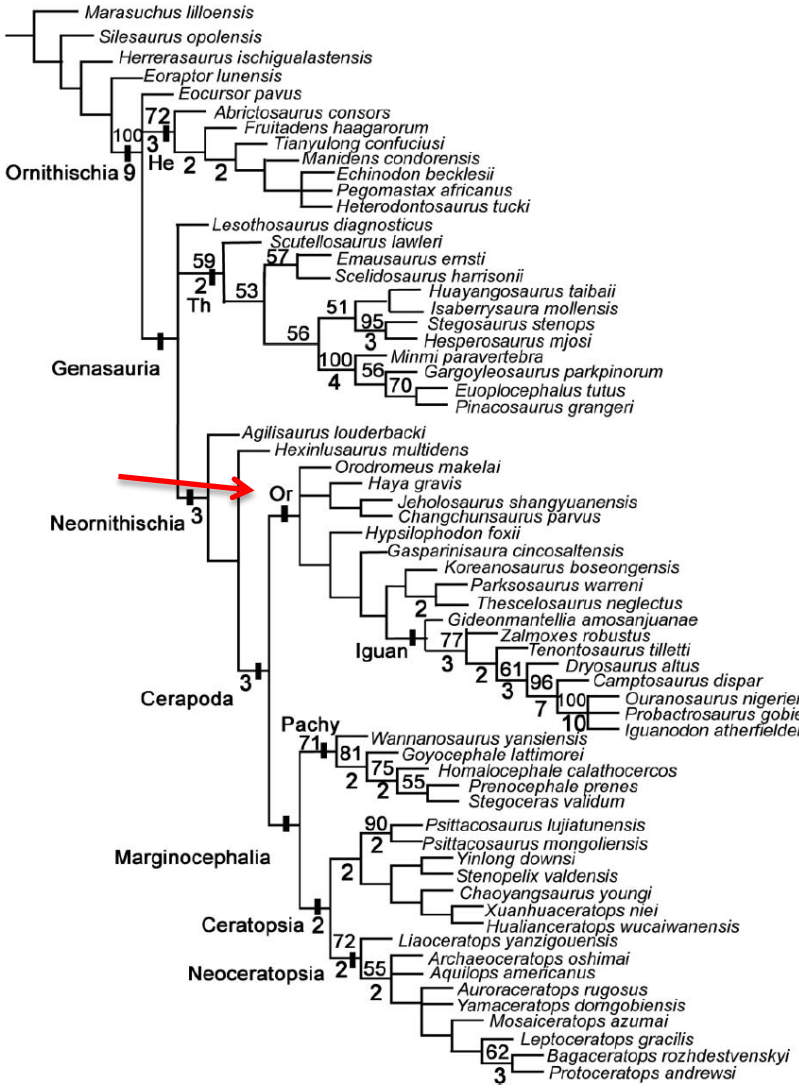

Figure 16. Reduced consensus tree derived by *a posteriori* pruning of eight unstable taxa (*Yueosaurus*, *Pisanosaurus*, *Yandusaurus*, *Zephylosaurus*, *Albalophosaurus Laquintasaura*, *Micropachycephalosaurus* and *Koreaceratops*) from 53,376 most parsimonious trees generated by the full analysis. Values above nodes represent bootstrap proportions. Values beneath nodes indicate Bremer support. Bremer support values of 1 are not shown. Abbreviations: Ch, Chaoyangsauridae; He, Heterodontosauridae; Iguan, Iguanodontia; Or, Ornithopoda; Pachy, Pachycephalosauria; Th, Thyreophora.

Han et al 2017

ORNITHISCHIA

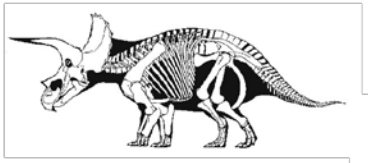

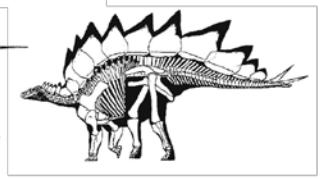

Marginocephalia

Ornithopoda

Thyreophora

Neornithischia

Asymmetrical enamel on teeth

Genasauria

Eocursor

Heterodontosauridae

Deep powerful skulls; Premaxillary tooth row ventral to maxillary tooth row; Jaw joint ventral to dentary tooth row

Hands reduced in size and reduced grasping ability

Expansión extremo distal de la tibia

Pisanosaurus

Saurischia

Backwards-pointing Pubis; Epaxial ossified tendons; Inset tooth row (for cheeks?)

ORNITHISCHIA

Broad Leaf-shaped Teeth with Large Denticles; Predentary Bone; 5 or more sacrals

Dinosauria

Heterodontosauridae

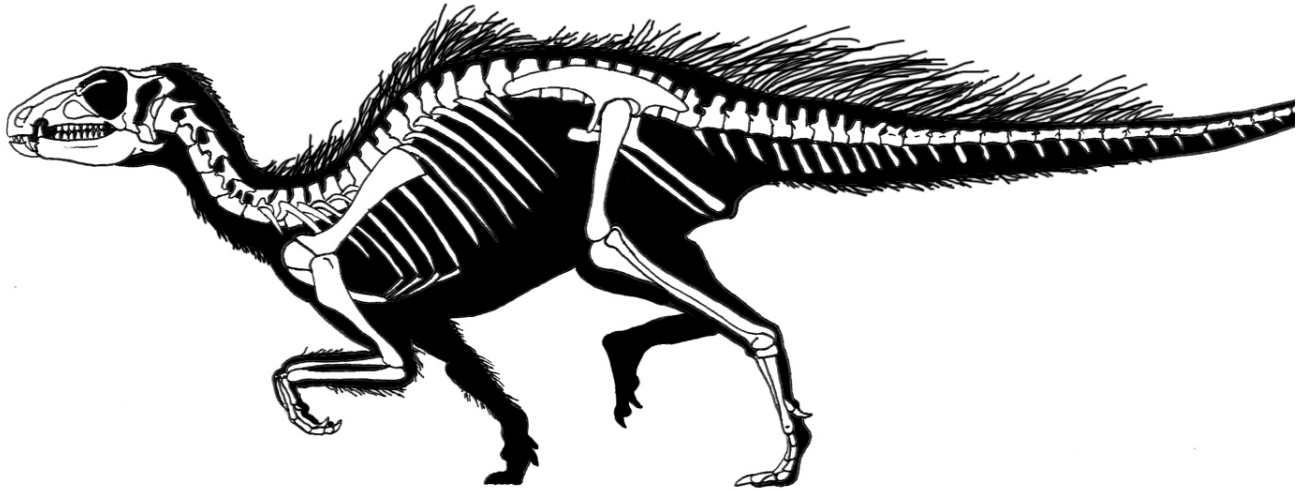

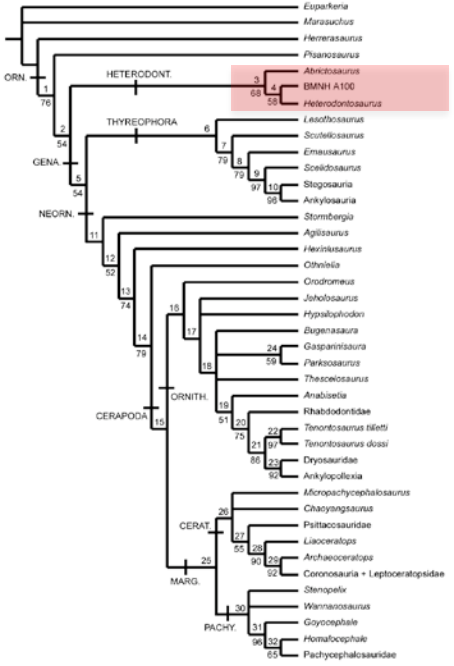

Heterodontosaurus tucki

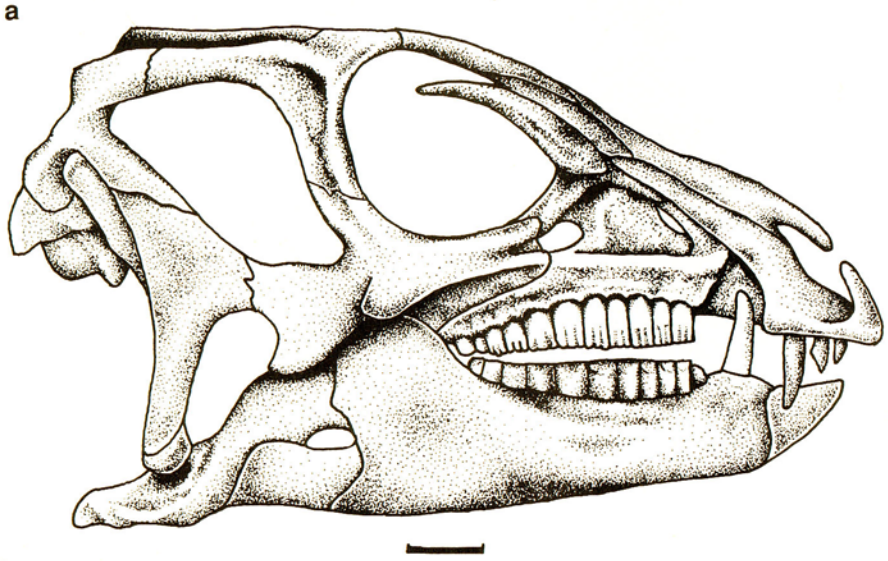

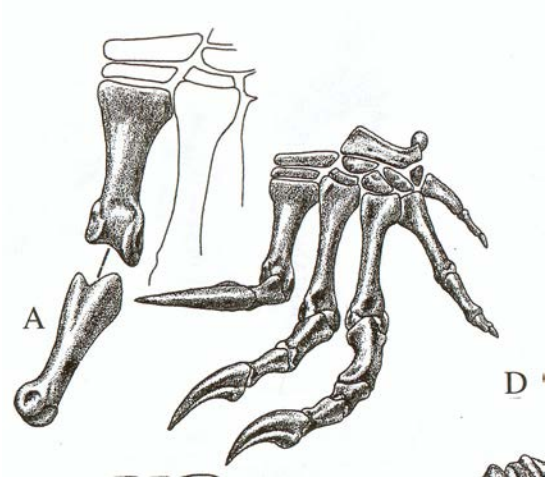

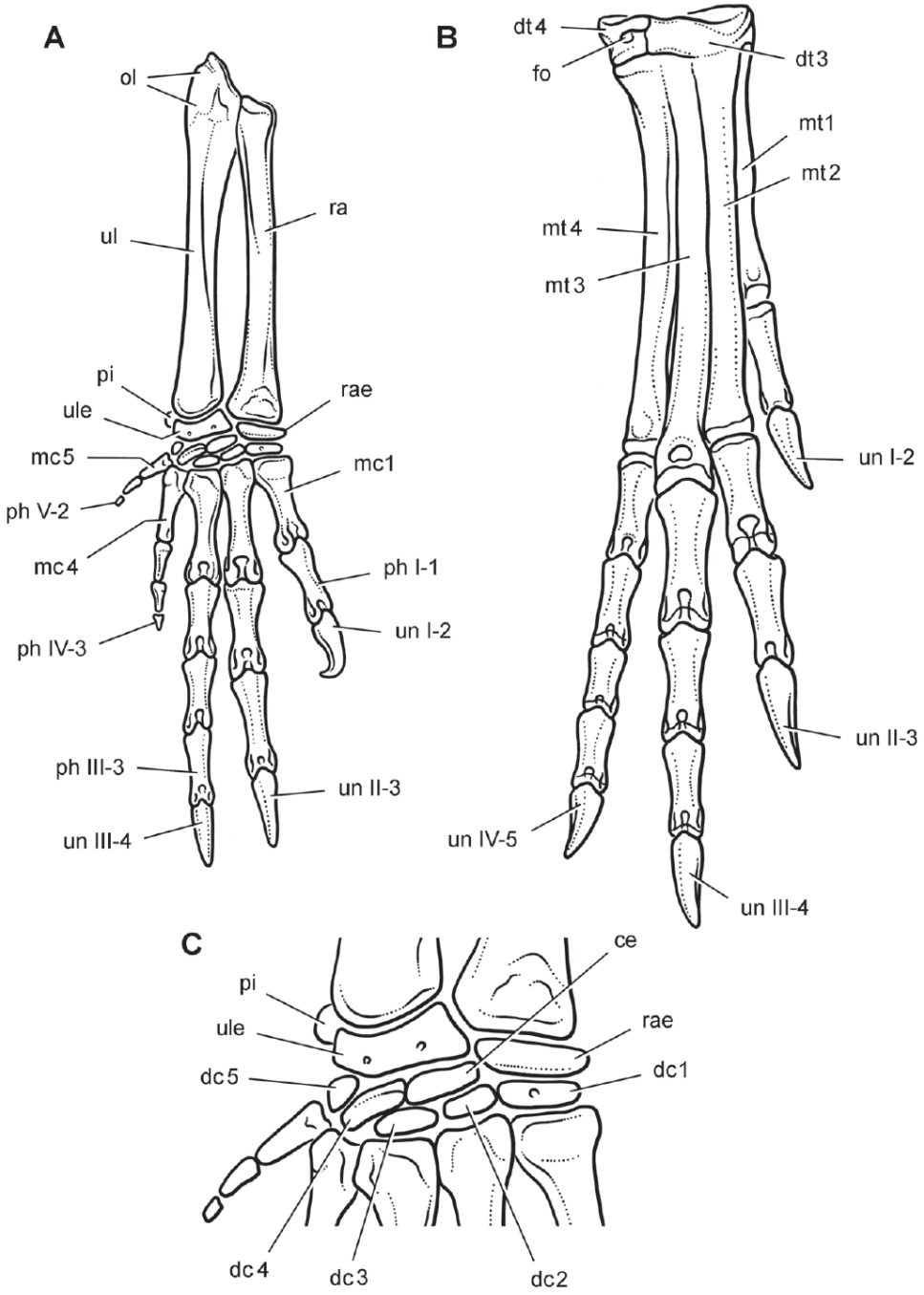

. Relative position of the lower jaw in *Heterodontosaurus tucki* from the Lower Jurassic Upnd Clarens formations of South Africa. Position of the lower jaw during occlusion (**A**) and ıpe (**B**) as seen in left lateral view of a cast of the cranium and lower jaws of adult specimen 1332. Scale bar equals 2 cm.

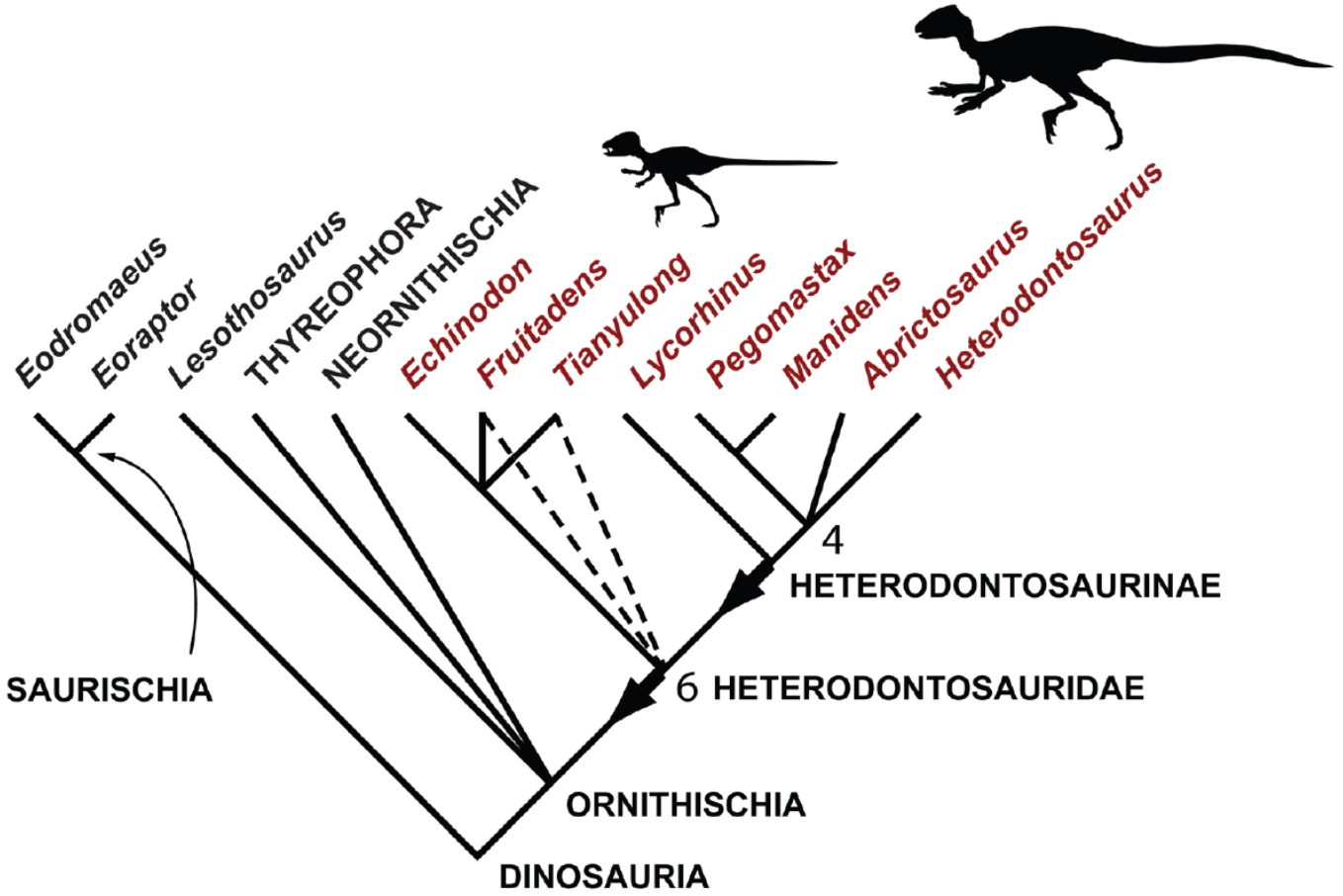

Figure 105. Phylogenetic hypothesis for heterodontosaurids based on character data assembled in this study. Consensus tree summarizing 6 minimum-length trees (38 steps) based on maximum parsimony analysis of 30 characters in 8 heterodontosaurid genera (consistency index = 0.79; retention index = 0.88; Appendix I). Outgroups (constrained as shown) include basal saurischians (*Eoraptor*, *Eodromaeus*) and representative ornithischians (*Lesothosaurus*, Thyreophora, Neornithischia). Dashed lines indicate loss of resolution with an increase of one step in tree length; numbers at nodes indicate the decay index when four poorly known heterodontosaurids (*Echinodon*, *Fruitadens*, *Lycorhinus*, *Pegomastax*) are removed from the analysis. Red text highlights heterodontosaurid genera; arrows indicate stem-based definitions for Heterodontosauridae and Heterodontosaurinae; body icons of *Tianyulong* and *Heterodontosaurus* are shown at appropriate relative size (based on Figures 30 and 72).

Heterodontosaurus es basal (no es un Ornithopoda, como previamente se pensaba)

A number of derived character states are absent in heterodontosaurids, but occur in all cerapodan ornithischians. These include: loss of the squamosal–quadratojugal contact; closure of the external mandibular fenestra (reversed in some psittacosaurids); reduction of the pubic peduncle of the ilium; development of an elongated rod-like prepubic process; modification of the *fossa trochanteris* into a distinct constriction separating the femoral head and greater trochanter; and the anteroposterior expansion of the greater trochanter of the femur relative to the anterior trochanter

The presence of a buccal emargination has previously been considered (Sereno 1986, 1999*a*) to be synapomorphic for a less inclusive clade of ornithischians, Genasauria, and absent in the basal ornithischian *Lesothosaurus diagnosticus*. This analysis alternatively suggests that the presence of a weak or incipient buccal emargination (generally correlated with the

Galton 1974; Olsen & Baird 1986), that heterodontosaurids are not members of Genasauria and are actually situated close to the base of Ornithischia. This basal position is supported by a number of characters (Appendix 4), including: absence of a spout-shaped mandibular symphysis; premaxillary crowns not expanded mesiodistally or apicobasally above the root; alveolar foramina absent medial to maxillary and dentary tooth rows; retention of epipophyses on cervical vertebrae; manus length more than 40% of the combined length of the humerus and radius; penultimate phalanges of the second and third manual digits more elongate than the proximal phalanges; extensor pits present on the dorsal surface of the distal end of metacarpals and manual phalanges; manual unguals strongly recurved with prominent flexor tubercles (Characters 97, 113, 126, 133, 156, 159, 162, 163: Appendix 2).

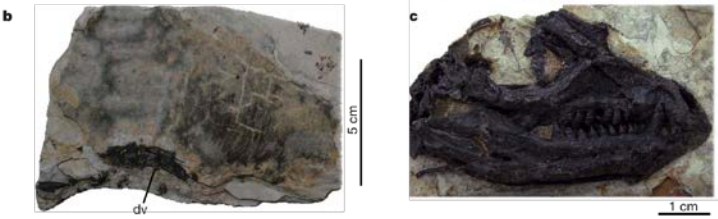

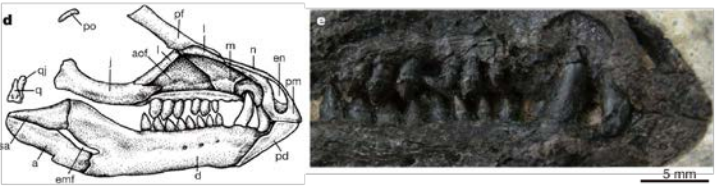

Figure 2 | Integumentary structures of *T. confuciusi* holotype (STMN 26-3) and others for comparison. **a**, Ventral to the cervical vertebral series. **b**, Dorsal to the dorsal vertebral series. **c**, Dorsal to the proximal–middle caudal vertebral series. **d**, Close-up of **c**. Arrows in **c** and **d** point to single filament exhibiting a clear, dark, midline 'stripe'. **e**, Schematic of long, central tail feather of *Epidexipteryx* (after ref. 12). **f**, Two types of integumentary filaments of *Sinornithosaurus* (after ref. 17).

Tianyulong

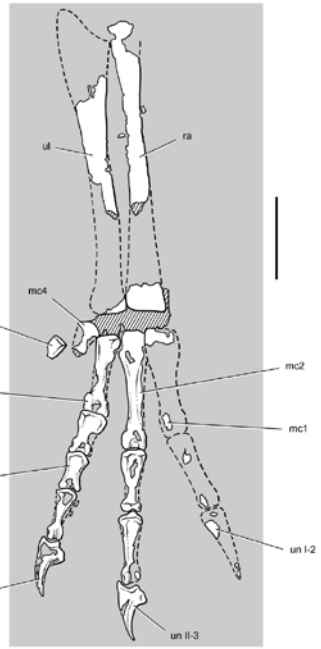

Figure 27. Forearm and manus of the heterodontosaurid *Tianyulong confuciusi* from the Lower Cretaceous Jehol Group of China. Left ulna, radius and manus for the most part in anterior or ventral view. Hatching indicates broken bone; dashed lines indicate estimated edges; tone indicates matrix. Scale bar equals 5 mm. Abbreviations: ***I-III*** digits I-III ***mc1-5*** metacarpal 1-5 ***ph*** phalanx ***ra*** radius ***ul*** ulna ***un*** ungual.

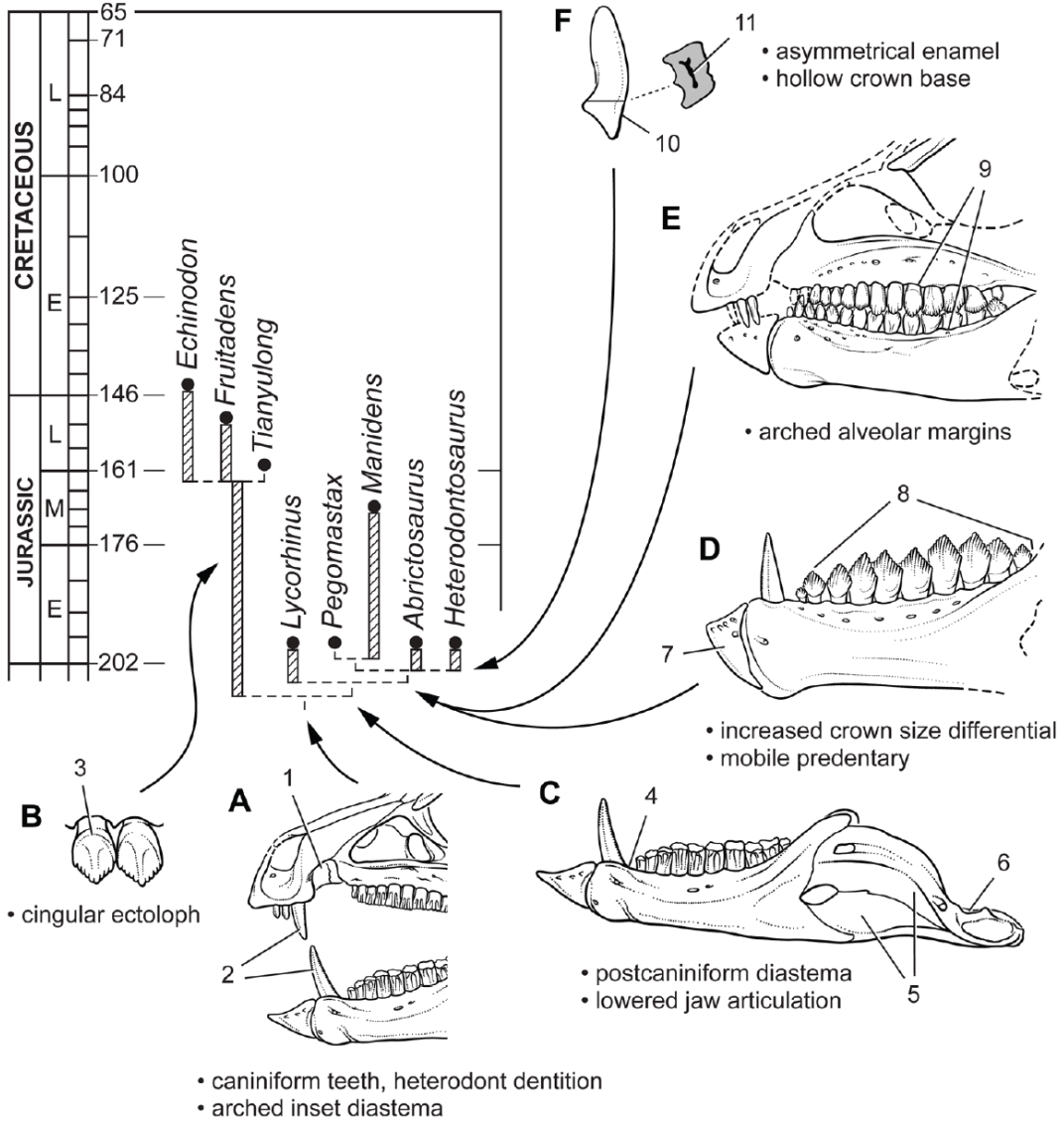

Figure 106. Evolution of key masticatory specializations among heterodontosaurids. **A** Heterodontosauridae **B** Simple-crowned heterodontosaurids **C** Heterodontosaurinae **D** Advanced heterodontosaurines **E** *Abrictosaurus* and *Heterodontosaurus* **F** *Heterodontosaurus*. Abbreviations: ***1*** arched inset diastema ***2*** heterodont dentition with caniniform teeth ***3*** cingular ectoloph ***4*** postcaniniform diastema ***5*** external mandibular fossa ***6*** lowered jaw articulation ***7*** mobile predentary articulating against saddle-shaped dentary articular surface ***8*** increased differential in crown size ***9*** arched alveolar margins in cheek dentition ***10*** asymmetrical enamel ***11*** hollow crown base.

Eocursor parvus

Although *Pisanosaurus* clearly demonstrates that some key cranial and dental characters related to herbivory (e.g. well-developed wear facets, inferred presence of cheeks, enlarged dentary) were present in ornithischians by the beginning of the Late Triassic, other ornithischian synapomorphies are either ambiguous (e.g. number of sacral vertebrae, pelvic morphology) or absent (e.g. a distal expansion of the tibia and corresponding features of the tarsus). By contrast, the more complete holotype specimen of *Eocursor* clearly possesses many key ornithischian features, including an increased number of sacral vertebrae, a strap-shaped preacetabular process of the ilium, an opisthopubic pelvis with a well-defined prepubic process, a blade-shaped anterior trochanter, a pendant fourth trochanter and a distally expanded tibia (Sereno 1999). *Eocursor* provides the earliest unambiguous evidence for the evolution of these features.

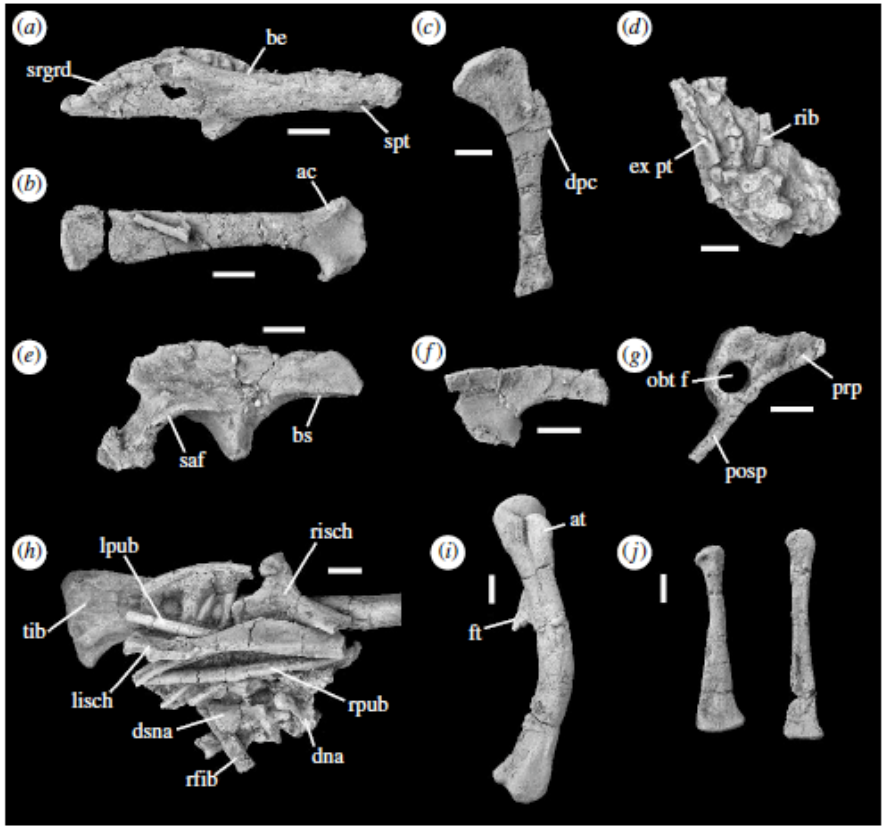

Figure 2. Anatomy of the holotype of *E. parvus* (SAM-PK-K8025). (*a*) Right mandible in lateral view. (*b*) Right scapula in lateral view. (*c*) Right humerus in posterior view. (*d*) Preserved manual phalanges in dorsal view. (*e*) Left ilium in lateral view (preacetabular process is missing). (*f*) Preacetabular process of right ilium in lateral view. (*g*) Prepubic process of left pubis in medial view. (*h*) Elements of pelvic region and hindlimb, including dorsal and sacral vertebrae, ischia (right ischium in medial view; left ischium in dorsal view), pubes, right tibia and fibula. (*i*) Right femur in lateral view. (*j*) Right metatarsals 2 (left) and 3 (right) in medial view. Scale bars, 10 mm. Abbreviations: ac, acromion process; at, anterior trochanter; be, buccal emargination; bs, brevis shelf; dna, neural arch of dorsal vertebra; dpc, deltopectoral crest; dsna, neural arch of dorsosacral vertebra; ex pt, extensor pit on dorsal surface of distal end of manual phalanx; fib, fibula; ft, fourth trochanter; lisch, left ischium; lpub, left pubis; obt f, obturator foramen; posp, pubic shaft; prp, prepubic process; risch, right ischium; rpub, right pubis; saf, supra-acetabular flange; spt, spout-shaped mandibular symphysis; srgrd, weak ridge on lateral surface of surangular; tib, tibia.

Eocursor parvus (Butler et al, 2007)

Reconstruction of type specimen SAM-PK-K8025, with missing elements restored after *Lesothosaurus* and *Stormbergia*. Rigorous skeletal shows what is known of SAM-PK-K8025.

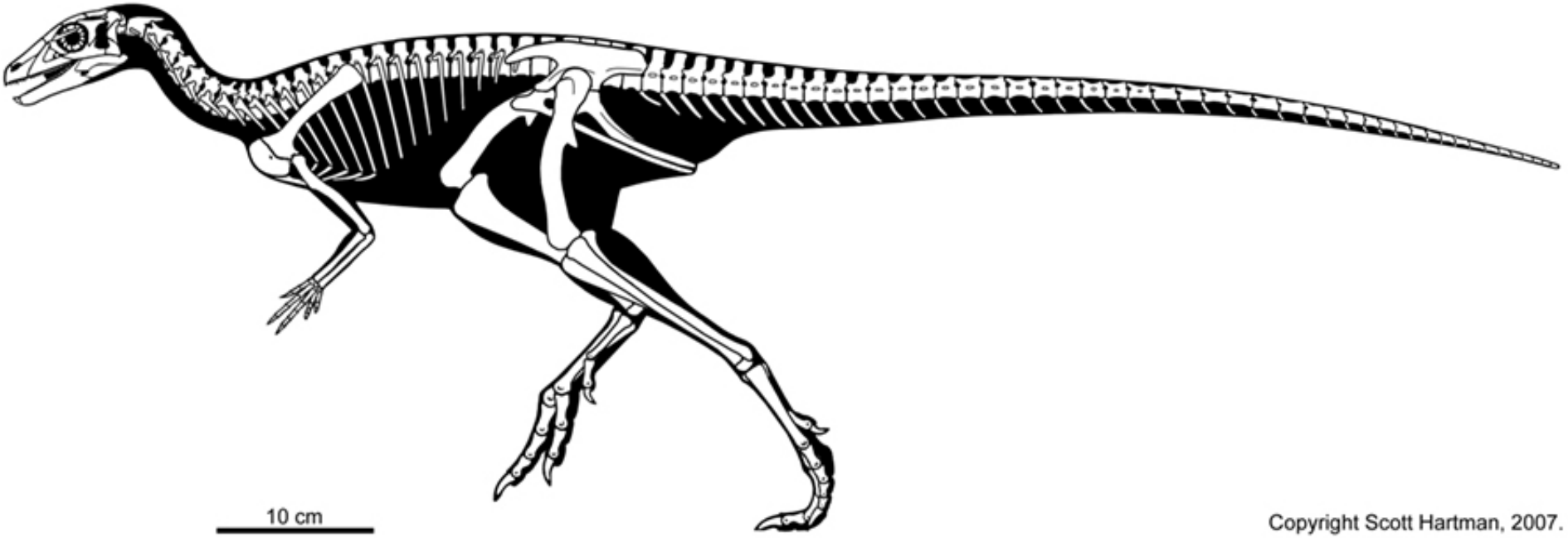

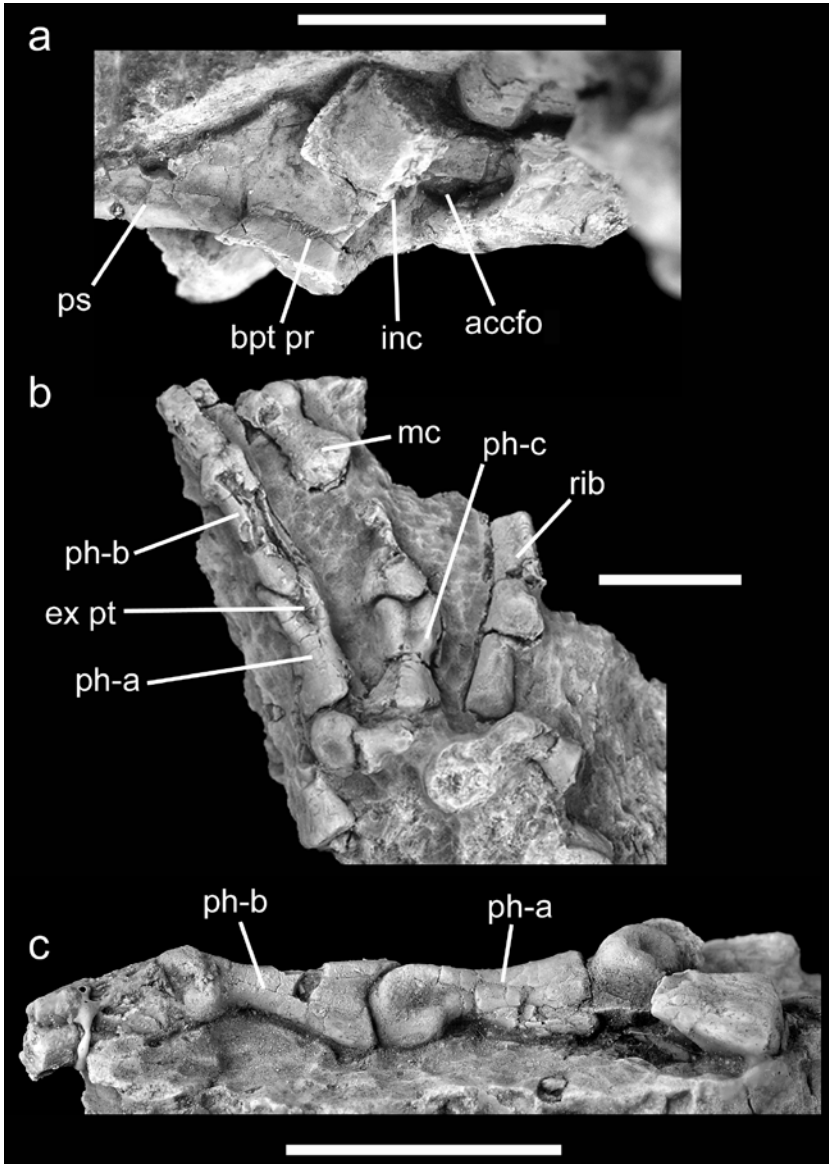

unusual features are evident. As in basal saurischians (Sereno 1993) and the Early Jurassic ornithischian *Heterodontosaurus* (Santa Luca 1980), the manus is robust and elongated relative to the humerus when compared with other ornithischians: the longest preserved phalanx is 17% of the length of the humerus, compared with the values of 9–11% in small ornithischians, such as *Lesothosaurus* (Thulborn 1972; Sereno 1991), *Hexinlusaurus* (He & Cai 1984; Barrett *et al.* 2005) and *Hypsilophodon* (Galton 1974), and 19% in *Heterodontosaurus* (Santa Luca 1980). Furthermore, in *Eocursor*, distal manual phalanges exceed proximal manual phalanges in length, and at least some manual phalanges possess tongue-like median dorsal and ventral intercondylar processes proximally and dorsal extensor pits and deep collateral ligament pits distally. These features are also present in heterodontosaurids and some basal saurischians (Santa Luca 1980; Sereno 1993), but absent in other ornithischians (Galton 1974; He & Cai 1984; Sereno 1991).

material, figure S2). Although previous analyses have interpreted the presence of an enlarged grasping manus (with elongated distal manual phalanges, prominent dorsal extensor pits and proximal intercondylar processes) as a feature unique to heterodontosaurids among ornithischians (Sereno 1986), this work suggests that this feature may represent a plesiomorphic dinosaurian condition, present in basal members of the ornithischian outgroup Saurischia (e.g. *Herrerasaurus*), the primitive and stratigraphically early ornithischian clade Heterodontosauridae and *Eocursor*.

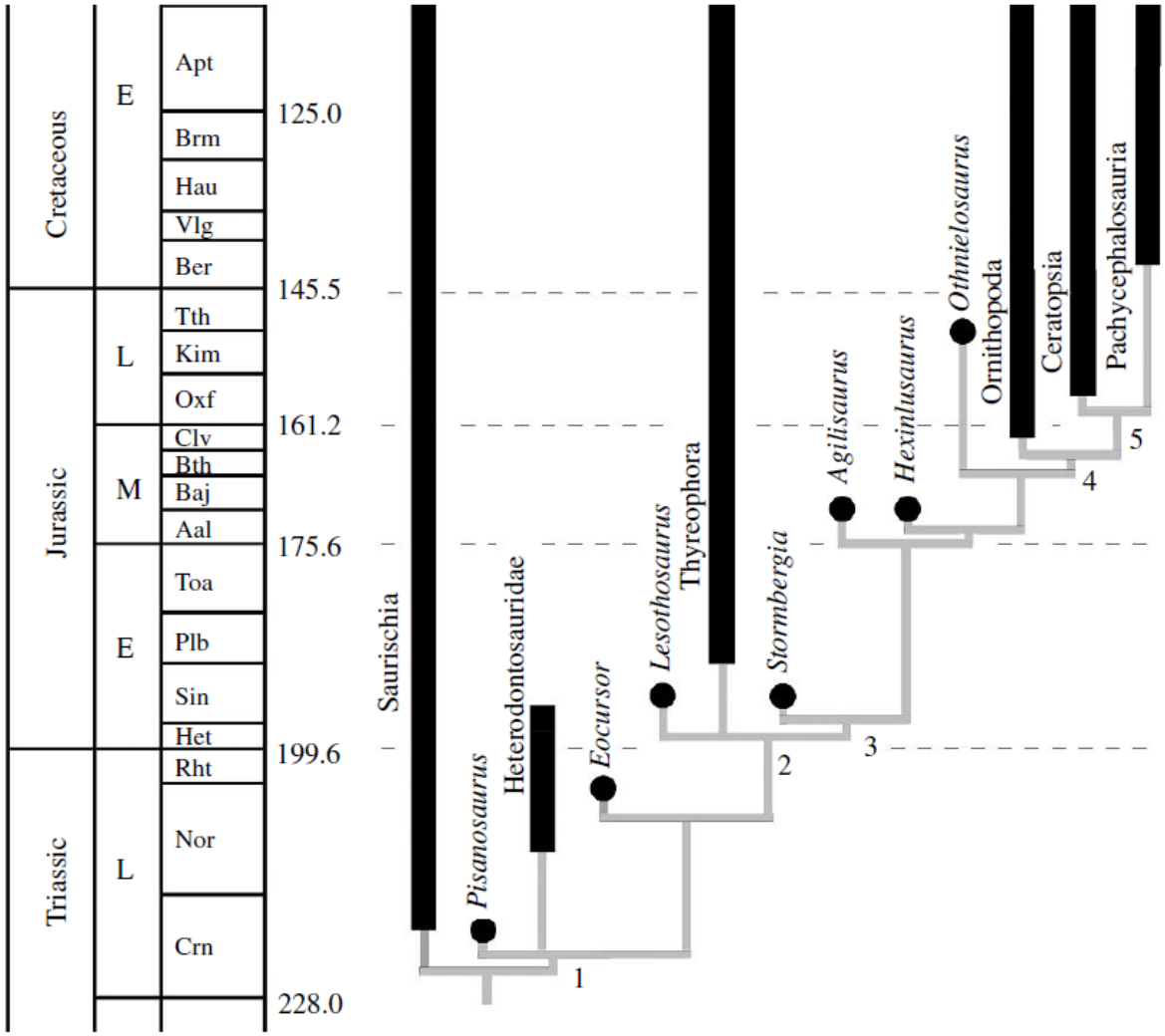

Figure 3. Temporally calibrated phylogeny of early ornithischian dinosaurs. The phylogeny is a simplified version of a cladogram produced by an analysis of 27 taxa and 150 characters (electronic supplementary material). Grey lines indicate ghost lineages. Minimum origination dates for major ornithischian clades include: Carnian (Late Triassic), Ornithischia; Hettangian (Early Jurassic), Genasauria, Thyreophora, Neornithischia; Callovian (Middle Jurassic), Cerapoda, Ornithopoda; Oxfordian (Late Jurassic), Marginocephalia. Numbers indicate clades: 1, Ornithischia; 2, Genasauria; 3, Neornithischia; 4, Cerapoda; 5, Marginocephalia.

Genasauria

Definición: *Ankylosaurus magniventris*, *Stegosaurus stenops*, *Parasaurolophus walkeri*, *Triceratops horridus*, *Pachycephalosaurus wyomingensis*, su ancestro común y todos los descendientes

Sinapomorfias:

1. Presencia de Proceso ventral del predentario bien desarrollado.
2. Sínfisis del dentario en forma de pico.
3. Proceso coronoides muy alto.
4. Pedúnculo púbico angosto en vista lateral.

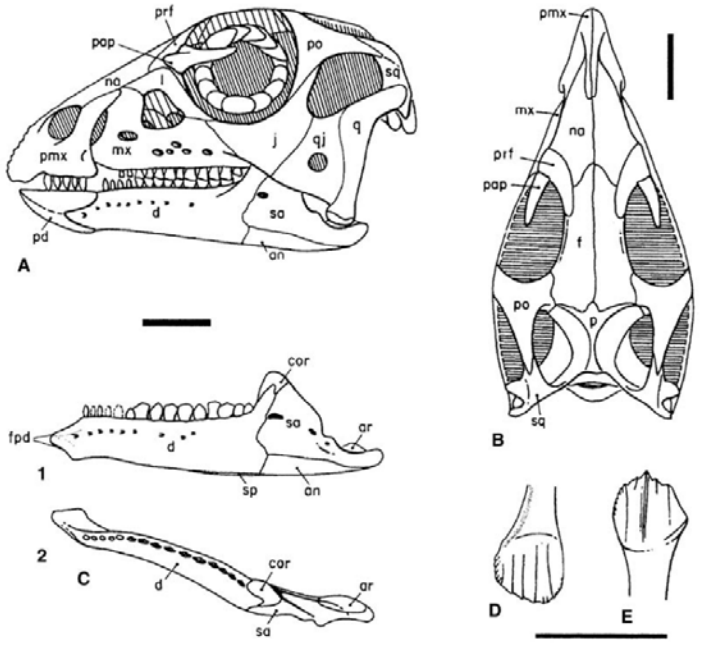

FIGURE 18.3. Skull and teeth of *Hypsilophodon foxii:* A, B, skull in left lateral and dorsal views; C, left lower jaw (without predentary) in lateral, 1, and dorsal, 2, views; D, maxillary crown in buccal view; E, dentary crown in buccal view. Scale = 2 cm (A, B, C), 1 cm (D, E). (After Galton 1974a.)

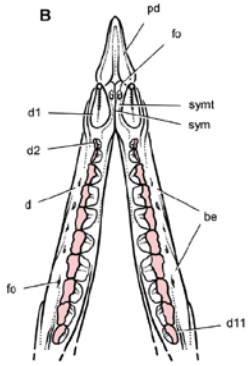

Heterodontosaurus

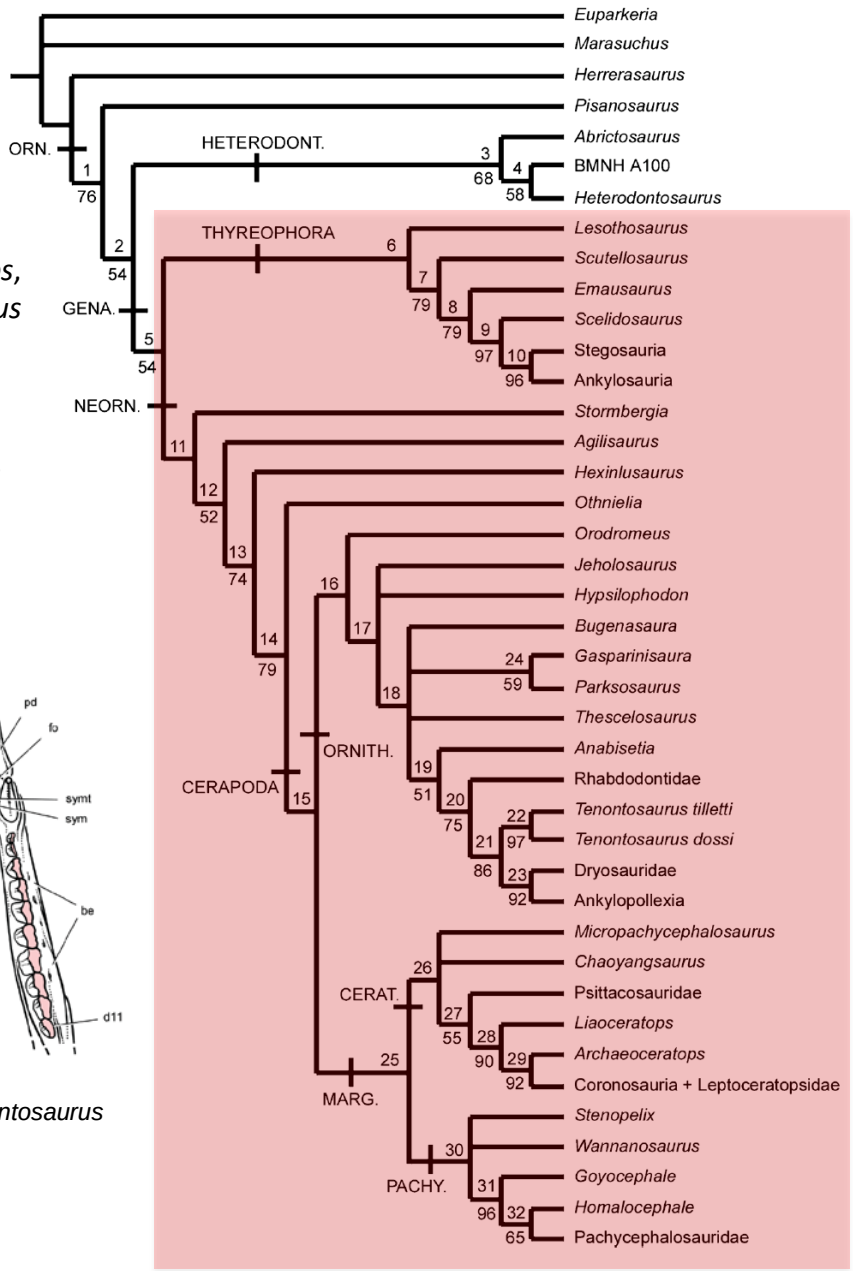

Gracias a *Eocursor* sabemos que antes del origen de Genasauria, la mano disminuyó de tamaño y perdió capacidad de "asir" (agarrar)

Sereno (1999) listed three characters supporting the monophyly of Genasauria (defined as a node-based taxon consisting of *Ankylosaurus*, *Triceratops*, their most recent common ancestor, and all descendants: Sereno, 1998): 1) ~~presence of a maxillary buccal emargination~~; 2) height of the coronoid process of the mandible at least 50% of the height of the dentary at mid-length; 3) pubic peduncle tapering in lateral view. All of these characters are present in *Hexinlusaurus* and *Agilisaurus*, demonstrating that these taxa are more derived than the basalmost ornithischian *Lesothosaurus*.

Cuestionado por nueva posición basal de *Heterodontosaurus*, sería un rasgo plesiomórfico

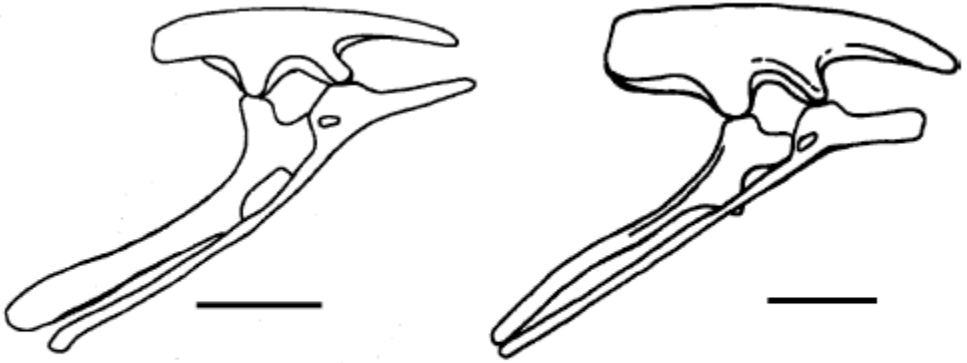

FIGURE 4. Reconstructed right pelves of *Hexinlusaurus multidens* and *Agilisaurus louderbacki* in lateral view. **A**, *Hexinlusaurus* (based on ZDI T6001). **B**, *Agilisaurus* (based on ZDM T6011). Note that the reconstruction of *Agilisaurus* differs somewhat from that provided by Peng (1997): th latter was based in part on material of *Hexinlusaurus*, which was regarded as a synonym of *Agilisaurus* by Peng. Scale bars equal 50 mm.

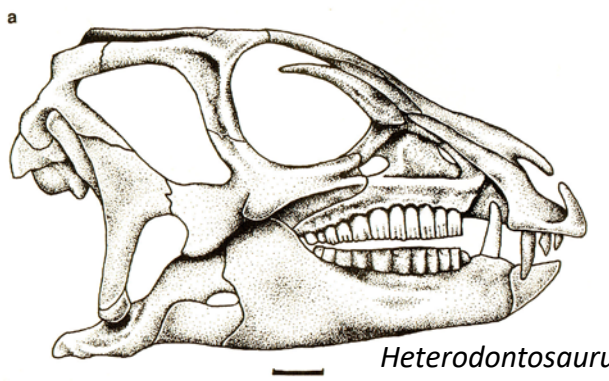

Heterodontosaurus

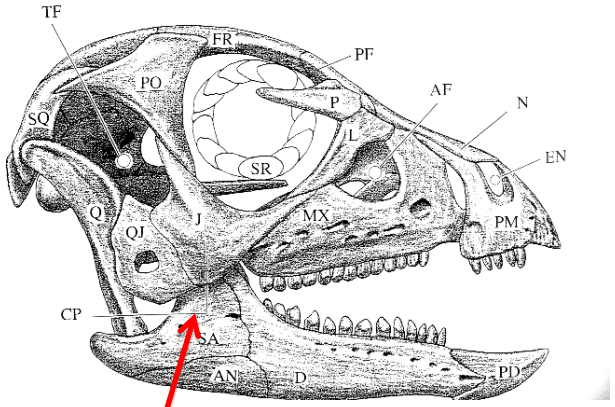

Hypsilophodon

Genasauria: proceso coronoide más elevado

Lesothosaurus diagnosticus

Butler 2005). The interpretation of the position of *Lesothosaurus* suggested by Sereno (1984, 1986, 1991*a*, 1999*a*) is based upon a number of putative synapomorphies supposedly shared by Genasauria and absent in *Lesothosaurus*; Butler (2005) recently demonstrated that most of these characters are either present in *Lesothosaurus* or absent in some basal thyreophorans/neornithischians. Butler (2005) sugges-

All previous and current interpretations of the exact phylogenetic position of *Lesothosaurus* are problematic and poorly supported. However, it seems clear that *Lesothosaurus* is positioned close to the base of Genasauria, as either the sister-taxon to this clade (Sereno 1986, 1999*a*), the most basal known neornithischian (Butler 2005), or the most basal thyreophoran (this analysis). In addition, autapomorphies appear to be difficult to delimit for *Lesothosaurus* (Butler 2005). Taken in combination, these observations suggest that the anatomy of *Lesothosaurus* may be close to that of the ancestral genasaurian and that this taxon remains a good 'ancestral' taxon for ornithischian functional studies.

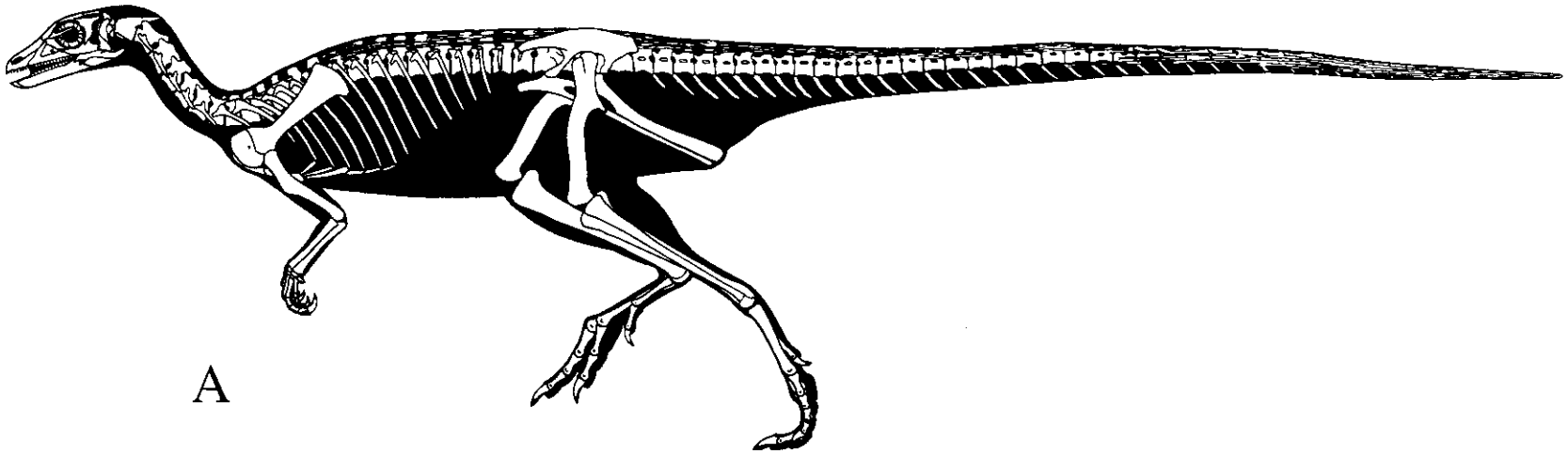

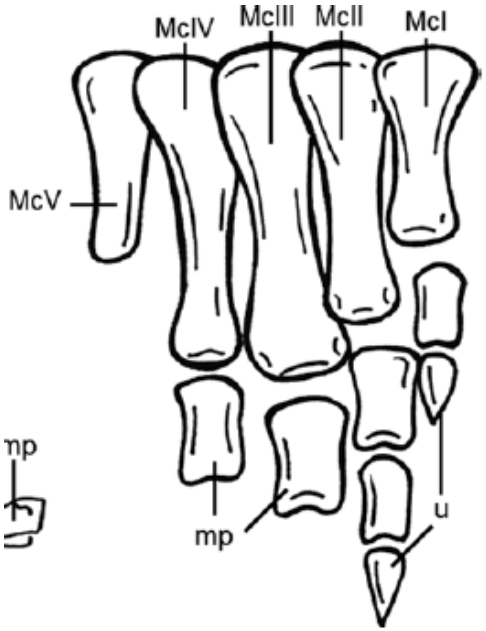

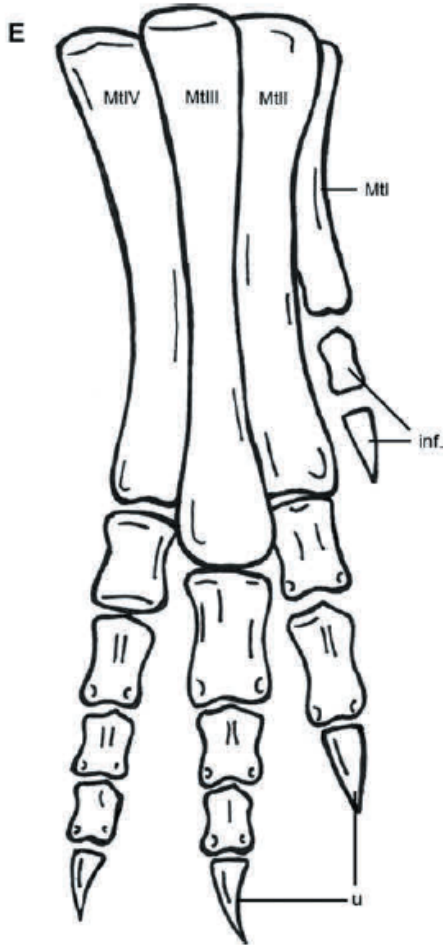

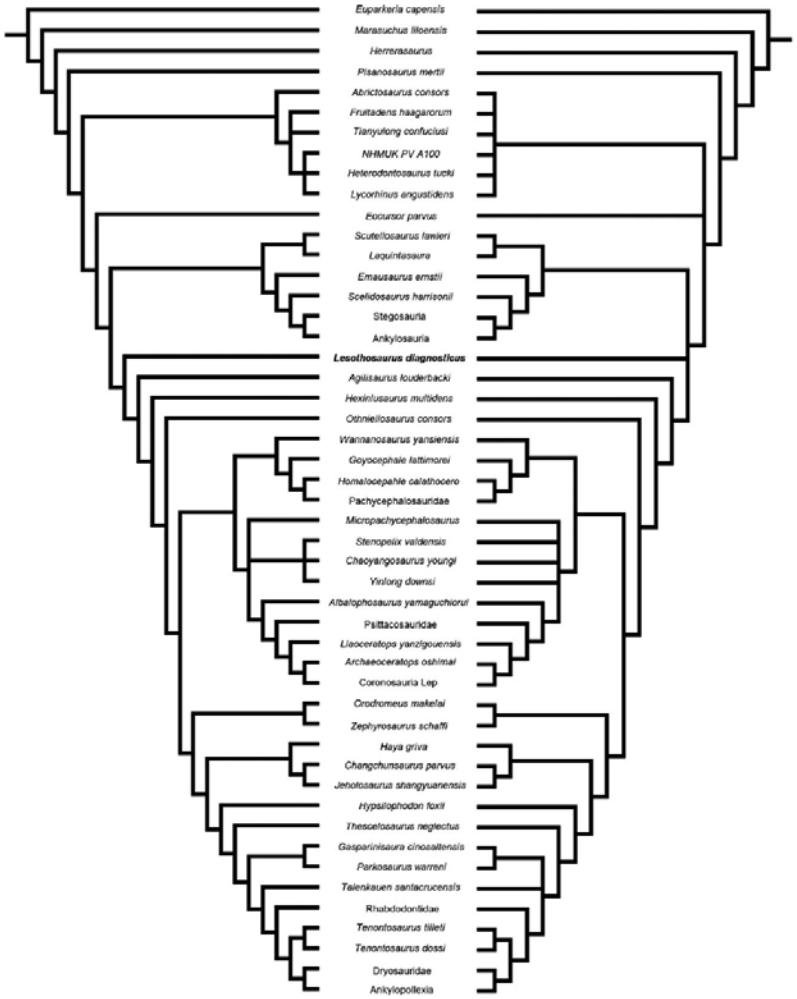

Figure 22. 50% majority rule (left) and reduced strict consensus (right) trees produced in the analysis in which *Lesothosaurus diagnosticus* and *Stormbergia dangershoeki* are synonymized and combined into a single taxonomic unit.

Baron et al 2016

Laquintasaura venezuelae

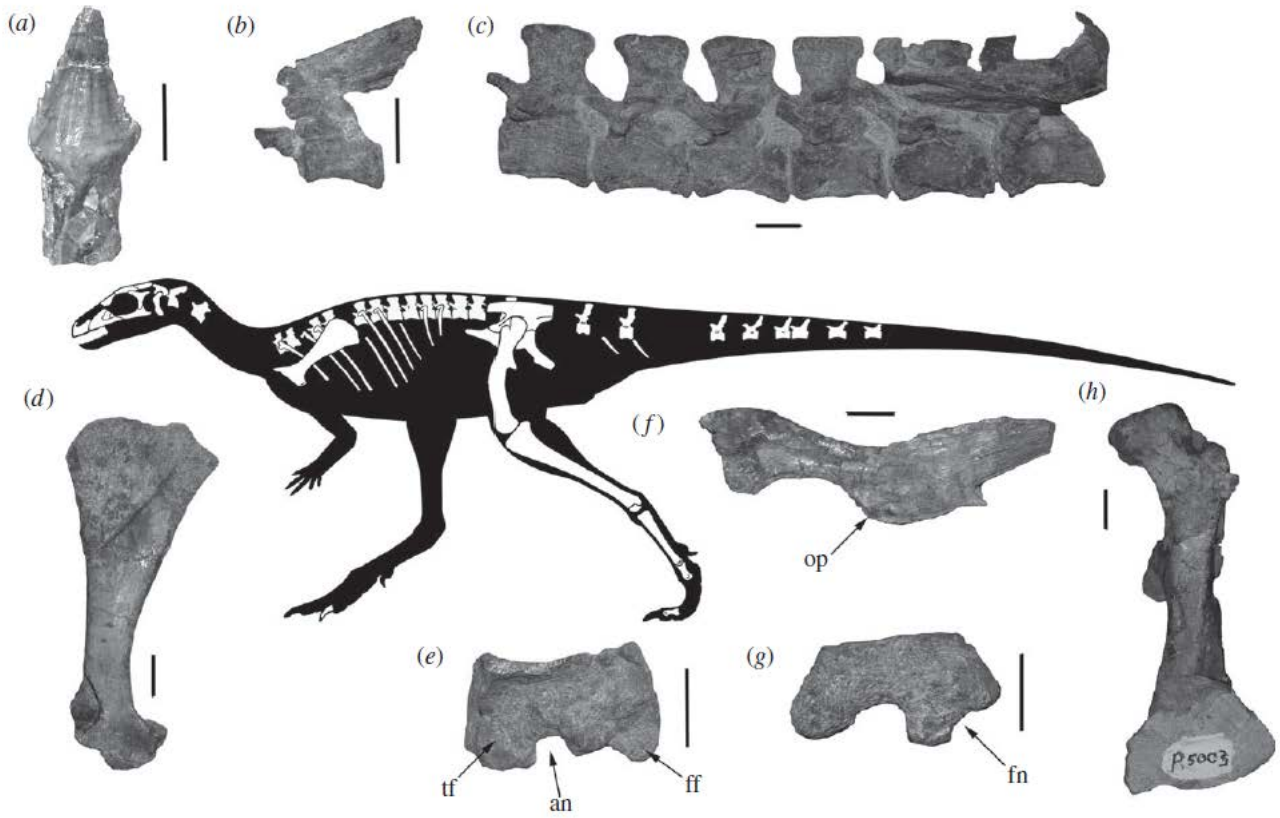

Figure 1. Composite reconstruction of *Laquintasaura venezuelae* gen. et sp. nov., with representative skeletal elements: (*a*) cheek tooth (MBLUZ P.1396: holotype) in labial view, (*b*) atlas–axis complex (MBLUZ P.1350) in left lateral view, (*c*) articulated middle and posterior dorsal vertebrae (MBLUZ P.5009) in right lateral view (reversed), (*d*) left scapula (MBLUZ P.5000) in lateral view, (*e*) left astragalocalcaneum (MBLUZ P.5005: paratype) in proximal view, (*f*) left ischium (MBLUZ P.5018: paratype) in lateral view, (*g*) left femur (MBLUZ P.5017: paratype) in distal view and (*h*) left femur (MBLUZ P.5003) in anterior view. Anterior notch, an; notch in fibular epicondyle, fn; fibular facet, ff; obturator process, op and tibial facet, tf. Scale bars, 2 mm (*a*) and 10 mm (*b*–*h*).

Barrett et al 2014

Laquintasaura venezuelae

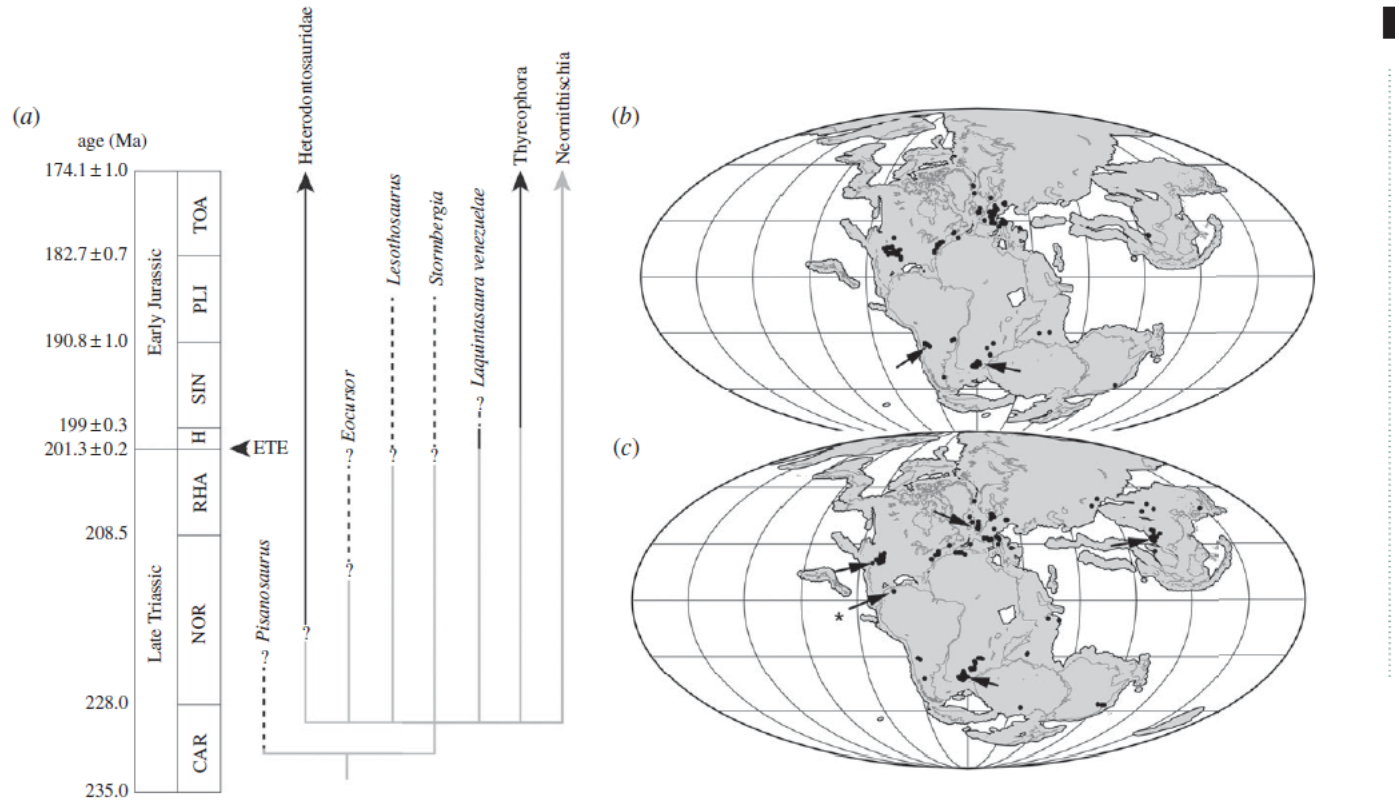

Figure 3. Phylogeny and temporal and spatial distributions of early ornithischians. (*a*) Simplified time-calibrated phylogeny. Lines in black are known ranges; grey lines are inferred (ghost) lineages; dashed lines and question marks indicate taxa with poorly constrained stratigraphic ranges; arrowheads signify clades that continue into the Middle Jurassic. Dinosaur localities in the Late Triassic (*b*) and Early Jurassic (*c*). Arrows indicate ornithischian localities; the asterisk signifies the *Laquintasaura* locality. Note the scarcity of palaeoequatorial dinosaur localities and limited palaeobiogeographical distribution of ornithischians in the Late Triassic and their subsequent spread in the Early Jurassic. Carnian, CAR; end-Triassic extinction event, ETE; Hettangian, H; Norian, NOR; Pliensbachian, PLI; Rhaetian, RHA; Sinemurian, SIN; Toarcian, TOA. See the electronic supplementary material for full details.

Barrett et al 2014

Isaberrysaura mollensis

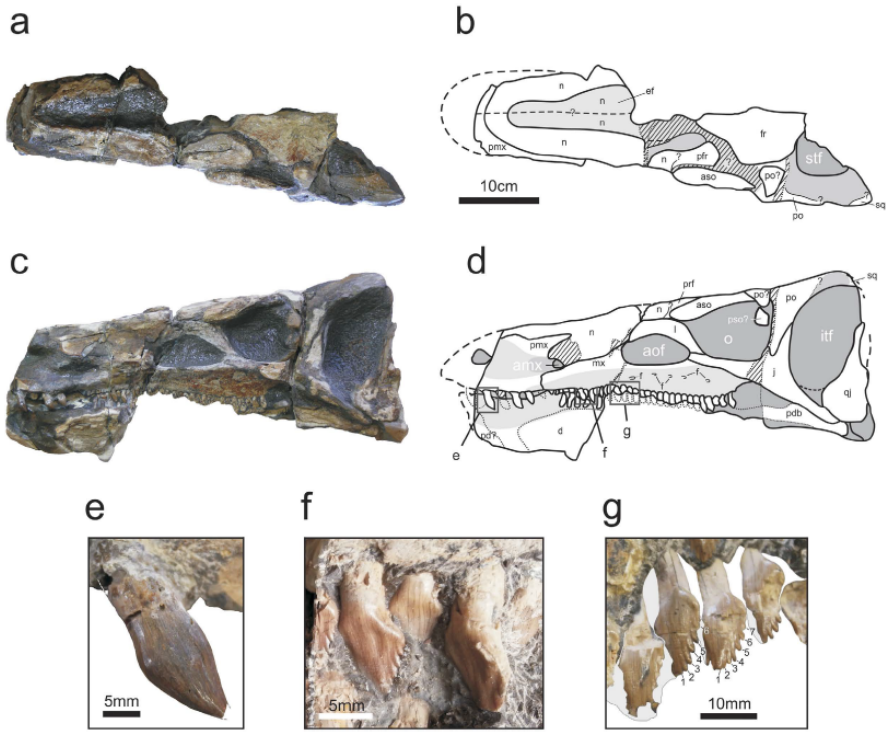

Figure 2. ***Isaberrysaura mollensis*** **gen. et sp. nov. holotype.** Skull in dorsal (**a** and **b**, photograph and drawing respectively), and left lateral (**c** and **d**, photograph and drawing respectively) views. (**e**) Premaxillary tooth; (**f**,**g**) maxillary teeth (g inverted). amf, anterior maxillary fossa; aof, antorbital fossa; aso, anterior supraorbital; d, dentary; ef, elliptical fossa; f, foramina; fr, frontal; ift, infratemporal fenestra; j, jugal; mx, maxilla; n, nasals; o, orbit; pd, predentary; pdb, postdentary bones; pmx, premaxilla; po, postorbital; pso: posterior supraorbital; prf, prefrontal; qj, quadratojugal; sq, squamosal; stf, supratemporal fenestra. 1–7 denticles. The drawings were processed using Adobe Photoshop CS2 Serial Number: 1045-1412-5685-1654-6343-1431.

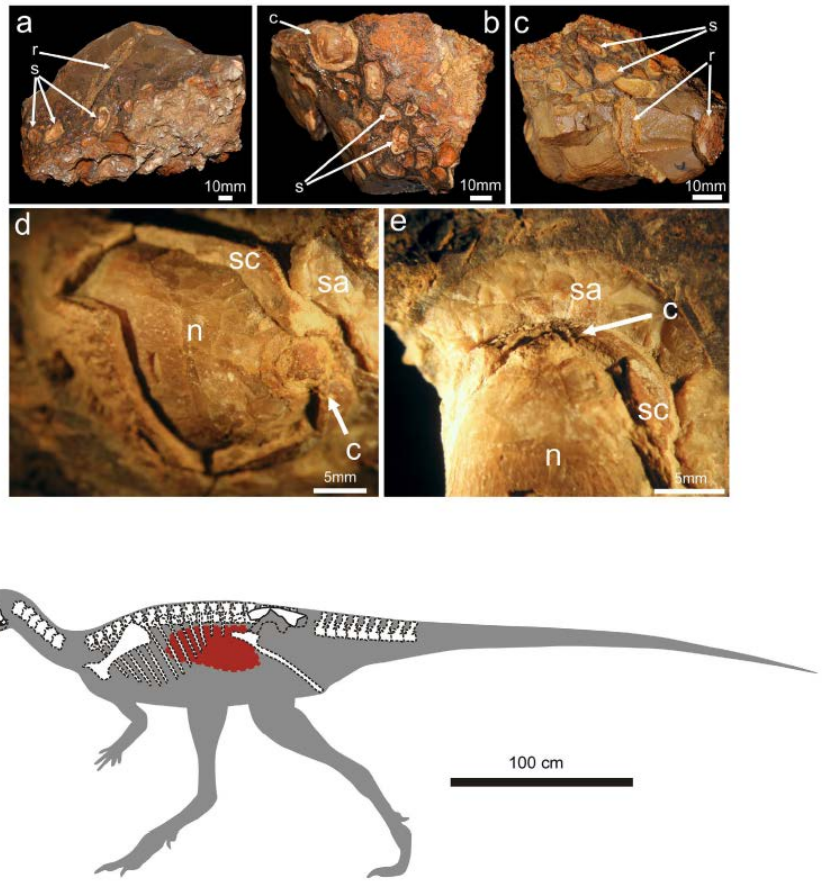

Figure 3. Gut content of *Isaberrysaura mollensis* gen. et sp. nov. (**a**–**c**), seeds of cycads (c), and other seeds (s); rib (r). (**d**,**e**) Detail of seeds of cycads: sarcotesta (sa), sclerotesta (sc), coronula (c), nucellus (n). (**f**) Location of the gut content in the reconstructed skeleton of *Isaberrysaura mollensis* gen. et sp. nov. The drawings were processed using Adobe Photoshop CS2 Serial Number: 1045-1412-5685-1654-6343-1431.

Salgado et al 2017

Isaberrysaura mollensis

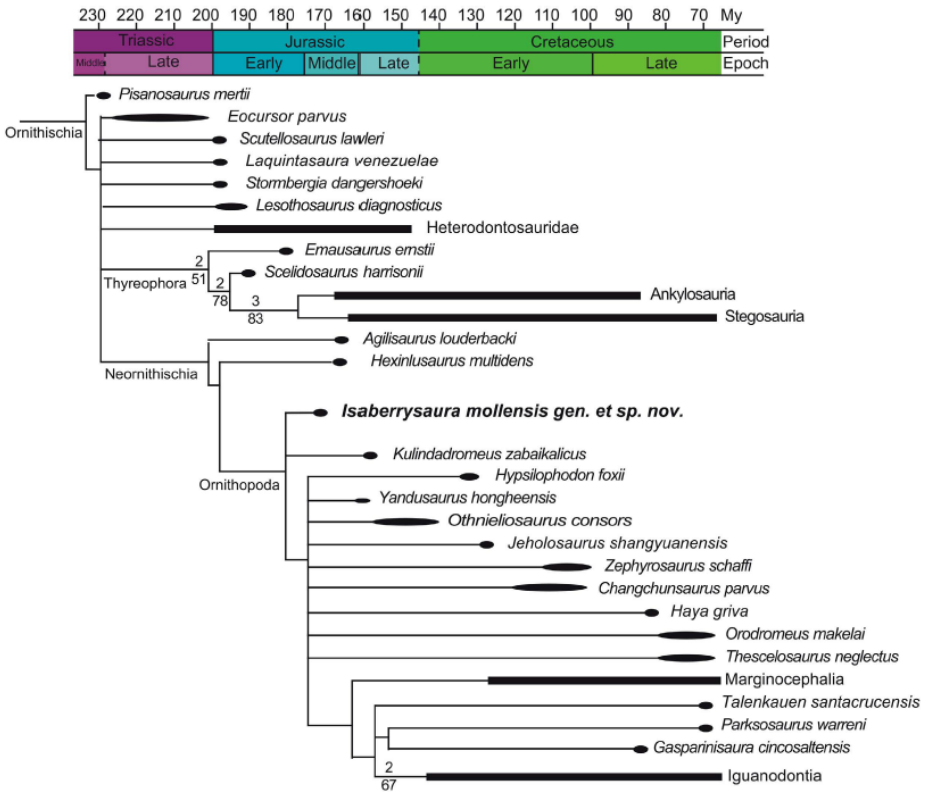

Figure 4. Phylogenetic position of *Isaberrysaura mollensis* gen. et sp. nov. Calibrated reduced strict consensus obtained after including the Argentinian taxon in the current iteration of the Butler *et al.*[17] dataset. Numbers over branches are Bremer support values over 1. Numbers below branches represent bootstrap support values over 50.

Salgado et al 2017

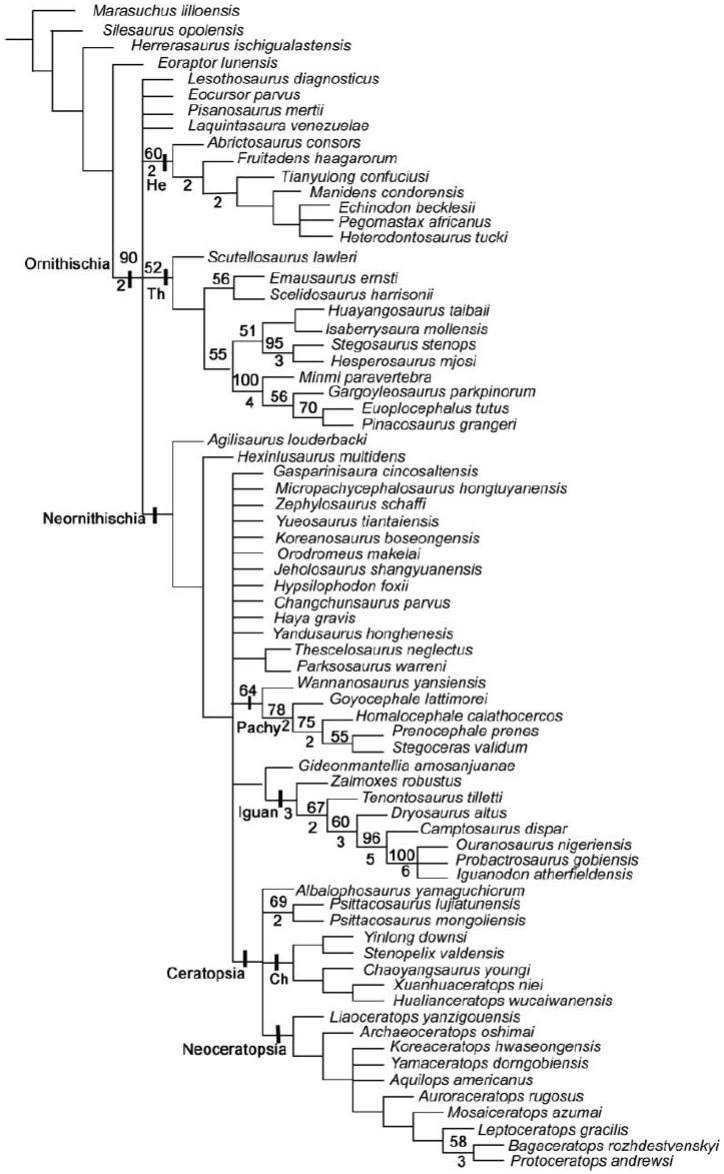

Figure 15. Strict consensus of 53,376 most parsimonious trees (MPTs) produced by analysing a data matrix of 72 taxa and 380 characters. Values above nodes represent bootstrap proportions. Values beneath nodes indicate Bremer support. Bremer support values of 1 are not shown. Abbreviations: Ch, Chaoyangsauridae; He, Heterodontosauridae; Iguan, Iguanodontia; Pachy, Pachycephalosauria; Th, Thyreophora.

Han et al 2017

Tyreophora

Definición: Todos los genasaurios más cercanos a *Ankylosaurus magniventris* que a *Parasaurolophus walkeri*, *Triceratops horridus*, *Pachycephalosaurus wyomingensis*.

Sinapomorfias:

1. Reborde horizontal en el surangular (ausente en estegosaurios).
2. Presencia de osteodermos poscraneales (ausente en *Lesothosaurus*).
3. Proceso anterior del jugal mediolateralmente más ancho que dorsoventralmente profundo (ausente en *Lesothosaurus*).

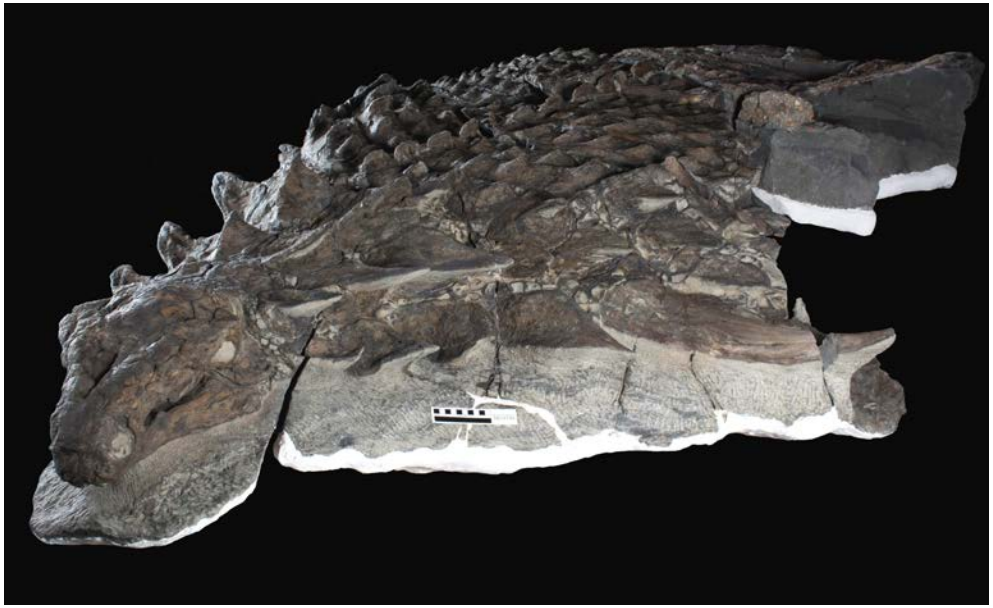

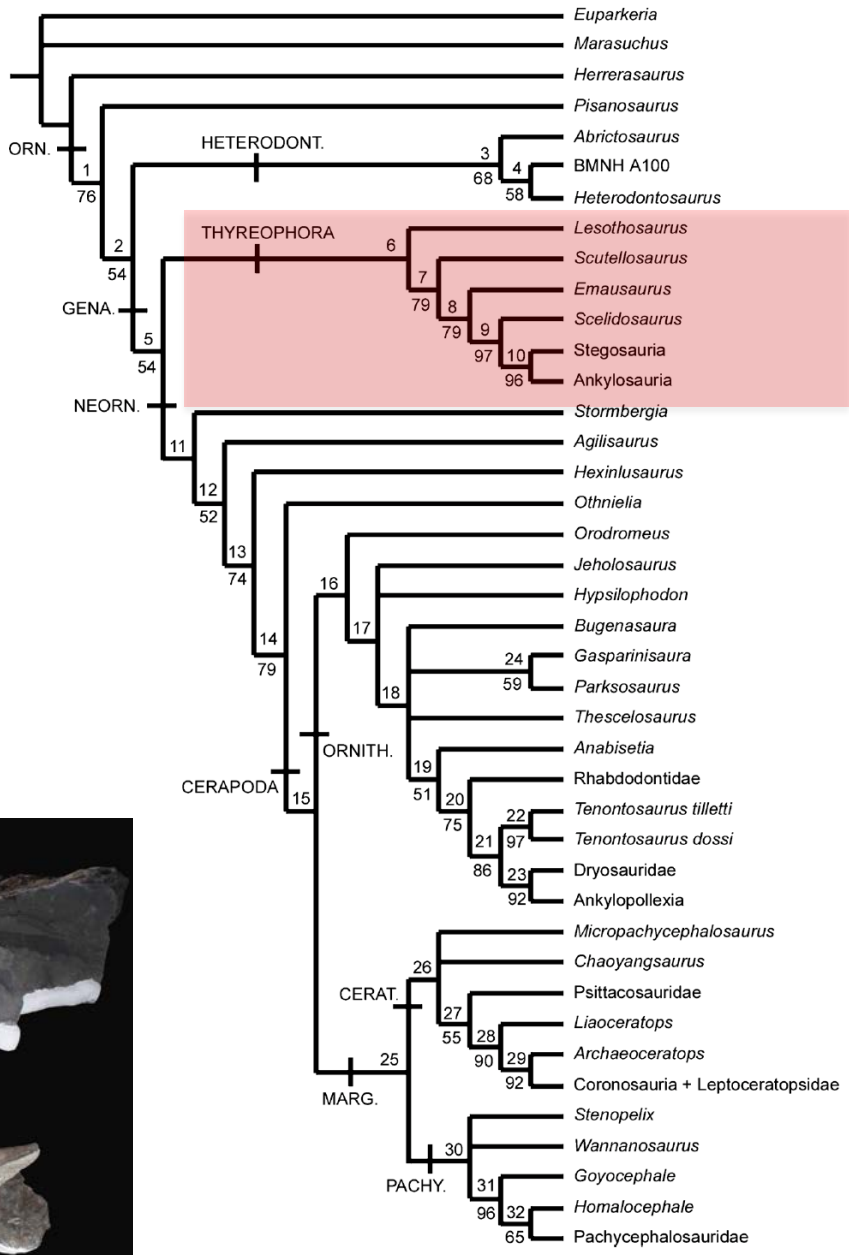

Thyreophora Nopcsa, 1915

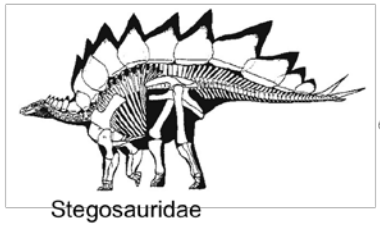

Stegosauridae

Huayangosauridae

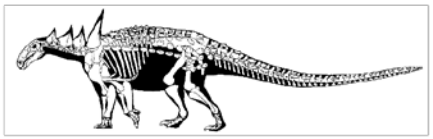

Nodosauridae

Polacanthidae

Ankylosauridae

Stegosauria

Paired plates and spikes;
Thagomizer

Tail club; Short triangular head; Triangular hornlets on skull; Complex nasal chambers

Ankylosauria

Osteoderms fused to skull; Rings of osteoderms on neck and shoulder; Extensive osteoderms over body; Wide across body

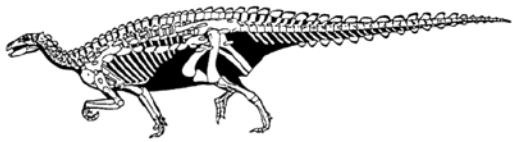

Scelidosaurus

Eurypoda

Scutellosaurus

Larger size; Heavier armor; Obligate quadrupedality

Neornithischia

THYREOPHORA

Osteoderms

Ornithischia

Tyreophora basales

Scutellosaurus lawleri

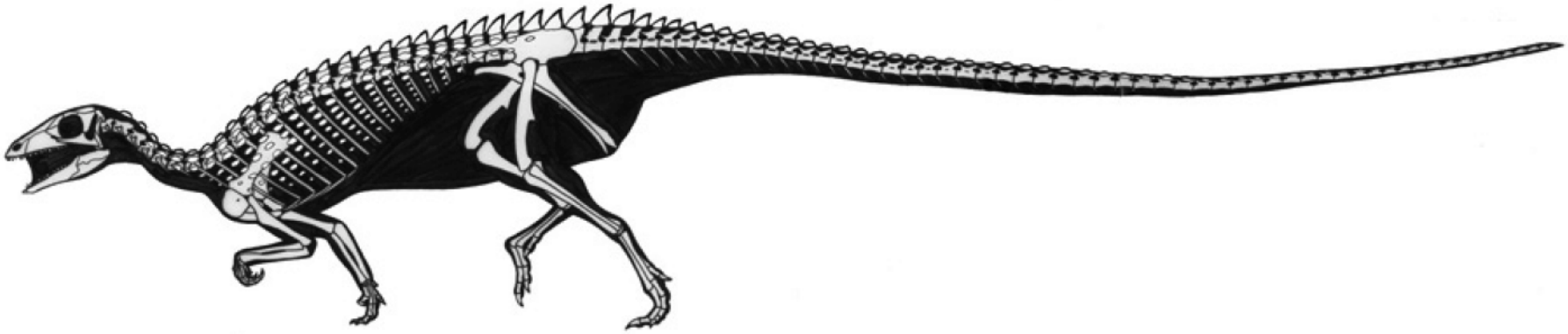

pero ya poseen una coraza compuesta de múltiples filas paralelas de huesos dérmicos dorsales y laterales

Los demás tyreophora tendieron a ser de mayor tamaño y a caminar cuadrúpedos. Formas basales como *Emausaurus* y *Scelidosaurus* presentan pequeñas pezuñas en las manos que delatan su tendencia a ser cuadrúpedos

Scelidosaurus harrisonii

eurypodans. It is also possible that the distribution of character states has been complicated by coding both Stegosauria and Ankylosauria as supraspecific clades: a full consideration of the phylogenetic position of *Scelidosaurus* requires an analysis that includes a large number of stegosaur and ankylosaur taxa. Unfortunately such an analysis has not yet

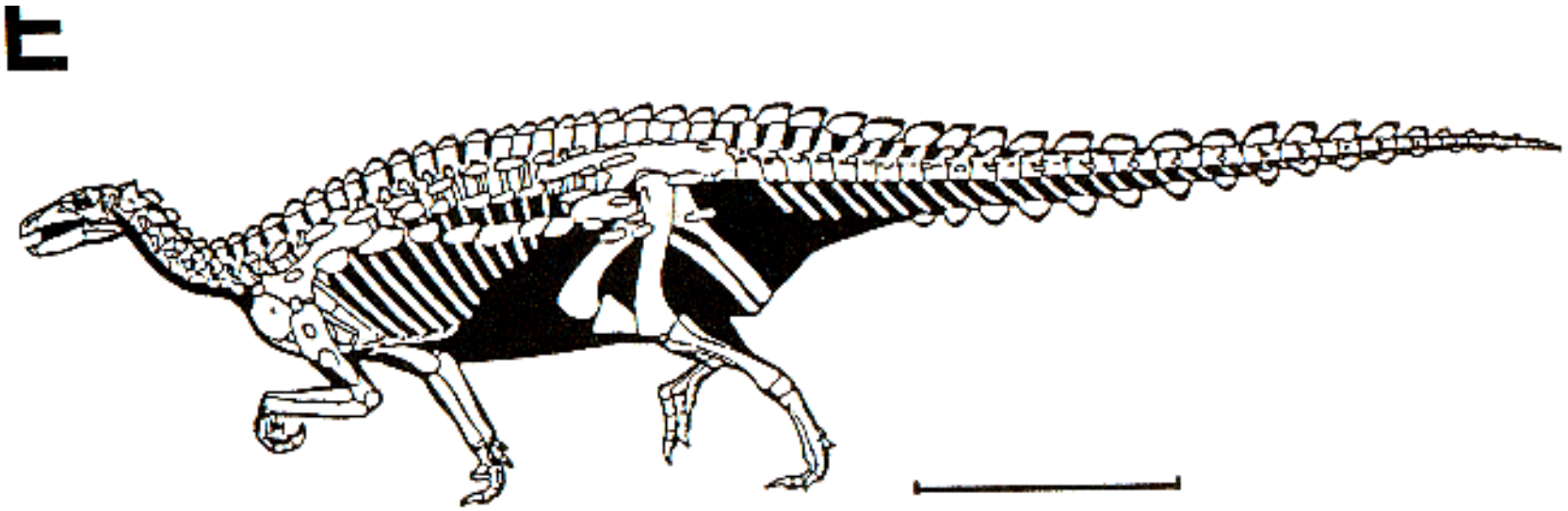

Scelidosaurus

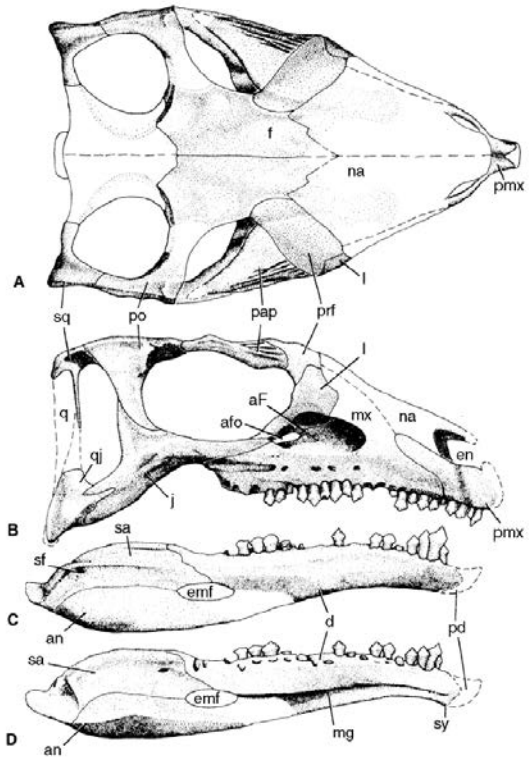

FIGURE 15.2. Skull and lower jaw of *Emausaurus ernsti*: A, B, skull in A, dorsal, and B, lateral views; C, D, lower jaw in C, lateral, and D, medial views. Scale = 10 cm. (After Haubold 1990[JSA6].)

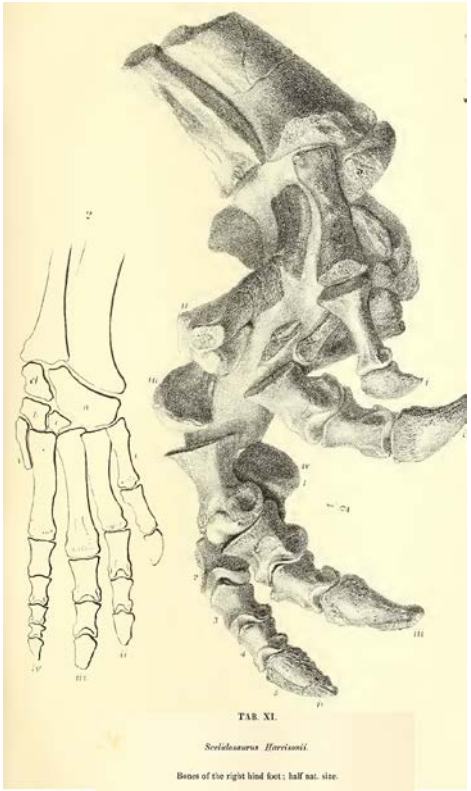

TAB. XI.

Scelidosaurus Harrisonii.

Bones of the right hind foot; half nat. size.

Fig.
1. Bones of the right hind foot, with the distal ends of the tibia and fibula, shewing the amount of dislocation with which they became finally petrified in the matrix.
2. Scheme of the bones of the hind feet, restored.

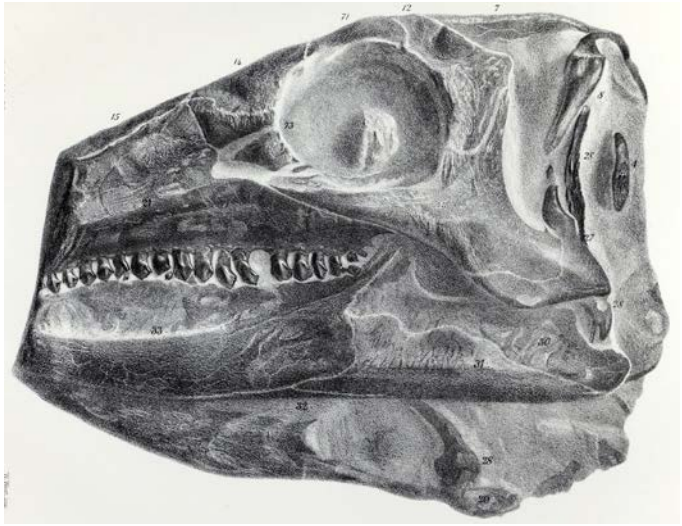

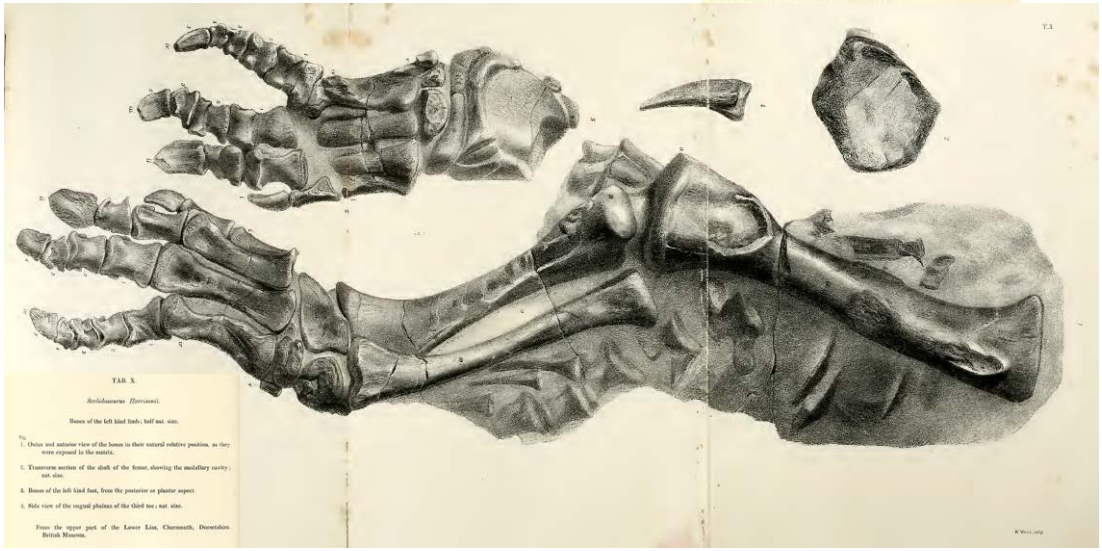

TAB. X.

Scelidosaurus Harrisonii.

Bones of the left hind limb; half nat. size.

Fig.
1. Outer and anterior view of the bones in their natural relative position, as they were exposed in the matrix.
2. Transverse section of the shaft of the femur, shewing the medullary cavity; nat. size.
3. Bones of the left hind foot, from the posterior or plaster aspect.
4. Side view of the ungual phalanx of the third toe; nat. size.

From the upper part of the Lower Lias, Charmouth, Dorsetshire. British Museum.

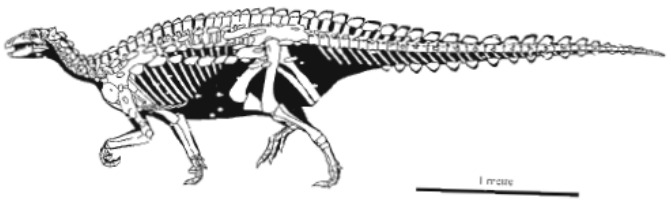

En ***Scelidosaurus*** y **Eurypoda** hay tres nuevos huesos supraorbitales en el techo del cráneo, de los cuales uno posiblemente deriva del palpebral

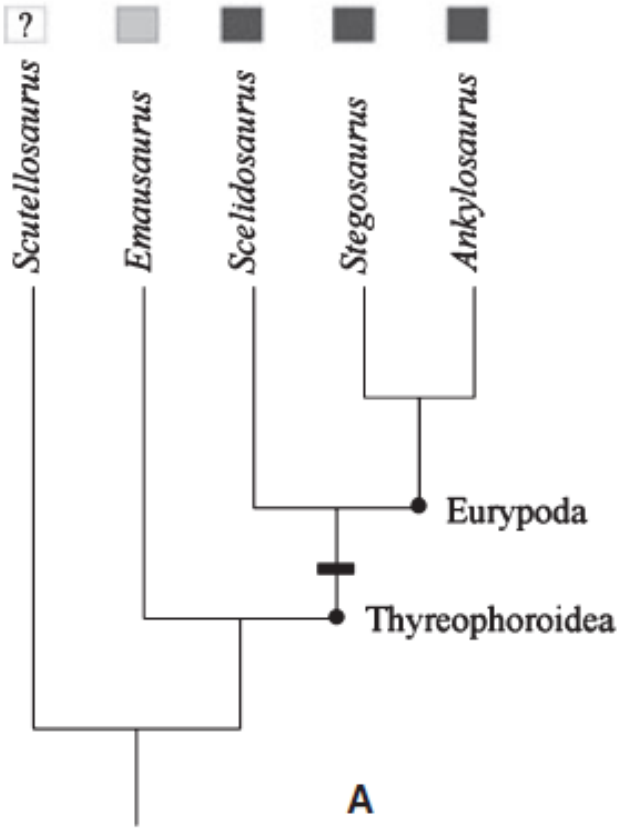

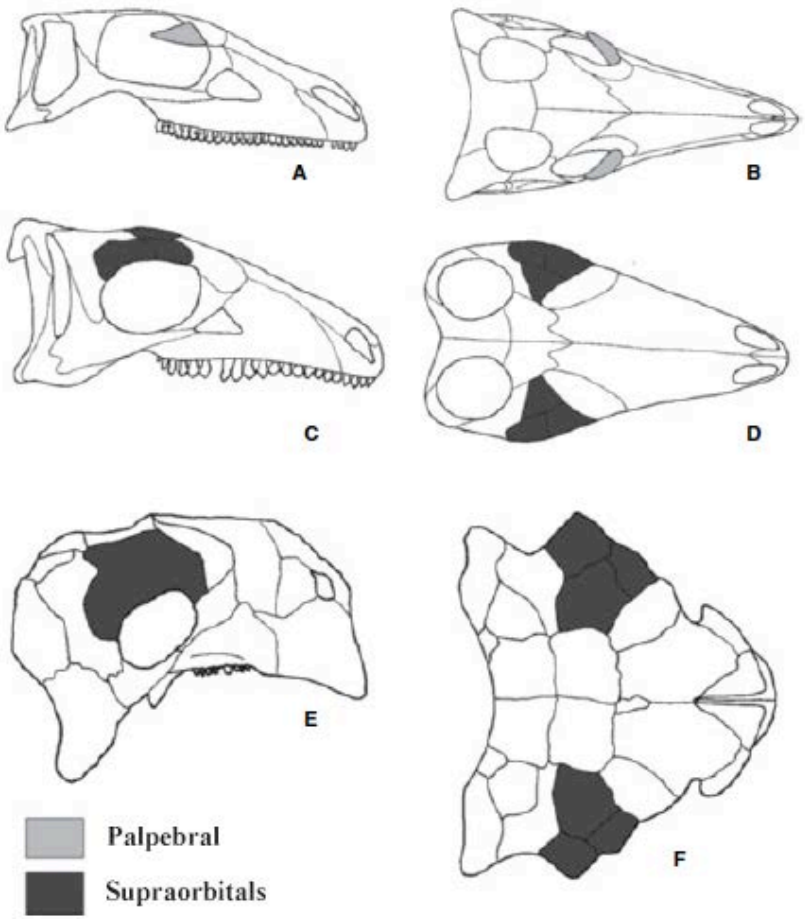

Fig. 4. Reconstructions of the skulls of thyreophoran dinosaurs, showing the locations of the palpebral and supraorbitals. A,B, *Emausaurus ernsti* in right lateral (A) and dorsal (B) view. C,D, *Scelidosaurus harrisonii* in right lateral (C) and dorsal (D) view. E,F, *Pinacosaurus grangeri* (after Vickaryous *et al.* 2004) in right lateral (E) and dorsal (F) view. Not to scale.

Eurypoda

Los Eurypoda (pies anchos) son Tyreophora totalmente cuadrúpedos en los cuales los metatarsos ya no se encuentran compactados sino "abiertos". El pie pasa a tener un aspecto "elefantino", señalando el paso de digitígrados a plantígrados. Los Eurypoda incluyen Stegosauria y Ankylosauria

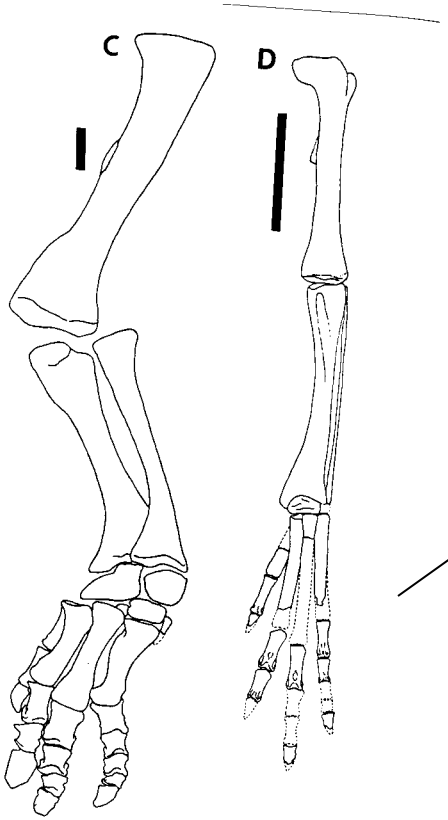

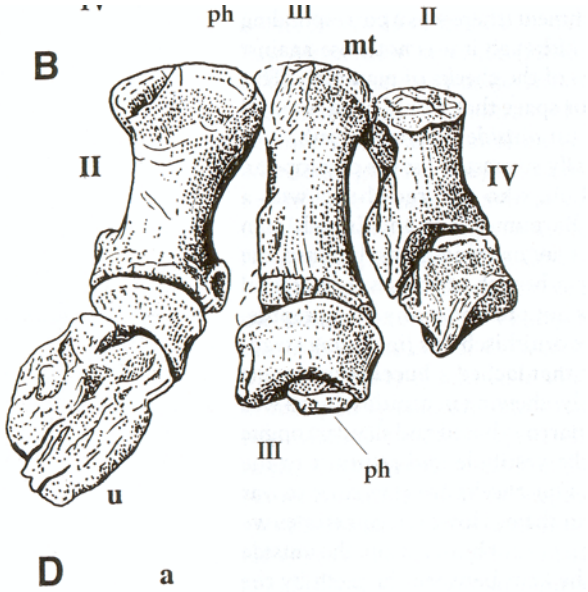

Tyreophora basales (*Scelidosaurus, Scutellosaurus*)

Eurypoda

Stegosauria

Definición: Todos los ornitisquios más cercanamente emparentados a *Stegosaurus stenops* que a *Ankylosaurus magniventris* (Galton, 1997)

Sinapomorfías (sensu Galton & Upchurch, 2004):

- Superficie dorsal de los parietales plana.
- Diámetro del canal neural de v. dorsales anteriores mayor a la mitad del centro vertebral.
- Arco neural dorsal 1.5 veces más alto que centro vertebral.
- Procesos transversos de vértebras dorsales inclinados 50˚.
- Espinas neurales de caudales anteriores anchas y bajas.
- Extremo proximal de la escápula con superficie mayor al coracoides.
- Tubérclo triceps prominente en húmero.
- Ulnare+intermeidum fusionados.
- Carpales distales ausentes.
- Proceso peracetabular desviado lateralmente unos 35˚.
- Presencia de escudo iliaco conformado por la fusión de procesos transversos sacrales.
- Dígito pedal I ausente.
- Dígito pedal III con máximo 3 falanges.
- Dígito pedal IV con máximo 3 falanges.
- 2 filas parasagitales de placas dérmicas.
- Tendones epaxiales osificados ausentes.

Maidment et al 2017

Stegosauria

Definición: Todos los ornitisquios más cercanamente emparentados a *Stegosaurus stenops* que a *Ankylosaurus magniventris* (Galton, 1997)

Sinapomorfías (sensu Galton & Upchurch, 2004):

- Superficie dorsal de los parietales plana.
- Diámetro del canal neural de v. dorsales anteriores mayor a la mitad del centro vertebral.
- Arco neural dorsal 1.5 veces más alto que centro vertebral.
- Procesos transversos de vértebras dorsales inclinados 50˚.
- Espinas neurales de caudales anteriores anchas y bajas.
- Extremo proximal de la escápula con superficie mayor al coracoides.
- Tubérclo triceps prominente en húmero.
- Ulnare+intermedium fusionados.
- Carpales distales ausentes.
- Proceso preacetabular desviado lateralmente unos 35˚.
- Presencia de escudo iliaco conformado por la fusión de procesos transversos sacrales.
- Dígito pedal I ausente.
- Dígito pedal III con máximo 3 falanges.
- Dígito pedal IV con máximo 3 falanges.
- 2 filas parasagitales de placas dérmicas.
- Tendones epaxiales osificados ausentes.

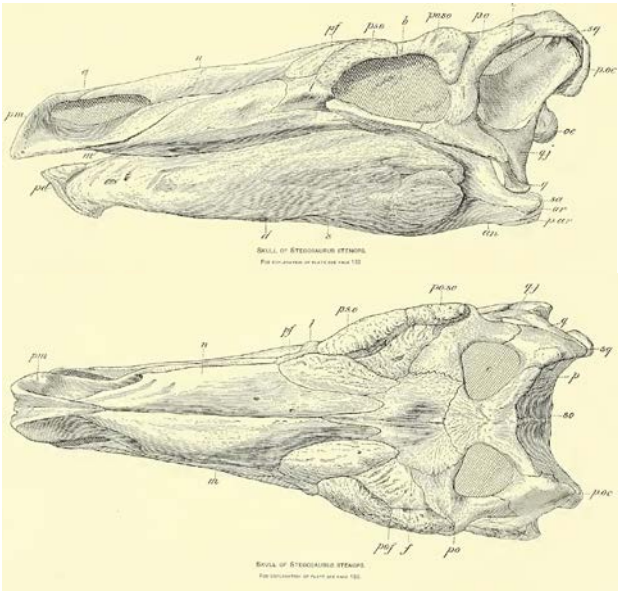

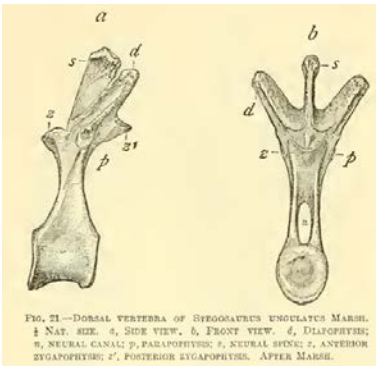

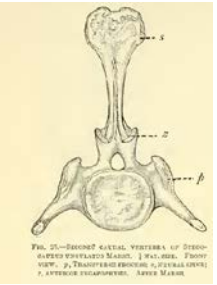

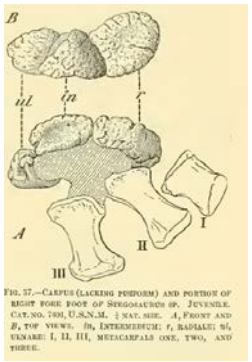

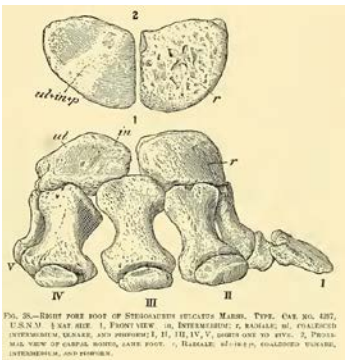

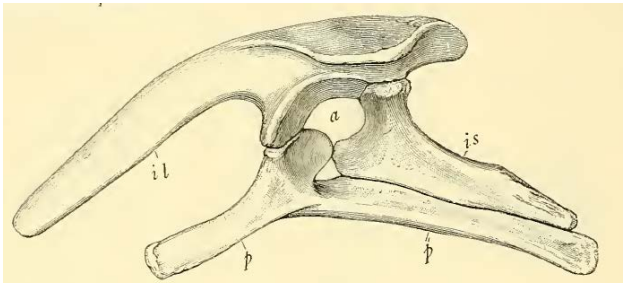

FIG. 42.—PELVIS OF STEGOSAURUS STENOPS MARSH. 1/10 NAT. SIZE. SIDE VIEW. *a*, ACETABULUM; *il*, ILIUM; *is*, ISCHIUM; *p*, PUBIS; *p'*, POSTPUBIS. AFTER MARSH.

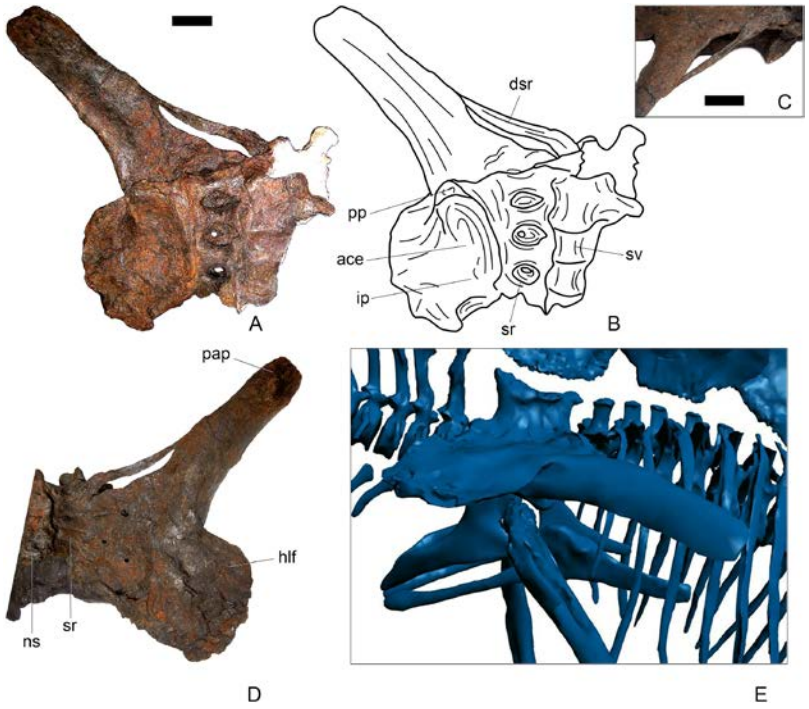

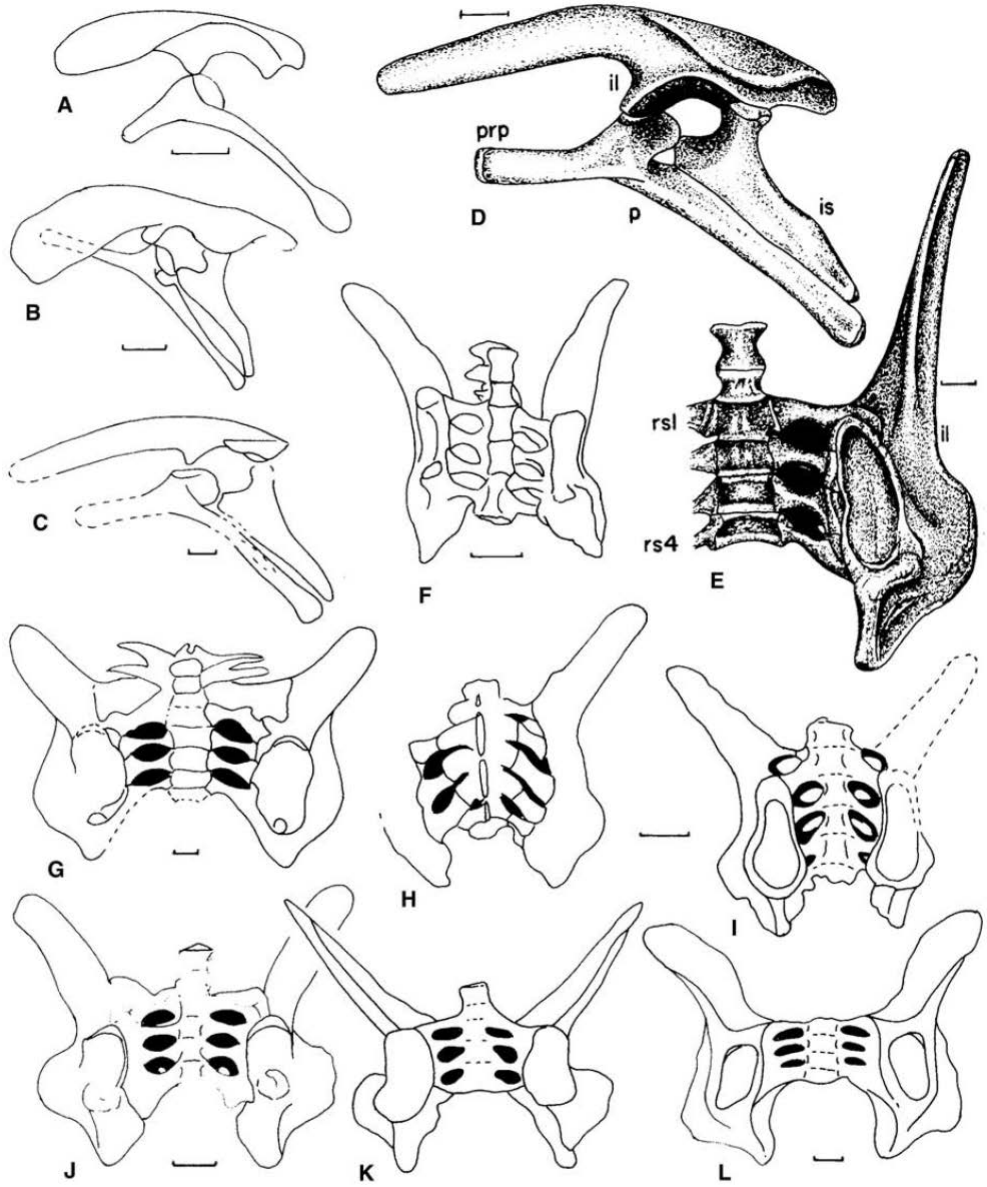

FIGURE 16.7. Left pelvic girdles (A–D) and sacra with ilia (E–L) in lateral (A–D), dorsal (H), and ventral views (E–G, I–L): A, F, *Huayangosaurus;* B, J, *Kentrosaurus;* C, *Lexovisaurus;* D, E, *Stegosaurus;* G, *Dacentrurus;* H, I, *Chungkingosaurus;* K, *Wuerhosaurus;* L, *Tuojiangosaurus*. Scale = 10 cm. (A, F after Zhou 1984; B, J after Hennig 1924; C after Galton 1985f; D, E after Gilmore 1914b; Ostrom and McIntosh 1966; G after Galton 1985f; H, I, L after Dong et al. 1983; K after Dong 1973.)

Los Stegosauria redujeron el tamaño de los filas de huesos dérmicos laterales y enfatizaron el tamaño de las más dorsales las cuales se transforman en placas verticalmente orientadas sobre el esqueleto axial. Hacia el extremo de la cola estas placas adquieren forma de estolón o púas defensivas.

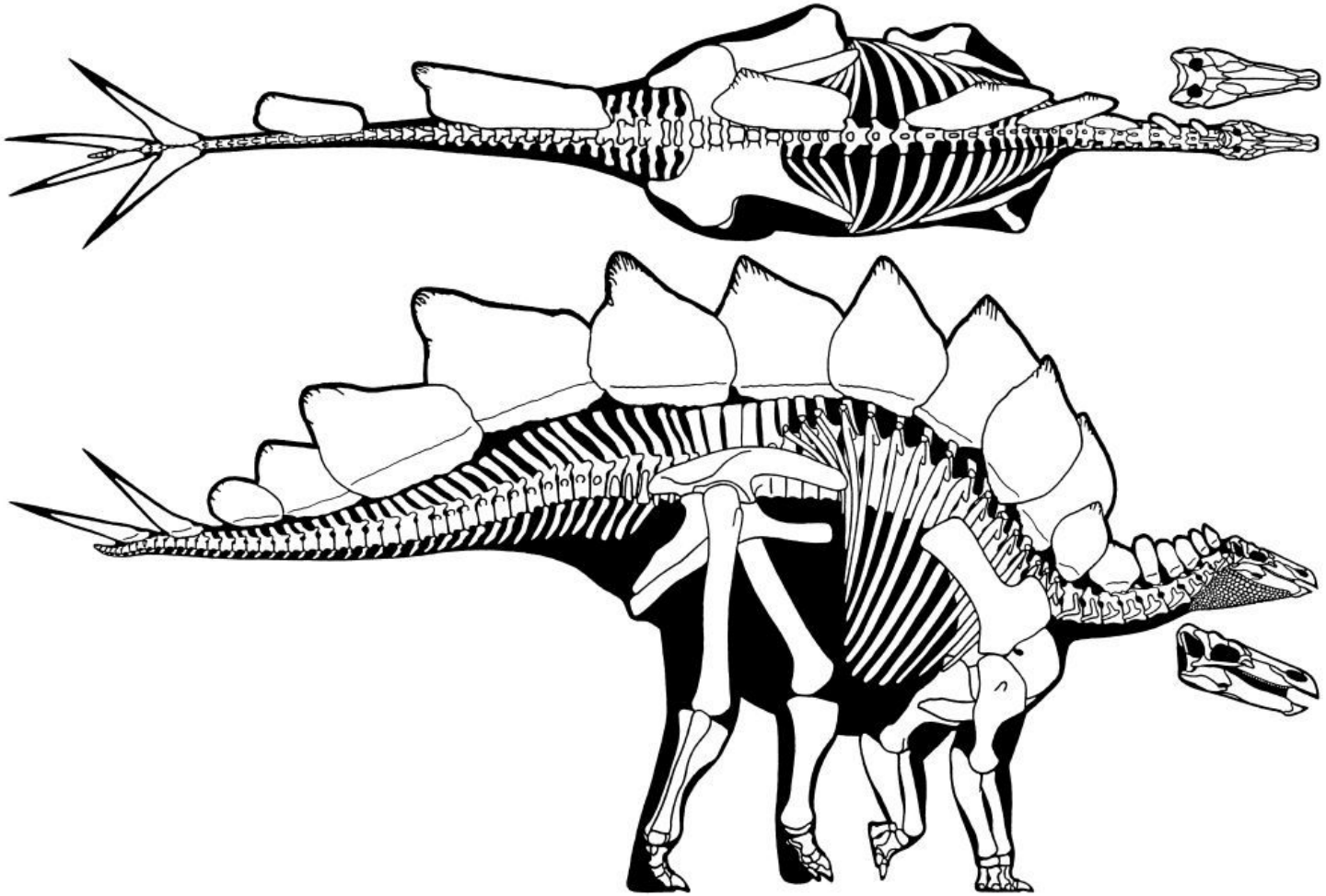

Filogenia de stegosaurios

FIG. 2. Strict consensus of six most parsimonious trees obtained when continuous data was excluded from the analysis.

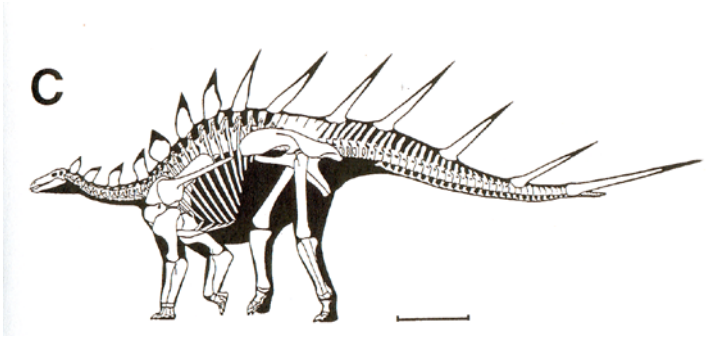

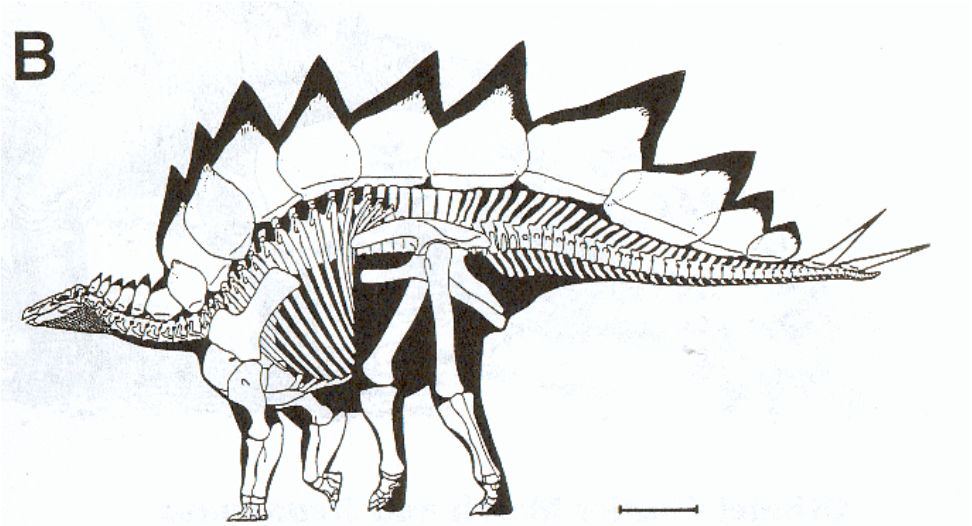

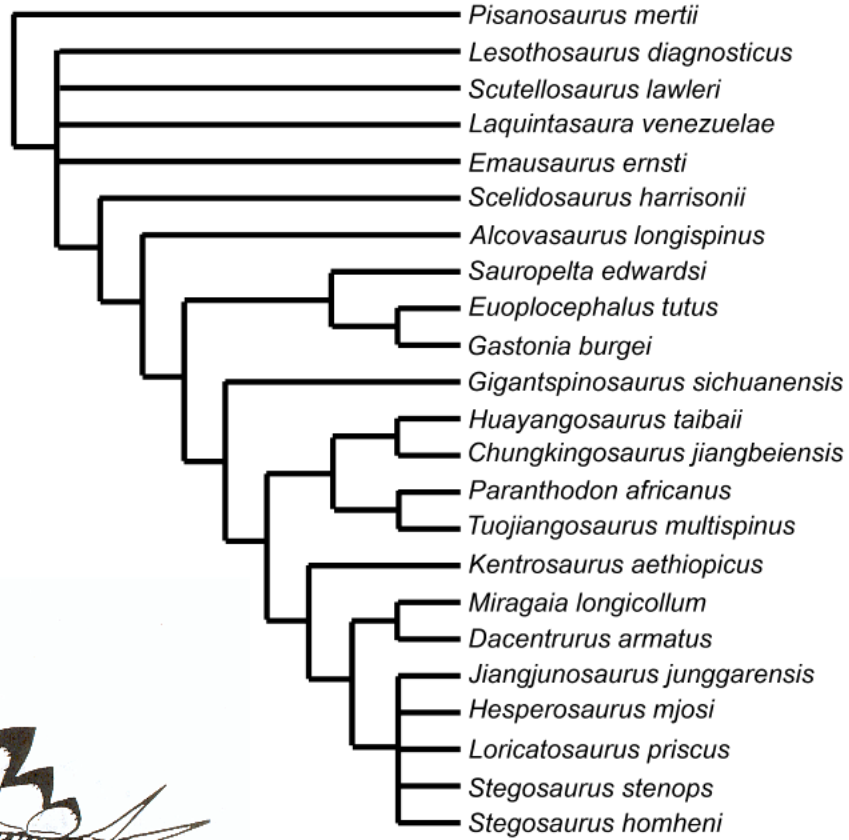

Raven & Maidment, 2017

Gigantspinosaurus sichuanensis

图 2　四川巨棘龙埋藏状态和两个“，”状的副肩棘

Fig. 2　Burial condition of *Gigantspinosaurus sichuanensis*, and two parascapular spines which are similar in outline to a ‘,’

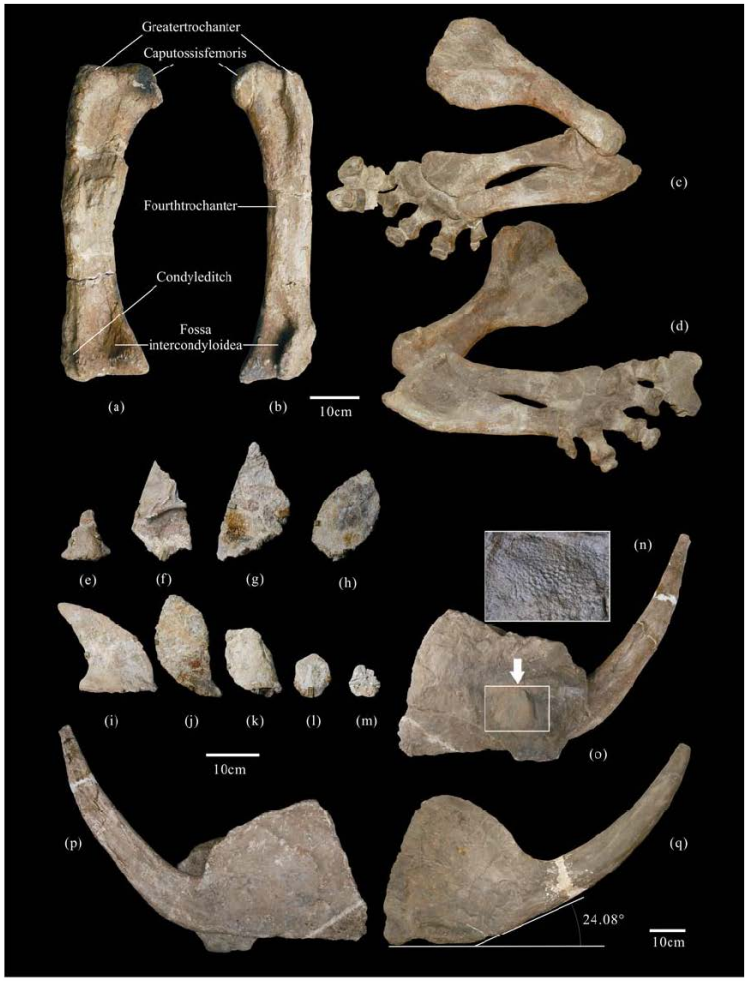

Fig. 5. Limb and Plate.
(a), left femur in posterior view; (b), right femur in posterior view; (c), left forelimb in dorsal view; (d), left forelimb in ventral view; (e),, left plate 1; (f), right plate 2; (g), left plate 3; (h), right plate 6; (i), right plate 9; (j), left plate 10; (k), right plate 13; (l), left plate 14; (m), right plate 15; (n), skin impression; (o), right parascapular spine in ventral view; (p), right parascapular spine in dorsal view; (q), left parascapular spine in dorsal view.

Huayangosauridae

Huayangosaurus es uno de los primeros Stegosauria, del Jurásico medio de China

Huayangosaurus taibaii

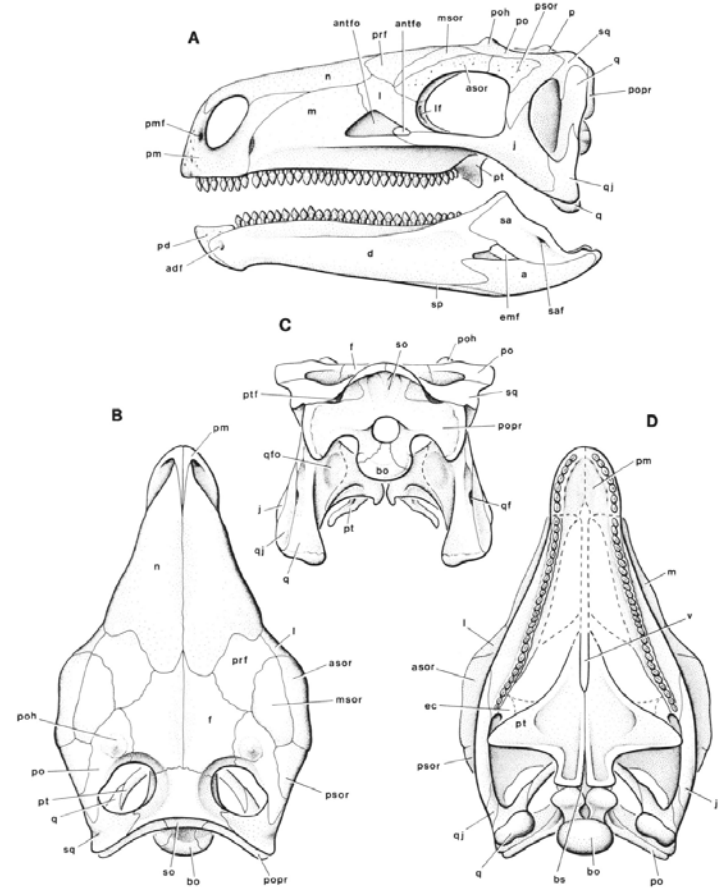

FIGURE 6. Reconstruction of the skull of *Huayangosaurus taibaii* in lateral (**A**), dorsal (**B**), posterior (**C**), and ventral (**D**) views. Abbreviations as in Figs. 1, 3, 5 plus: **adf**, anterior dentary foramen; **antfe**, antorbital fenestra; **antfo**, antorbital fossa; **bs**, basisphenoid; **lf**, lacrimal foramen; **pmf**, premaxillary foramen; **saf**, surangular foramen.

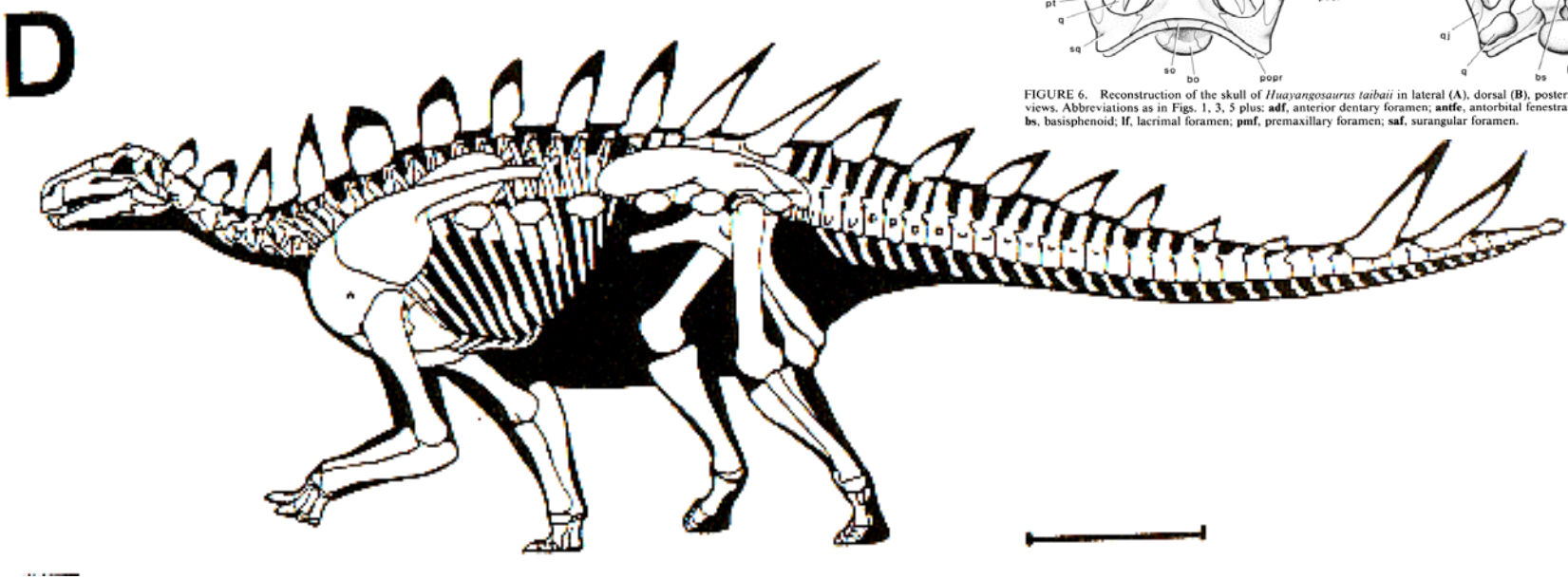

Stegosauridae

Los demás Stegosauria difieren de *Huayangosaurus* en el cráneo, el cual se torna bajo y angosto. También las extremidades posteriores se hacen mucho más largas que las anteriores

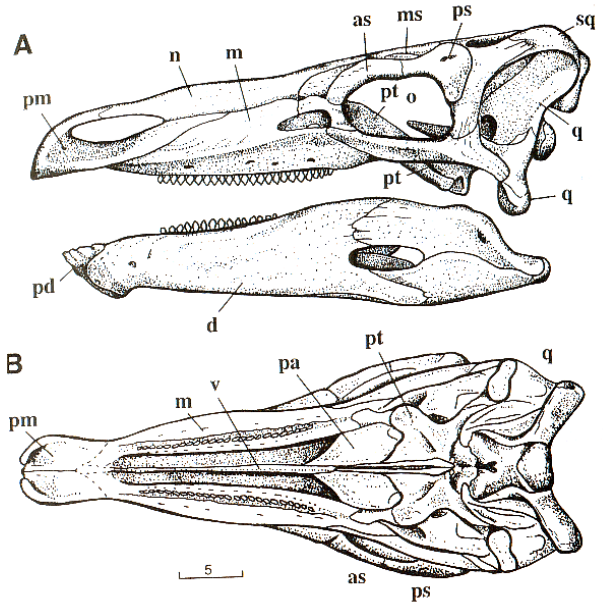

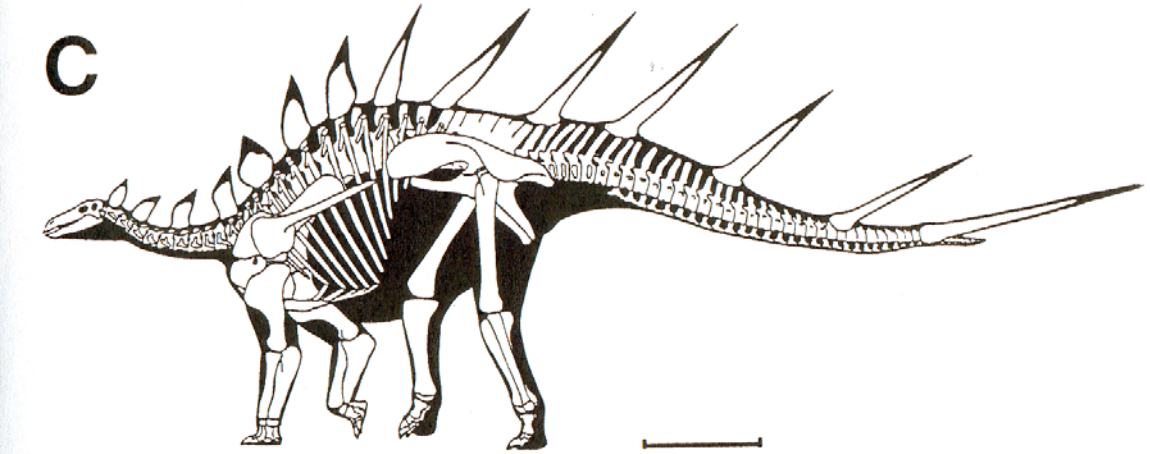

Kentrosaurus

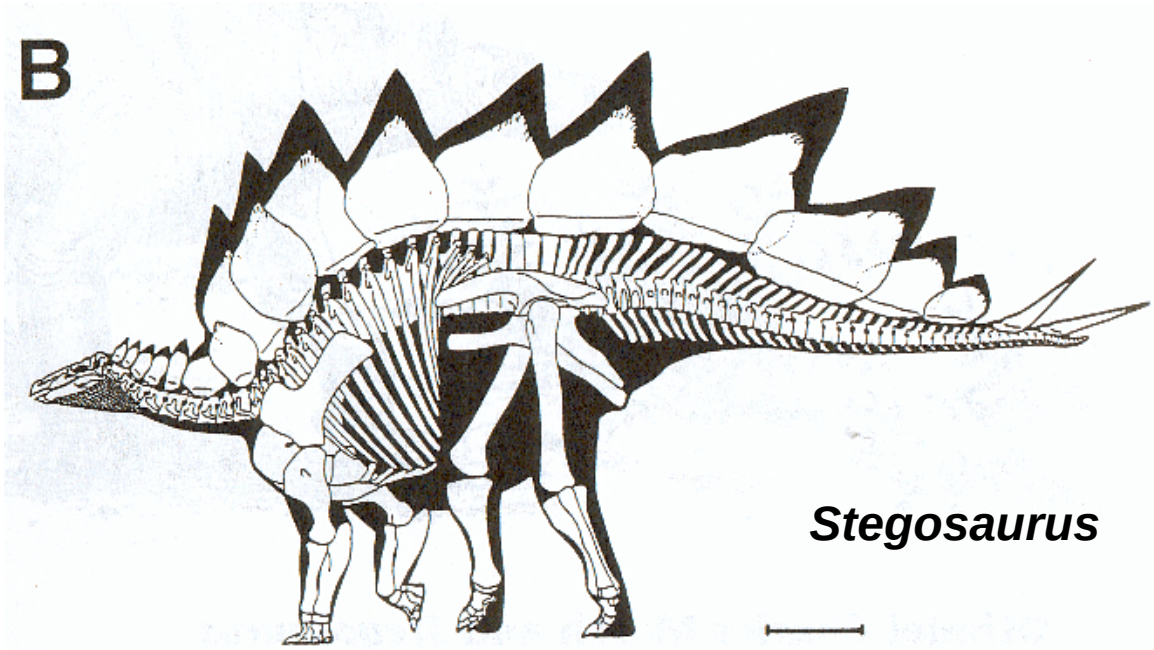

Stegosaurus

Miragaia longicollum

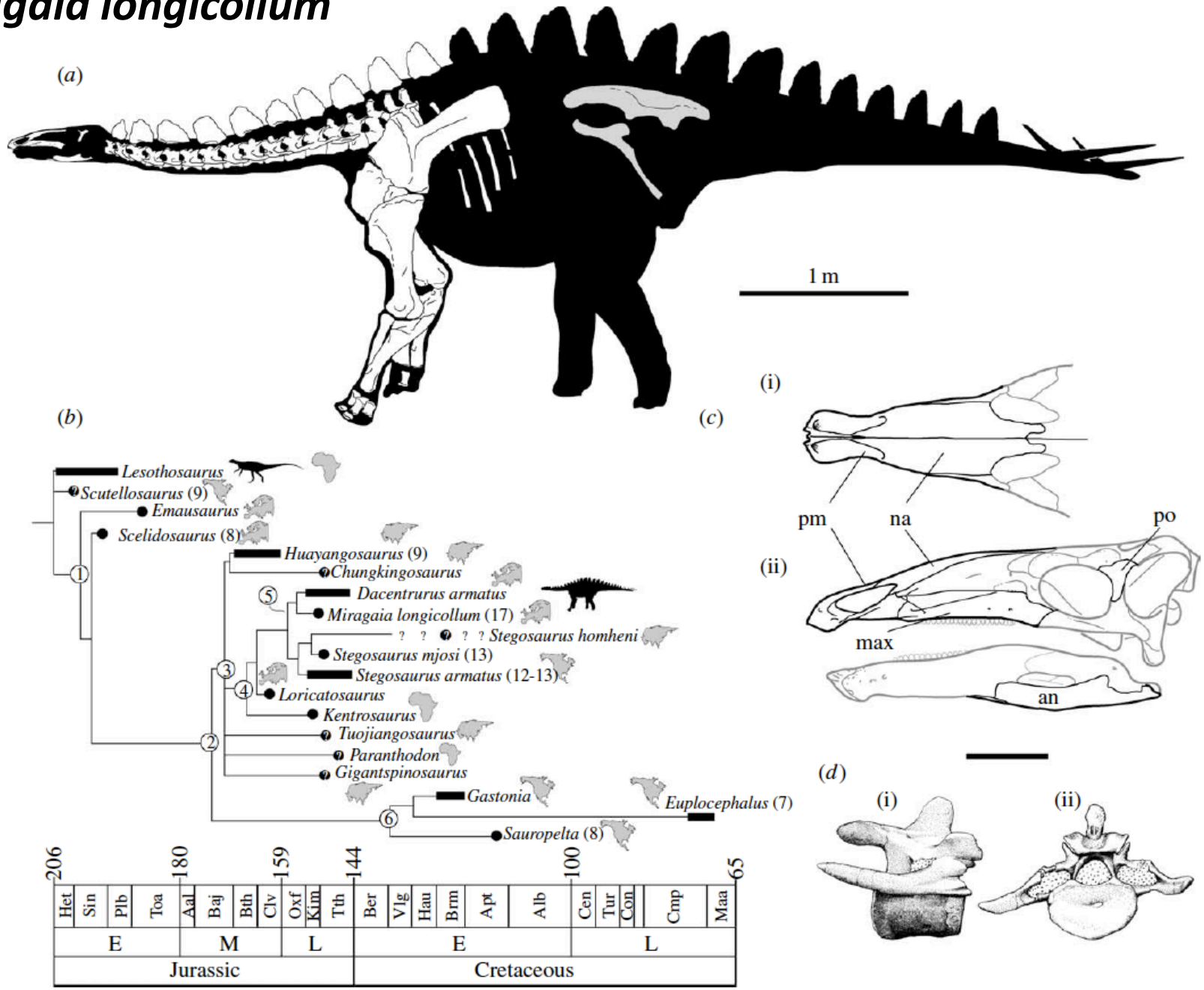

Ankylosauria

Definición: Todos los ornitisquios más cercanamente emparentados a *Ankylosaurus magniventris que a Stegosaurus stenops* (Galton, 1997).

Los Ankylosauria evolucionaron otra forma de armadura, rellenando los espacios entre las filas de huesos dérmicos con osículos más pequeños, creando una coraza sólida sobre el cuello y el tronco. Las aperturas del cráneo se cierran por los huesos que las rodean y osificaciones accesorias

Sinapomorfías:

Osteoderms fused to skull; Rings of osteoderms on neck and shoulder; Extensive osteoderms over body; Wide across body

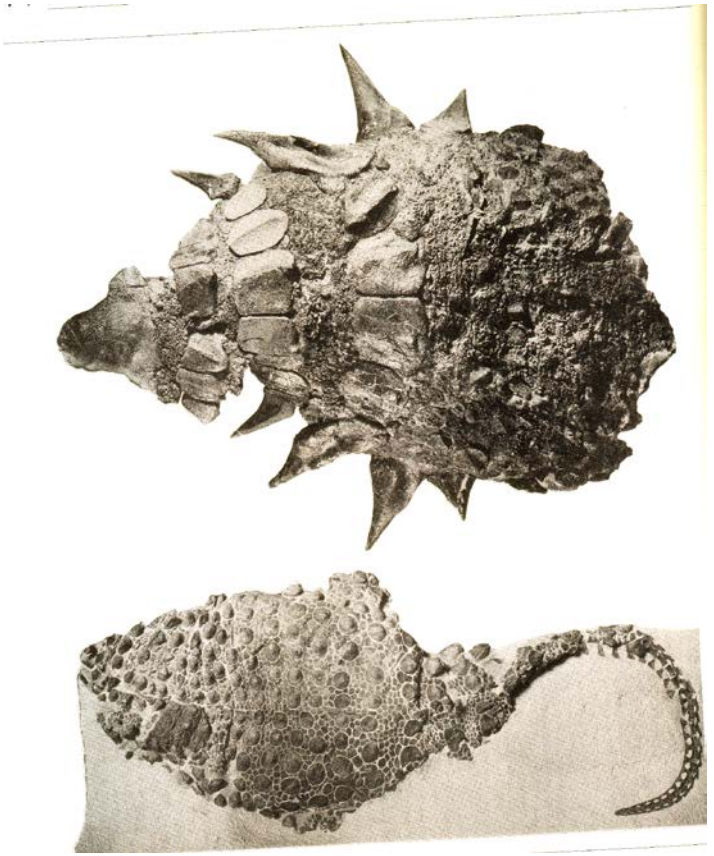

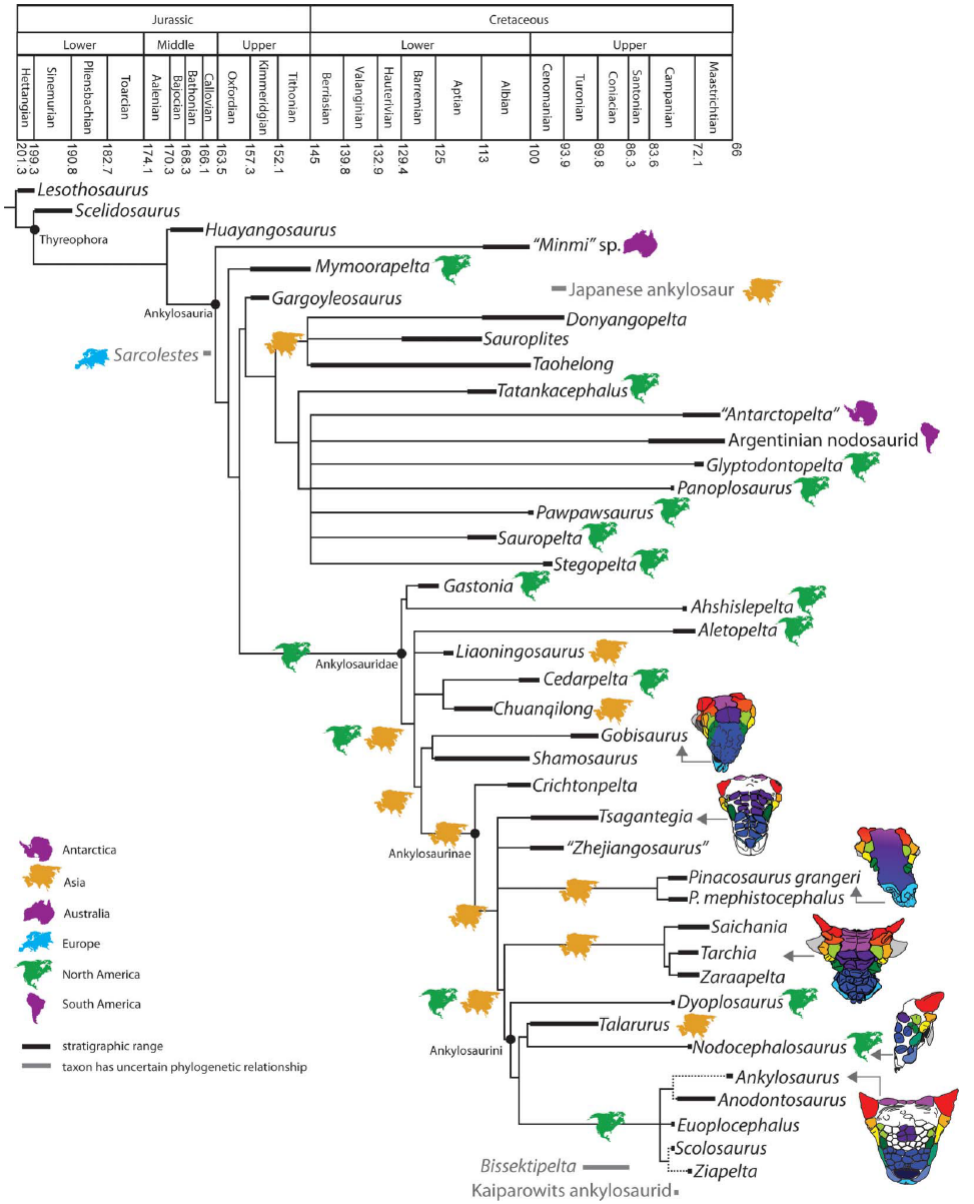

Figure 12. Time-calibrated phylogeny of the Ankylosauridae and selected nodosaurids and other thyreophorans, based on the 50% majority rule tree with biogeographical information from the Statistical Dispersal-Vicariance Analysis (S-DIVA analysis) using RASP (Reconstruct Ancestral State in Phylogenies); potential interrelationships between ankylosaurins, from the maximum agreement subtree, are represented by dashed lines.

Gargoyleasaurus parkpinorum: evolución de la pelvis ankylosauriana

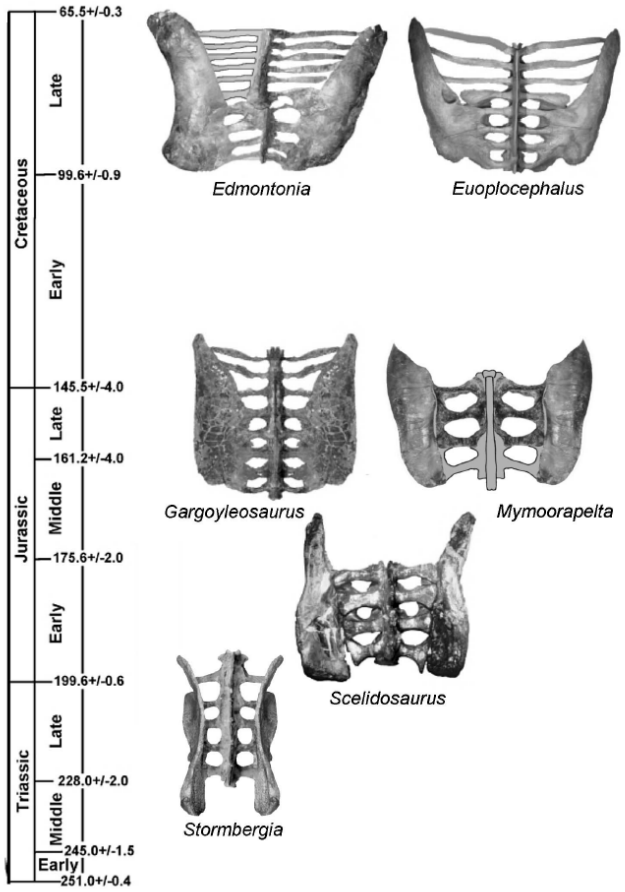

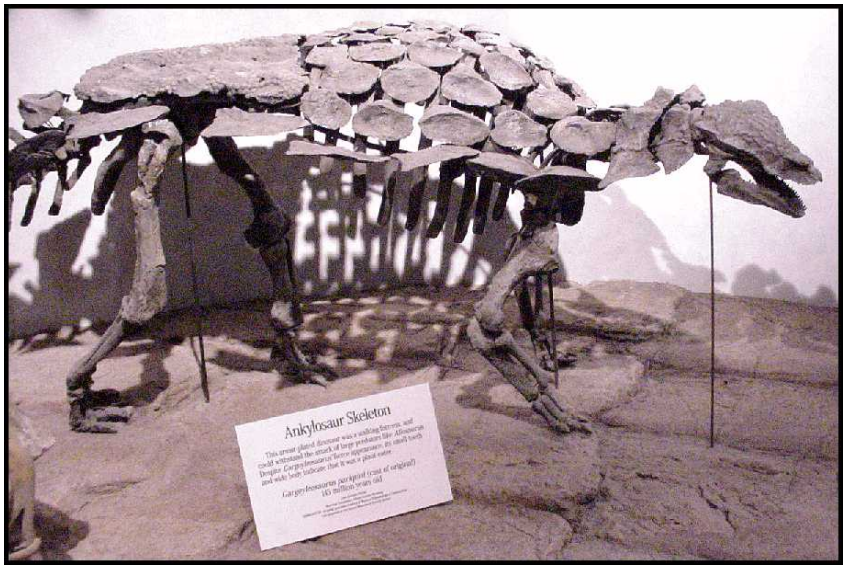

Figure 6. The origin and evolution of the ankylosaur pelvis can be approximated from this chronostratigraphic distribution of various pelves seen in dorsal view. In the basal ornithischian condition, represented by *Stormbergia* (reconstructed), the ilia are near vertical plates of bone. In the earliest ankylosauromorph, respresented by *Scelidosaurus,* the dorsal rim of the iliac blade and postacetabulum have rotated towards the lateral side so as to overhang the femur head, and an incipient synsacrum developed. In addition, the elongation of the sacral ribs is accompanied by the medial rotation of the preacetabular process. In the earliest ankylosaur, represented by *Gargoyleosaurus*, the ilium has assumed a nearly horizontal position and a synsacrum was developed including both caudals and posterior dorsals. In contrast, the preacetabulum of *Mymoorapelta* curved ventrally for reasons not clear; regardless, this specialization suggests that *Mymoorapelta* is not the close sister taxon to later ankylosaurs. Further evolution of the ankylosaur pelvis resulted in divergence of the ilia, seen in nodosaurids, represented by *Edmontonia*, but especially in ankylosaurids, represented by *Euoplocephalus*. In addition, there was further elongation of the sacral ribs. Not to scale. See also Fig. 10.
doi:10.1371/journal.pone.0079887.g006

Nodosauridae

Los Ankylosauria de dividen en Nodosauridae y Ankylosauridae. Los Nodosauridae presentan cráneos bajos y angostos que sostenían con el hocico apuntando ligeramente hacia abajo

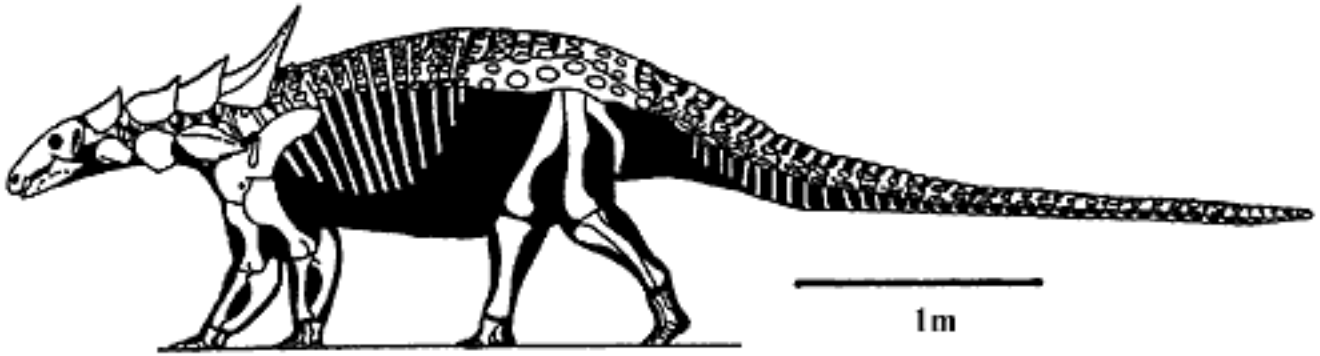

Sauropelta

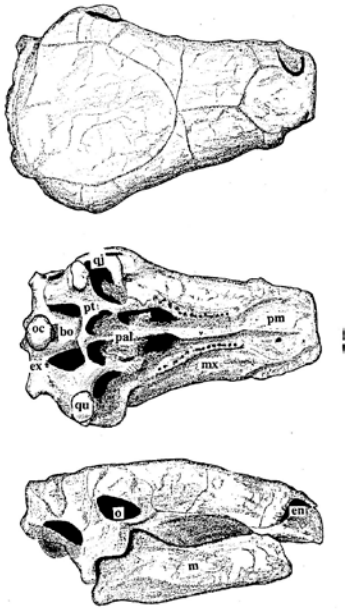

Filogenia de Nodosauridae

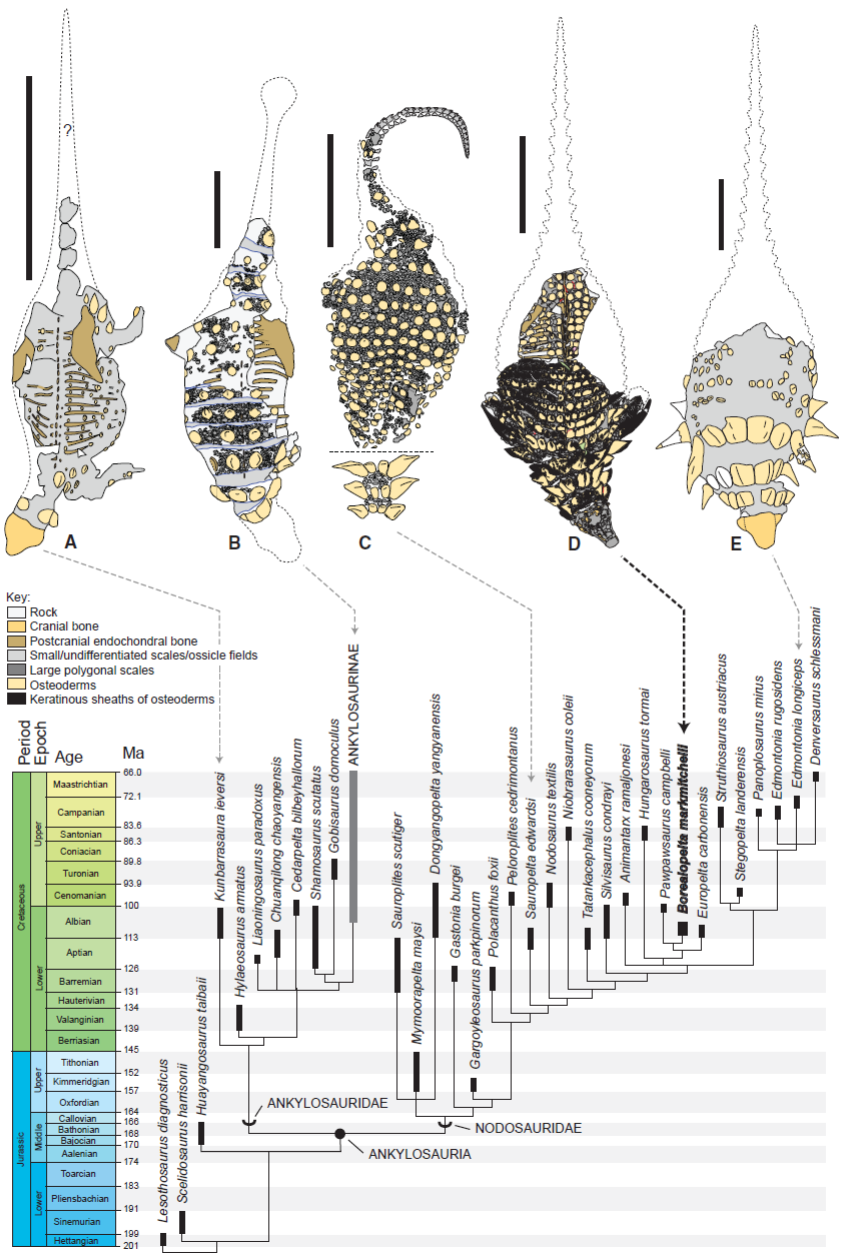

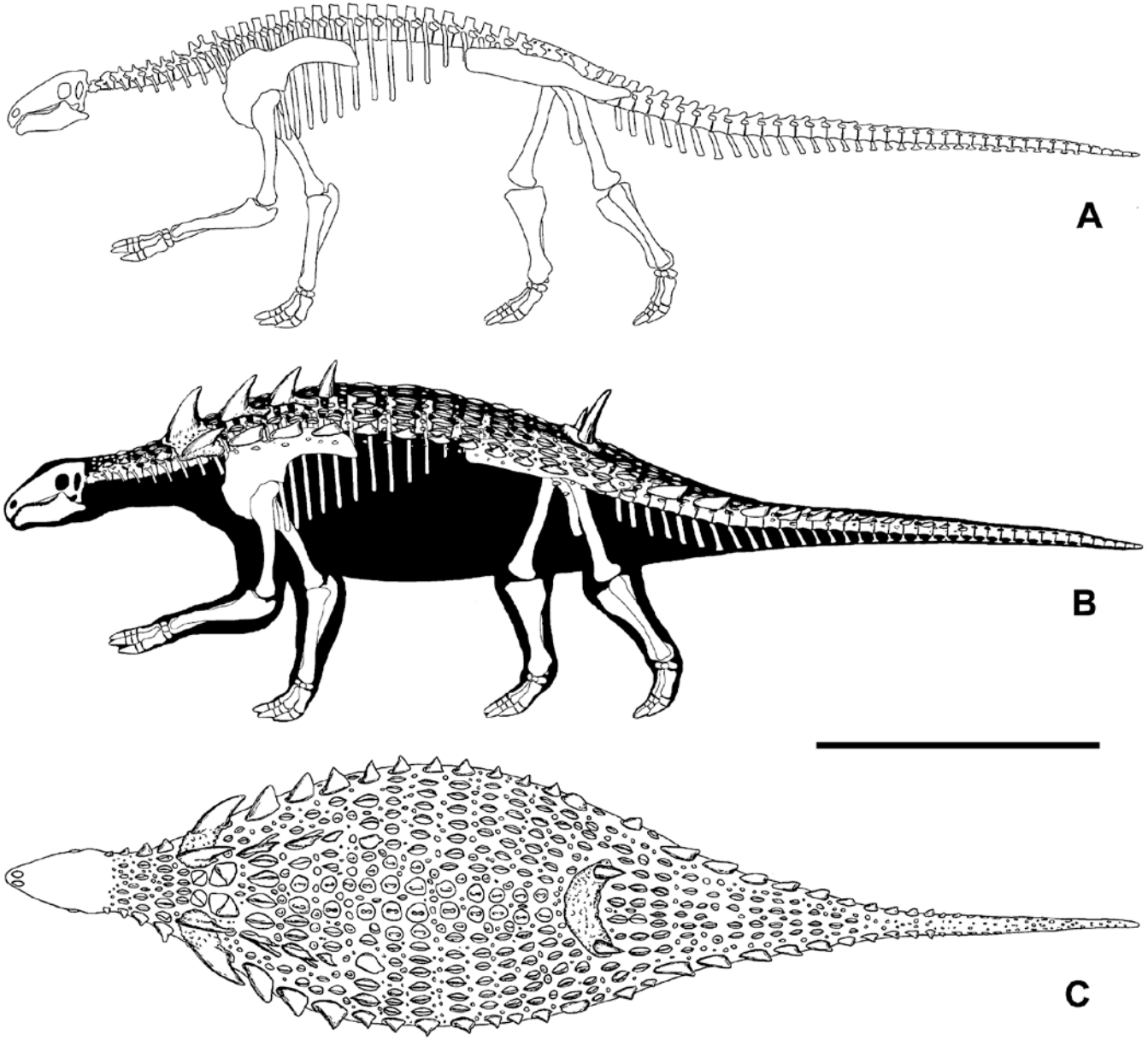

Fig. 11 Skeletal and dermal armor reconstruction of *Hungarosaurus tormai*. **a** Skeletal reconstruction in left lateral view, **b** skeletal reconstruction with dermal armor in left lateral view, **c** dermal armor reconstruction in dorsal view. *Scale bar* equals 1 m

~~Ankylosauridae~~ basal:

Gastonia subfamilia Polacanthinae

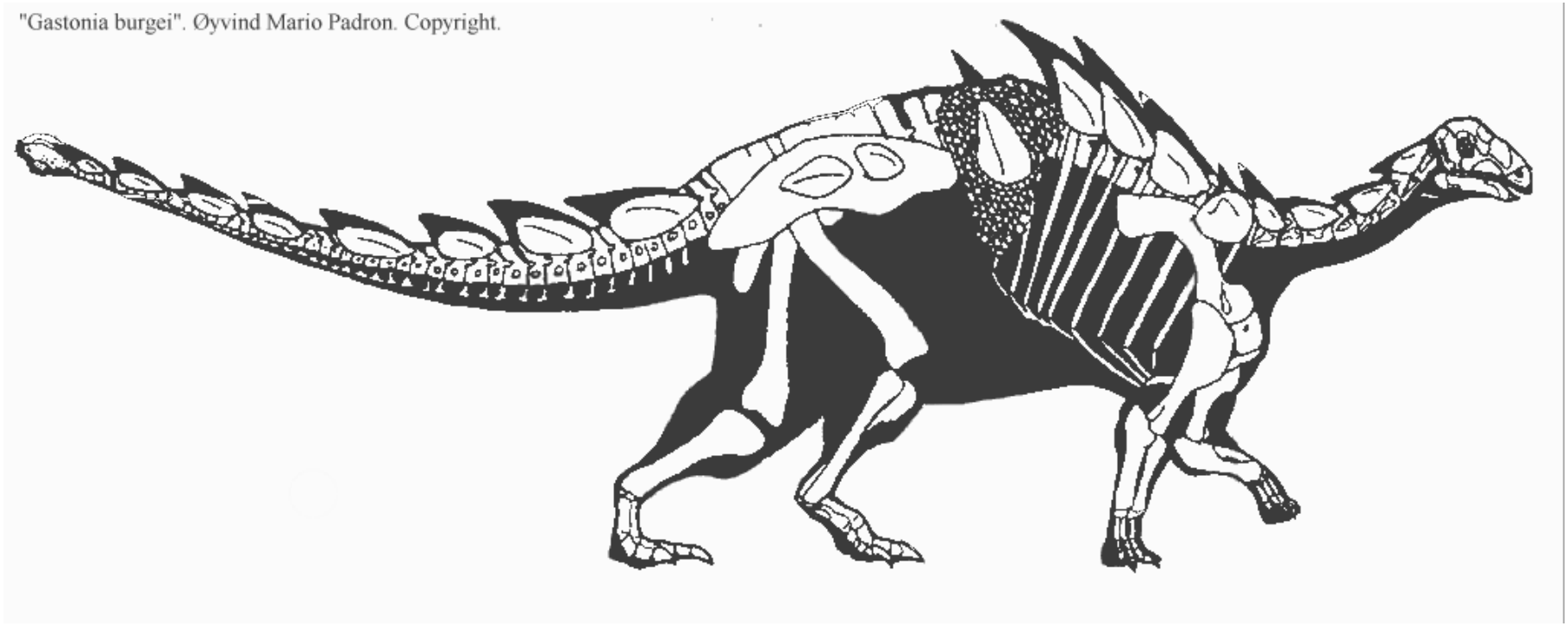


A
1 m

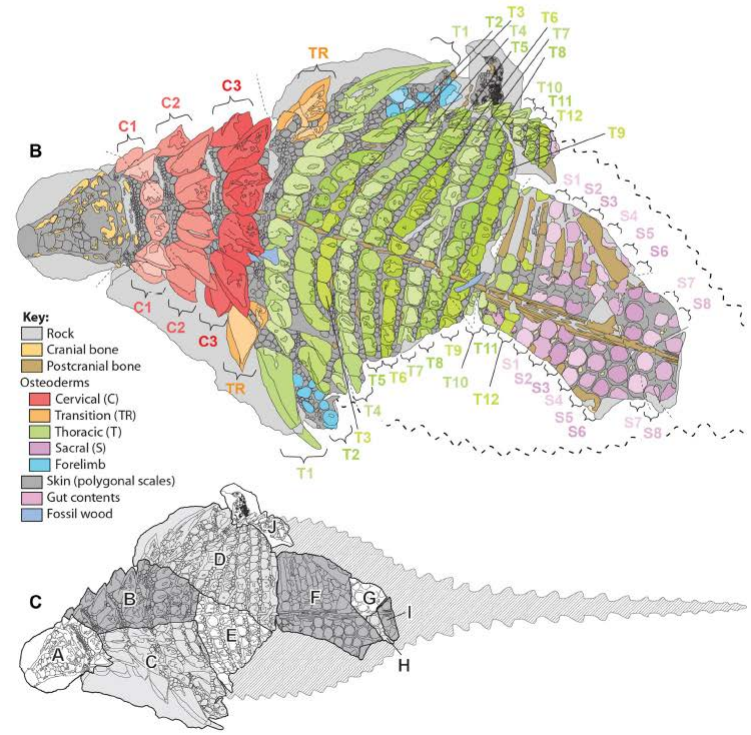
B
C1
C2
C3
TR
T1
T2
T3
T4
T5
T6
T7
T8
T9
T10
T11
T12
S1
S2
S3
S4
S5
S6
S7
S8
Key:
Rock
Cranial bone
Postcranial bone
Osteoderms
Cervical (C)
Transition (TR)
Thoracic (T)
Sacral (S)
Forelimb
Skin (polygonal scales)
Gut contents
Fossil wood
C
A
B
C
D
E
F
G
H
I
J

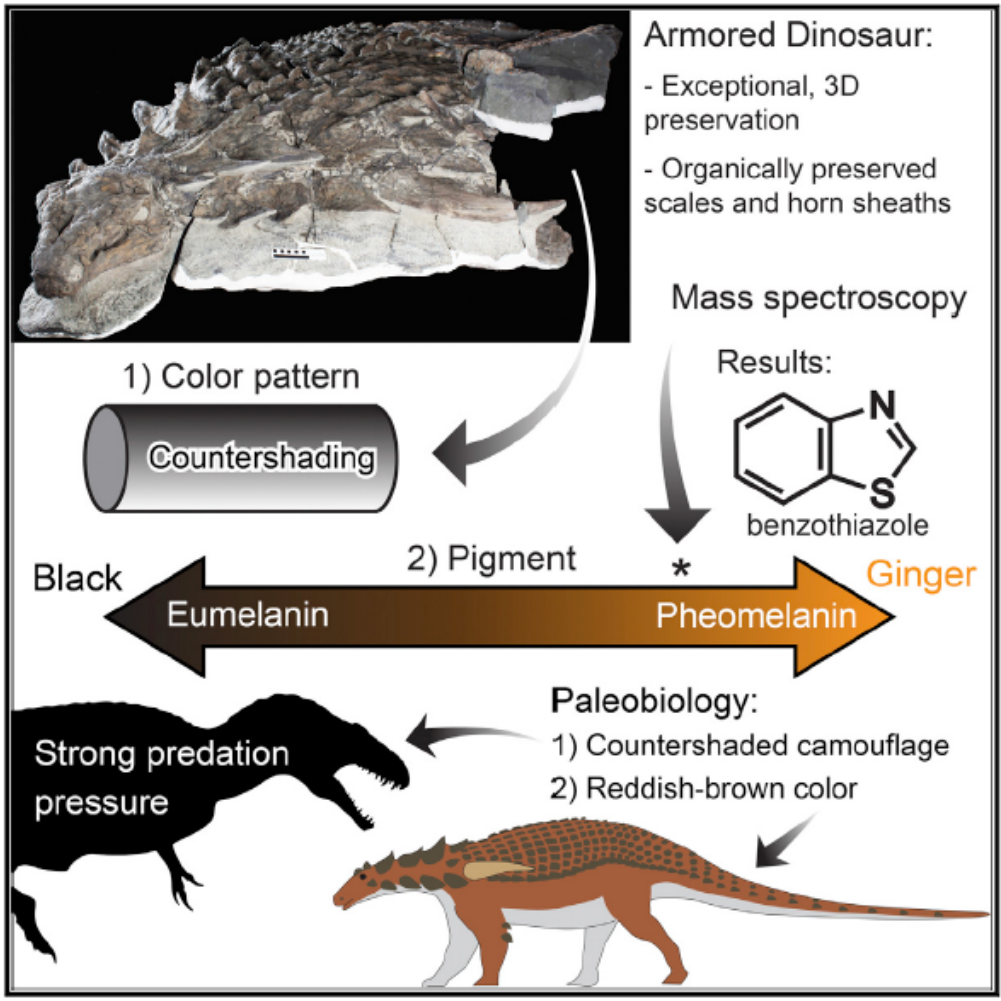
Armored Dinosaur:
- Exceptional, 3D preservation
- Organically preserved scales and horn sheaths
Mass spectroscopy
Results:
N
S
benzothiazole
1) Color pattern
Countershading
2) Pigment
*
Black
Ginger
Eumelanin
Pheomelanin
Paleobiology:
1) Countershaded camouflage
2) Reddish-brown color
Strong predation pressure

Ankylosauridae

Definición: Todos los ankylosaurios más cercanos a *Ankylosaurus* que a *Nodosaurus*.

Cráneos más anchos con osteodermos triangulares fusionados a las esquinas posteriores del cráneo. También presentan una cola terminada en un garrote formado por dos pares de osteodermos en forma de cuña.

Minotaurasaurus

Saichania

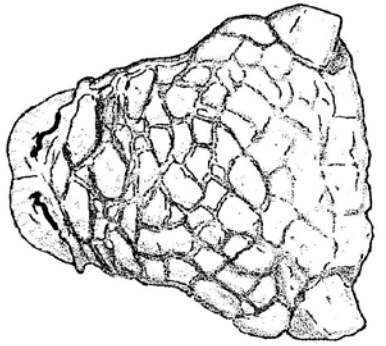

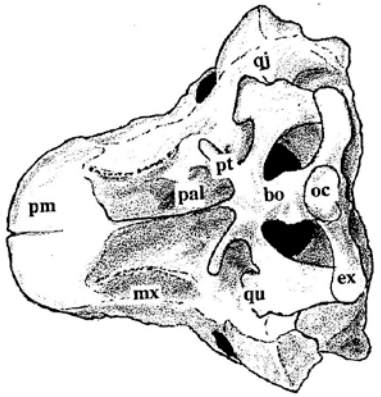

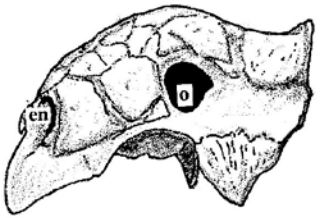

Sinapomorfías:

- arched antorbital region (Character 6); reversed to flat in *Talarurus*, and the clade of Mongolian ankylosaurines; also present in *Panoplosaurus.*
- maxilla bordering the anterior margin of the internal nares (Character 14); except in *Pinacosaurus grangeri*, where the premaxilla borders the internal nares
- respiratory passage with anterior and posterior loops
- rugose cranial ornamentation (Character 20); present only in basal members of the clade
- prezygapophyses and neural spines overlap more than half the length of the adjacent vertebra
- coracoid longer than wide (Character 114), ACCTRAN; reversed from the basal condition in ankylosaurs
- distal width of tibia greater than proximal width
- coracoid with straight anterior margin
- fused sternal plates
- crenulated osteoderm margins
- no gular osteoderms
- cervical half rings with an underlying bony band

Tail club; Short triangular head; Triangular hornlets on skull; Complex nasal chambers

Ankylosauridae y evolución del “Tail-Club”

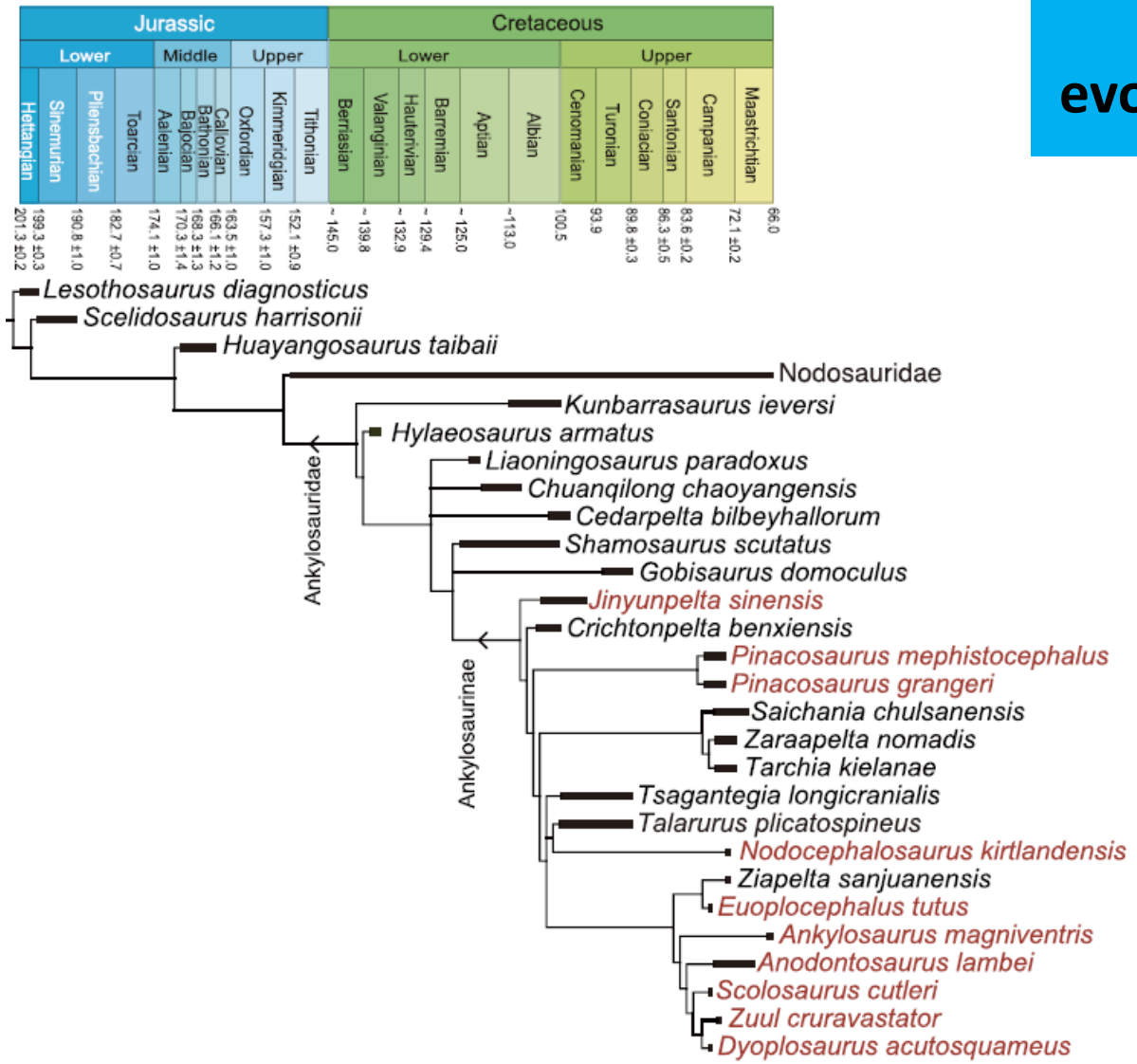

Figure 10. Temporal calibration of the simplified derivative strict reduced consensus tree produced by phylogenetic analysis. Taxa in red text have a tail club knob. The geologic numerical ages and coloring follow International Chronostratigraphic Chart 2017/02.

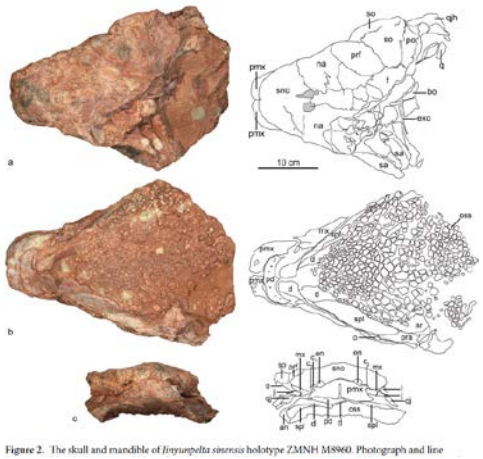

Figure 2. The skull and mandible of *Jinyunpelta sinensis* holotype ZMNH M8960. Photograph and line

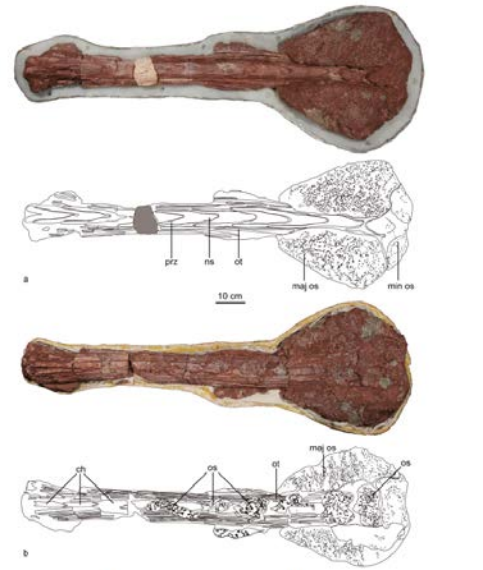

Figure 6. The tail club *Jinyunpelta sinensis* paratype ZMNH M8963 in dorsal (a) and ventral (b) views. Abbreviations: ch, chevron; maj os, major osteoderm of the tail club knob; min os, minor osteoderm of the tail club knob; ns, neural spine; os, osteoderm; ot, ossified tendon; prz, prezygapophyses.

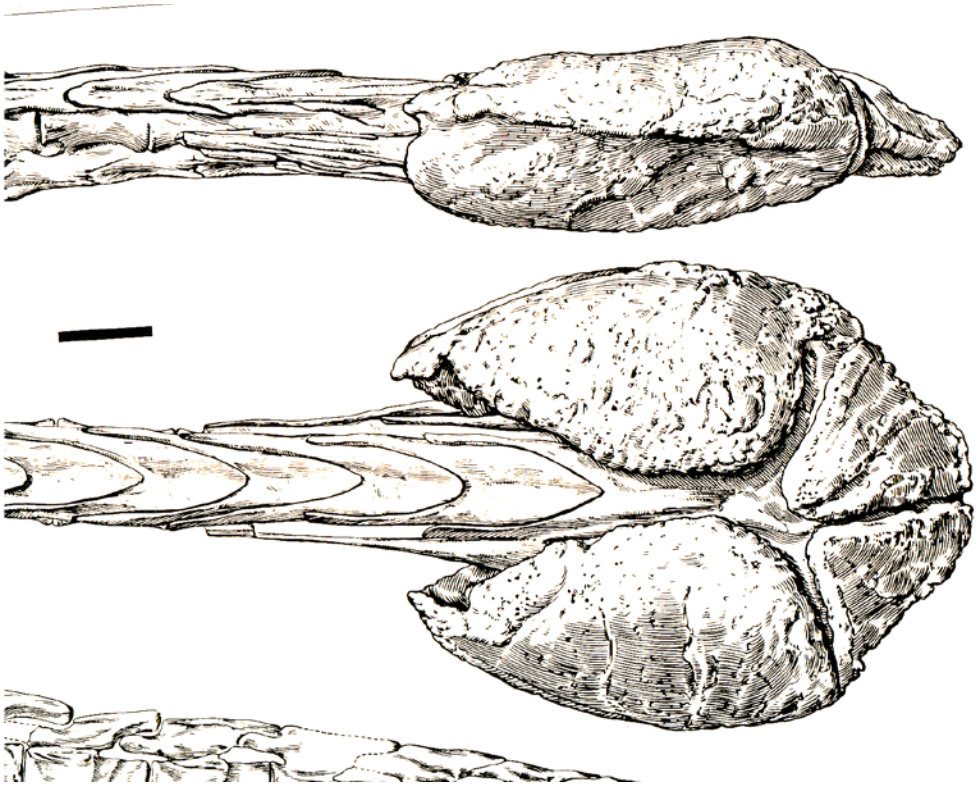

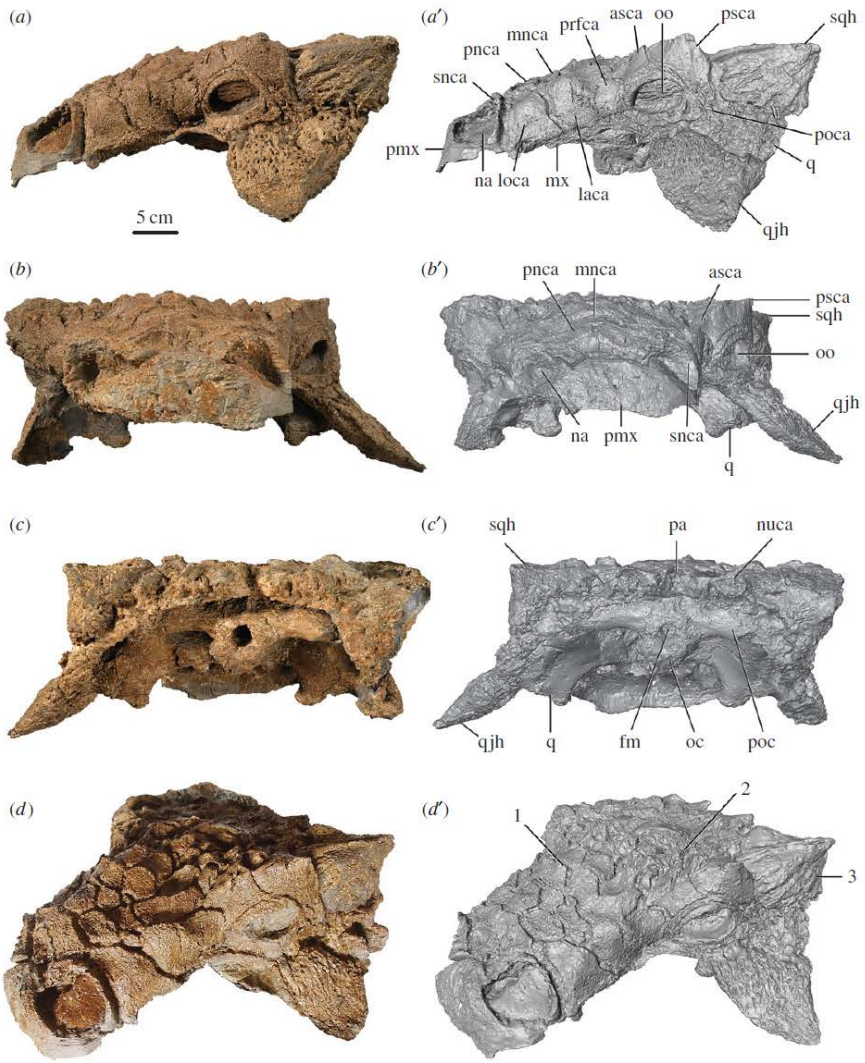

Figure 2. Holotype of *Zuul crurivastator*, ROM 75860, skull in (*a*) left lateral, (*b*) anterior, (*c*) posterior and (*d*) oblique left anterodorsal views. (*a*′–*d*′) are digital models of the skull. Diagnostic characters for *Z. crurivastator* include (1) imbricated frontonasal caputegulae, (2) peaked, pyramidal prefrontal and middle supraorbital caputegulae and (3) prominent apicobasal furrows on the squamosal horns. Abbreviations are as follows: asca, anterior supraorbital caputegulum; fm, foramen magnum; laca, lacrimal caputegulum; loca, loreal caputegulum; mnca, median nasal caputegulum; mx, maxilla; na, external naris; nuca, nuchal caputegulum; oo, ocular osteoderm; oc, occipital condyle; pa, parietal; pmx, premaxilla; pnca, postnarial caputegulum; poc, paroccipital process; poca, postocular caputegulum; prfca, prefrontal caputegulum; psca, posterior supraorbital caputegulum; q, quadrate; qjh, quadratojugal horn; snca, supranarial caputegulum; sqh, squamosal horn.

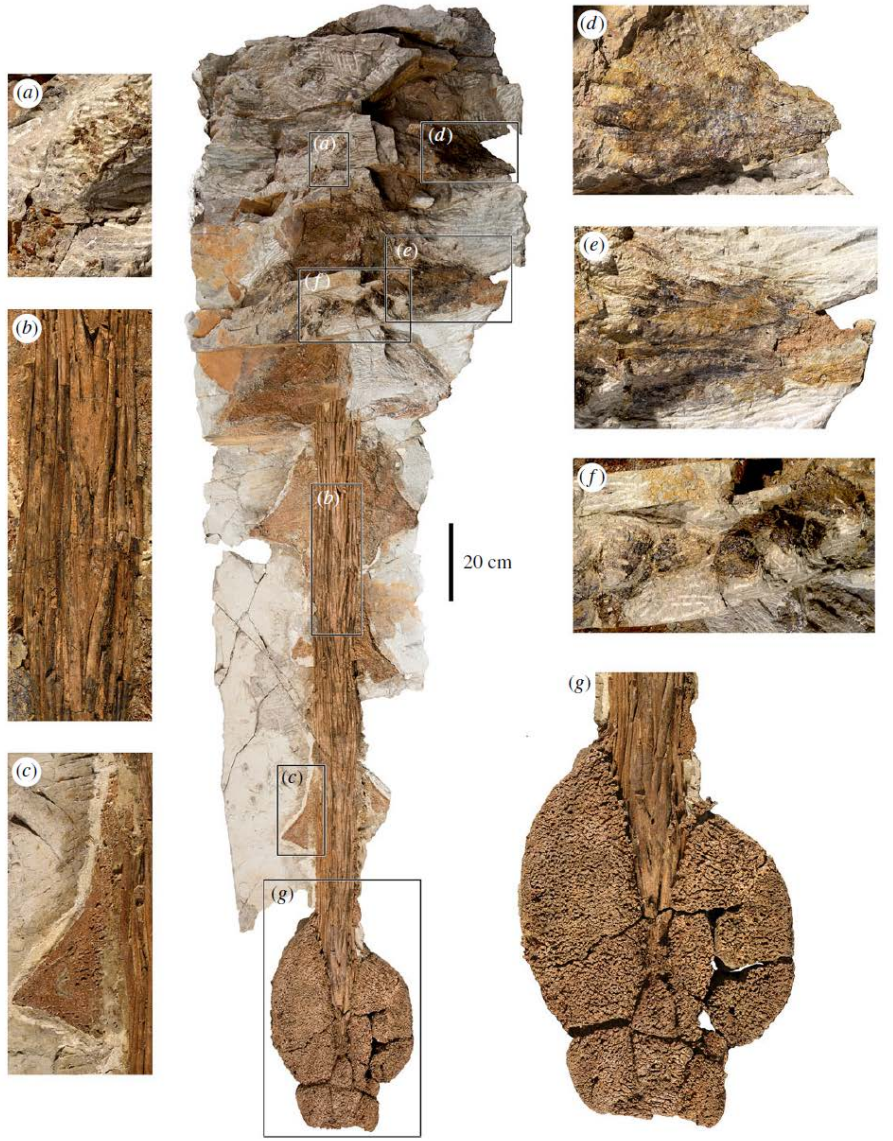

Figure 6. Overview of the tail of *Zuul crurivastator* ROM 75860 in dorsal view, with insets of detailed anatomy. (*a*) Field of ossicles in the anterior portion of the tail. (*b*) Detail of the neural arches of the handle caudal vertebrae, and ossified tendons. (*c*) Left caudal osteoderm from the seventh pair. (*d*) Preserved epidermal sheath on the right caudal osteoderm from the second pair. (*e*) Preserved epidermal sheath on the right caudal osteoderm from the third pair. (*f*) Epidermal scales lacking bony cores, arranged in a transverse row at the third pair of caudal osteoderms. (*g*) Close-up of the tail club knob.

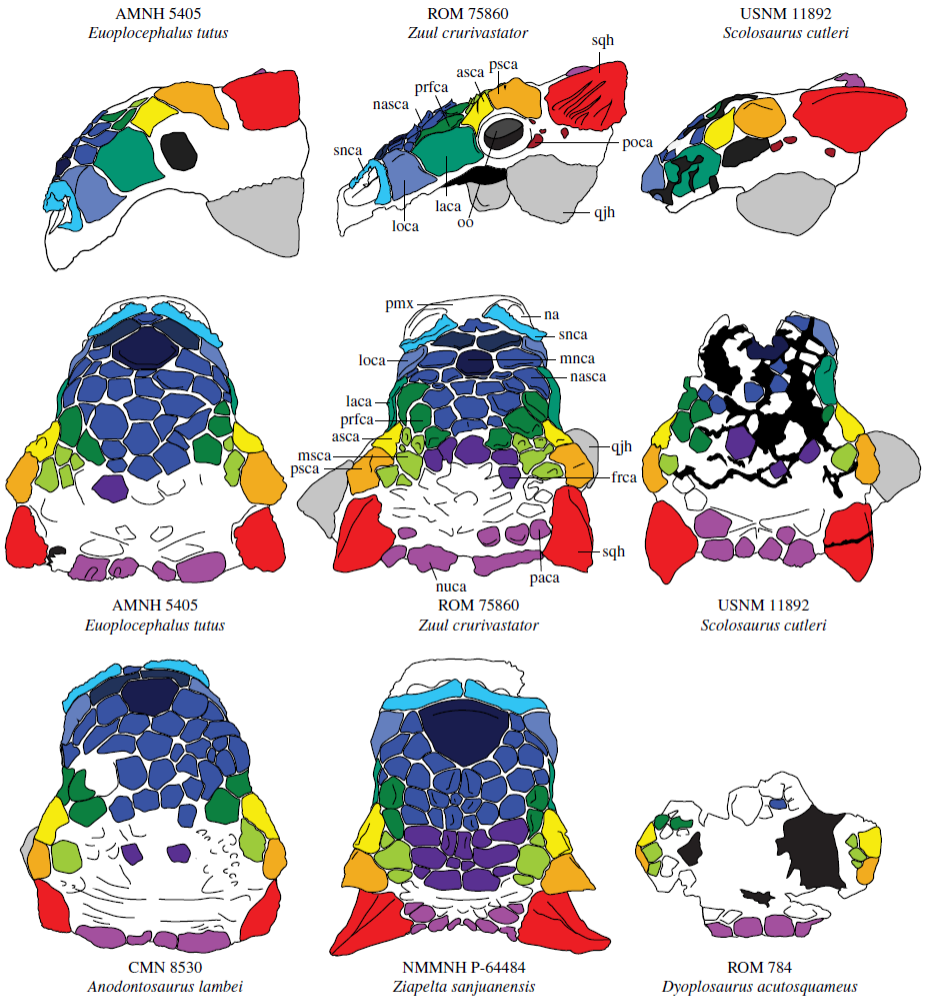

Figure 5. Cranial ornamentation of ankylosaurins compared, in dorsal and lateral views. Abbreviations are as follows: asca, anterior supraorbital caputegulum; frca, frontal caputegulum; laca, lacrimal caputegulum; loca, loreal caputegulum; mnca, median nasal caputegulum; msca, middle supraorbital caputegulum; na, external naris; nasca, nasal caputegulae; nuca, nuchal caputegulum; oo, ocular osteoderm; paca, parietal caputegulum; pmx, premaxilla; pnca, postnarial caputegulum; poca, postocular caputegulum; prfca, prefrontal caputegulum; psca, posterior supraorbital caputegulum; qjh, quadratojugal horn; snca, supranarial caputegulum; sqh, squamosal horn. Skulls are scaled to the same anteroposterior length.

Liaoningosaurus paradoxus

Fig.1 The holotype of *Liaoningosaurus paradoxus* (Xu et al., 2001)

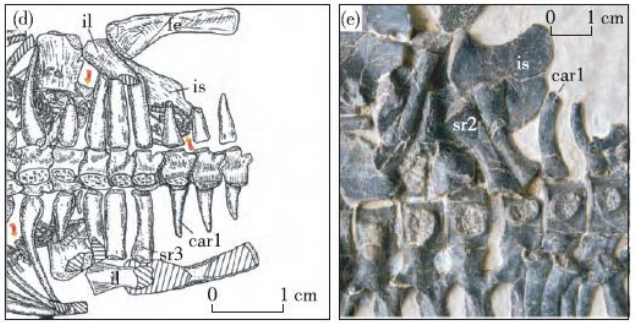

Fig. 4 Partial skeleton of the holotype of *Liaoningosaurus paradoxus* (IVPP V12560) in (a) to (c) and the sacral region of two Triassic marine reptiles in (d) and (e)

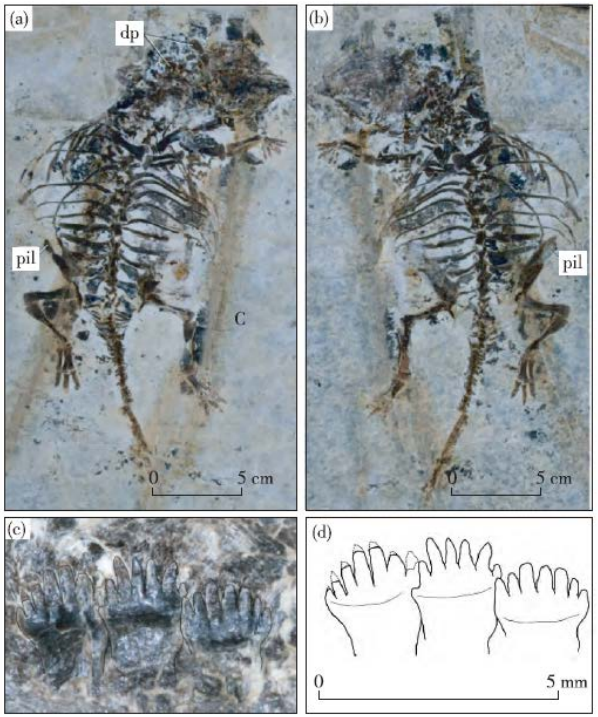

Fig.2 New specimen of *Liaoningosaurus paradoxus* (xhpm-1206)

(a) the positive dorsal view; (b) the negative counterparts of the skeleton; (c) three maxillary teeth in lateral view, showing fork-like crown; (d) the outline of (c)

dp-dorsal bony plate around the shoulder girdle; pil-preacetabular process of the ilium

Fig.5 Reconstruction of *L. paradoxus*

Neornithischia

Definición: Todos los genasaurios más cercanos a *Parasaurolophus walkeri que a Ankylosaurus magniventris* o *Stegosaurus stenops.*

Sinapomorfias:

1. Proceso obturador del ísquion en forma de legüeta.
2. Articulación entre costilla sacral y pedúnculo isquiádico.
3. Esmalte asimétrico? (en Cerapoda y quizá formas basales).

Hasta recientemente, Neornithischia se consideraba equivalente a **CERAPODA**, un grupo definido por nodo, como todos los descendientes del ancestro común más reciente compartido por *Parasaurolophus* (**ORNITHOPODA**) y *Triceratops* (**MARGINOCEPHALIA**). Algunos taxa que se consideraban como miembros de Ornithopoda (ej. *Othnielia*) ahora se considera que van por fuera de Cerapoda, es decir, son neornitiquios basales

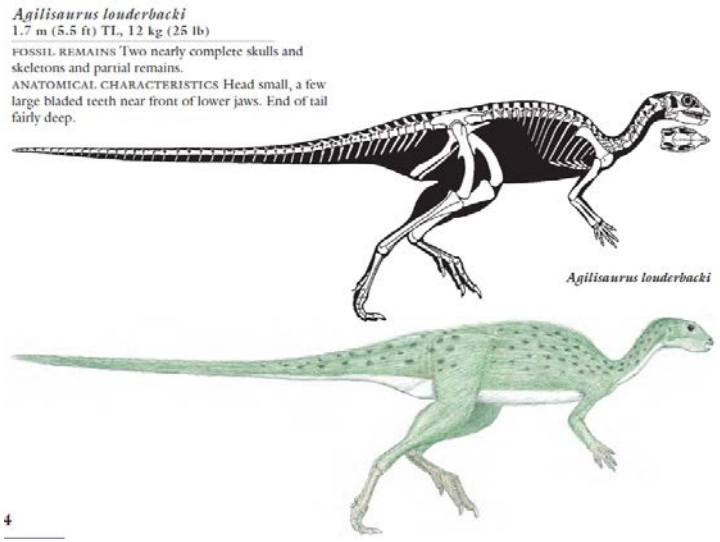

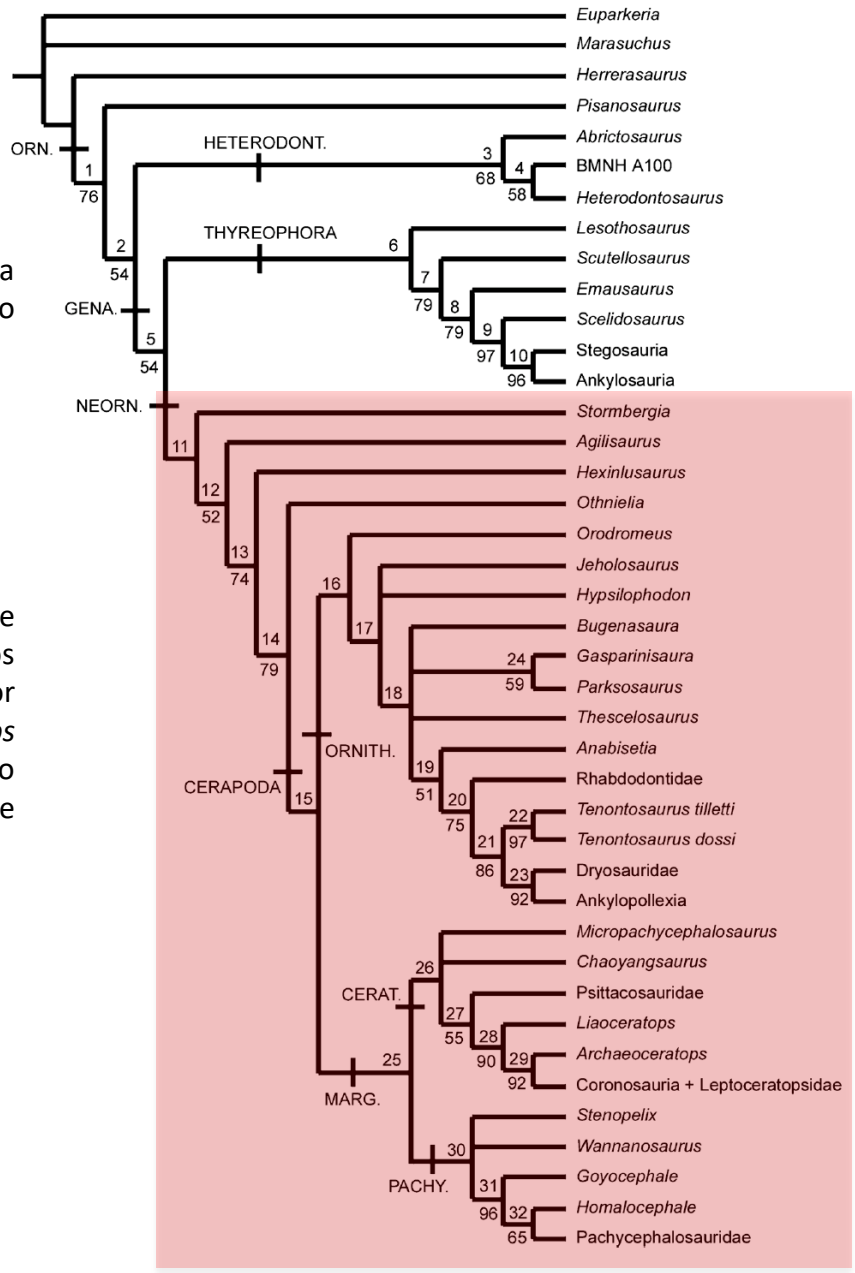

Concepto de Ornithopoda e “Hypsilophodontidae”:

Hasta hace poco se utilizaba de manera amplia para ornitisquios bípedos/facultativamente bípedos. Ahora se ha aclarado que algunos ornitisquios previamente considerados ornithopodos (especialmente aquellos clasificados dentro de un grupo “hypsilophodontidae” de ornitópodos pequeños) caen por fuera de Cerapoda, y son por lo tanto neornitisquios basales. Esto indica que los Cerapoda descienden de una organización que previamente se reconocía como “hypsilophodontida” (pequeños herbívoros bípedos)

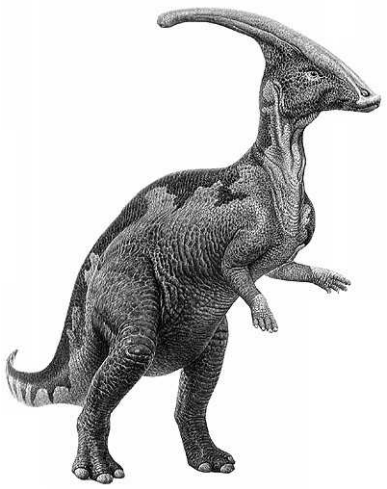

Ornithopoda

“Hypsilophodontidae”

Marginocephalia

Sinapomorfías

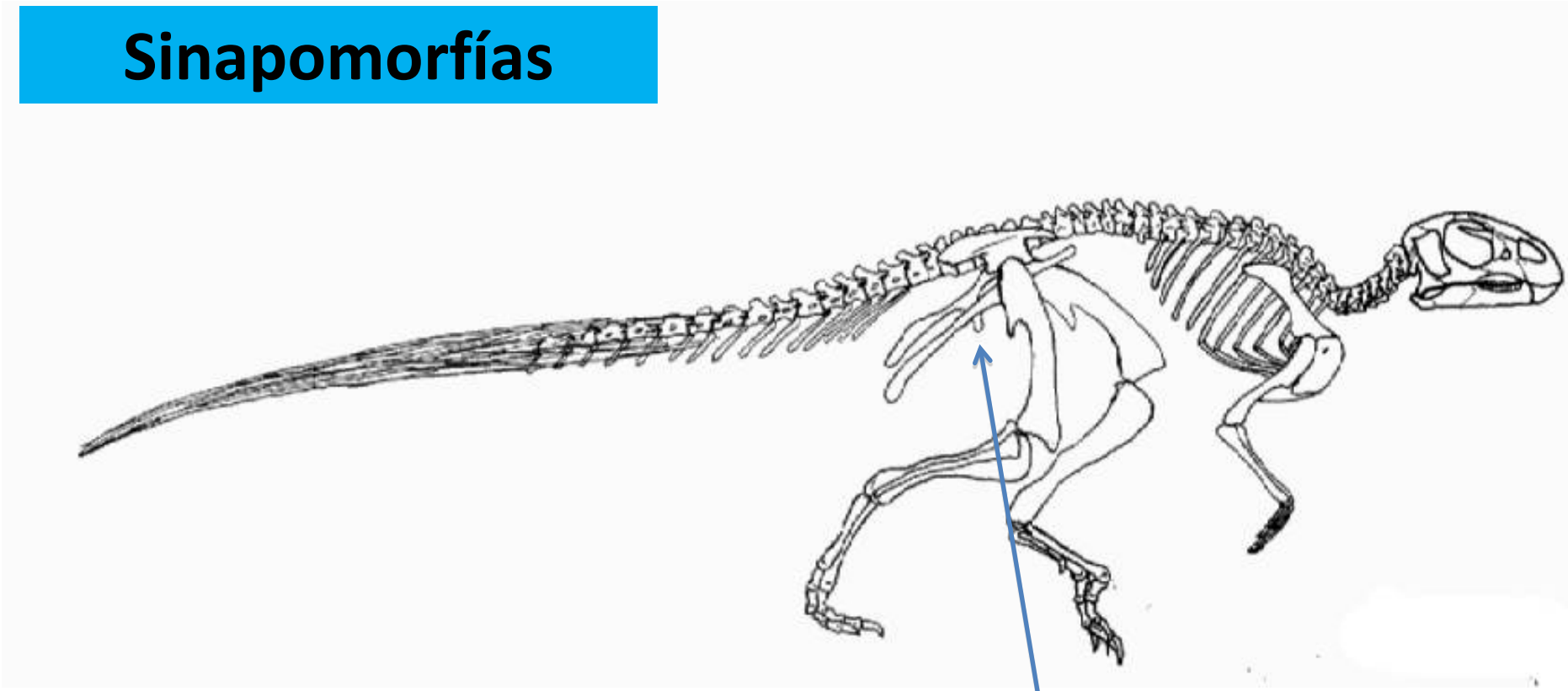

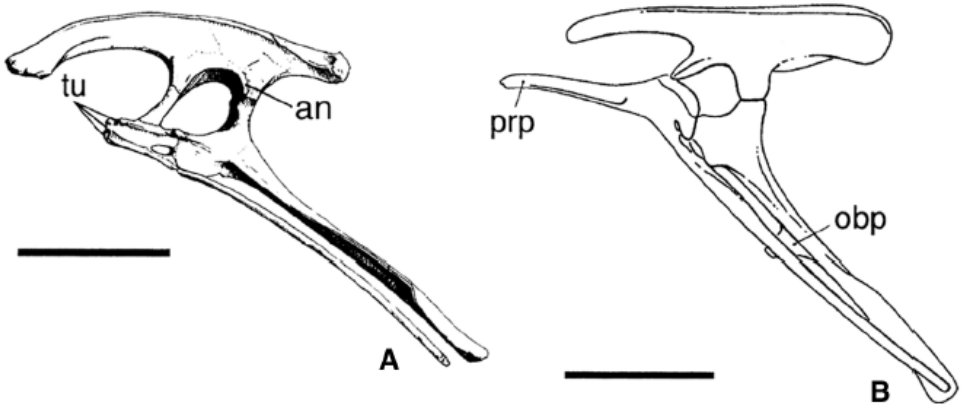

FIGURE 18.10. A, Pelvis of *Heterodontosaurus tucki* in left lateral view; B, pelvis of *Hypsilophodon foxii* in left lateral view. Scale = 5 cm (A), 10 cm (B). (A after Santa Luca 1980; B after Galton 1974a.)

Synapomorfía de Neornithischia:
Proceso obturador en el isquión

Sinapomorfías

Nanosaurus agilis

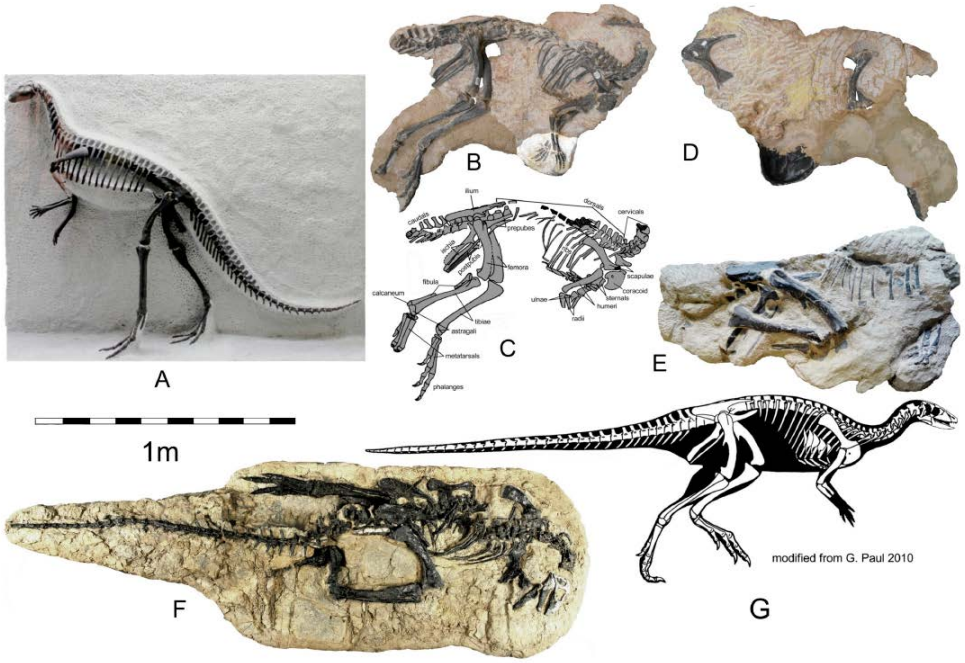

Figure 8. *Nanosaurus agilis* Marsh, 1877. (A) Mounted skeleton at the Peabody Museum of Natural History, YPM VP 1882, the holotype of "*Laosaurus consors*" Marsh, 1894b, type species of "*Othnielosaurus*" Galton, 2007 as "*O. consors*" (Marsh, 1894b). A great deal of plaster of Paris obscures details of some of the bones. (B) Headless juvenile specimen (BYU 163) from near Willow Springs, Emery County, Utah, (C) with interpretative sketch. This specimen was well illustrated and described by Galton and Jensen (1973). (D) Opposite side of (BYU 163) showing *Allosaurus* lacrymal and lateral side of left femur in window. (E) Another headless partial skeleton (UW 24823) preserved three-dimensionally from near Alcova, Wyoming. This specimen is a little larger than BYU 163. (F) "Barbara" (SMA 0010), the most complete and articulated specimen that was excavated at the Howe Ranch, Wyoming (photo from H.J. Siber, Athal Saurier Museum). (G) Composite skeletal reconstruction courtesy Greg Paul (independent paleoartist).

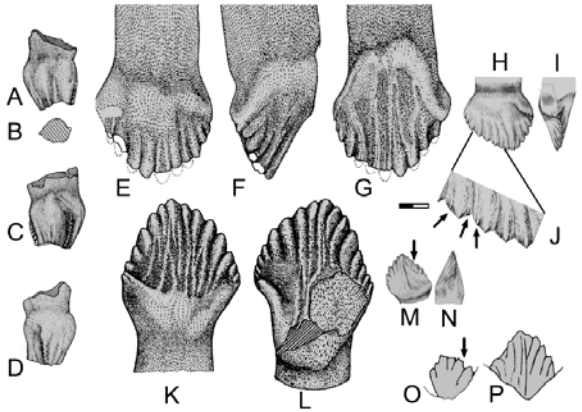

Figure 10. *Nanosaurus agilis* Marsh, 1877. Premaxillary (YPM VP 9522) tooth in (A) anterior; (B) cross section at broken surface, (C) posterior, and (D) marginal views. Maxillary tooth (YPM VP 1882) in (E) lingual, (F) marginal, and (G) labial views. Juvenile maxillary tooth with multi-cuspid cusps in (H) lingual, (I) marginal view, (J) enlarged crown margin showing multi-cusp (arrows) (adapted from Bakker and others, 1990). Dentary tooth (YPM VP 1882) in (K) labial and (L) lingual views. Juvenile dentary tooth in (M) labial (multi-cuspid at arrow) and (N) marginal views; USNM V 5829 (O) posterior tooth with multi-cuspid crown (arrow), and (P) mid-dentary tooth without multicuspid crown; see figure 7I, arrows, for size of teeth. The presence of multi-cuspid crowns was originally used to separate "*Drinker*" from "*Othnielosaurus*," but this specimen shows both crown types occur in the same specimen. Scale for A to I and K to N = 2 mm.

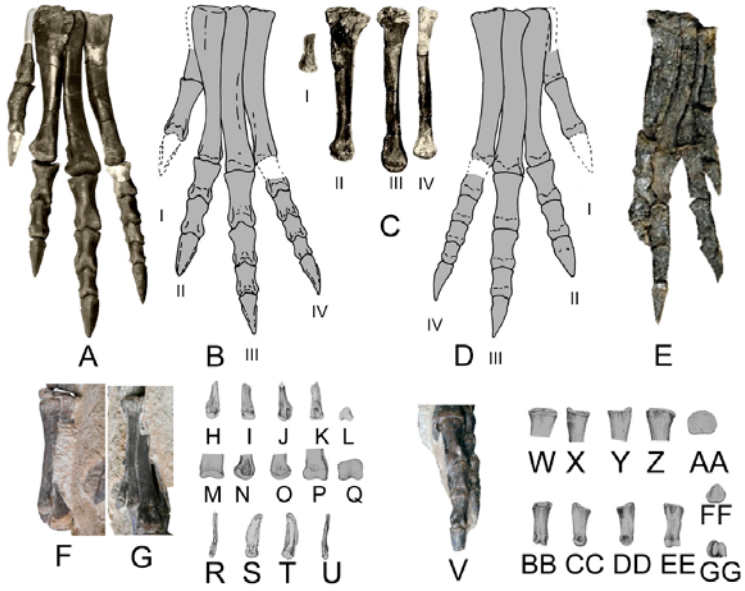

Figure 18. *Nanosaurus agilis* Marsh (1877). Nearly complete, gracile left pes (YPM VP 1822) in (A) anterior view, (B) sketch of anterior side, (C), metatarsals in medial view, and (D) sketch of posterior side. Although the first digit (I) is present, it is short and there were only three functional digits (II to IV); Boyd (2015) considers this foot the derived state in ornithischians. (E) Articulated left pes (SMA 0010) in posterior view. Right metatarsals (BYU 163) in (F) anterior view, and left metatarsals in (G) anterior view. Metatarsal I ("*Drinker nisti*" courtesy of R.T. Bakker, Houston Museum of Natural History) in (H) anterior, (I) medial, (J) lateral, (K) posterior, and (L) distal views; distal end of metatarsal III in (M) anterior, (N) lateral, (O) medial, (P) posterior, and (Q) distal views; metatarsal V in (R) anterior, (S) lateral, (T) medial, and (U) posterior views. Articulated left pes phalanges (BYU 163) in (V) anterior view. Proximal end of phalanx I-1 ("*Drinker nisti*" courtesy of R.T. Bakker, Houston Museum of Natural History) in (W) anterior, (X) lateral, (Y) medial, (Z) posterior, and (AA) proximal views; phalanx II?/IV?-1 in (BB) anterior, (CC) lateral, (DD) medial, (EE) posterior, (FF) proximal, and (GG) distal views. Scales in cm.

Placas intercostales

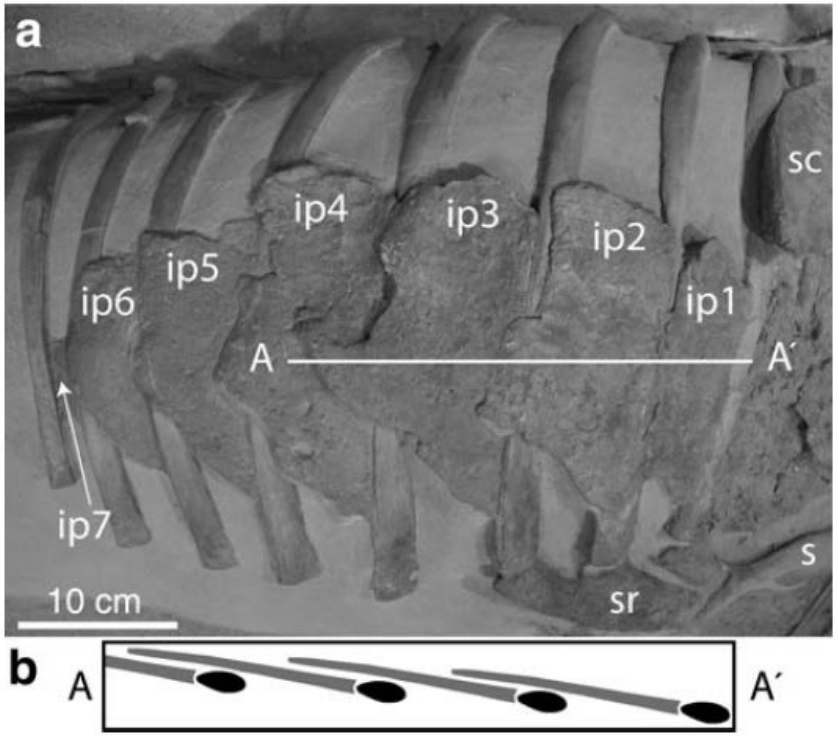

Fig. 1 **a** Right lateral view of the rib cage of NCSM 15728 (*Thescelosaurus* sp.) showing the morphology and placement of the intercostal plates on the thoracic cavity. The dorsal half of ip3 is reconstructed to match the portion of the plate that was removed for sampling. **b** Cartoon showing the position of the intercostal plates (*gray*) in relation to the dorsal ribs (*black*) in cross-sectional view along line A to A′. Abbreviations: *ip1-7* intercostal plates 1–7, *s* sternum, *sc* scapula, *sr* sternal ribs

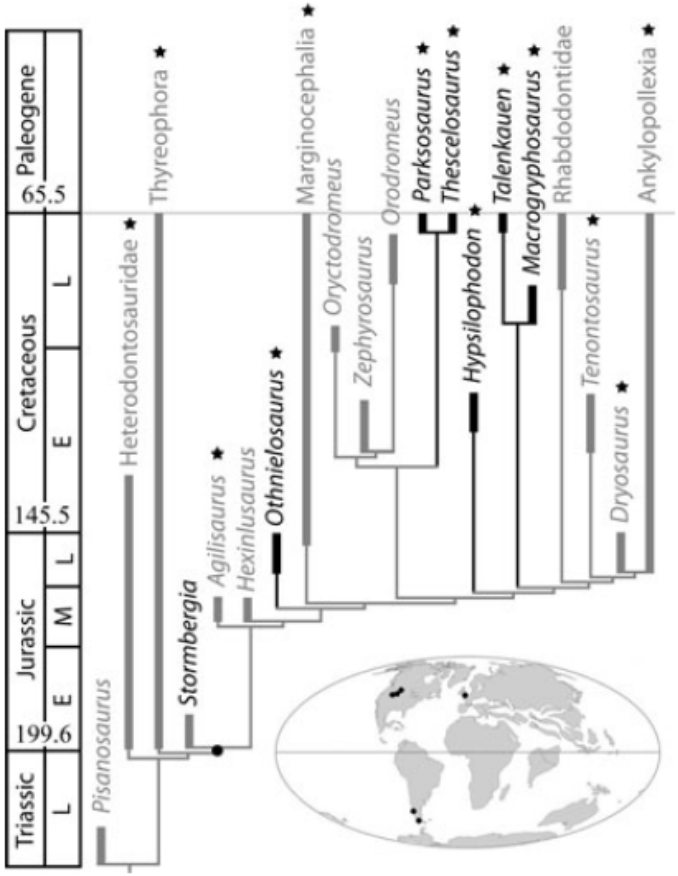

NEORNITISQUIOS (MUY!) BASALES: *Agilisaurus,* y *Hexinlusaurus (=Yandusaurus),* tienen las synapomorfías de Genasauria pero carecen de las synapomorfías de Cerapoda. Habían sido antiguamente considerados como ornitópodos hypsilofodontes.

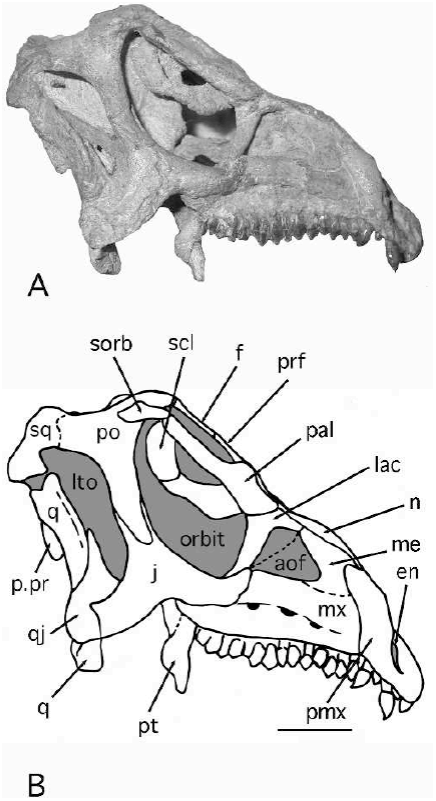

FIGURE 3. Holotype skull of *Agilisaurus louderbacki* (ZDM T6011). **A**, right lateral view. **B**, outline drawing of the skull. Note the excavated area on the ascending process of the maxilla that lies rostral to the antorbital fossa, and the palpebral/supraorbital bar that traverses the orbit. **Abbreviations**: as for Figure 1 with the addition of: **en**, external naris; **me**, maxillary embayment; **pmx**, premaxilla; **pt**, pterygoid flange; **sorb**, supraorbital. Scale bar equals 20 mm.

Cerapoda (= Neornithischia, sensu Sereno, 1999) has been diagnosed on the basis of the following synapomorphies: 1) premaxilla-maxilla diastema present; 2) asymmetrical enamel on maxillary and dentary tooth crowns; 3) predentary equal in length to premaxilla; 4) anterior trochanter finger-shaped; 5) ventral acetabular flange absent; 6) supraacetabular rim absent; 7) ischial peduncle of ilium projecting laterally. All of these characters are absent in *Agilisaurus*; characters 2, 4, 5, and 7 are absent in *Hexinlusaurus* (characters 1 and 3 cannot be determined for this taxon), but character 6 is present. This suggests that neither *Agilisaurus* nor *Hexinlusaurus* is a cerapodan and thereby excludes them from Ornithopoda. However, the presence of a cerapodan synapomorphy in *Hexinlusaurus* suggests that this taxon is more derived than *Agilisaurus* (see also Norman et al., 2004b). As both taxa lack dermal armour and other thyreophoran synapomorphies (e.g., Sereno, 1999), this distribution of character states suggests that they should be regarded as basal ornithischians, Genasauria incertae sedis. The absence of asymmetrically distributed enamel on the teeth of *Xiaosaurus* (Dong and Tang, 1983) suggests that this taxon also lies outside of Cerapoda: unfortunately, the fragmentary material of this genus does not allow further consideration of its phylogenetic position and it should be regarded as Ornithischia incertae sedis until more information becomes available.

Apparent support is also weak for the position of *Agilisaurus* and *Hexinlusaurus* as basal neornithischians. However, bootstrap support for the node supporting the clade *Othnielia* + Cerapoda, to the exclusion of *Agilisaurus* and *Hexinlusaurus*, is relatively high (79%) in the reduced bootstrap analysis (Fig. 4). Five unambiguous characters (Appendix 4) suggest that *Hexinlusaurus* is more closely related to cerapodans than *Agilisaurus*. This is of interest as many authors have synonymised the two, although recent work (Barrett

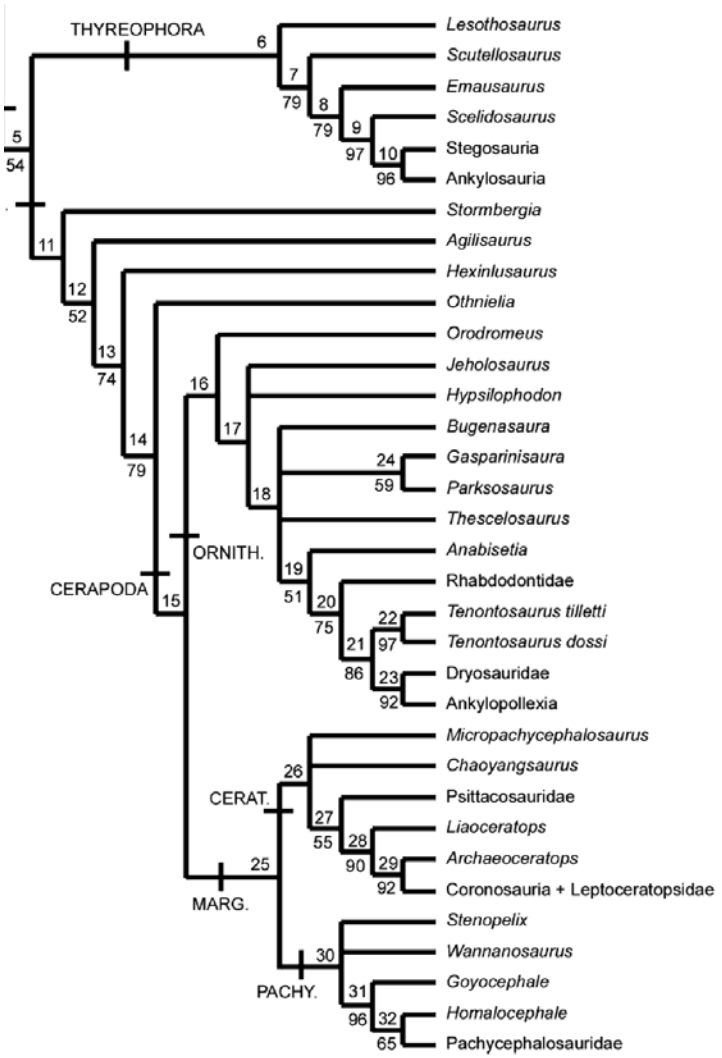

Othnielia (=Othnielasaurus), previamente considerado un ornitópodo “hypsilophodontido”, se encuentra cerca, pero por fuera de Cerapoda (buena aproximación de lo que sería el primer Cerapoda).

Ojo: dientes con esmalte asimétrico en Othnielia sugieren que el rasgo precede el nodo Cerapoda, donde se ha propuesto como synapomorfía

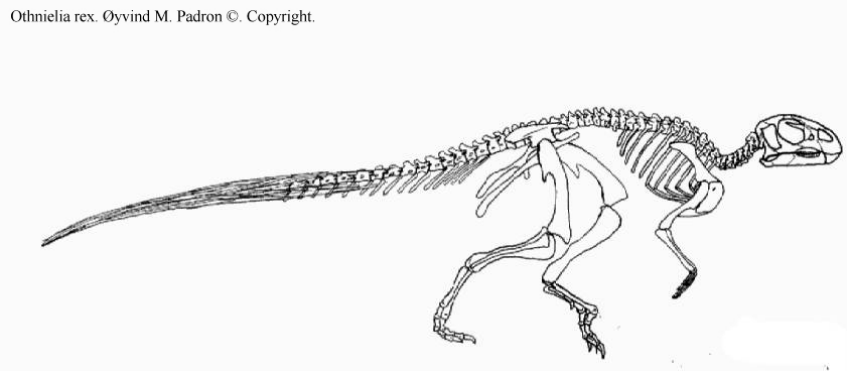

Referral of *Stormbergia* to Neornithischia is supported by only a single unambiguous character (possession of an obturator process on the ischium, Character 184, Appendix

recovered by this analysis excludes *Othnielia* from Cerapoda, as a result of the retention of a relatively short postacetabular process (Character 174, Appendix 2) and a relatively reduced and splint-like first metatarsal (Character 211, Appendix 2). However, the position of *Othnielia* appears to be unstable and weakly supported and this may reflect the near-absence of cranial data for this taxon.

Hypsilophodontidae, as generally conceived (Weishampel & Heinrich 1992), does not form a monophyletic clade; instead ‘hypsilophodontids’ appear to represent a paraphyletic grade of basal neornithischian and basal ornithopod taxa (see below). More derived ornithopod relationships generally follow that suggested by previous authors (e.g. Weishampel *et al.* 2003).

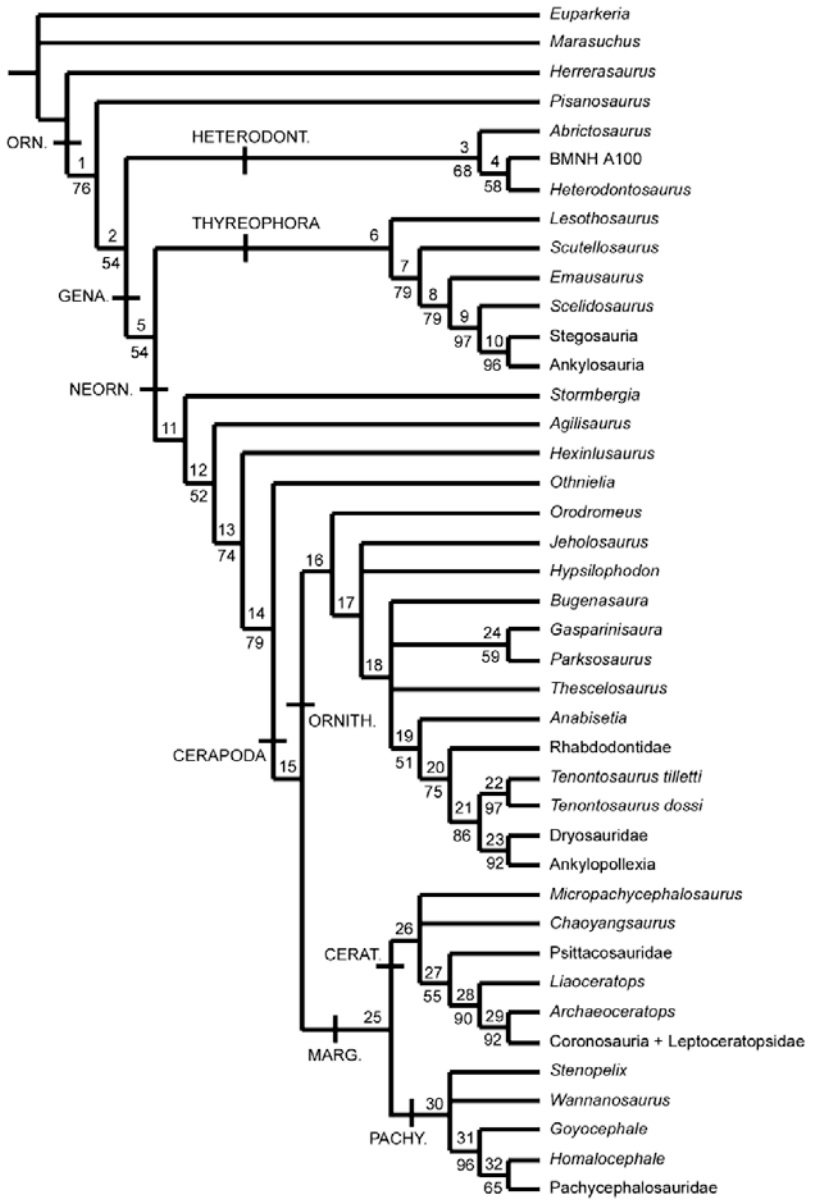

Figure 4 Derivative strict reduced consensus tree derived by *a posteriori* pruning of five unstable taxa (*Echinodon*, *Lycorhinus*, *Zephyrosaurus*, *Talenkauen* and *Yandusaurus*) from the set of 756 most parsimonious trees (MPTs) generated by the full analysis. The number above each node is a unique identifier used in the tree description (see Appendix 4). The number beneath a node represents the bootstrap proportion for that node (taken from the reduced bootstrap analysis). Note the increased levels of bootstrap support for a number of nodes when compared to Fig. 2. Abbreviations: ORN., Ornithischia; HETERODONT., Heterodontosauridae; GENA., Genasauria; NEORN., Neornithischia; ORNITH., Ornithopoda; MARG., Marginocephalia; CERAT., Ceratopsia; PACHY., Pachycephalosauria.

Nanosaurus agilis

Based on the "Barbara" specimen collected by the Aathal Museum. Additional information from type specimen BYU ESM-163R. Rigorous skeletal drawing shows what is known of Barbara.

Kulindadromeus zabakalicus

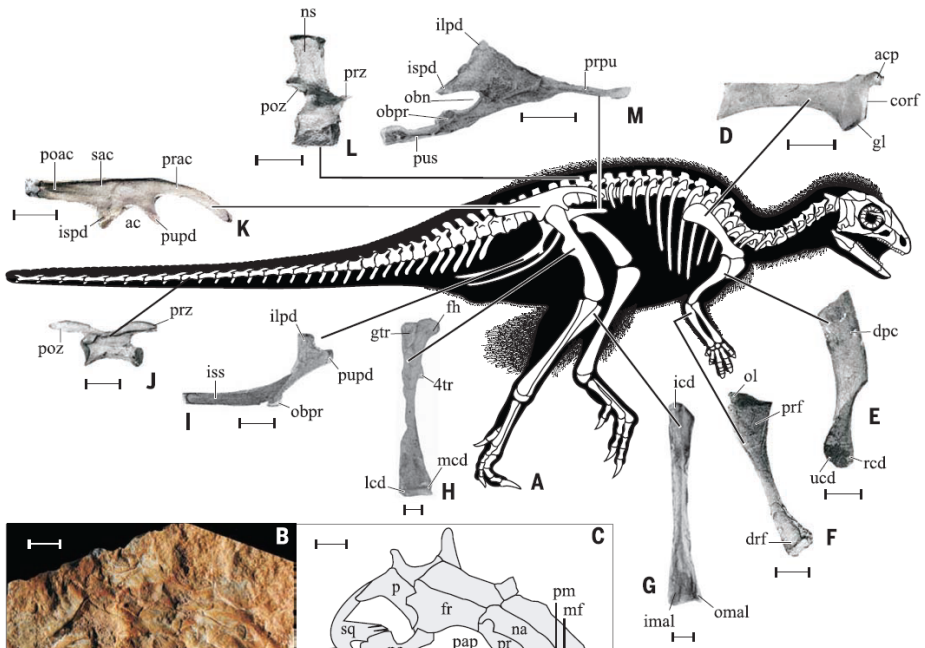

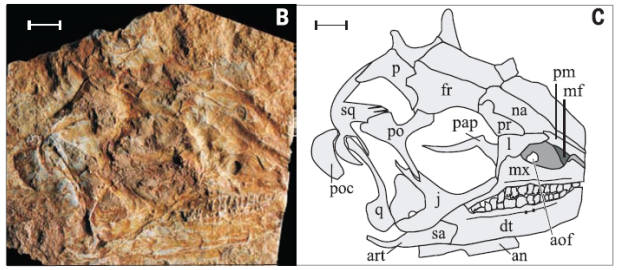

Fig. 1. Skeletal anatomy of *Kulindadromeus zabaikalicus*. (**A**) Composite skeletal reconstruction; photograph (**B**) and line drawing (**C**) of the holotype skull (INREC K3/109) in right lateral view; (**D**) proximal portion of right scapula (INREC K3/204) in lateral view; (**E**) right scapula (INREC K3/134) in caudolateral view; (**F**) left ulna (INREC K3/205) in medial view; (**G**) right tibia (INREC K3/207) in caudal view; (**H**) right femur (INREC K3/206) in cranial view; (**I**) right ischium (INREC K3/124) in lateral view; (**J**) distal caudal vertebra (INREC K3/202) in right lateral view; (**K**) mirror image of left ilium (INREC K3/113) in lateral view; (**L**) dorsal vertebra (INREC 3/112) in right lateral view; (**M**) mirror image of left pubis (INREC K3/114) in lateral view. Scale bars, 10 mm. Abbreviations: ac, acetabulum; acp, acromial process; an, angular; aof, antorbital fossa; art, articular; cor, coracoid facet; dpc, deltopectoral crest; drf, distal radial facet; dt, dentary; fh, femoral head; fr, frontal; gl, glenoid; ilpd, iliac peduncle; imal, inner malleolus; ispd, ischial peduncle; iss, ischial shaft; j, jugal; l, lacrimal; lcd, lateral condyle; mcd, medial condyle; mf, maxillary fenestra; mx, maxilla; na, nasal; obn, obturator notch; obpr, obturator process; ns, neural spine; ol, olecranon process; omal, outer malleolus; p, parietal; pap, palpebral; pm, premaxilla; po, postorbital; poac, postacetabular process; poc, paroccipital process; poz, postzygapophysis; pr, prefrontal; prac, preacetabular process; prf, proximal radial facet; prpu, prepubic process; prz, prezygapophysis; pupd, pubic peduncle; pus, pubic shaft; q, quadrate; qj, quadratojugal; rap, rostral ascending process; rcd, radial condyle; sa, surangular; sac, supraacetabular crest; sq, squamosal; ucd, ulnar condyle; 4tr, fourth trochanter.

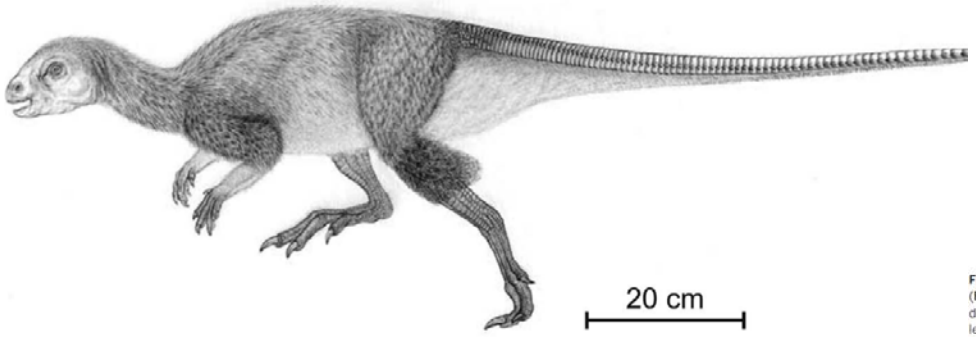

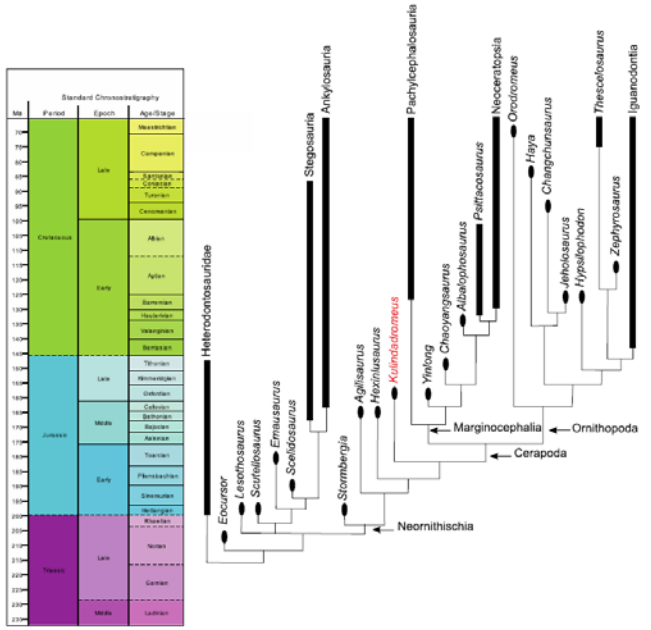

Fig. S11. Phylogenetic relationships of *Kulindadromeus zabaikalicus* among ornithischian dinosaurs, as a result of the inclusion of *Kulindadromeus* in a recently published analysis of ornithischian phylogeny. Time-calibrated strict consensus tree of the 4 most parsimonious trees (tree length = 571; consistency index excluding uninformative characters = 0.42; retention index = 0.7). In this hypothesis, *Kulindadromeus* is the sister-taxon of Cerapoda.

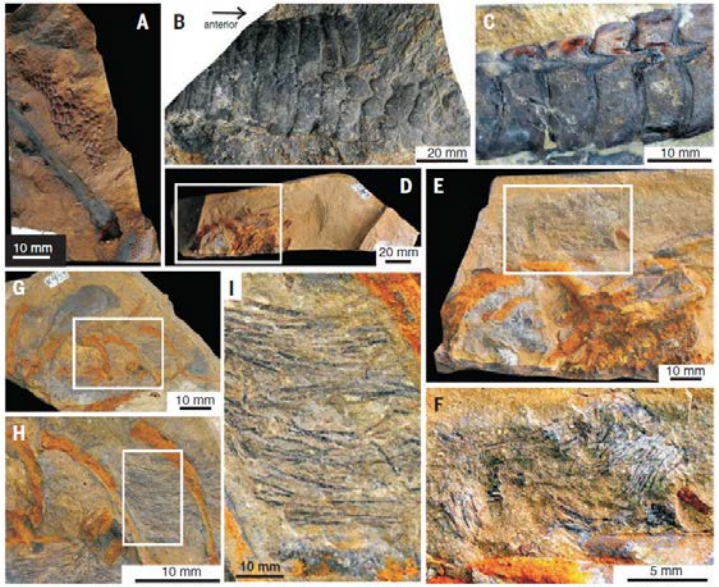

Fig. 2. Epidermal scales and featherlike structures of *Kulindadromeus zabaikalicus*. (**A**) Scales around the distal tibia and the tarsus (INREC K4/57); (**B**) double row of scales above the proximal part of the tail (INREC K4/94) in dorsal view; (**C**) close-up of the left row of caudal scales (INREC K4/117) in dorsal view; (**D**) partial skull (INREC K4/22) in right lateral view, with (**E** and **F**) detail of areas indicated in (D) and (E) showing filamentous structures; (**G**) left part of ribcage (INREC K4/33), with (**H** and **I**) detail of areas indicated in (G) and (H) showing filamentous structures.

Cerapoda

Definición: *Parasaurolophus walkeri*, *Triceratops horridus*, su ancestro común reciente y todos sus descendientes (Butler et al, 2008).

Contenido: Marginocephalia + Ornithopoda

Sinapomorfías:

1) Coronas maxilares que se estrechan hacia la raíz.
2) Esmalte asimétrico en dientes maxilares.
3) Coronas dentarias con estrías linguales.
4) Diastema maxilar.

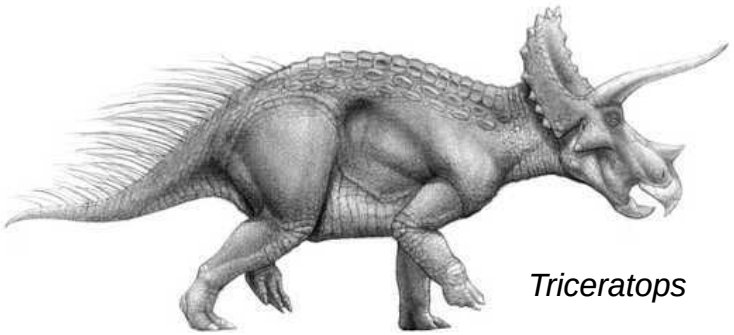

Triceratops

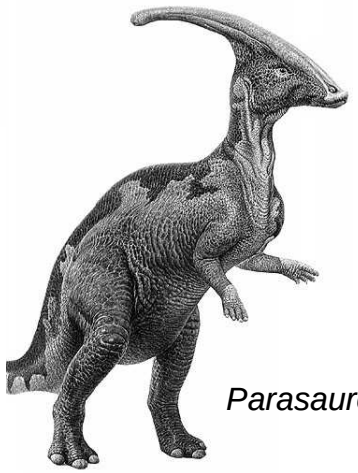

Parasaurolophus

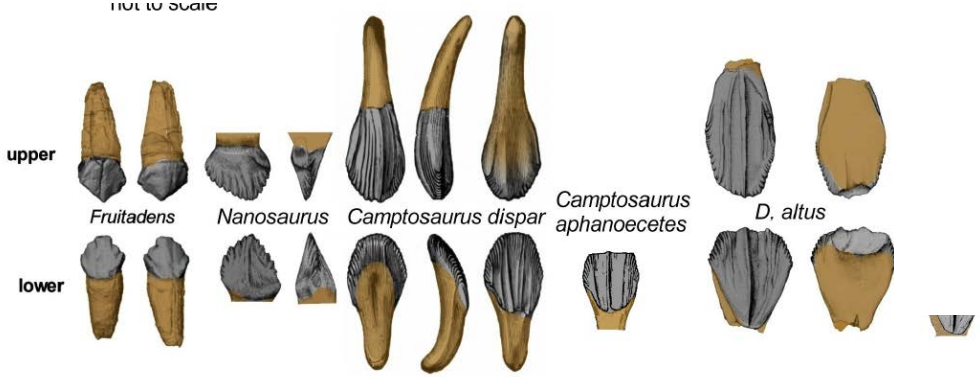

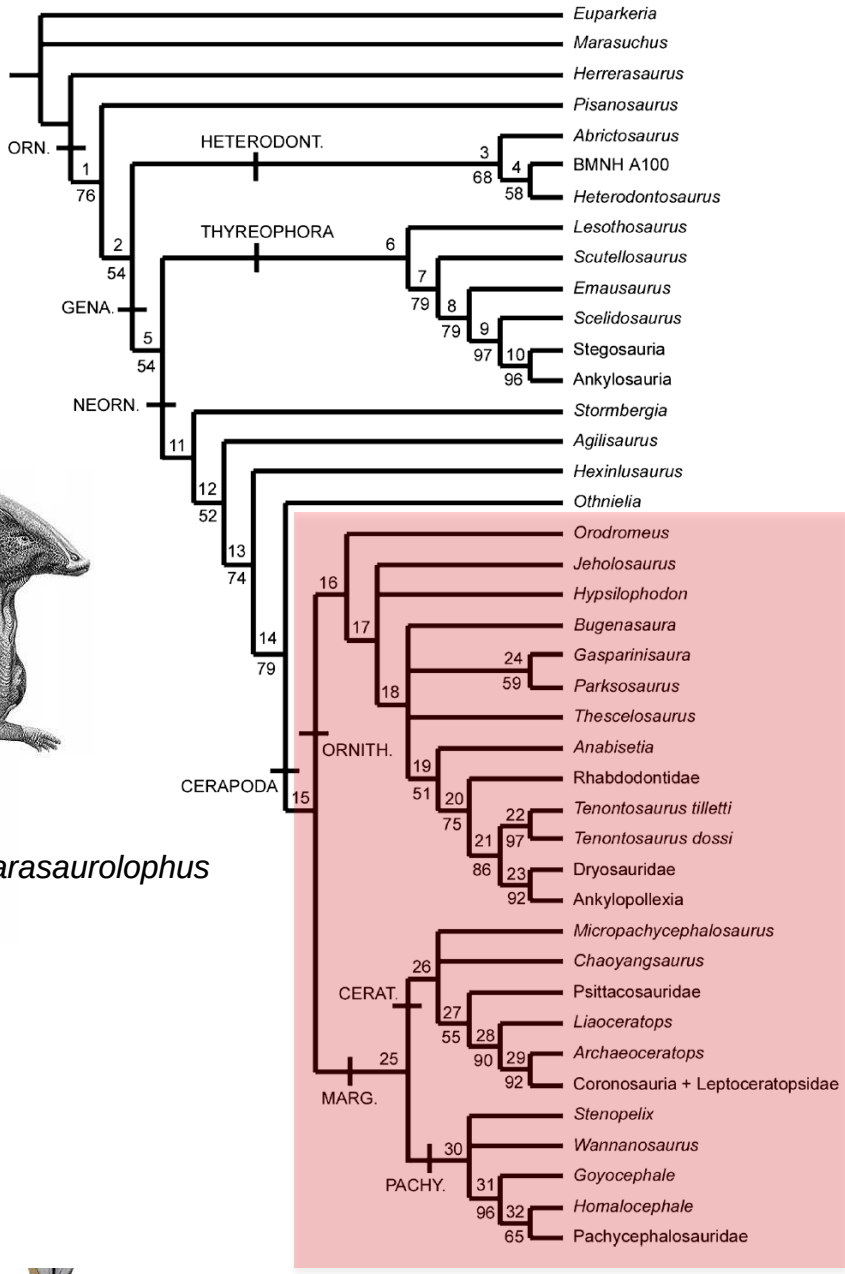

Cerapoda Sereno, 1986

presencia de un espacio (diastema) entre los dientes del premaxilar y el maxilar, y la reducción del número de dientes premaxilares a cinco o menos; predentario y premaxilar de igual longitud. Dientes con esmalte asimétrico (este rasgo es equívoco, ya que está presente en Othnielia, y ausente de ornitópodos basales. Tb fue independientemente adquirido en Heterodontosauridae, demostrando su plasticidad evolutiva)

Hypsilophodon (Ornithopoda)

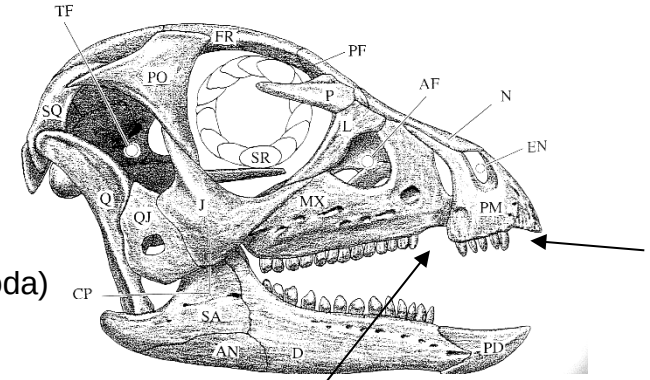

5 ó menos dientes

Diastema entre premaxilar y maxilar

Esmalte asimétrico

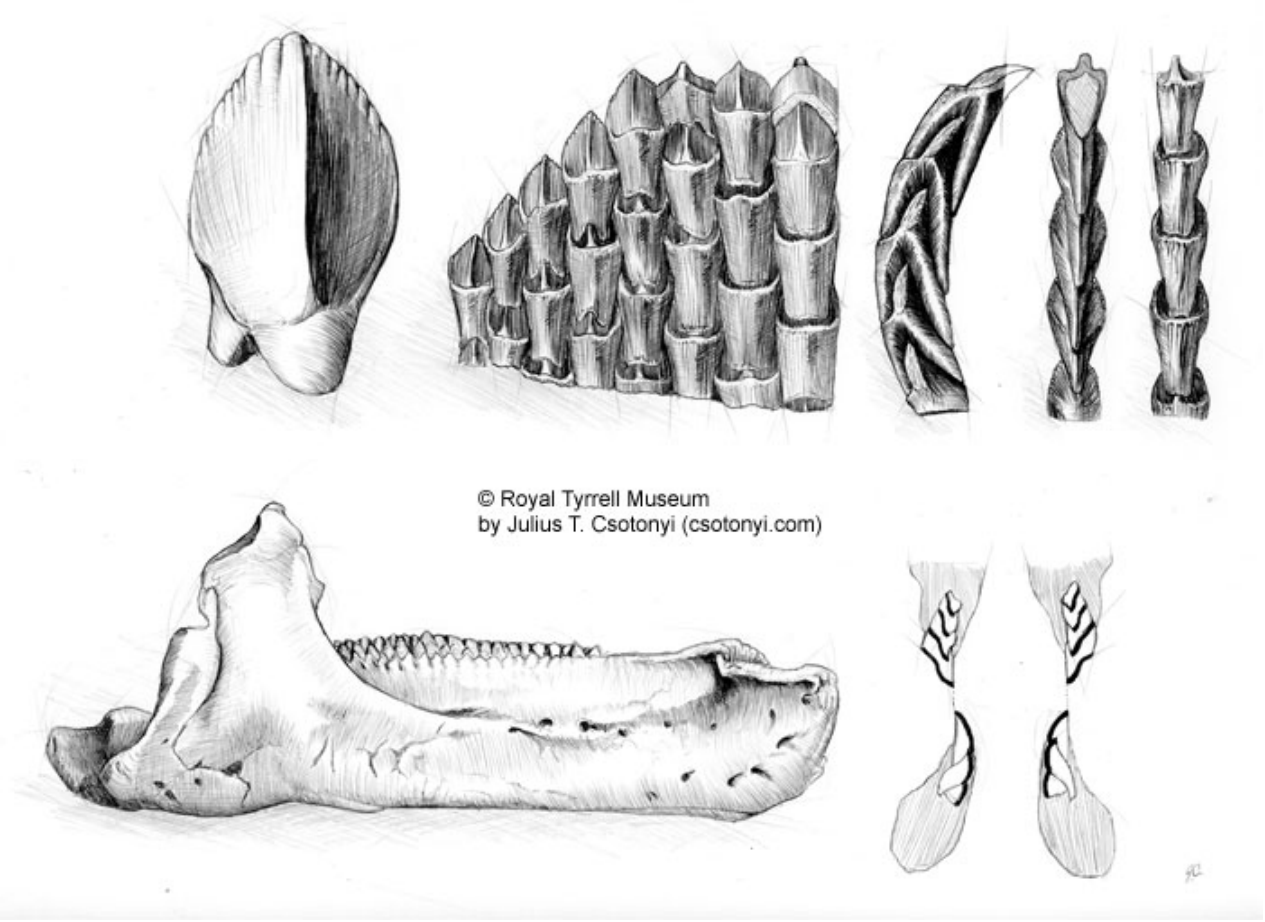

Marginocephalia

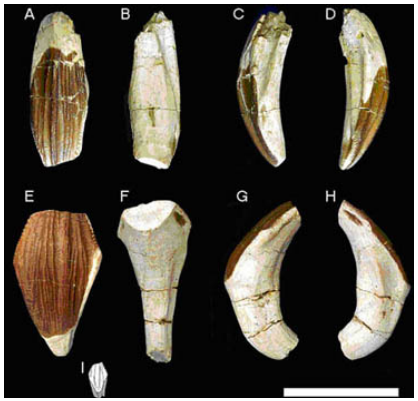

Ornithopoda

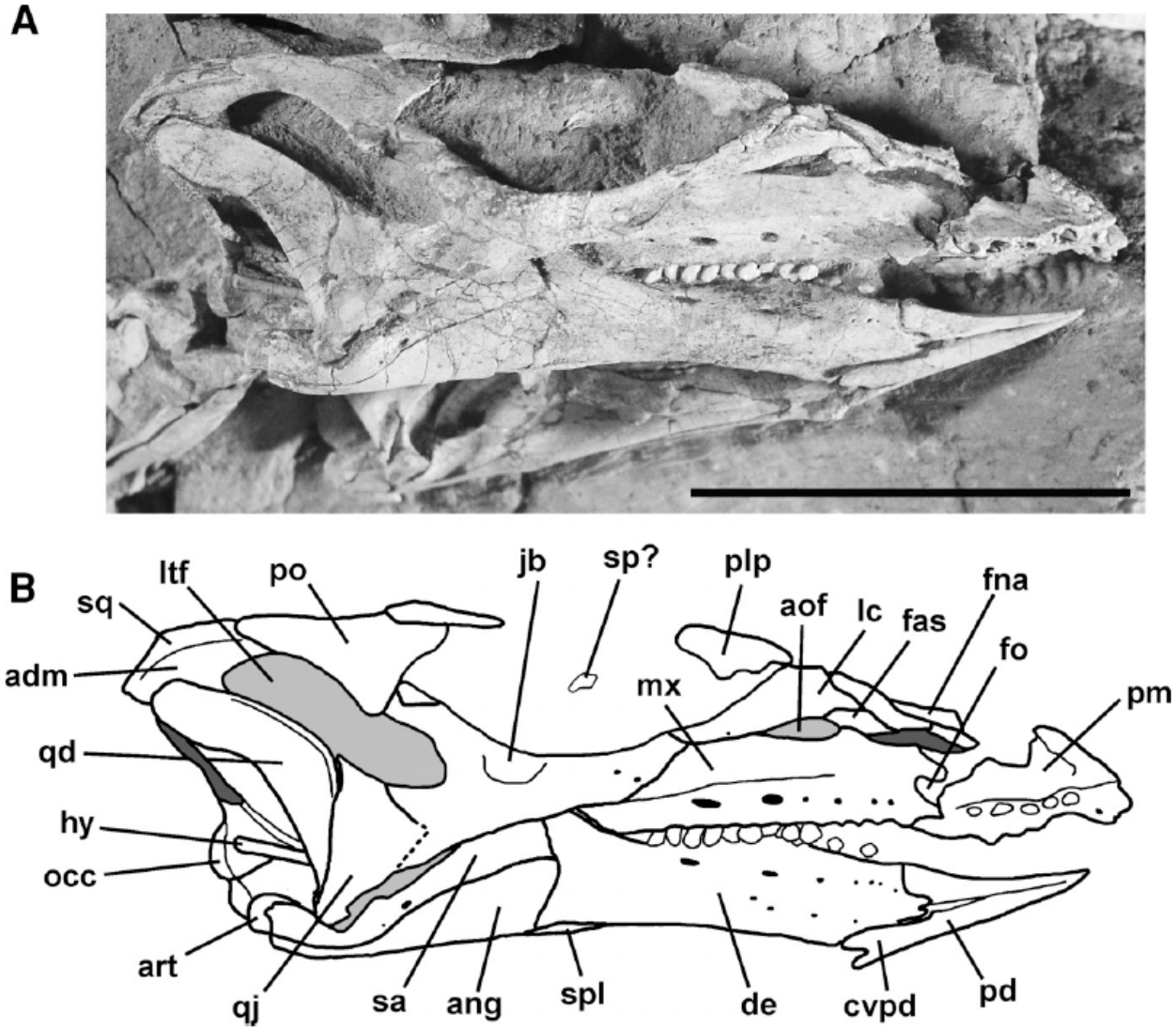

Sin embargo, *Changchunsaurus*, y *Orodromeus* son ornitópodos basales que carecen de esmalte asimétrico.
Reversión, o **Paralelismo**.

Ornithopoda

Definición: Todos los cerápodos más cercanos a *Parasaurolophus walkeri* que ha *Triceratops horridus.*

Sinapomorfías:

1. Presence of a fossa-like depression on the premaxilla-maxilla boundary.
2. Pterygoid mandibular process short, terminates at or above maxillary tooth row.
3. Predentary long and about equal in length to the premaxilla
4. Prominent femoral ligament sulcus.

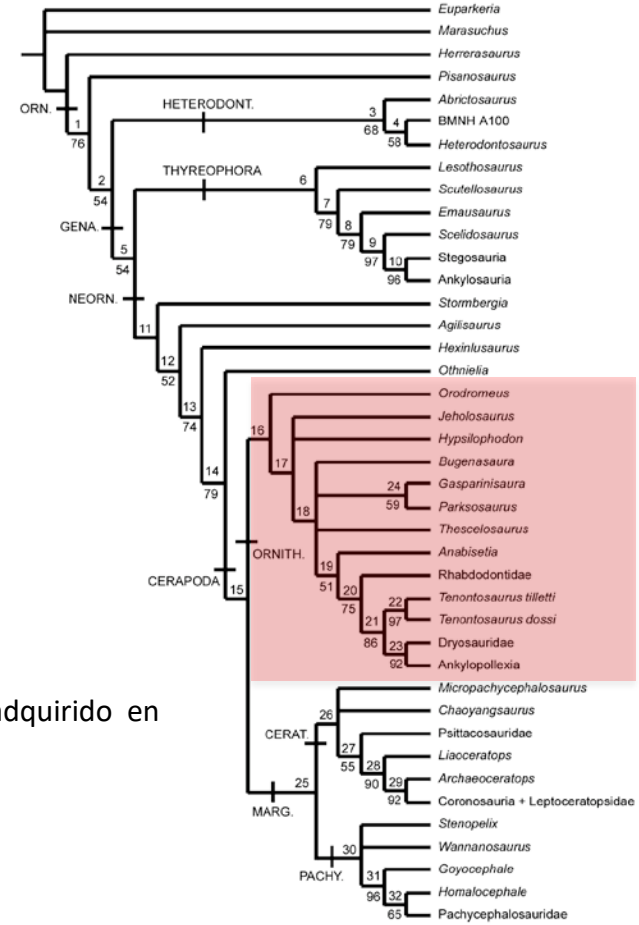

Otras posibles Sinapomorfías de Ornithopoda:

1. articulación pleurokinética que permite mover los dientes maxilares,

2. Hilera de dientes por arriba de articulación mandibular (independientemente adquirido en heterodontosauridae)

3. Borde inferior y dientes del premaxilar por debajo de los del maxilar

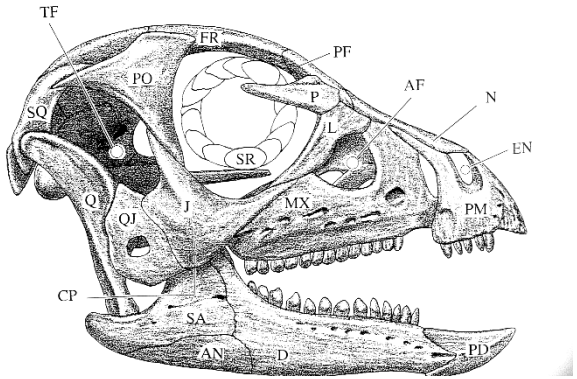

Hypsilophodon

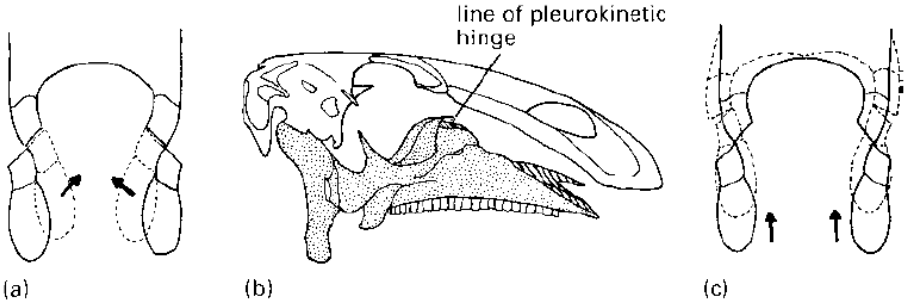

Ornithopod jaw mechanics: the lower jaws of *Heterodontosaurus* (a) slide outwards as they close, hence producing a kind of 'chewing', whereas later ornithopods have a pleurokinetic hinge, which allows the cheek portion of the skull and the maxillary teeth, shown stippled in (b), to move outwards as the jaws close (c). (Modified from Norman and Weishampel, 1985.)

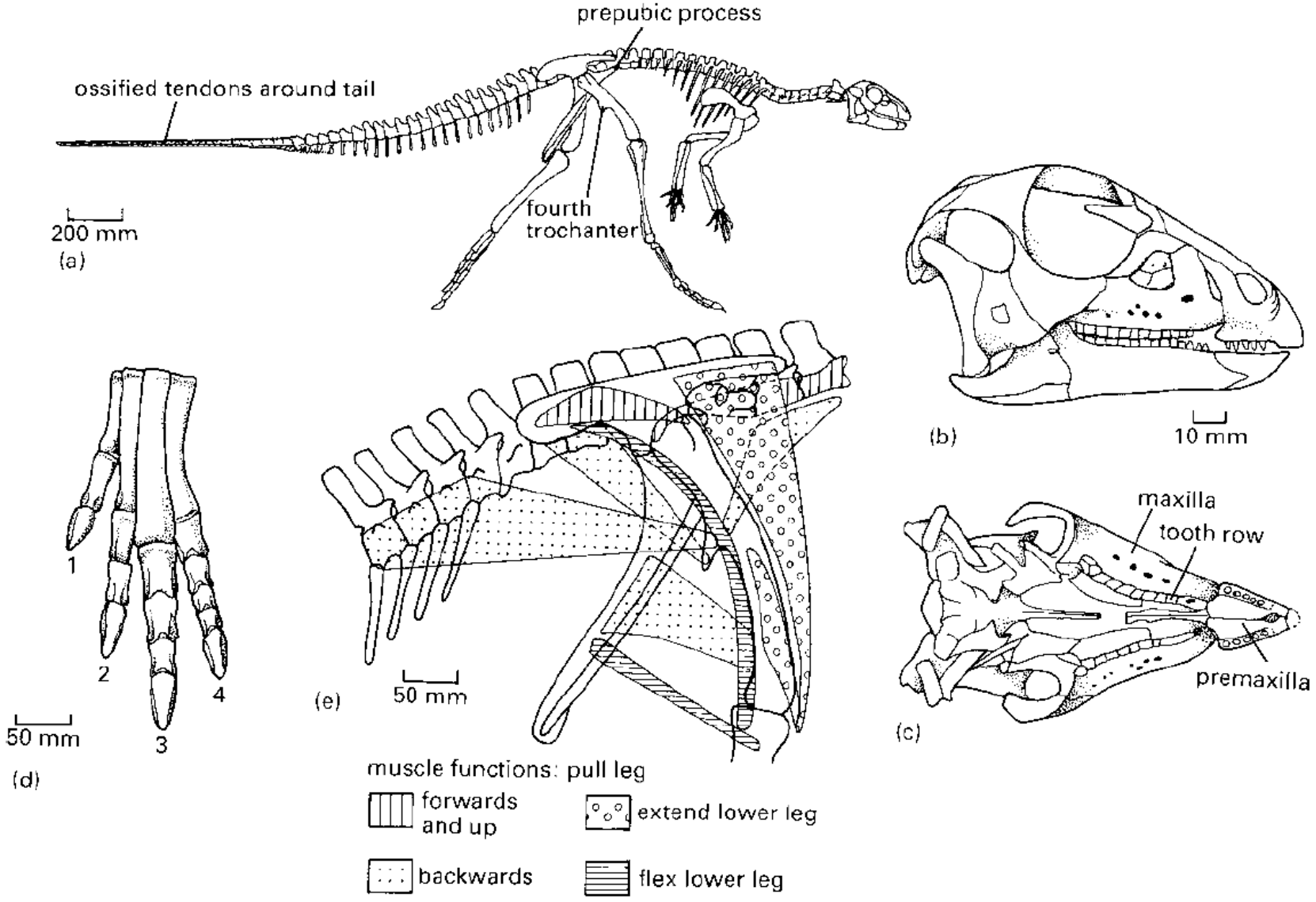

Fig. 8.12 The ornithopod *Hypsilophodon*: (a) skeleton in running pose; (b, c) skull in lateral and ventral views; (d) foot in anterior view; (e) restoration of the muscles of the pelvis and hindlimb, coded according to their functions. (After Galton 1974.)

ORNITHOPODA

Styracosterna

Greatly enlarged nares; much larger size; Spike thumb; metacarpals II-IV hoof-like; metacarpal V opposable

Camptosauridae

Dryosauridae

Ankylopollexia

Well-developed pleurokinetic hinge

Rhabdodontidae

Tenontosaurus

Dryomorpha

Thescelosauridae

Hypsilophodontidae

Iguanodontia

Larger size; Premaxilla toothless; Enlarged naris; 6 or more sacrals

Marginocephalia

Othnielosaurus

ORNITHOPODA

Premaxillary lower margin ventral to maxillary tooth row; Mandibular articulation ventral to dentary tooth row; Pleurokinetic hinge joint in cranium

Cerapoda

Neornithischia

ORNITHOPODA

“Hypsilophodontidae”

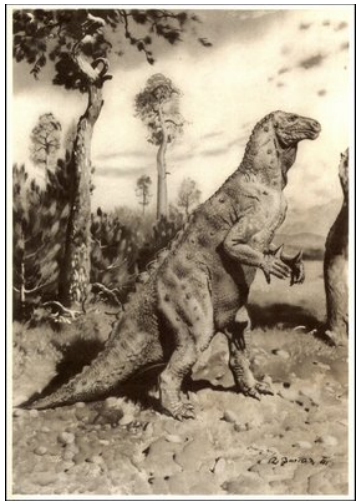

Iguanodon

Ankylopollexia

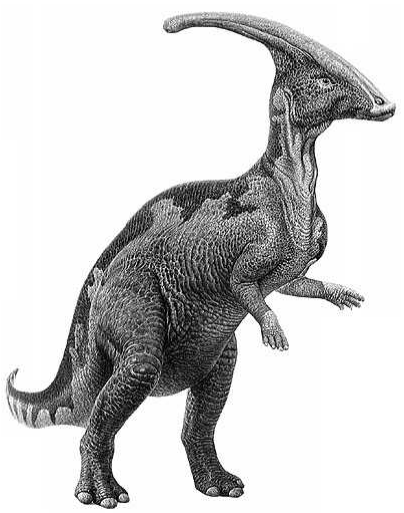

Hadrosauria

Se ha establecido que muchos “hypsilofodontes” son más cercanos a Iguanodon que a Hypsilophodon, documentando la transición desde la organización “hypsilofodonte” a formas de mayor tamaño y con la espina-pulgar (Ankyllopolexia).

De manera similar, se ha establecido que Hadrosauria pertenecen a ankylopollexia, descendiendo directamente de formas con espina-pulgar (hay formas con espina-pulgar más cercanas a hadrosauria que otras) .

La mayoría de los “hypsilophodontes” resultaron ser más cercanos a Parasaurolophus que a Hypsilophodon Puntualmente Dryosauridae, Thescelosaurus, y Tenontosauridae ahora se les considera miembro de un grupo denominado **Iguanodontia.**

Synapomorfías con Parasaurolophus:
Aumenta tamaño corporal, aumentan las aperturas nasales

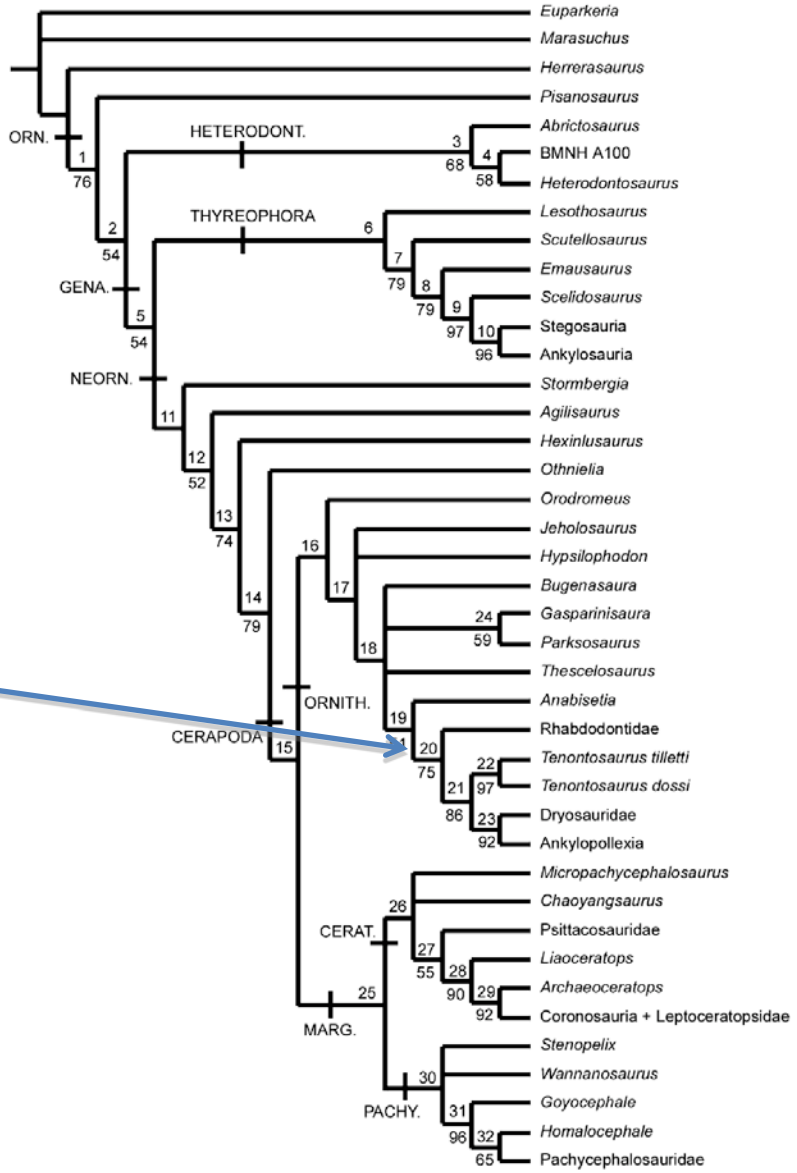

Figure 4 Derivative strict reduced consensus tree derived by *a posteriori* pruning of five unstable taxa (*Echinodon*, *Lycorhinus*, *Zephyrosaurus*, *Talenkauen* and *Yandusaurus*) from the set of 756 most parsimonious trees (MPTs) generated by the full analysis. The number above each node is a unique identifier used in the tree description (see Appendix 4). The number beneath a node represents the bootstrap proportion for that node (taken from the reduced bootstrap analysis). Note the increased levels of bootstrap support for a number of nodes when compared to Fig. 2. Abbreviations: ORN., Ornithischia; HETERODONT., Heterodontosauridae; GENA., Genasauria; NEORN., Neornithischia; ORNITH., Ornithopoda; MARG., Marginocephalia; CERAT., Ceratopsia; PACHY., Pachycephalosauria.

Jeholosauridae

Sinapomorfías:

1. Rama caudal del Yugal ahorquillada.
2. Sínfisis del ísquion alargada.

Jeholosaurus shangyuanensis

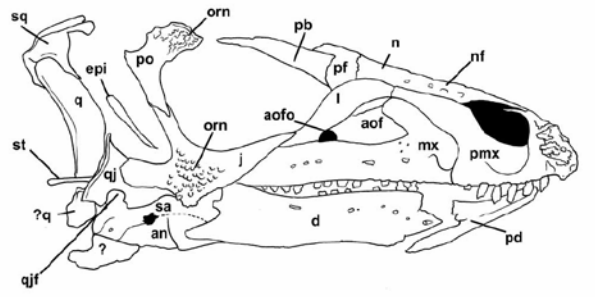

FIGURE 6. Outline drawing of the referred skull and mandible of *Jeholosaurus shangyuanensis* (IVPP V15716) in right lateral view. Abbreviations: an, angular; aof, antorbital fossa; aofo, antorbital fenestra; d, dentary; epi, epipterygoid; j, jugal; l, lachrymal; mx, maxilla; mxt, maxillary teeth; n, nasal; nf, nasal foramina; orn, ornamentation; pb, palpebral; pd, predentary; pf, prefrontal; pmx, premaxilla; po, postorbital; q, quadrate; qj, quadratojugal; qjf, quadratojugal foramen; sa, surangular; sq, squamosal; st, stapes.

Haya griva

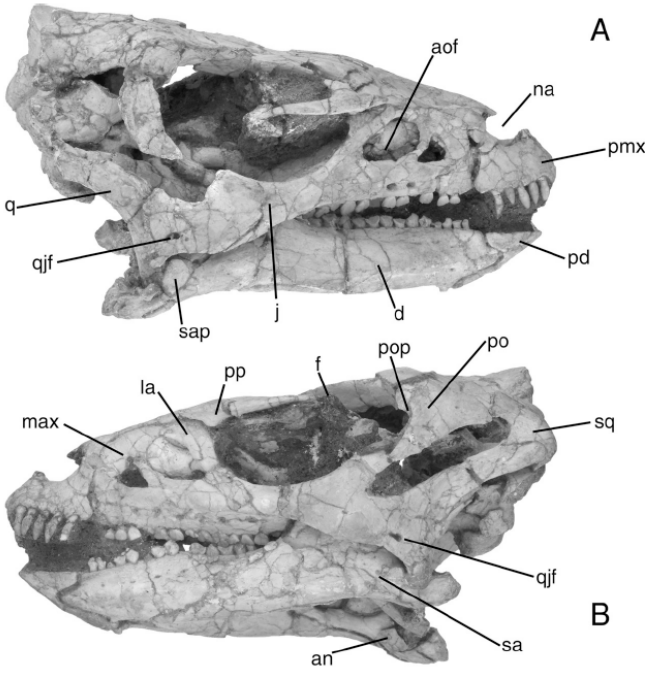

Changchunsaurus parvus

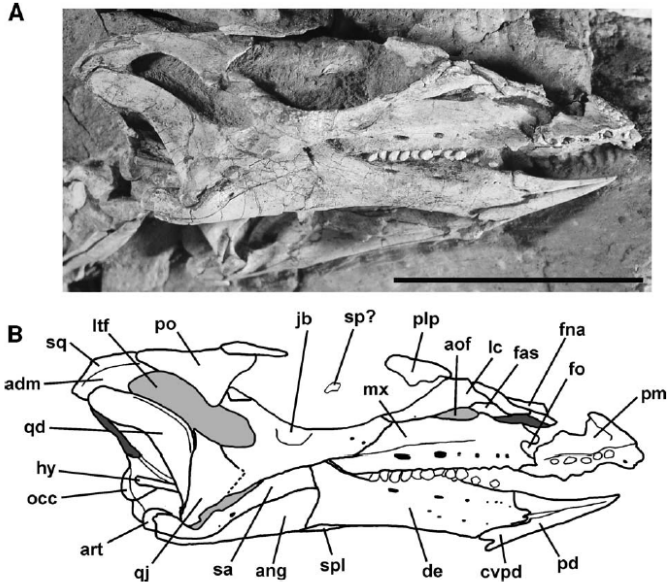

FIGURE 1. JLUM L0403-j-Zn2, holotype skull of *Changchunsaurus parvus* from the Quantou Formation (Aptian–Cenomanian) of Jilin Province, China. Light grey infill indicates sediment, dark grey infill indicates broken bone surface, dashed line indicates an uncertain sutural relationship. **A**, skull in right lateral view; **B**, interpretive line drawing (note that the left mandible and cervical vertebrae have been excluded for ease of interpretation). **Abbreviations**: **adm**, concavity for adductor musculature (M. adductor mandibulae superficialis); **ang**, angular; **aof**, antorbital fossa; **art**, articular; **cvpd**, caudoventral process of predentary; **de**, dentary; **fas**, fragment of ascending process of maxilla; **fna**, fragment of nasal; **fo**, fossa on rostral margin of maxilla, adjacent to premaxilla/maxilla suture; **hy**, hyoid; **itf**, infratemporal fenestra; **jb**, jugal boss; **lc**, lacrimal; **mx**, maxilla; **occ**, occipital condyle; **pd**, predentary; **plp**, palpebral; **pm**, premaxilla; **po**, postorbital; **qd**, quadrate; **qj**, quadratojugal; **sa**, surangular; **sp**, sclerotic plate; **spl**, splenial; **sq**, squamosal. Scale bar equals 50 mm.

Iguanodontia

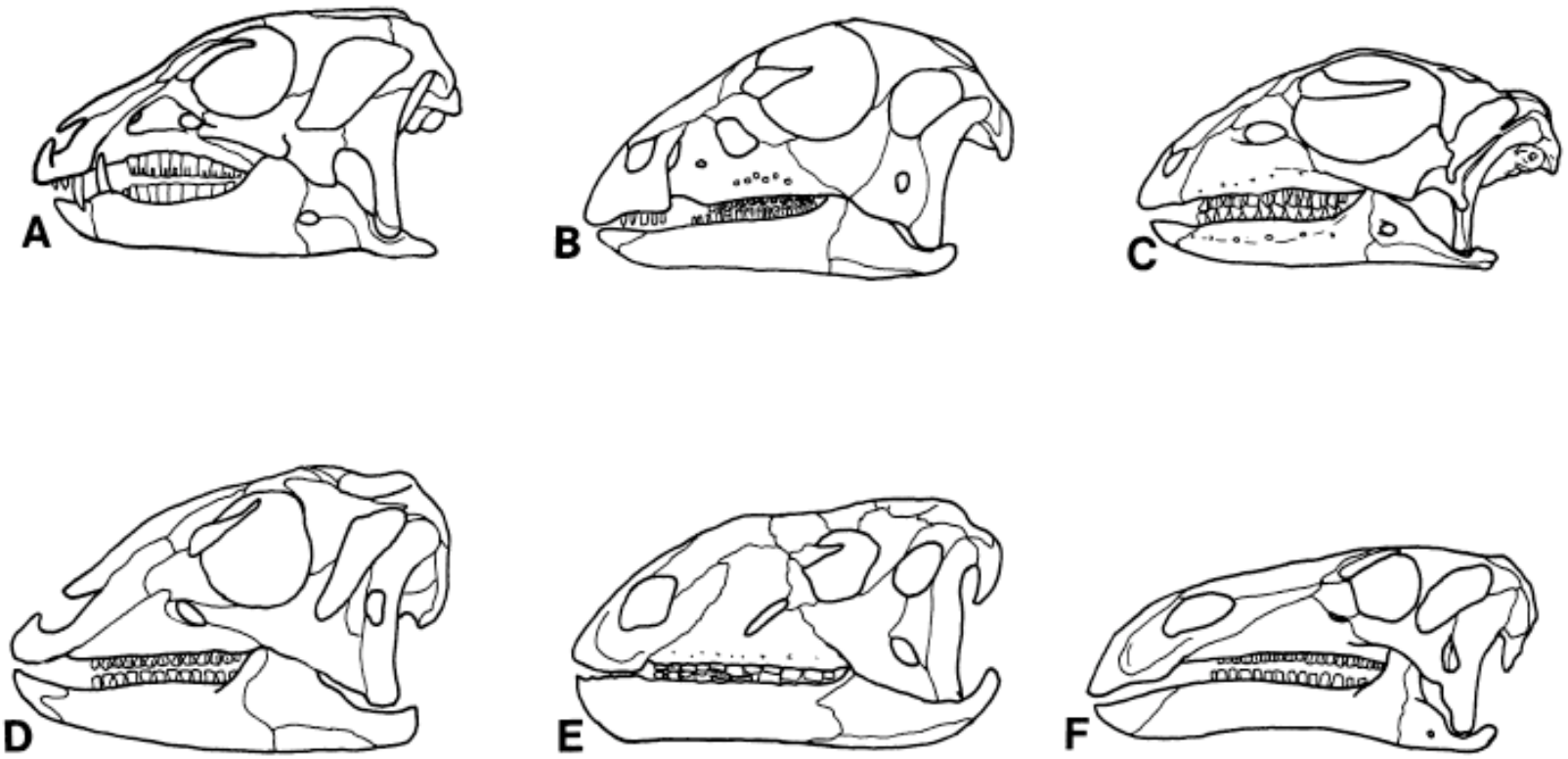

FIGURE 11. Comparisons of the skulls in lateral view of (**A**) *Heterodontosaurus* (after Weishampel and Witner, 1990), (**B**) *Hypsilophodon* (after Galton, 1974), (**C**) *Gasparinisaura*, (**D**) *Dryosaurus* (after Galton, 1983), (**E**) *Tenontosaurus* (after Sues and Norman, 1990) and (**F**) *Iguanodon* (after Norman, 1980). Not to scale.

Gasparinisauria, Thescelosaurus, Anabisetia : son más cercano a Iguanodontia que a Hypsilophodon (stem iguanodontia, pero aún son de tamaño pequeño)

Comparten con Iguanodontia las siguientes synapomorfías:

6 o más vertebras sacrales
Perdida de dientes premaxilares

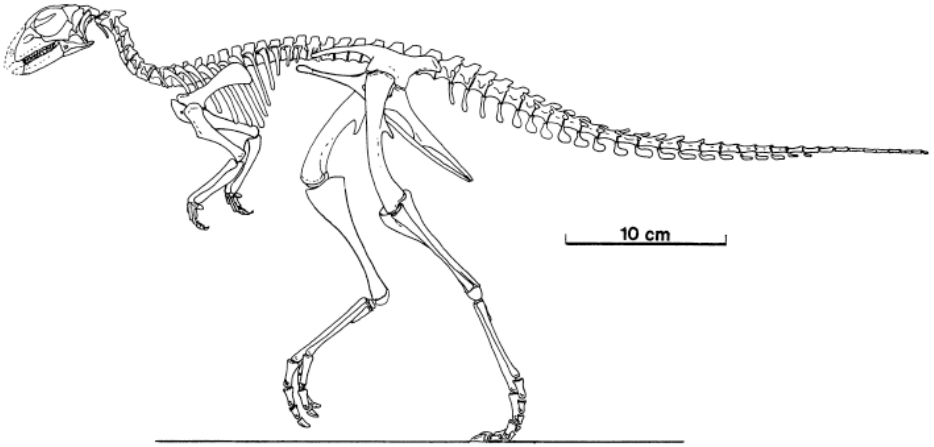

FIGURE 15. Skeletal restoration of *Gasparinisaura cincosaltensis*.

retention index of 0.88 was obtained (Fig. 13). *Gasparinisaura cincosaltensis* is clearly nested among Iguanodontia (*Tenontosaurus* + Dryomorpha), sharing the follow derived features: 12) circular or ovate antorbital fossa, 13) small external antorbital opening, 14) parallel dorsal and ventral margins of the dentary (Fig. 11C–F), and 15) sinuous dorsal margin of the iliac blade (independently developed in *Heterodonthosaurus*; Santa Luca, 1980) (Fig. 12C–F).

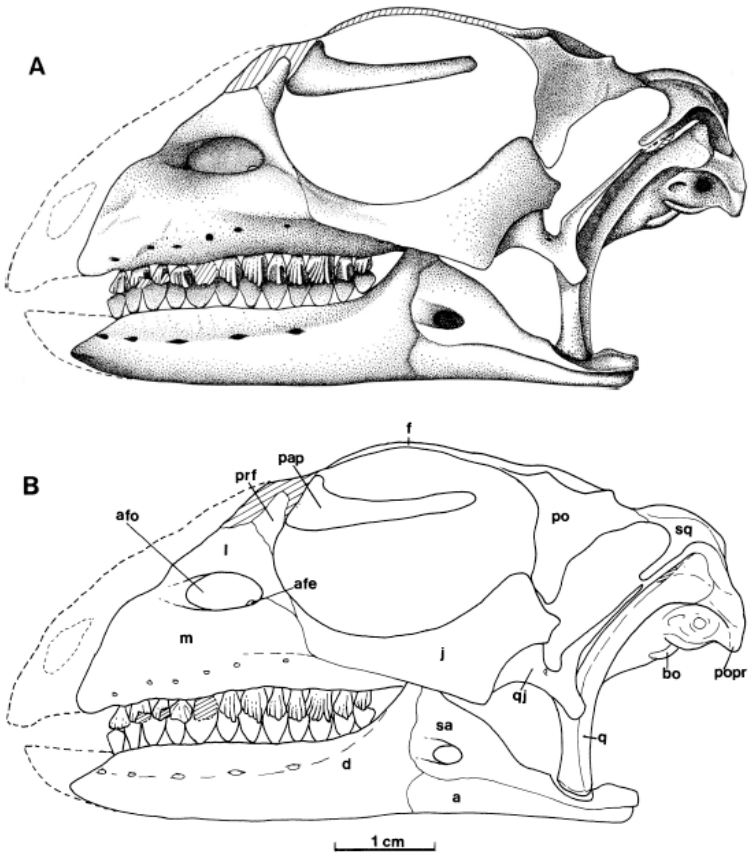

FIGURE 2. Skull of *Gasparinisaura cincosaltensis* (MUCPv-208, holotype) in lateral view (**A** and **B**). Abbreviations: **a**, angular; **afe**, antorbital fenestra; **afo**, antorbital fossa; **bo**, basioccipital; **d**, dentary; **f**, frontal; **j**, jugal; **l**, lacrimal; **m**, maxilla; **p**, parietal; **pap**, palpebral; **po**, postorbital; **popr**, paroccipital process; **prf**, prefrontal; **q**, quadrate; **qj**, quadratojugal; **sa**, surangular; **sq**, squamosal.

Elasmaria

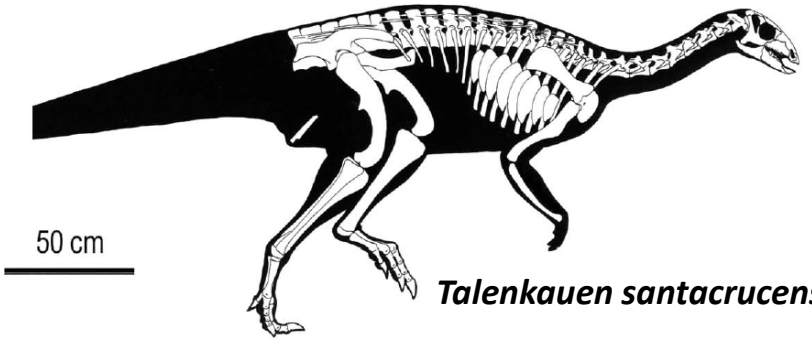

Talenkauen santacrucensis

Macrogryphosaurus gondwanicus

3- Reconstruction of *Macrogryphosaurus gondwanicus* sp.nov., including all preserved materials in white.

Gasparinisaura cincosaltensis

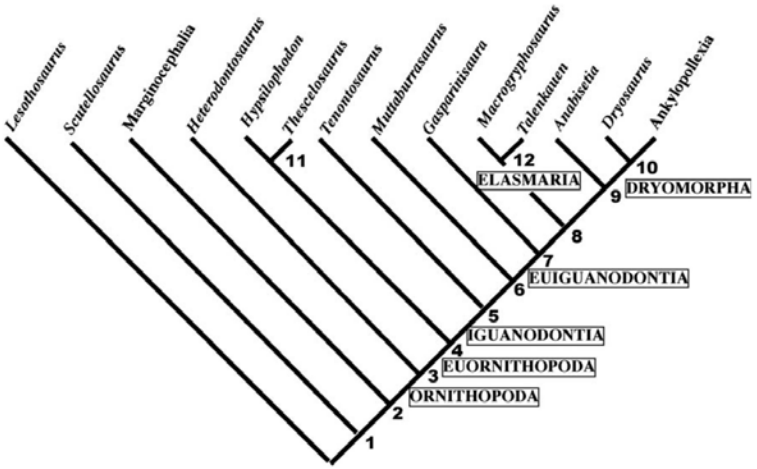

Fig.14- Cladogram depicting phylogenetic relationships of *Macrogryphosaurus gondwanicus* sp.nov. within ornithopoda, and the placement of Elasmaria. L = 88; CI = 0.625; RI = 0.742; RC = 0.463.

Calvo et al 2007

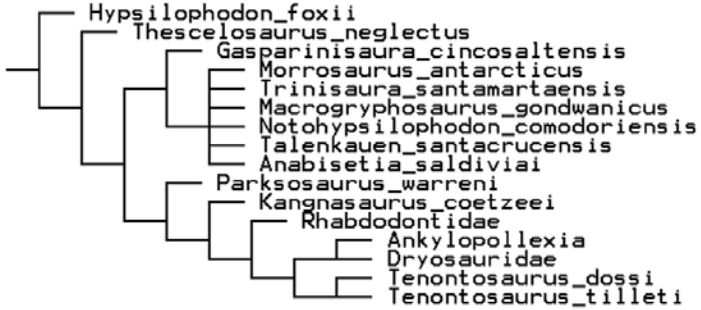

Fig. 7. Strict consensus tree showing derived iguanodontian interrelationships.

Rozadilla et al 2016

Clado Gondwánico?

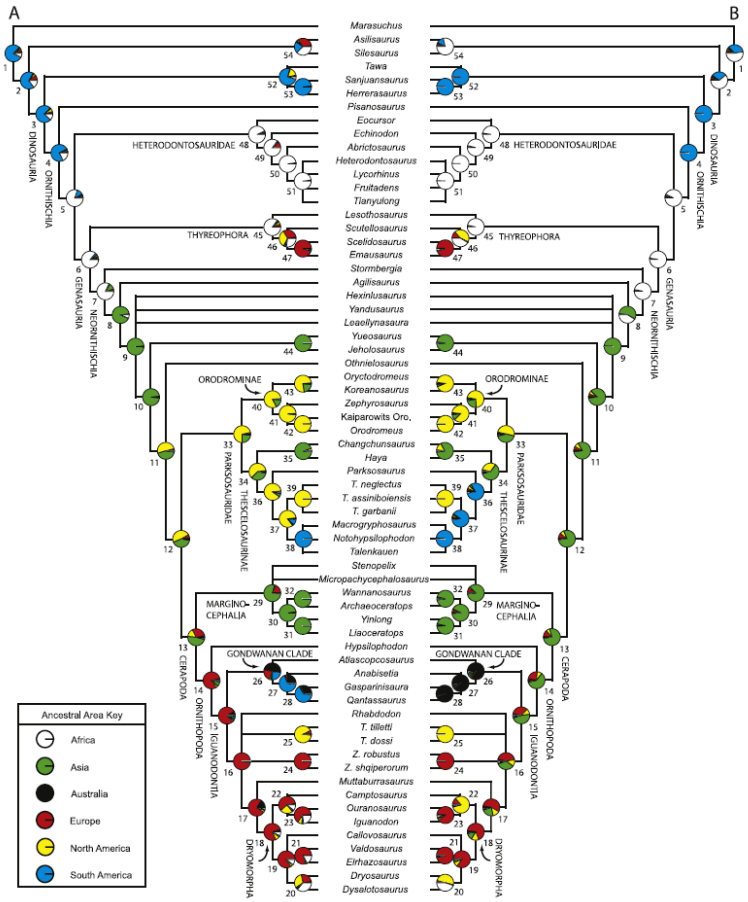

Figure 4 **Likelihood-based reconstructions of ancestral geographic areas.** Results obtained when all branch lengths were equal (A) versus results obtained when time calibrated branch lengths were included and set equal to inferred missing fossil records (B). Tree topology based on Fig. 2. The pie charts at each node represent the level of support for each ancestral area (See Table S5 for values). Each color represents a different geographic area (see key). Numbers next to nodes refer to Table S5.

Boyd 2015

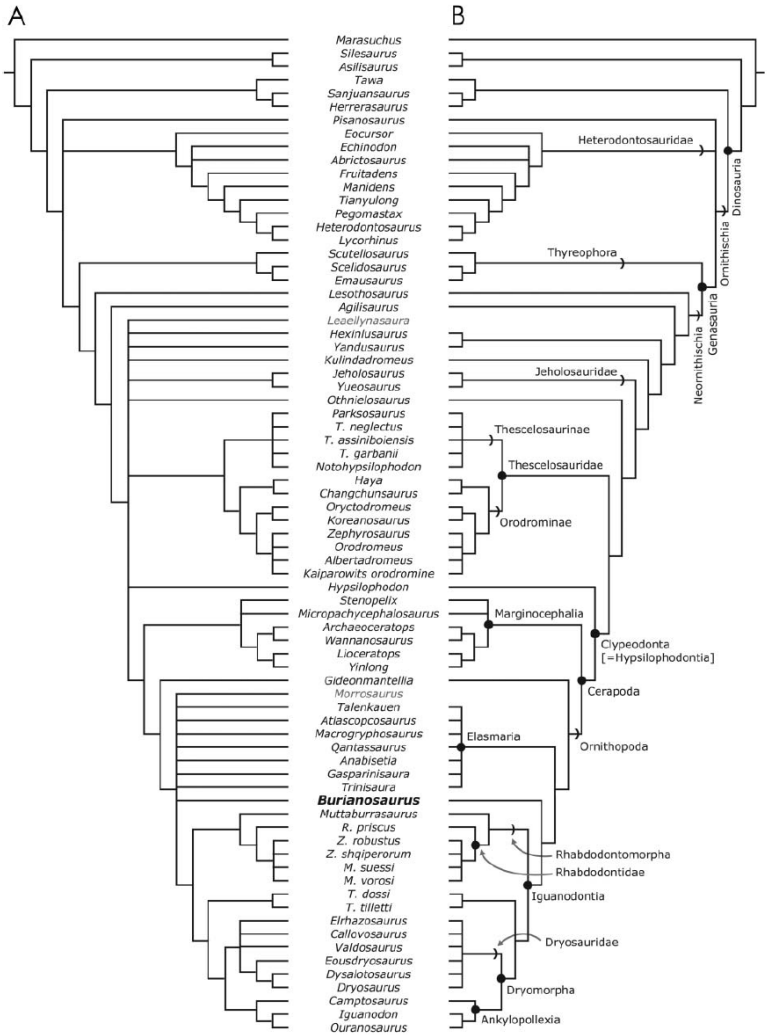

Figure 4. Topologies resulting from analysis of the modified Boyd (2015) data set of neornithischian dinosaur relationships. **A,** strict consensus topology calculated from 82,133 most parsimonious trees (MPTs) resulting from the analysis of the full data set. **B,** strict consensus topology calculated from 13,547 MPTs resulting from analysis of the data set after the removal of the operational taxonomic units (OTUs) *Leaellynasaura* and *Morrosaurus*.

Madzia et al 2018

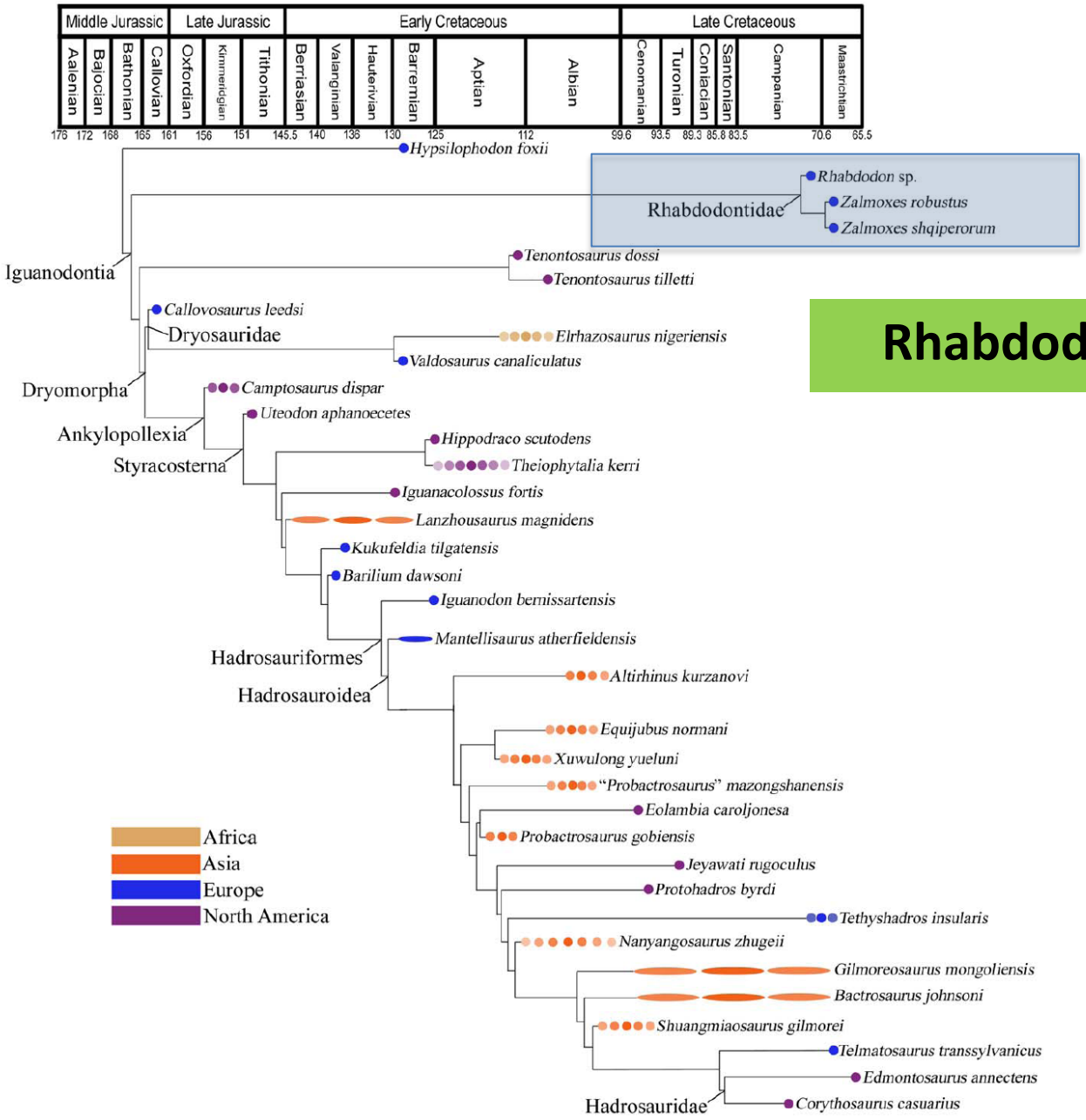

Rhabdodontidae

Figure 1. Phylogeny and Temporal and Geographical Occurrences of Basal Iguanodonts. Time-calibrated phylogeny of basal iguanodonts using the maximum agreement subtree of 16,270 MPTs calculated in PAUP. Timescale based upon Walker and Geissman [39]; numerical ages are in millions of years. Uncertainty in taxon ages indicated by lighter circles or ellipses. The branches leading to *Edmontosaurus* and *Corythosaurus* have been extended into the Santonian to reflect the probable age of the oldest known hadrosaurid, the lambeosaurine *Aralosaurus* [9,40].
doi:10.1371/journal.pone.0036745.g001

Rhabdodontidae

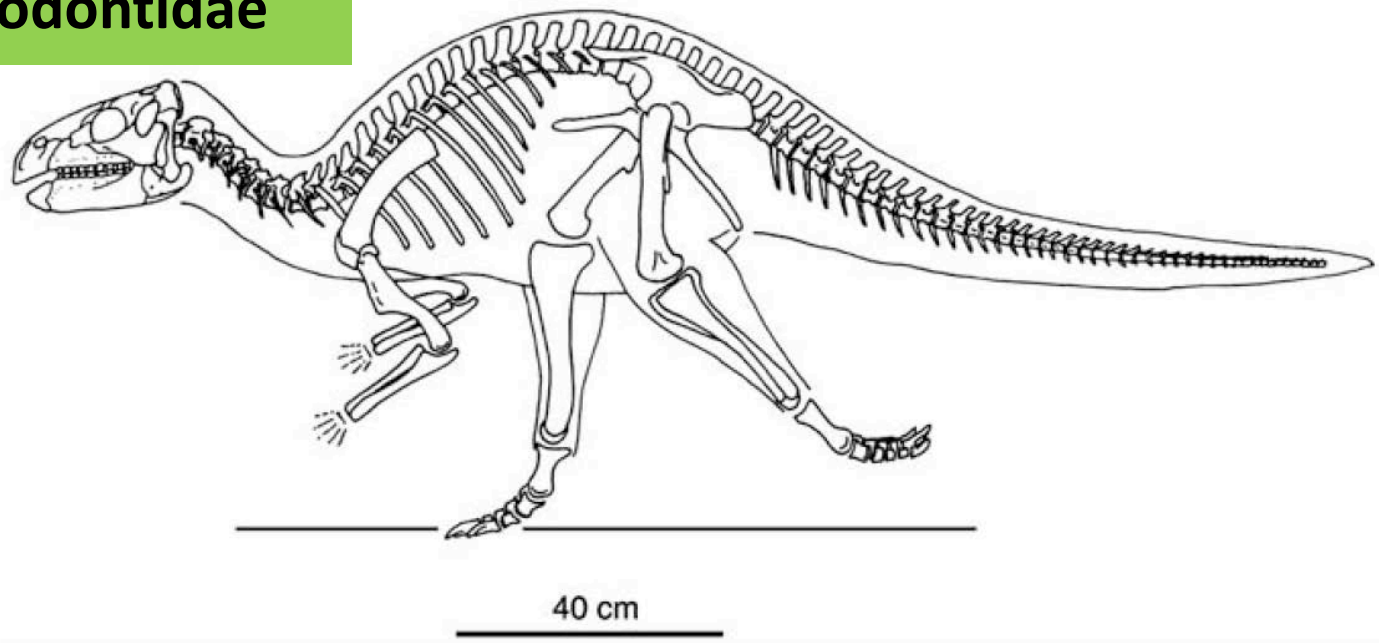

Figure 36 Skeletal reconstruction of *Zalmoxes robustus*. The vertebral count in the presacral and caudal series is based on *Hypsilophodon foxii* (Galton 1974b).

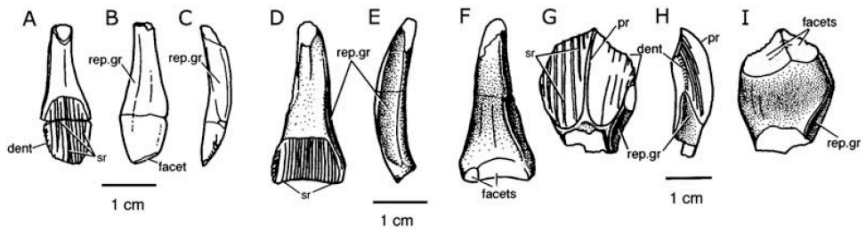

Figure 13 *Zalmoxes robustus*. Maxillary tooth (FGGUB R.0022) in buccal (**A**), lingual (**B**: showing single, small wear facet) and mesial (**C**) views. Maxillary tooth (FGGUB R.0022) in buccal (**D**), mesial (**E**) and lingual (**F**: showing two wear facets) views. Dentary tooth (FGGUB R.0006) in lingual (**G**), mesial (**H**) and buccal (**I**: showing two wear facets) views. Abbreviations: dent = marginal denticles on crown; facet(s) = wear facets; pr = primary ridge; rep.gr = grooves to accommodate the margins of crowns of replacement teeth; sr = secondary ridges.

RHABDODONTIDAE novum

DIAGNOSIS. A node-based taxon consisting of the most recent common ancestor of *Zalmoxes robustus* and *Rhabdodon priscus* and all the descendants of this common ancestor. It is diagnosed by the following features: more than 12 sharp ridges on the lingual side of the crowns of the dentary teeth, a straight to slightly convex dorsal margin of the ilium in lateral view and a distinctly bowed femur in anterior view. Potential apomorphies of Rhabdodontidae also include strong twisting of the preacetabular process of the ilium, a narrow, poorly defined acetabular margin on the ilium and the absence of metatarsal V.

Rhabdodontidae

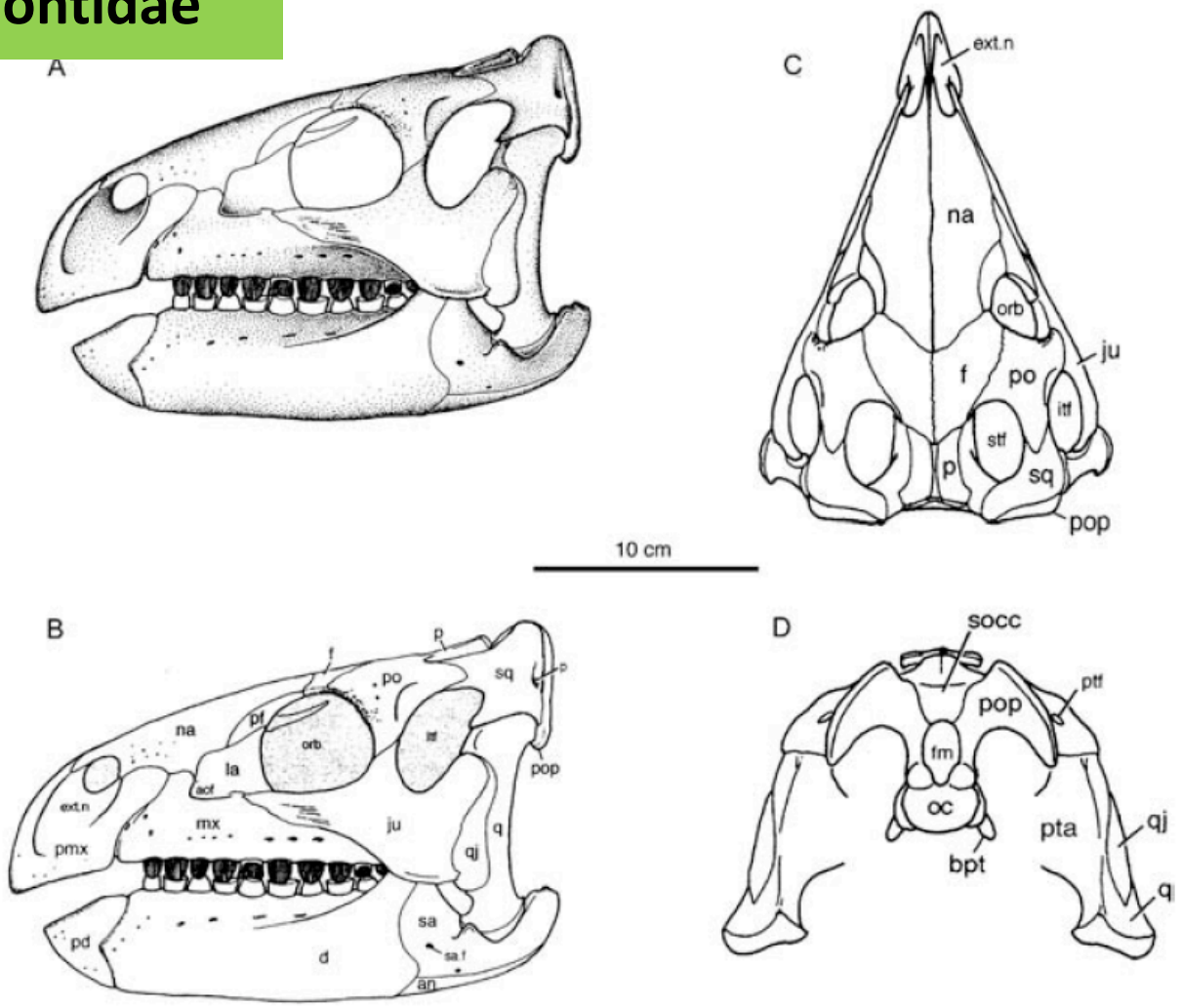

Figure 2 *Zalmoxes robustus*. **A.** Skull reconstruction in left lateral view. **B.** Outline with labelled features. **C.** Skull reconstruction in dorsal view. **D.** Skull reconstruction in occipital view. Abbreviations: an = angular; aof = external antorbital fenestra; bpt = basipterygoid process; d = dentary; ext.n = external naris; f = frontal; fm = foramen magnum; itf = infratemporal fenestra; ju = jugal; la = lacrimal; mx = maxilla; na = nasal; oc = occipital condyle; orb = orbital cavity; p = parietal; pd = predentary; pf = prefrontal; pmx = premaxilla; po = postorbital; pop = paroccipital process; pta = pterygoid ala of quadrate; ptf = post-temporal foramen; q = quadrate; qj = quadratojugal; sa = surangular; sa.f = surangular fenestra; socc = supraoccipital; sq = squamosal; stf = supratemporal fenestra.

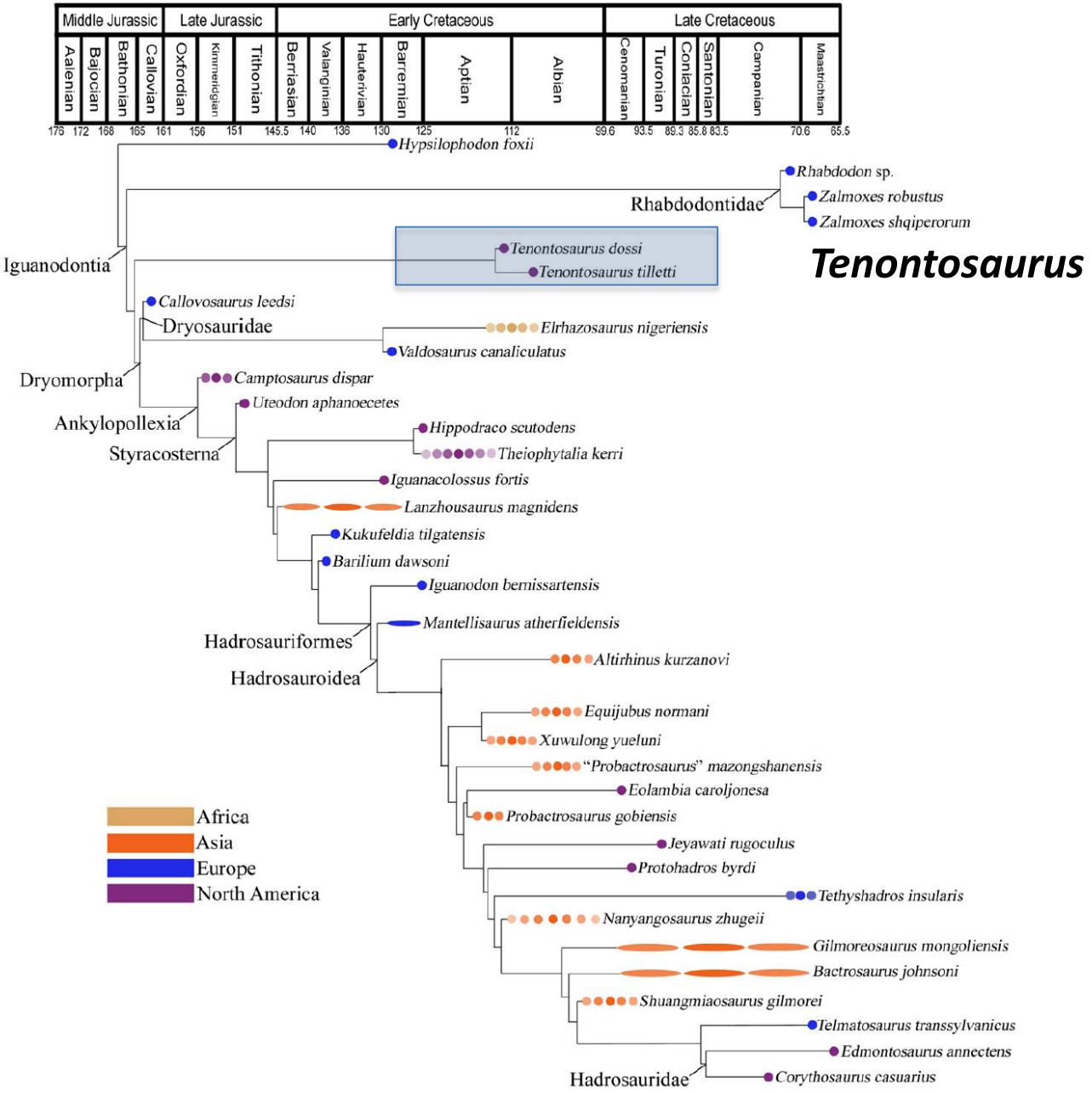

Figure 1. Phylogeny and Temporal and Geographical Occurrences of Basal Iguanodonts. Time-calibrated phylogeny of basal iguanodonts using the maximum agreement subtree of 16,270 MPTs calculated in PAUP. Timescale based upon Walker and Geissman [39]; numerical ages are in millions of years. Uncertainty in taxon ages indicated by lighter circles or ellipses. The branches leading to *Edmontosaurus* and *Corythosaurus* have been extended into the Santonian to reflect the probable age of the oldest known hadrosaurid, the lambeosaurine *Aralosaurus* [9,40].
doi:10.1371/journal.pone.0036745.g001

Tenontosaurus (6,5-8 mts)

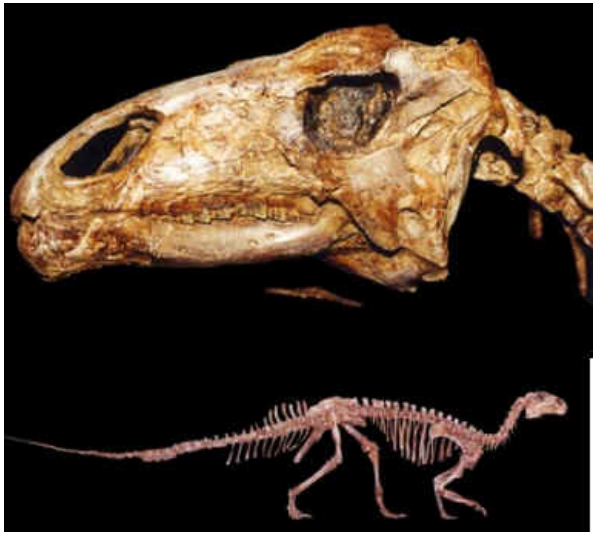

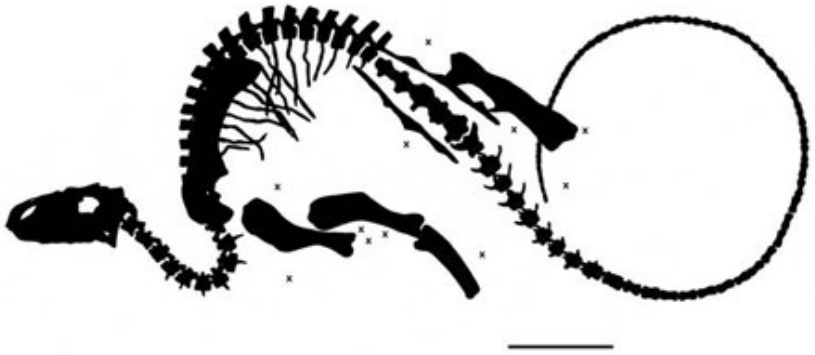

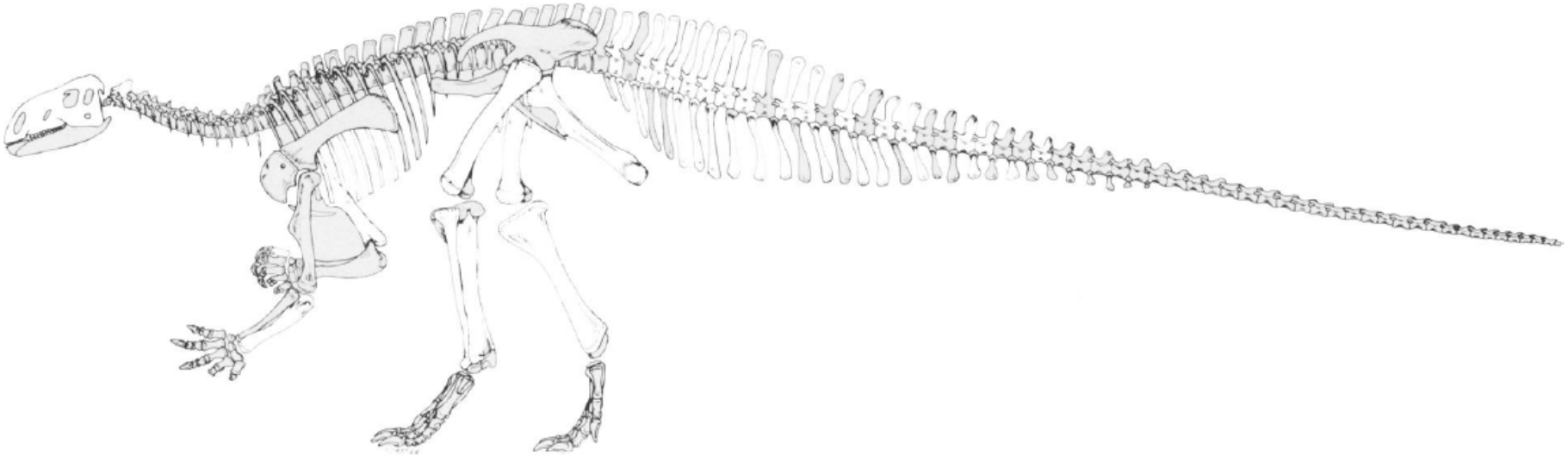

FIGURE 23. Reconstruction of the skeleton of *Tenontosaurus tilletti*.

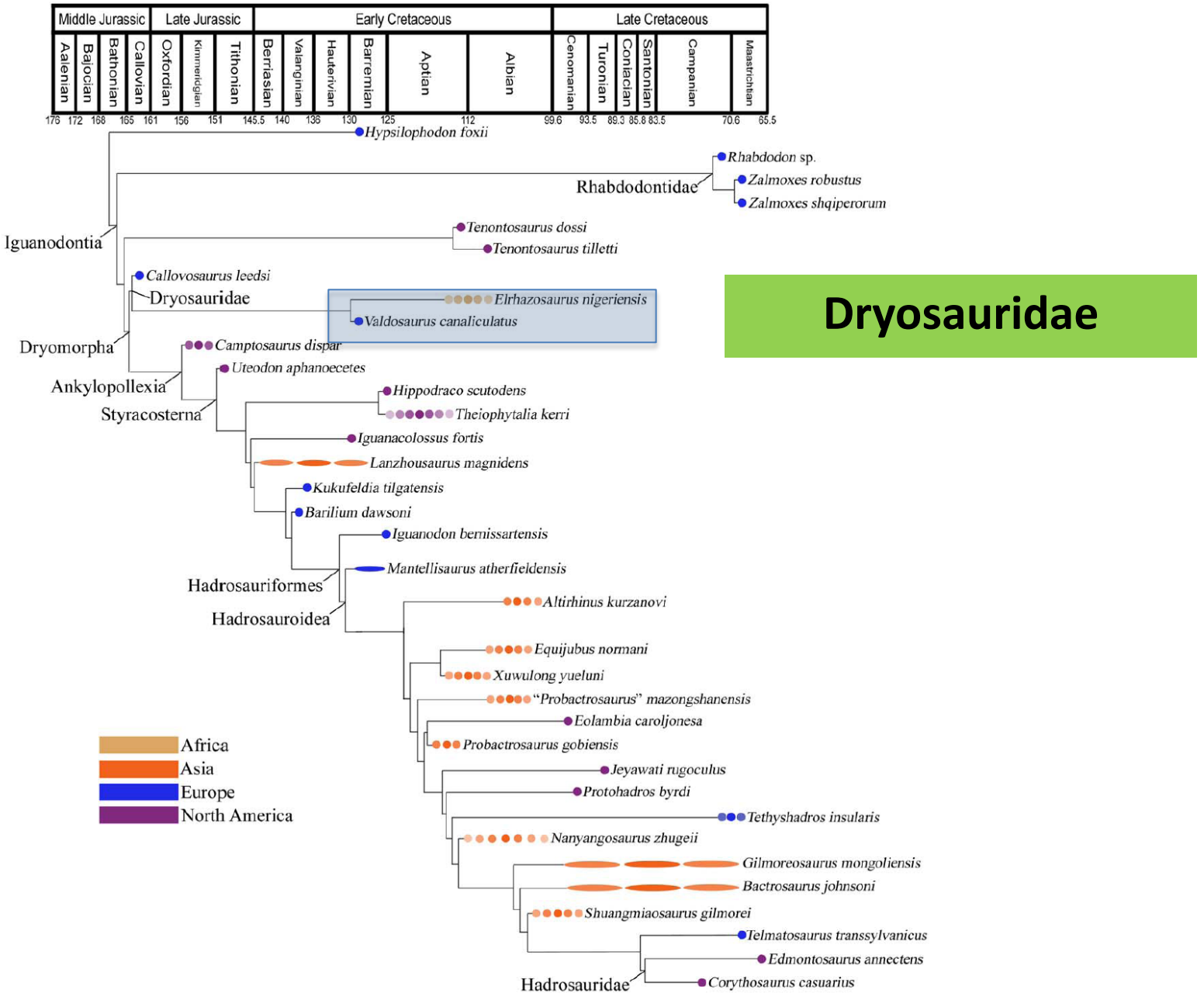

Dryosauridae

Figure 1. Phylogeny and Temporal and Geographical Occurrences of Basal Iguanodonts. Time-calibrated phylogeny of basal iguanodonts using the maximum agreement subtree of 16,270 MPTs calculated in PAUP. Timescale based upon Walker and Geissman [39]; numerical ages are in millions of years. Uncertainty in taxon ages indicated by lighter circles or ellipses. The branches leading to *Edmontosaurus* and *Corythosaurus* have been extended into the Santonian to reflect the probable age of the oldest known hadrosaurid, the lambeosaurine *Aralosaurus* [9,40].
doi:10.1371/journal.pone.0036745.g001

Dryosauridae

TEXT-FIG. 11. Time-calibrated strict component consensus tree generated by reanalysis of the McDonald *et al.* (2010) iguanodontian dataset. Full details of the analysis can be found in the text and in the Electronic Supplement. Dryosauridae is highlighted in the grey box: outline maps adjacent to taxa indicate provenance. Abbreviations: Alb, Albian; Apt, Aptian; Baj, Bajocian; Bar, Barremian; Ber, Berriasian; Cam, Campanian; Cen, Cenomanian; E, Early; Hau, Hauterivian; Kim, Kimmeridgian; L, Late; M, Middle; Maa, Maastrichtian; Oxf, Oxfordian; Tth, Tithonian; Tur, Turonian.

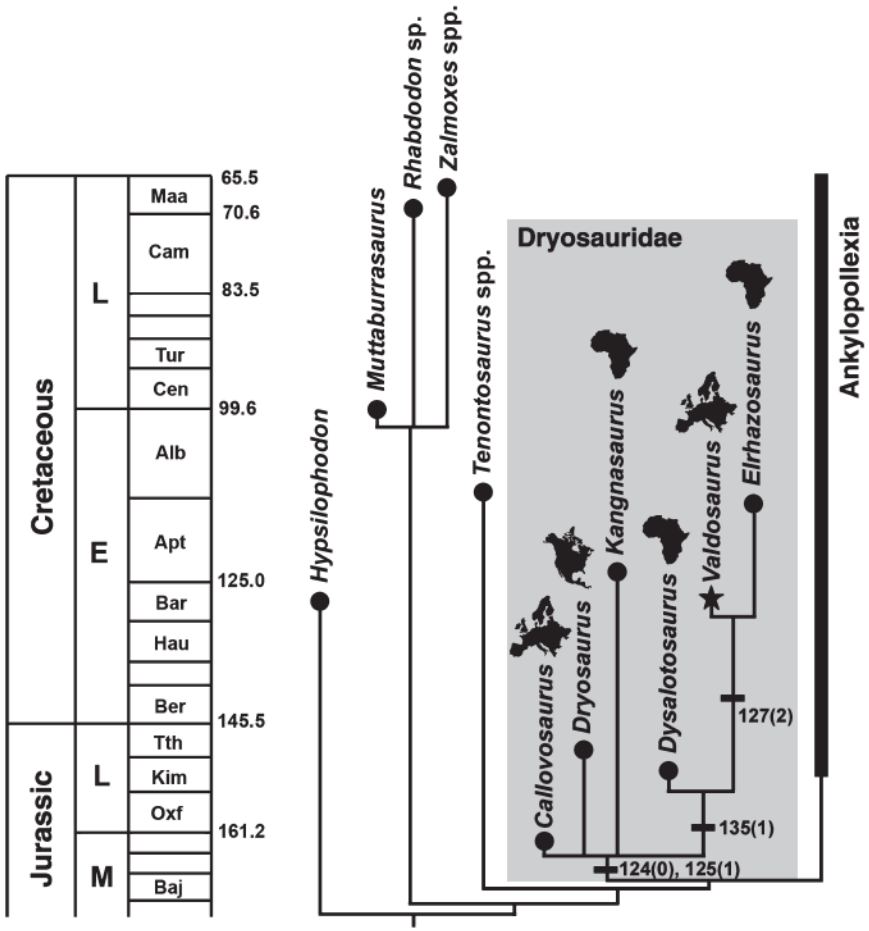

Dryosaurus

(2,5-5 mts)

Ankylopollexia

Los demás Iguanodontia conocidos pertenecen a la Ankylopollexia (Pulgar acorazado). Los Ankylopollexia se caracterizan por poseer una garra ungual cónica defensiva en el primer dedo de la mano, con la primer falange del dígito I ausente (posiblemente fusionada) o comprimida, en forma de disco. También poseen una articulación pleurokinética más desarrollada

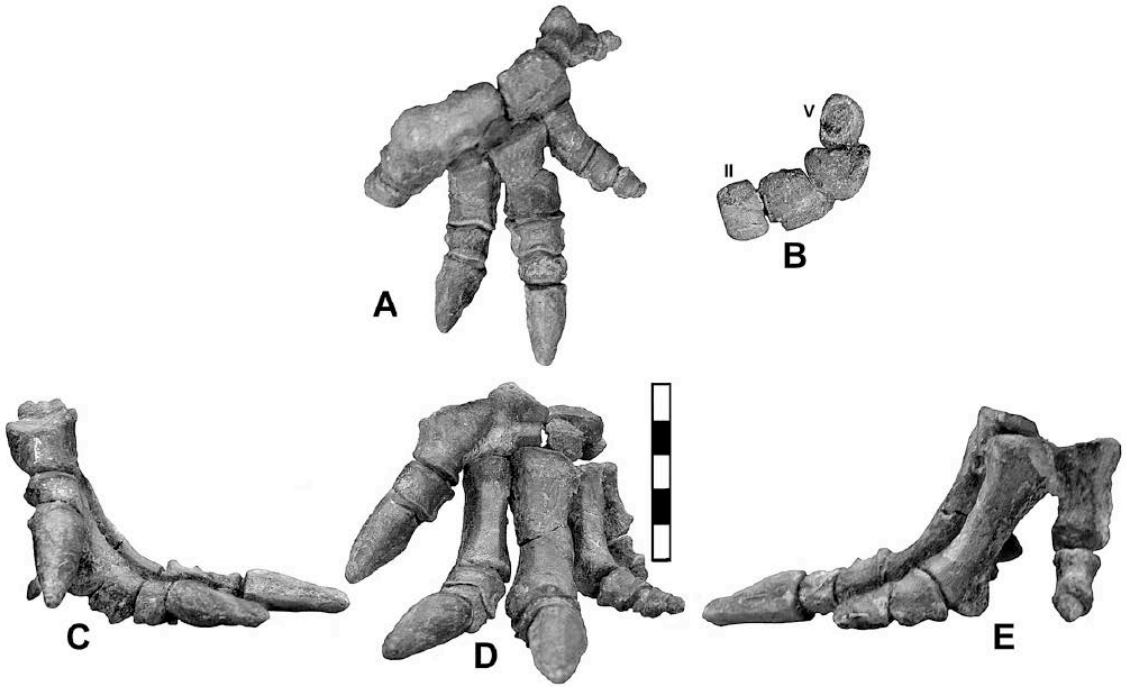

Fig. 46.—Reconstructed manus and wrist of *Camptosaurus aphanoecetes*. **A,** dorsal view; **B,** dorsal view of metacarpals in articulation (metacarpal I is fused to the radiale and is not included); **C,** medial view; **D,** extensor side; **E,** lateral view. Note the divergence of digit IV relative to digit III caused by the wedge shape of metacarpal IV in B. Scale units are cm.

ORNITHOPODA

Styracosterna

Greatly enlarged nares; much larger size; ~~Spike thumb~~; metacarpals II-IV hoof-like; metacarpal V opposable

Camptosauridae

Dryosauridae

Ankylopollexia

Well-developed pleurokinetic hinge

Spike thumb

Rhabdodontidae

Tenontosaurus

Dryomorpha

Thescelosauridae

Hypsilophodontidae

Iguanodontia

Larger size; Premaxilla toothless; Enlarged naris; 6 or more sacrals

Marginocephalia

Othnielosaurus

ORNITHOPODA

Premaxillary lower margin ventral to maxillary tooth row; Mandibular articulation ventral to dentary tooth row; Pleurokinetic hinge joint in cranium

Cerapoda

~~Senasauria~~

Neornithischia

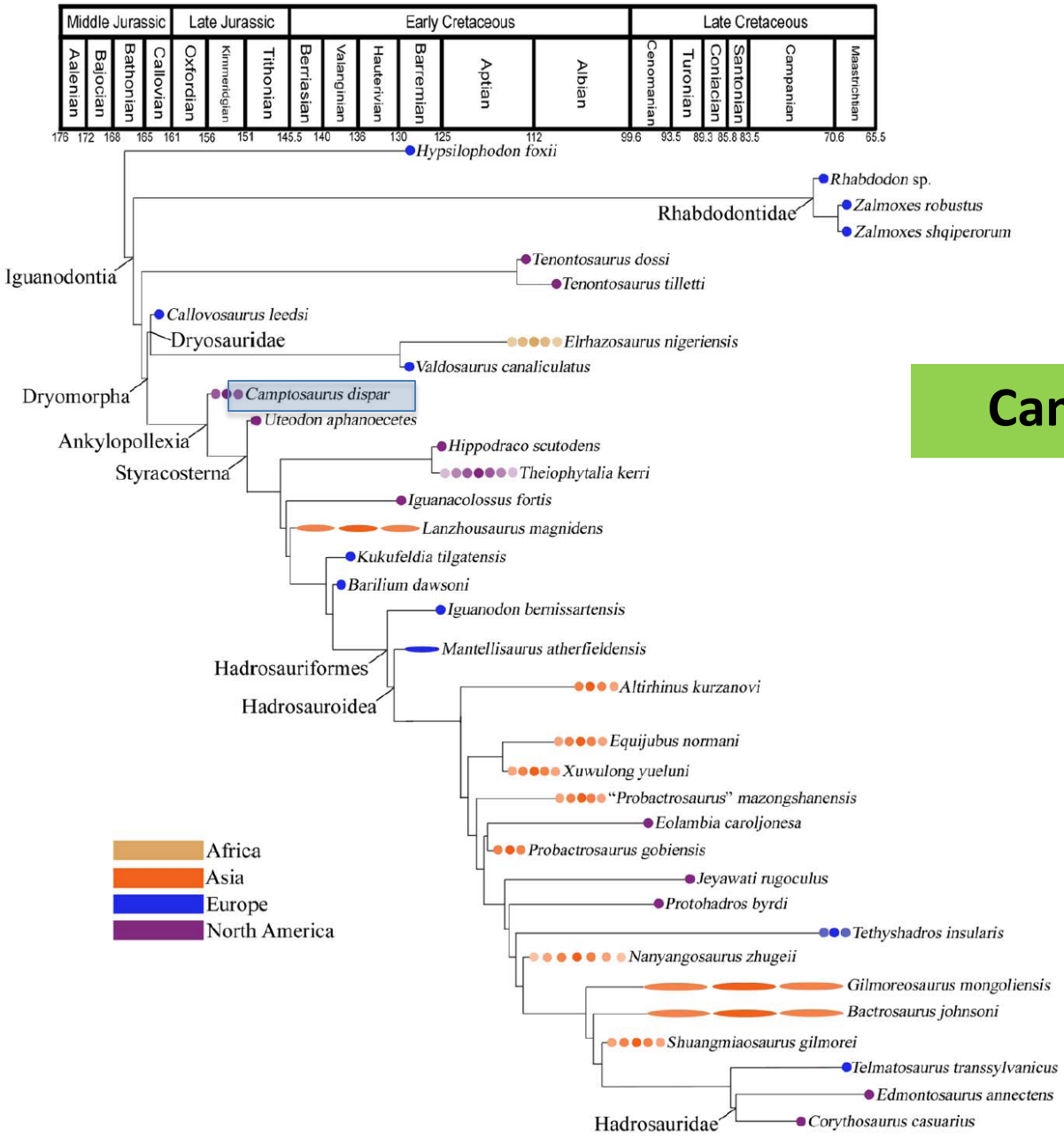

Camptosauridae

Figure 1. Phylogeny and Temporal and Geographical Occurrences of Basal Iguanodonts. Time-calibrated phylogeny of basal iguanodonts using the maximum agreement subtree of 16,270 MPTs calculated in PAUP. Timescale based upon Walker and Geissman [39]; numerical ages are in millions of years. Uncertainty in taxon ages indicated by lighter circles or ellipses. The branches leading to *Edmontosaurus* and *Corythosaurus* have been extended into the Santonian to reflect the probable age of the oldest known hadrosaurid, the lambeosaurine *Aralosaurus* [9,40].
doi:10.1371/journal.pone.0036745.g001

Camptosauridae

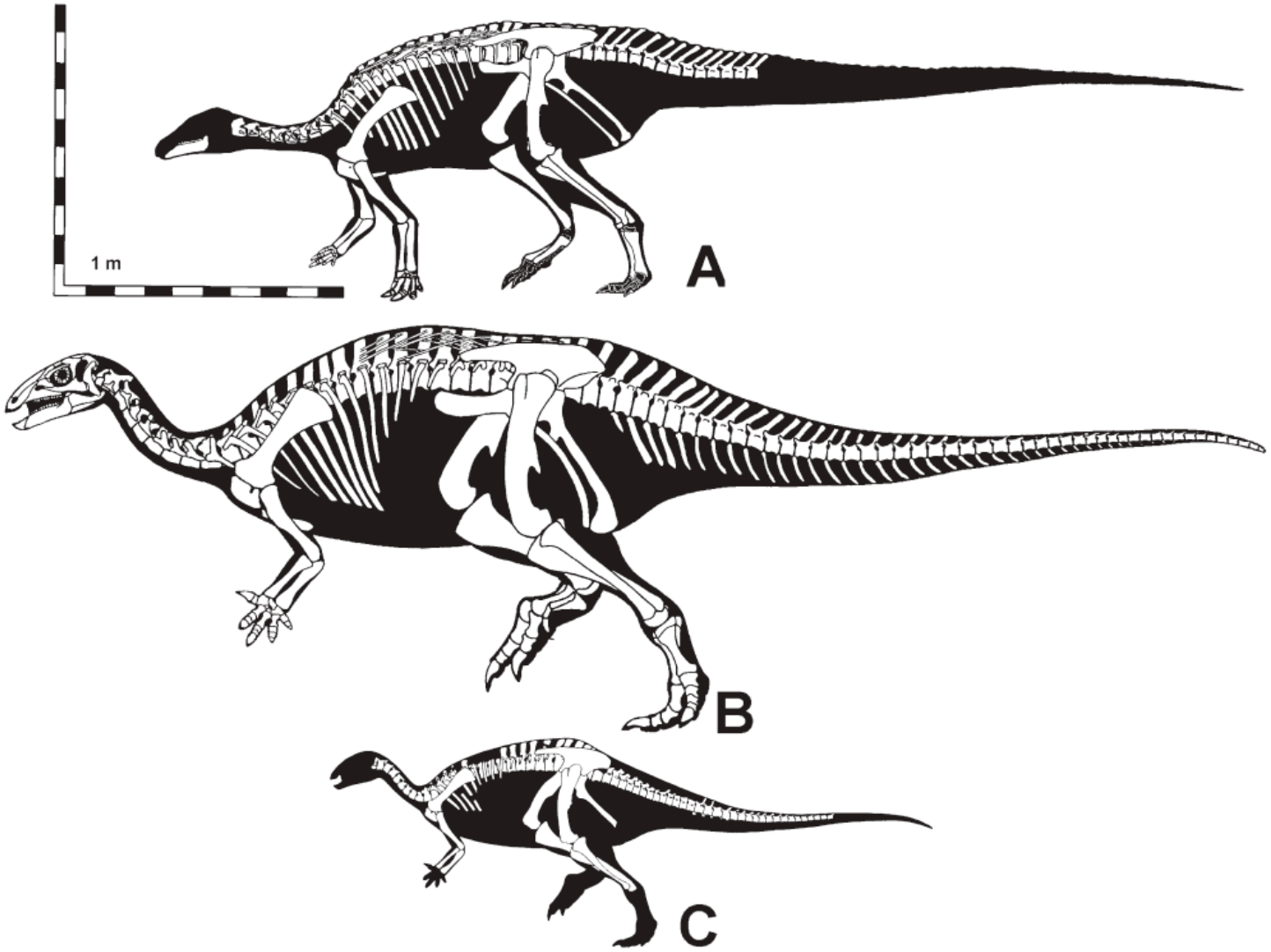

Fig. 34.—Skeletal reconstructions of *Camptosaurus*. **A,** *C. aphanoecetes*; **B,** *C. dispar* (adult); **C,** *C. dispar* (juvenile based on USNM 2210, holotype *C. nanus*). B, C courtesy of Gregory Paul.

Styracosterna

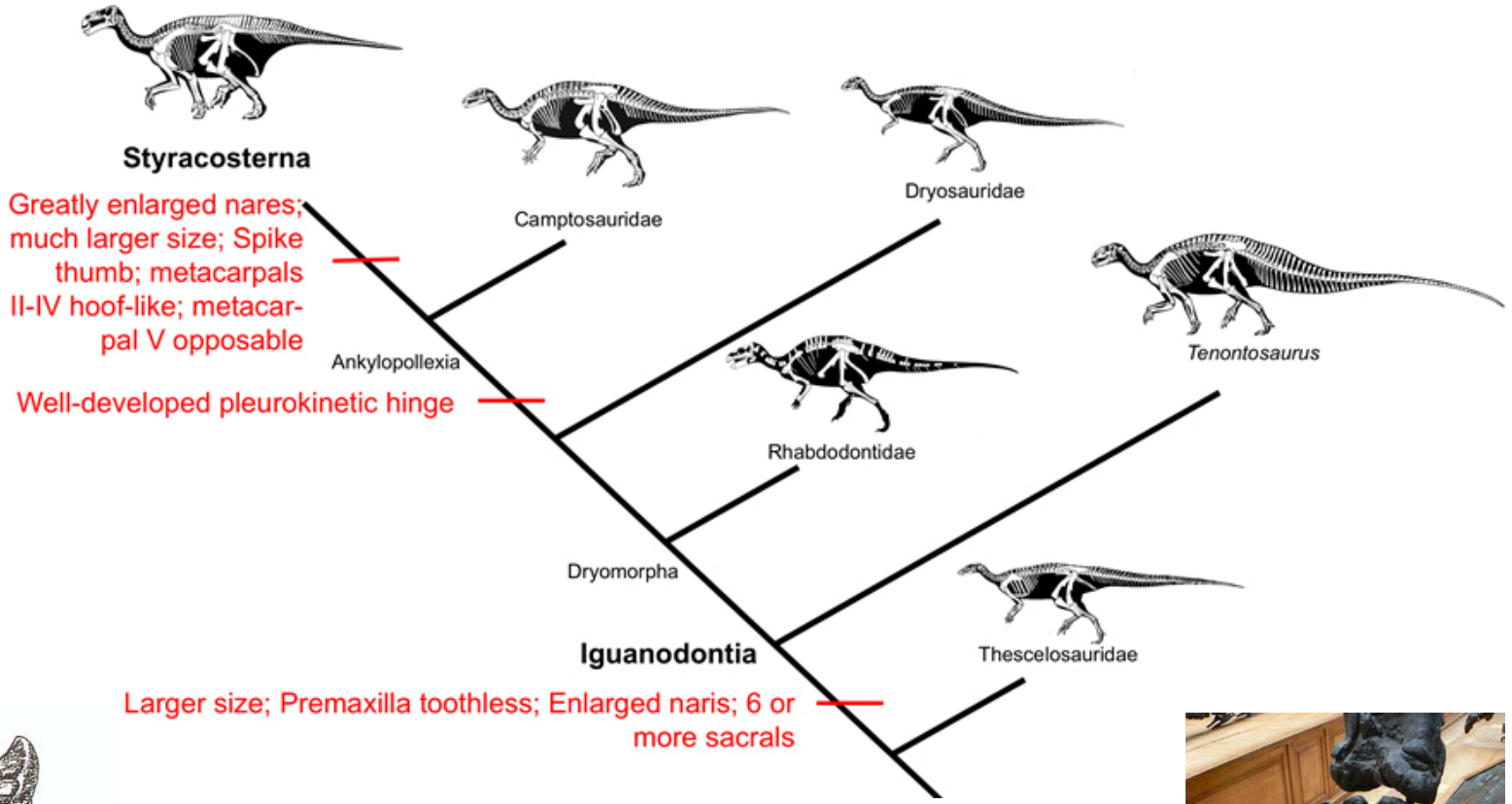

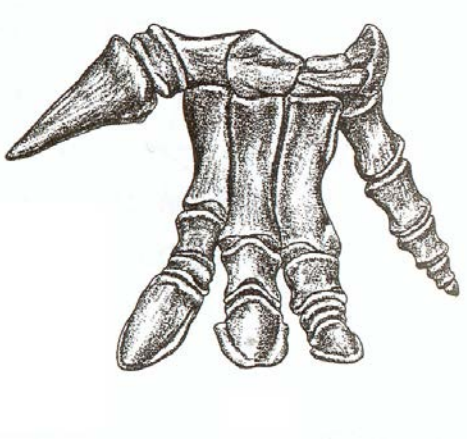

Pulgar-espina más desarrollada, pezuñas en dedos 2-4, y dedo 5 oponible

Pérdida de las falanges del dedo 1 del pie
(tb perdidas en Gasparinisaura y Dryosauridae, pero aún presentes en Tenontosaurus y Camptosauridae)

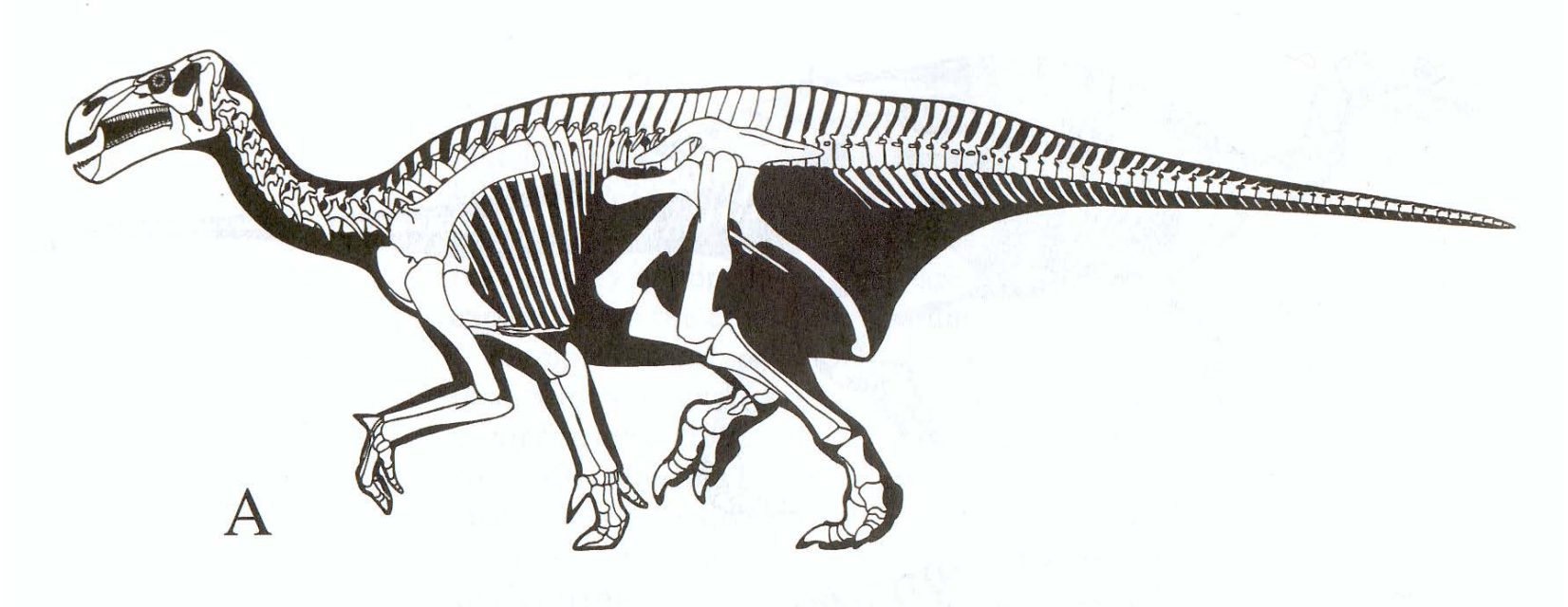

Iguanodon

Ouranosaurus presenta rostro distal expandido + o - cuadrangular (“pico de pato”), espinas neurales altas.
Algunos dicen que es más cercano a hadrosauria

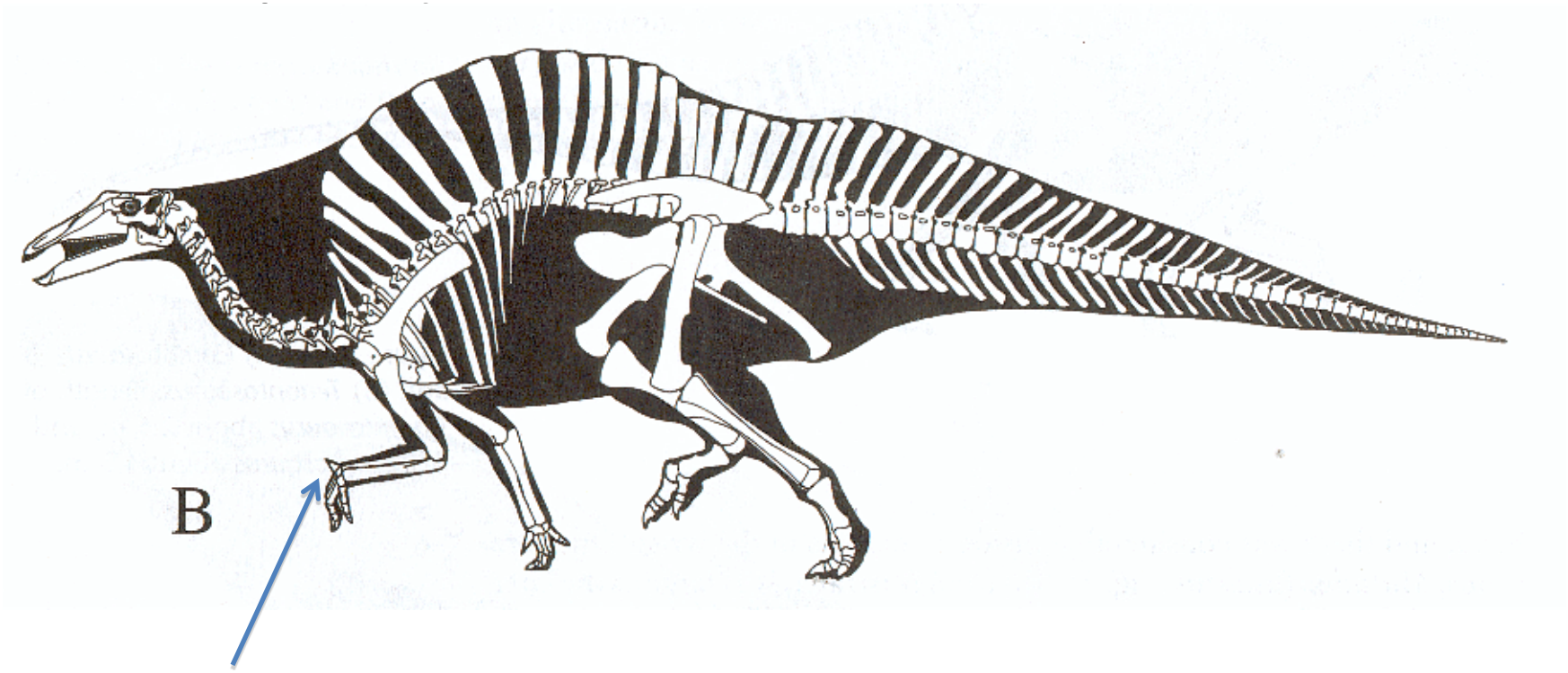

Pulgar-espina aún presente

Ouraunosaurus

Hadrosauroidea Cope, 1869

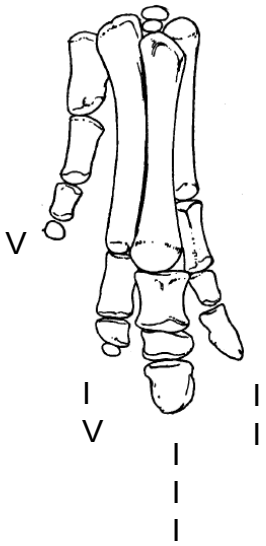

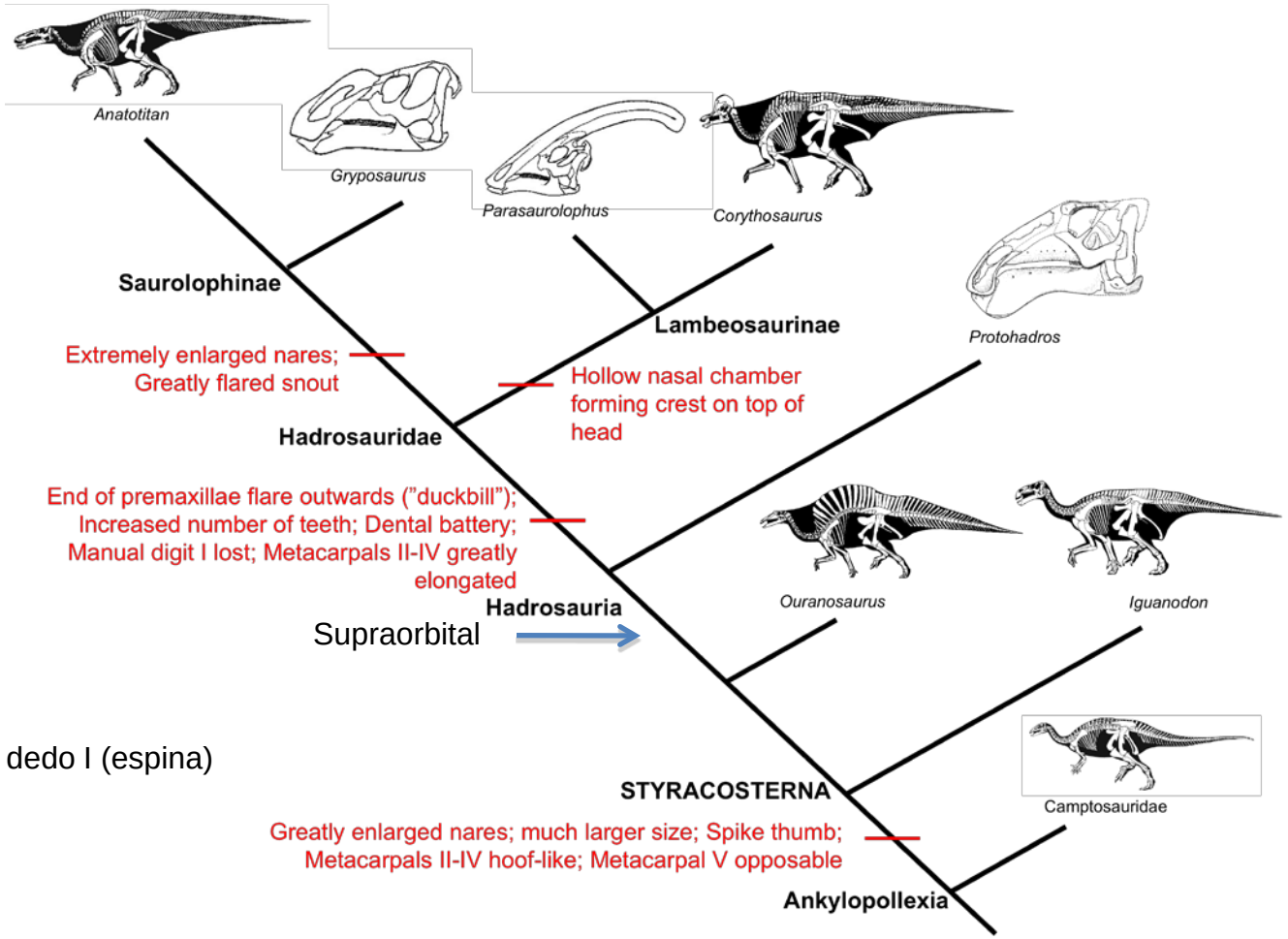

Mano de Hadrosauria: pérdida dedo I (espina)

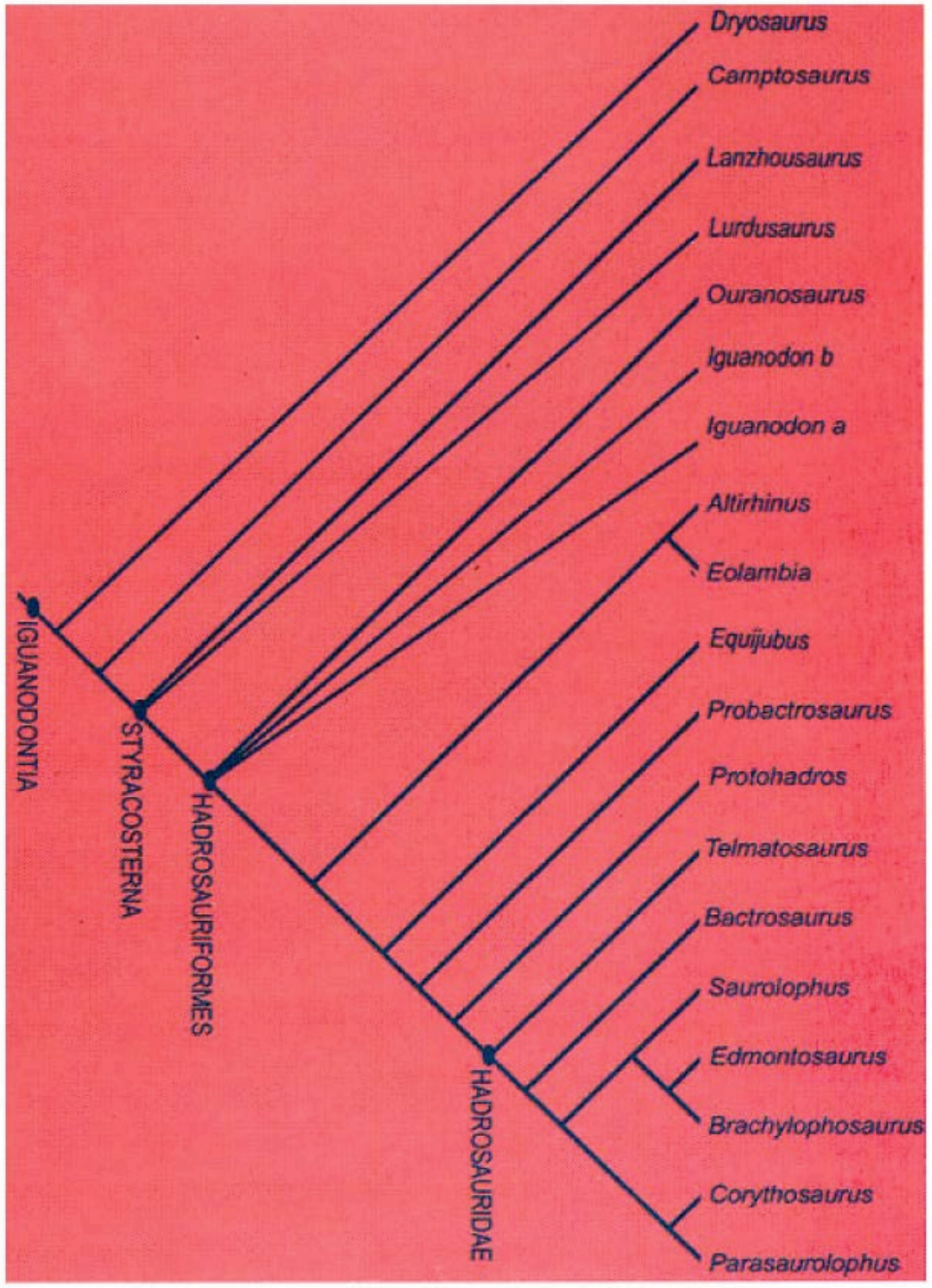

Formas con espina-pulgar indican la presencia de este rasgo en los ancestros de hadrosauria (que lo han perdido secundariamente)

Antiguamente se asumía que todas estas formas eran un grupo hermano a hadrosauria (Iguanodontidae)

Origen de hueso supraorbital de **Hadrosauria** a partir del palpebral

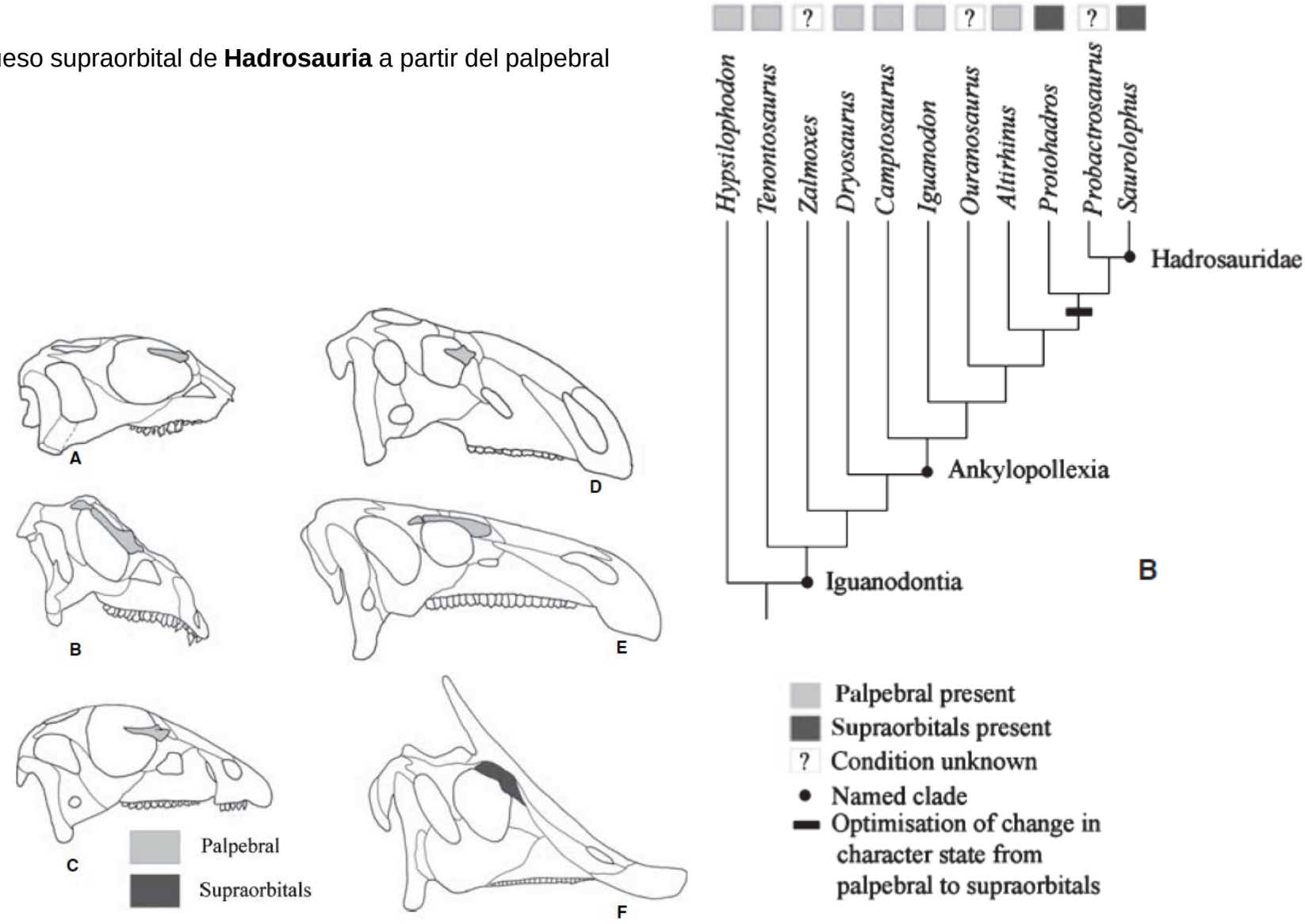

Fig. 7. Skulls of non-marginocephalian neornithischians in lateral view. A,B, skulls of non-cerapodan neornithischians (after Barrett *et al.* 2005); A, *Hexinlusaurus multidens,* ZDM T6001; B, *Agilisaurus louderbacki,* ZDM T6011. C–F, reconstructions of the skulls of ornithopods; C, *Hypsilophodon foxii* (after Norman *et al.* 2004a); D, *Tenontosaurus tilletti* (after Norman 2004); E, *Iguanodon bernissartensis* (after Norman 1980); F, *Saurolophus angustirostris* (after Maryanska & Osmólska 1981). Not to scale.

Filogenia de Hadrosauria

Hadrosaurios basales: muchos se pensaron más cercano a Iguanodon (ej, probactrosaurus)

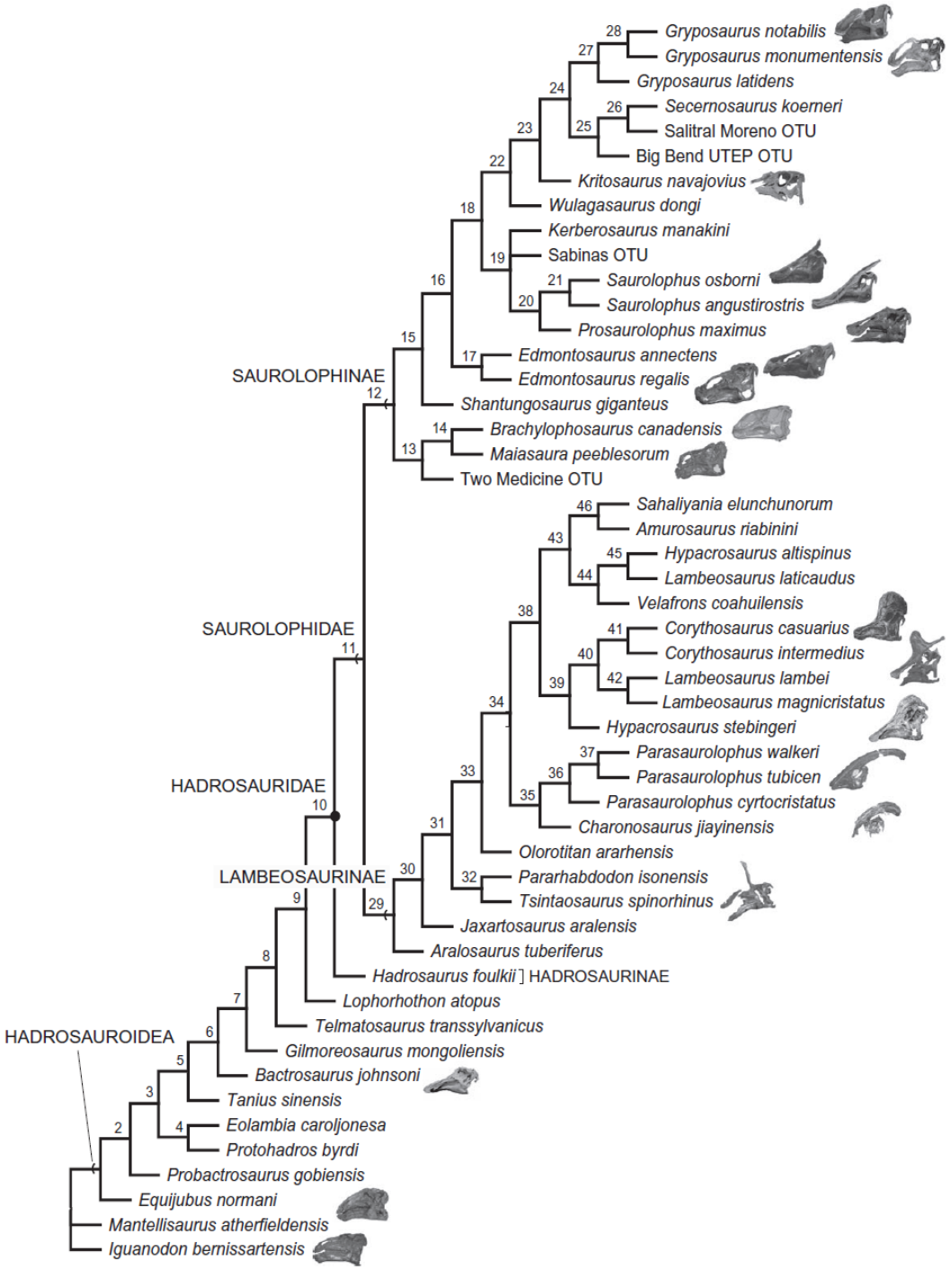

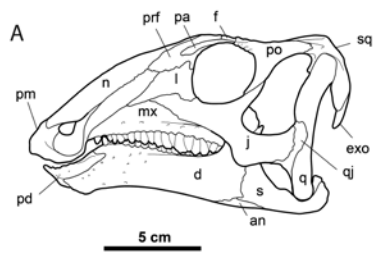

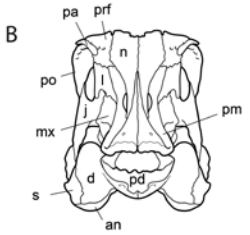

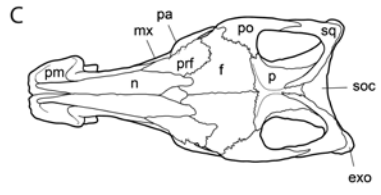

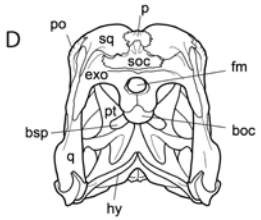

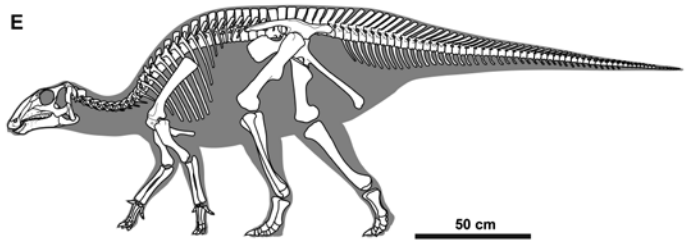

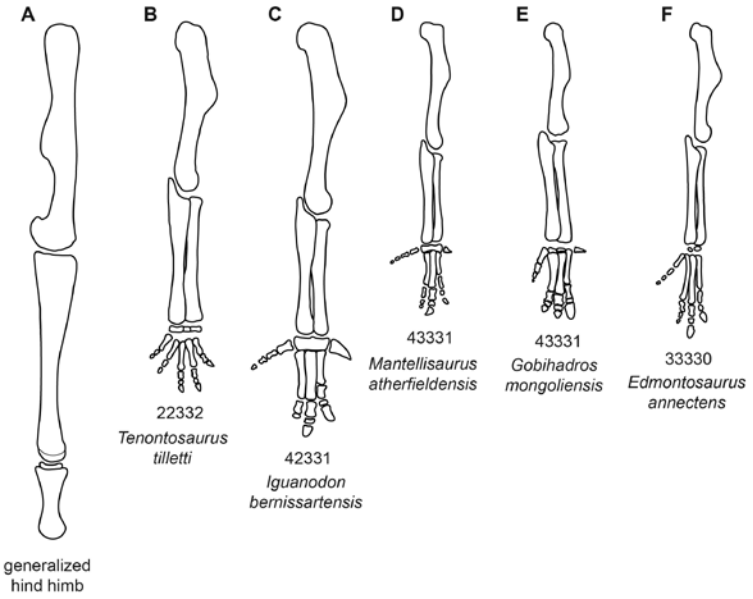

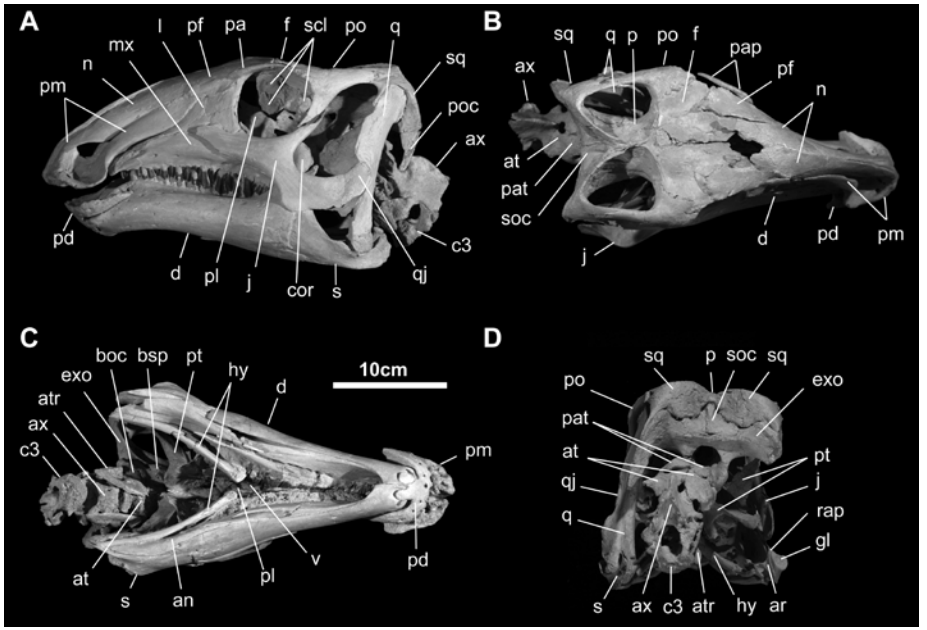

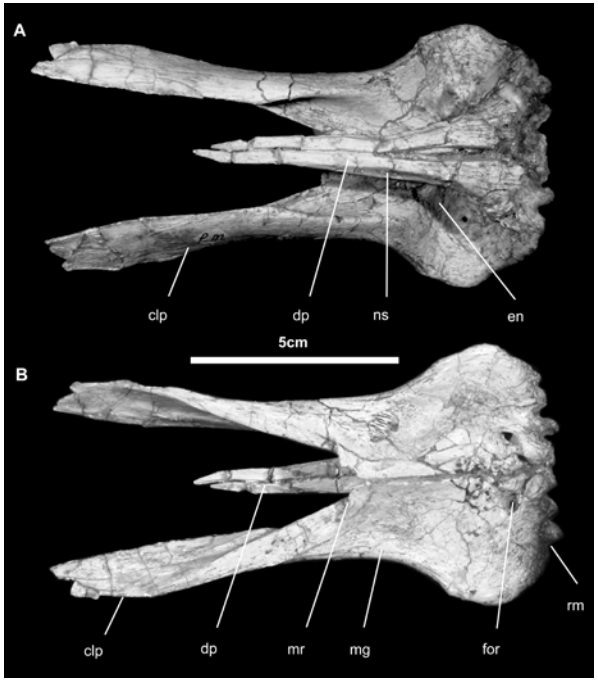

Unpublished, No tomar fotos!!!

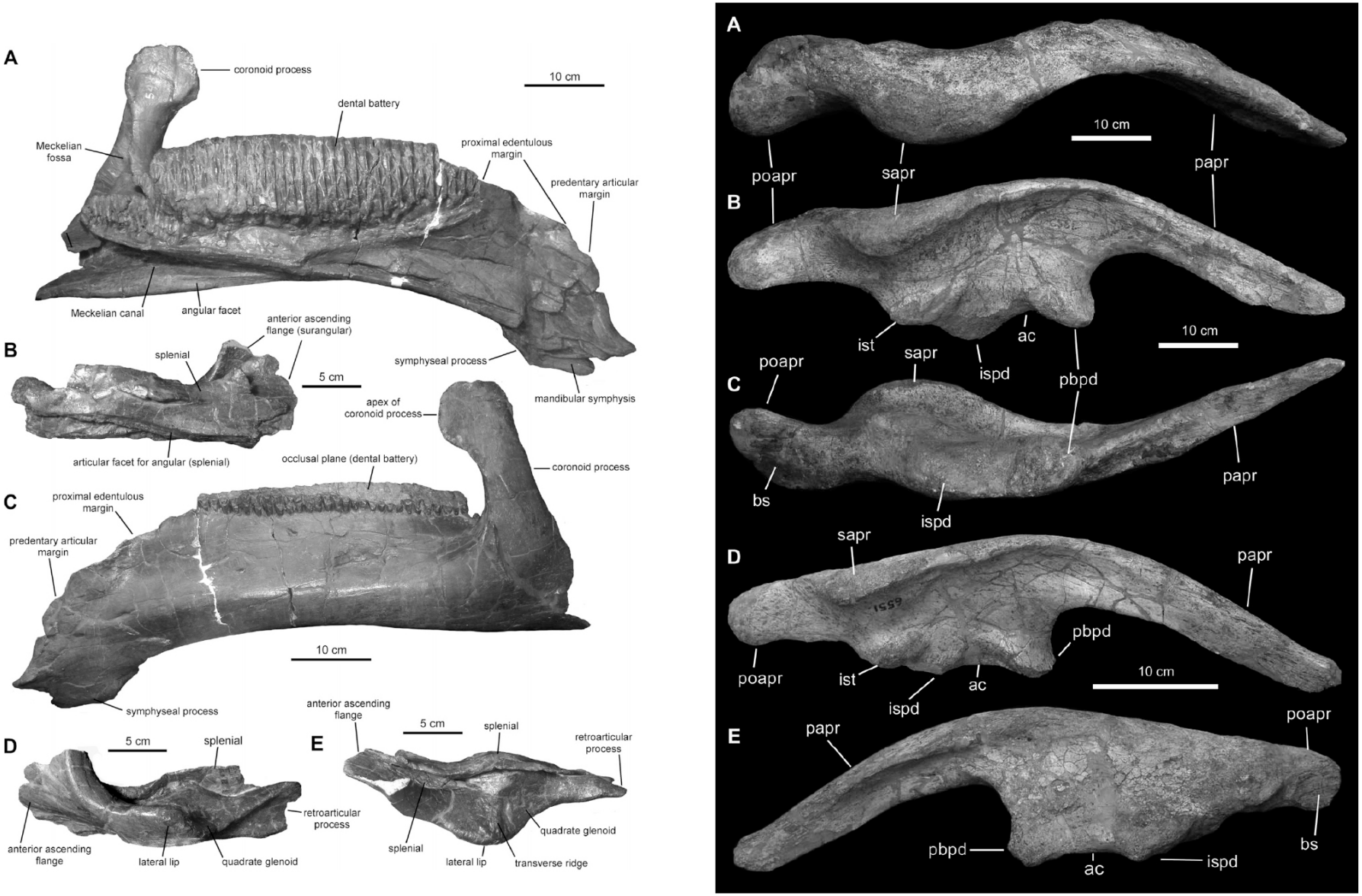

FIGURE 13. Selected pelvic elements of *Gilmoreosaurus mongoliensis*. **A–C,** right ilium (lectotype, AMNH FARB 30735) in dorsal, lateral, and ventral views. **D–E,** right ilium (AMNH FARB 30736) in lateral and medial views. Abbreviations in appendix 2.

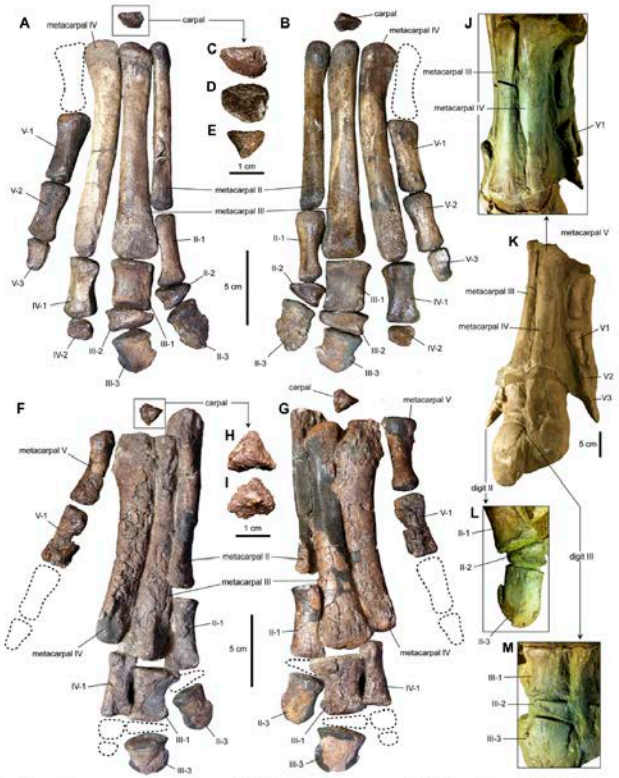

Fig. 10. Manus of *Edmontosaurus annectens*. A and B, Right manus of LACM 23504 in dorsal and palmar views, respectively. C–E, Right carpal element of LACM 23504. D is shown in proximal view. C and E being orthogonal to D. F and G, left manus of LACM 23504 in palmar and dorsal views, respectively. H and I, Left carpal element of LACM 23504 displayed in two undetermined views orthogonal to each other. J–M, Dorsal views of the left manus of SM R4036.

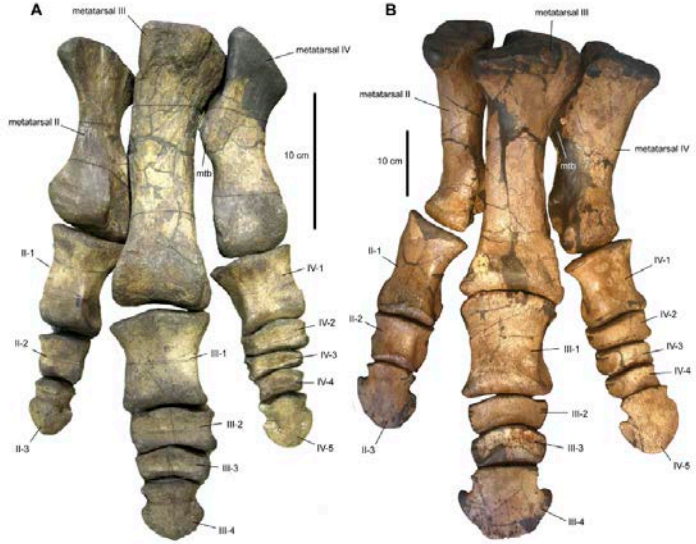

Fig. 14. Pedes of *Edmontosaurus annectens*. A, Left pes of LACM 23504 in dorsal view. B, Left pes of LACM 23502 in dorsal view.

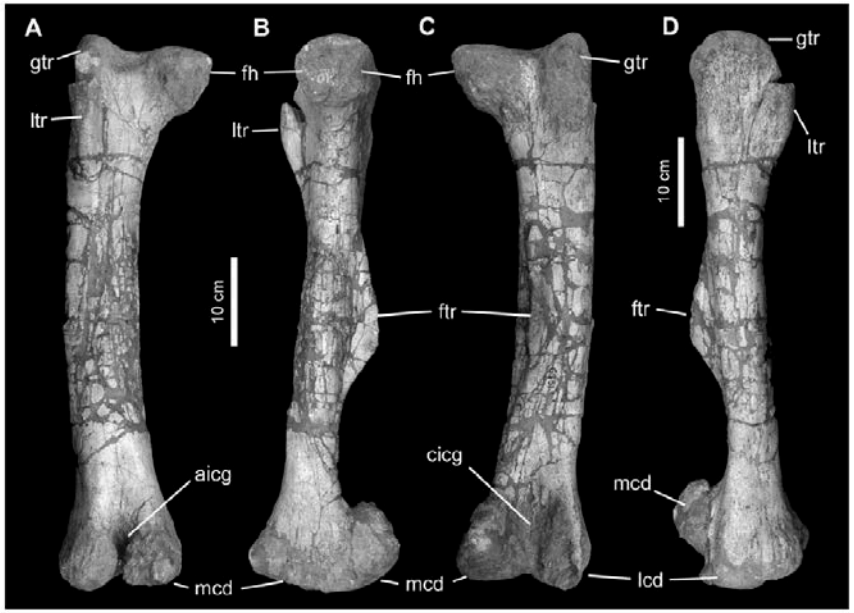

FIGURE 15. Right femur of *Gilmoreosaurus mongoliensis* (AMNH FARB 30741). **A**, anterior; **B**, medial; **C**, posterior; **D**, lateral. Abbreviations in appendix 2.

Figure 14. *Magnapaulia laticaudus*, **humeri.** LACM 17715 (holotype), right humerus in craniomedial (A), caudal (B), caudolateral (C), and cranial (D) views. LACM 17712, partial right humerus in craniomedial (E) and caudal (F) views. LACM 17716, right humerus in craniomedial (G) and caudal (H) views.

Marginocephalia

Definición: Todos los cerápodos más cercanos a *Triceratops horridus* que a *Parasaurolophus walkeri*.

Conenido: Ceratopsia y Pachycephalosauria

Sinapomorfías:

1) Reborde Parietoescamosal en la parte posterior del techo craneal.
2) Espciamiento entre acetábulos.
3) Ausencia de proceso obturador del ísquion.
4) Exclusión del premaxilar en narinas externas.
5) Proceso anterior dle pubis dorsoventralmente plano.

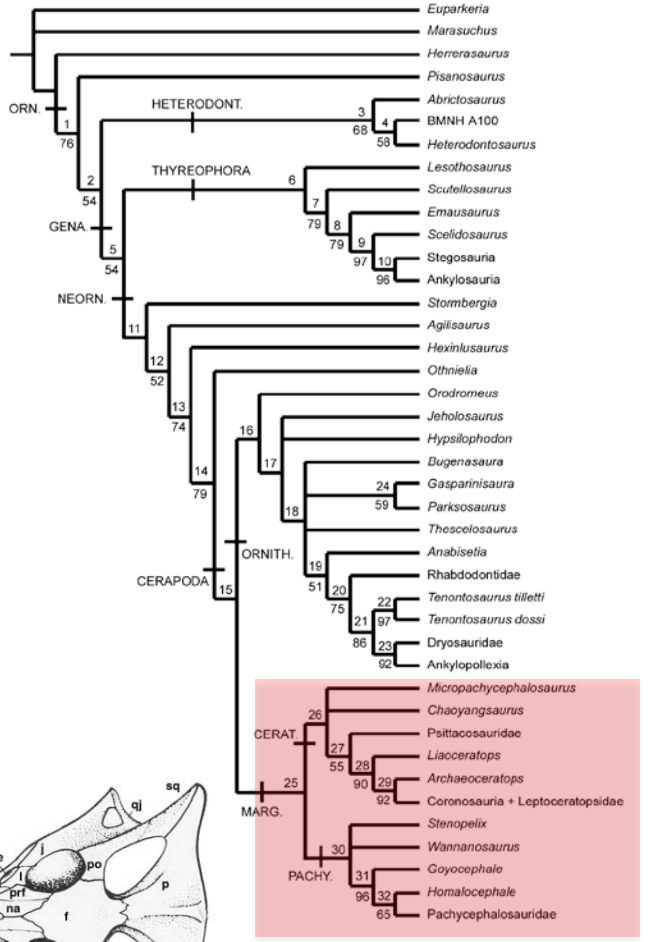

Three key characters have been identified by previous authors (Sereno 1984, 1986, 1987, 1999*a*, 2000; Cooper 1985; Maryańska & Osmólska 1985) as supporting marginocephalian monophyly: posterior expansion of the parietosquamosal obscures the occiput in dorsal view, premaxillae excluded from the border of the internal nares, postpubis reduced or absent (Characters 68, 84, 188/189, Appendix

A number of other potential marginocephalian synapomorphies are identified here. Unambiguous synapomorphies include: absence of elliptic fossa on the nasals (although a fossa is present in at least one basal ceratopsian, *Liaoceratops yanzigouensis*), three premaxillary teeth, elongate and strap-like scapula blade and the absence of an obturator process on the ischium (Characters 19, 112, 150, 184, Appendix 2). ACCTRAN indicates additional potential synapomorphies, most of which have rather uncertain distributions and suffer from missing data. For example, node-like ornamentation is present on the jugal–postorbital bar and angular (Characters 41, 108, Appendix 2) of pachycephalosaurs and the basal ceratopsians *Chaoyangsaurus youngi* and *Archaeoceratops oshimai*. However, the distribution of this character remains uncertain as ornamentation is absent in other basal ceratopsians such as Psittacosauridae.

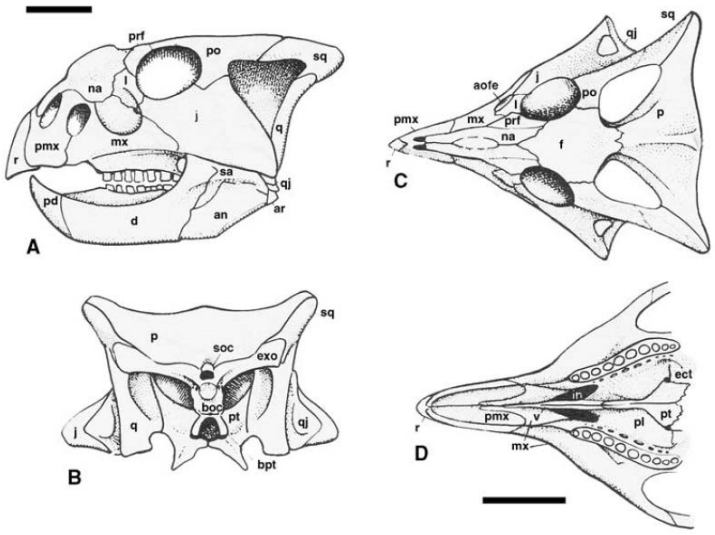

FIGURE 22.3. Skull of *Bagaceratops rozhdestvenskyi:* A, lateral; B, occipital; C, dorsal; and D, palatal views. Scale = 5 cm. (After Maryańska and Osmólska 1975.)

- 15 sinapomorfías según Han et al 2017.
- Grupo hermano de Heterodontosauridae ? (Xu et al 2006): solo un rasgo.

MARGINOCEPHALIA

Leptoceratopsidae

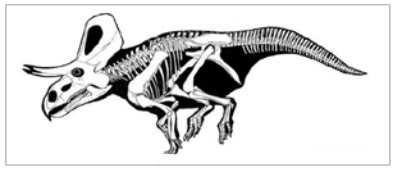

Zuniceratops

Ceratopsidae

Protoceratopsidae

Even larger size; Nasal horn; Shearing dental battery

Ceratopsoidea

Psittacosauridae

Larger size; Postorbital horns

Coronosauria

Enlarged frill; Enlarged skull; Obligate quadrupedality

Archaeoceratops

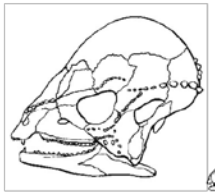

Quadrupedality

Pachycephalosauridae

Neoceratopsia

Homalocephale

Frill

Dome

Ceratopsia

Thickened skull roof; Small ossifications along ridge of skull

Pachycephalosauria

Rostral bone; Jugals form pointed “horns”

Ornithopoda

MARGINOCEPHALIA

Shelf of bone extending back over occipital region of skull

Genasauria

Ceratopsia

Definición: Todos los marginocéfalos más cercanos a *Triceratops horridus* que a *Pachycephalosaurus wyomingensis.*

Sinapomorfías:

1) presencia de un hueso rostral en la punta anterior del cráneo, lo cual les otorga su apariencia de "pico de loro".

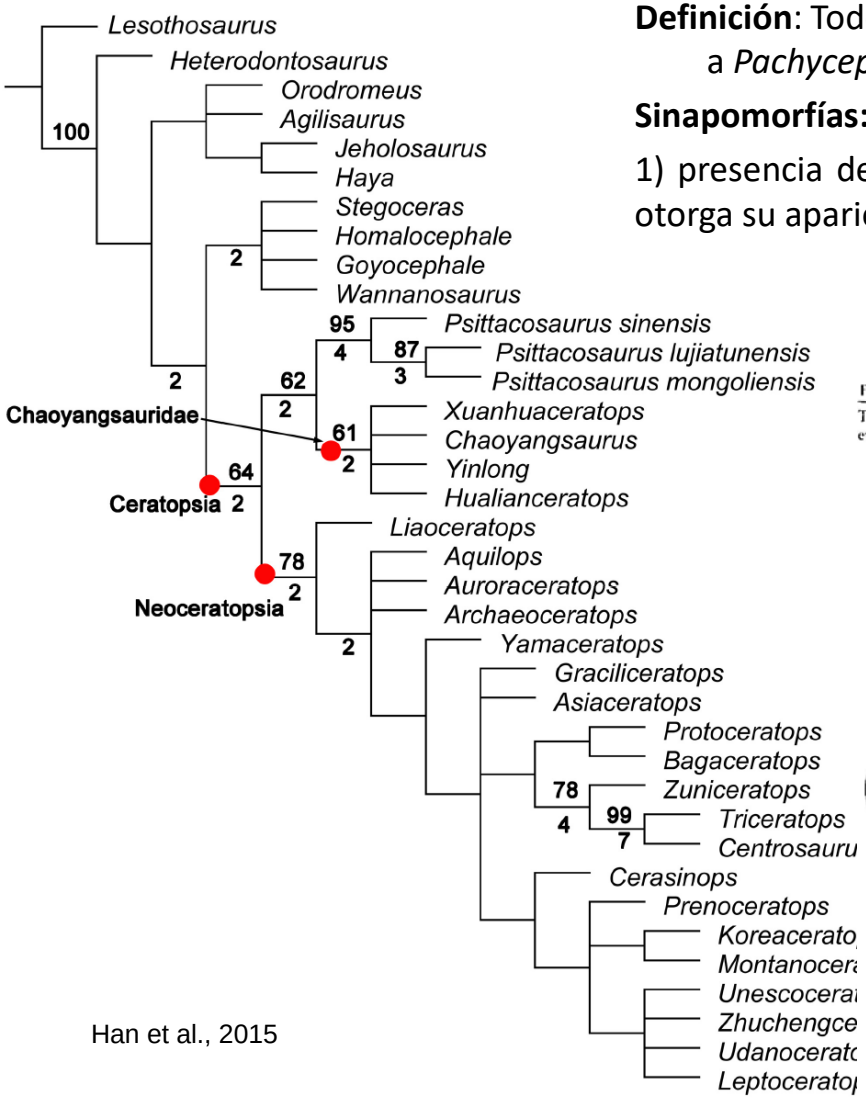

Han et al., 2015

Fig 10. Strict consensus tree of 216 most parsimonious trees produced by analysing a data matrix of 37 taxa and 210 characters (values above 1) is shown below and to the left of nodes, and bootstrap values are labeled to the left and above the nodes (values above

doi:10.1371/journal.pone.0143369.g010

FIGURE 10.2
This ceratopsian skull shows the key evolutionary novelties of the ceratopsians.

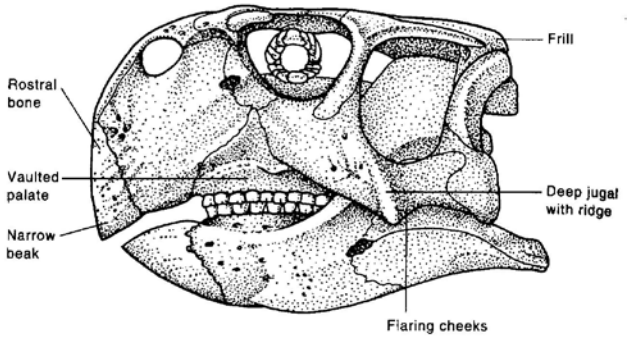

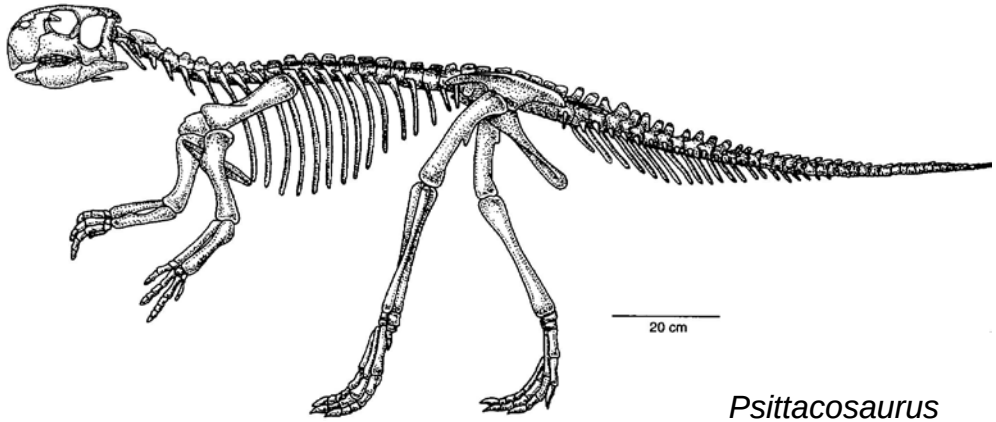

Psittacosaurus

Yinlong downsi

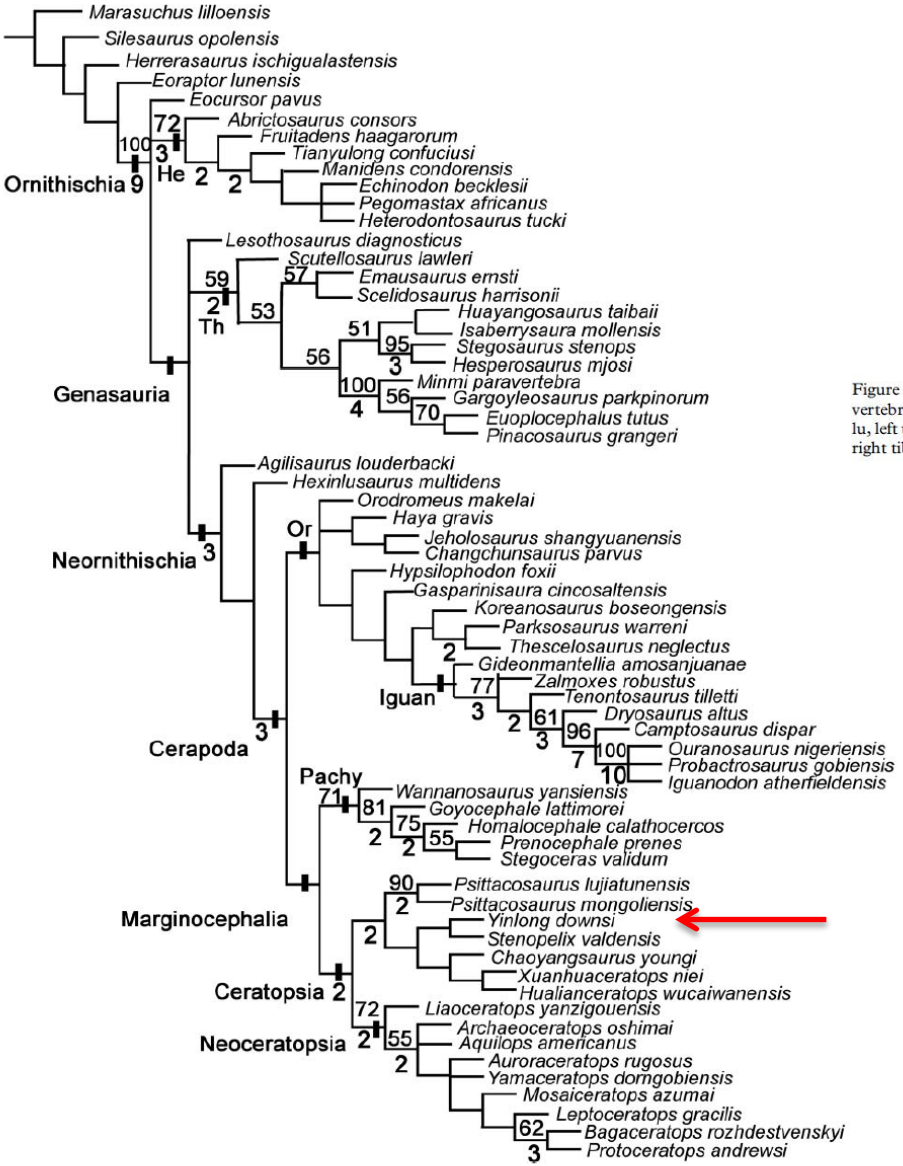

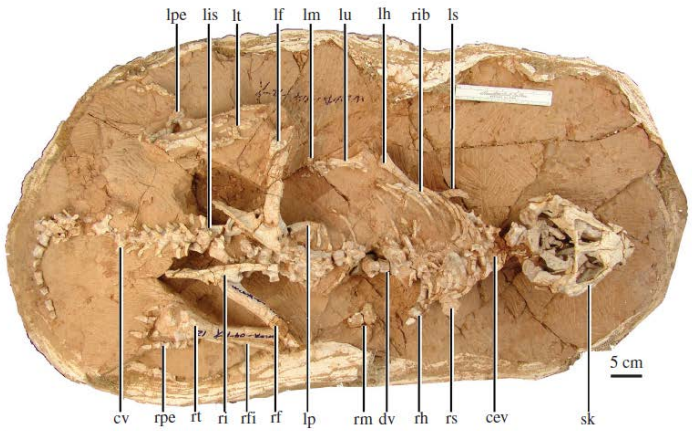

Figure 1. *Yinlong downsi* (IVPP V14530, holotype). Abbreviations: cev, cervical vertebrae; cv, caudal vertebrae; dv, dorsal vertebrae; lf, left femur; lh, left humerus; lis, left ischium; lm, left manus; lp, left pubis; lpe, left pes; ls, left scapula; lt, left tibia; lu, left ulna; rf, right femur; rfi, right fibula; rh, right humerus; ri, right ilium; rm, right manus; rpe, right pes; rs, right scapula; rt, right tibia; sk, skull. Scale bar, 5 cm.

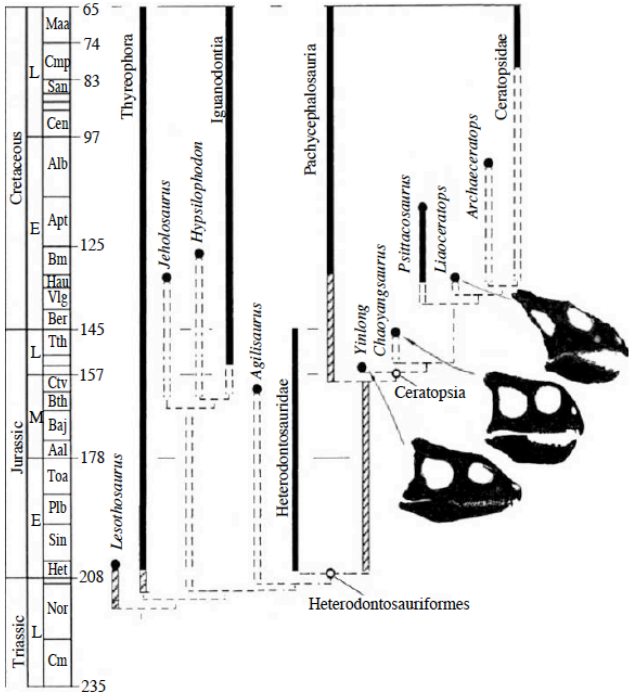

Figure 16. Reduced consensus tree derived by *a posteriori* pruning of eight unstable taxa (*Yueosaurus*, *Pisanosaurus*, *Yandusaurus*, *Zephylosaurus*, *Albalophosaurus Laquintasaura*, *Micropachycephalosaurus* and *Koreaceratops*) from 53,376 most parsimonious trees generated by the full analysis. Values above nodes represent bootstrap proportions. Values beneath nodes indicate Bremer support. Bremer support values of 1 are not shown. Abbreviations: Ch, Chaoyangsauridae; He, Heterodontosauridae; Iguan, Iguanodontia; Or, Ornithopoda; Pachy, Pachycephalosauria; Th, Thyreophora.

Han et al., 2017

Figure 3. A single most parsimonious tree recovered showing the phylogenetic position of *Yinlong downsi* and the interrelationships of the Cerapoda. The proposed tree plotted against geological time indicates the timing of the major cranial changes among the Ceratopsia. The Marginocephalia node is supported by 22 synapomorphies and the Heterodontosauriformes by nine synapomorphies (see electronic supplementary material).

Xu et al 2006

Chaoyangosauridae

Yinlong: “stem” Ceratopsia. Nótese que el yugal no forma “espinas”. Primordio del hueso rostral!

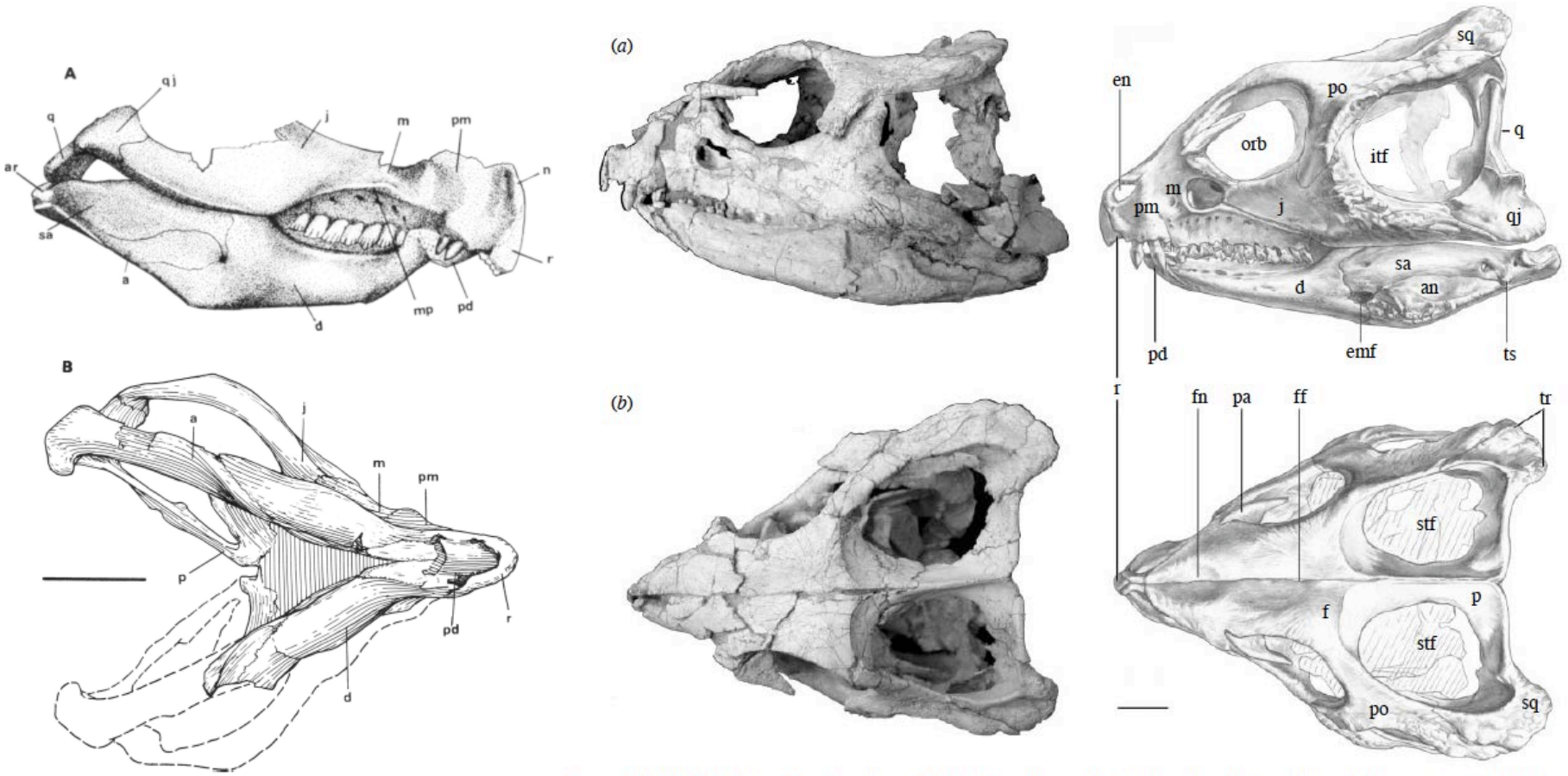

Figure 2. IVPP V14530. (*a*) Skull and mandible in lateral view. (*b*) Skull in dorsal view. Abbreviations: an, angular; d, dentary; emf, external mandibular fenestra; en, external naris; f, frontal; ff, fossa on frontals; fn, fossa on nasals; itf, infratemporal fenestra; j, jugal; m, maxilla; p, parietal; pa, palpebral; pd, predentary; pm, premaxilla; po, postorbital; q, quadrate; qj, quadratojugal; r, rostral bone; sa, surangular; sq, squamosal; stf, supratemporal fenestra; tr, tubercle row; ts, tubercle on surangular. Scale bar, 2 cm.

FIGURE 2. Skull of holotype of *Chaoyangsaurus youngi*, IGCAGS V371, in right lateral (**A**) and ventral (**B**) views. **Abbreviations**: **a**, angular; **ar**, articular; **d**, dentary; **j**, jugal; **m**, maxilla; **mp**, maxillary process; **n**, nasal; **p**, pterygoid; **pd**, predentary; **pm**, premaxilla; **q**, quadrate; **qj**, quadratojugal; **sa**, surangular; **r**, rostral. Scale bar equals 3 cm.

Xu et al 2006

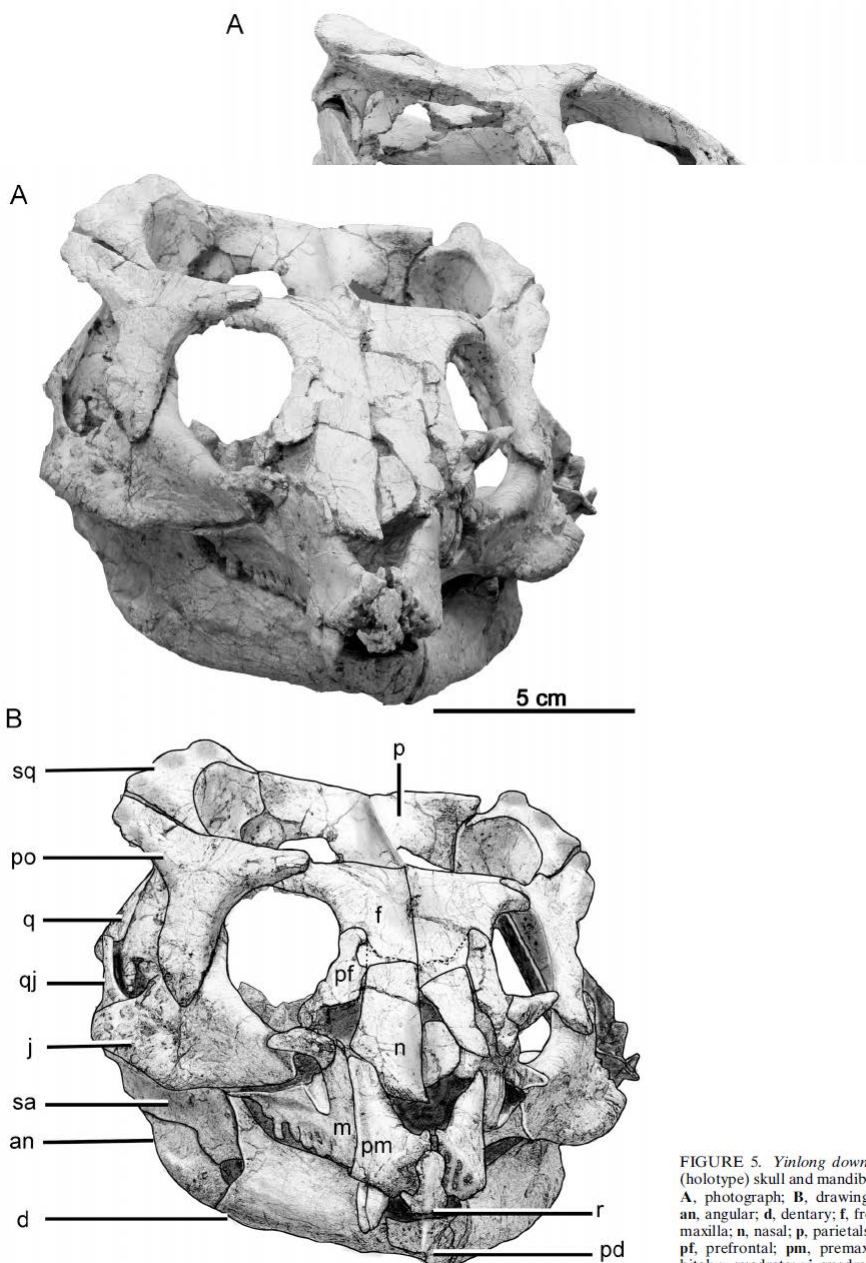

FIGURE 1
(holotype)
view. **A**, p
tions: **an**, a
tary; **emf**,
frontal; **j**,
nasal; **pd**, p
maxilla; **po**
ratojugal;
squamosal;

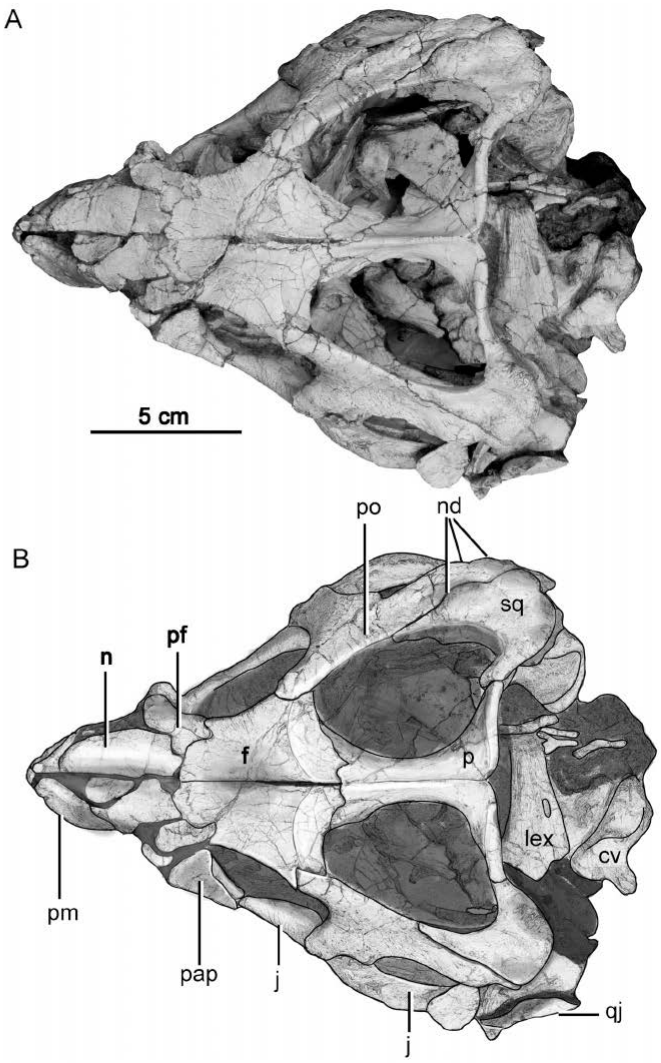

FIGURE 5. *Yinlong downsi* IVPP V14530 (holotype) skull and mandible in rostral view. **A**, photograph; **B**, drawing. **Abbreviations**: **an**, angular; **d**, dentary; **f**, frontal; **j**, jugal; **m**, maxilla; **n**, nasal; **p**, parietals; **pd**, predentary; **pf**, prefrontal; **pm**, premaxilla; **po**, postor-

Psittacosauridae

Psittacosaurus es un género son varias especies (15, pero 9 válidas actualmente), aunque también hay series ontogenéticas. Un segundo posible género es *Hongshanosaurus* (Sereno, 2010).

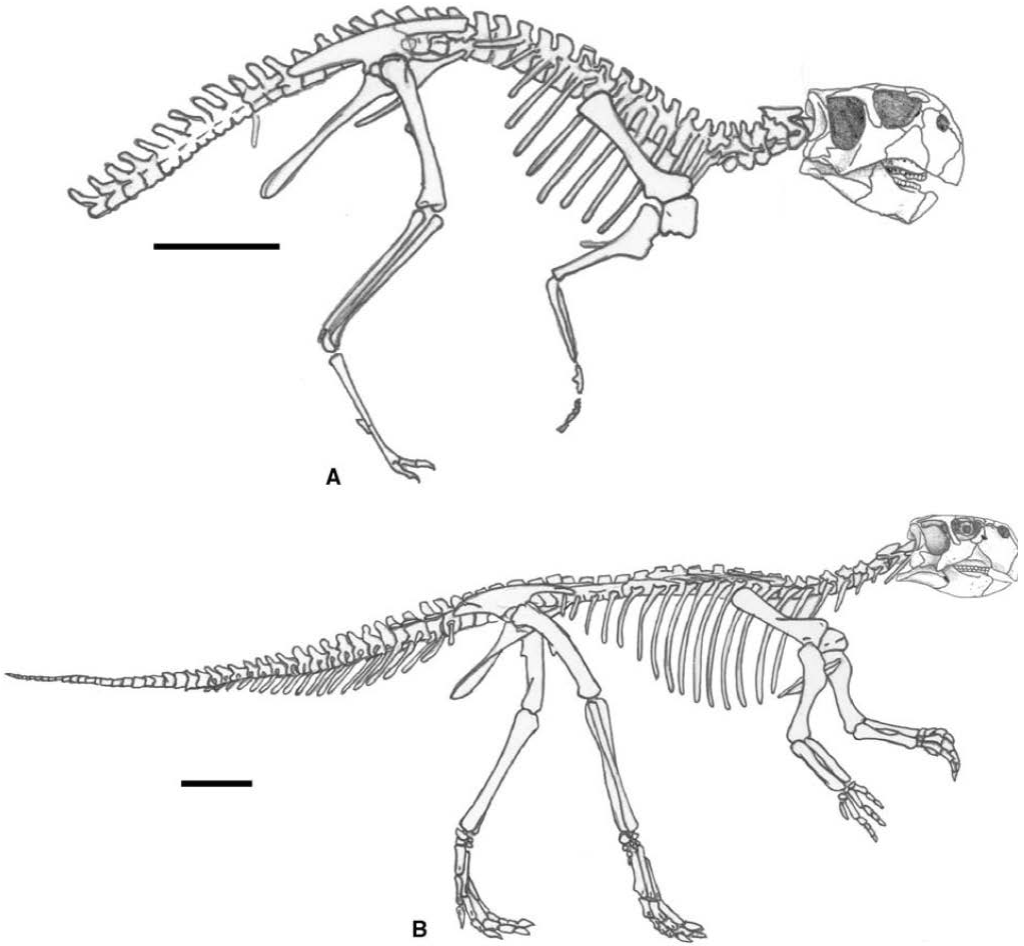

FIGURE 22.1. *Psittacosaurus* skeletons in right lateral view: A, *Psittacosaurus neimongoliensis;* B, *Psittacosaurus mongoliensis.* Scale = 10 cm. (A after Russell and Zhao 1996; B after Osborn 1924c.)

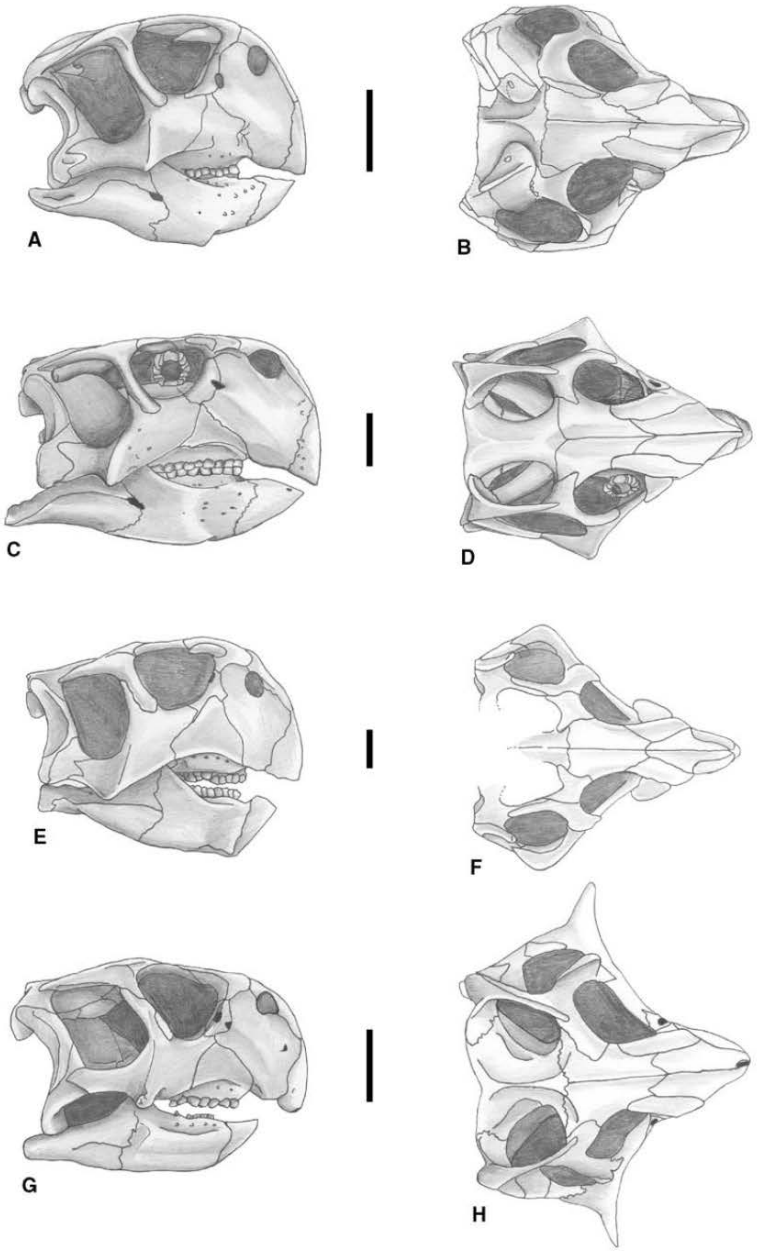

FIGURE 22.4. Skulls of *Psittacosaurus.* A, B, *Psittacosaurus meileyingensis* in lateral, A, and dorsal, B, views; C, D, *Psittacosaurus mongoliensis* in C, lateral, and D, dorsal views; E, F, *Psittacosaurus neimongoliensis* in E, lateral, and F, dorsal views; G, H, *Psittacosaurus sinensis* in G, lateral and H, dorsal views. Scale = 2 cm (A–F), 3 cm (G, H). (A–D, G, H after Sereno 1990b; E, F after Russell and Zhao 1996.)

Psittacosauridae: Yugal forma “espinas”

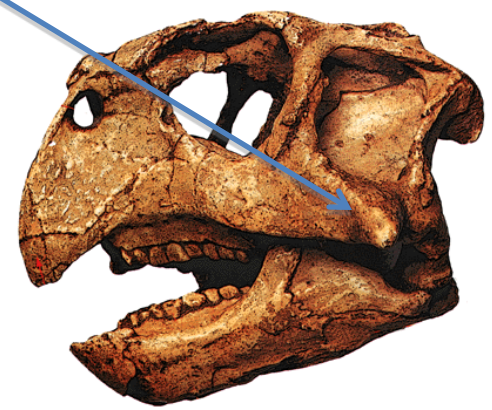

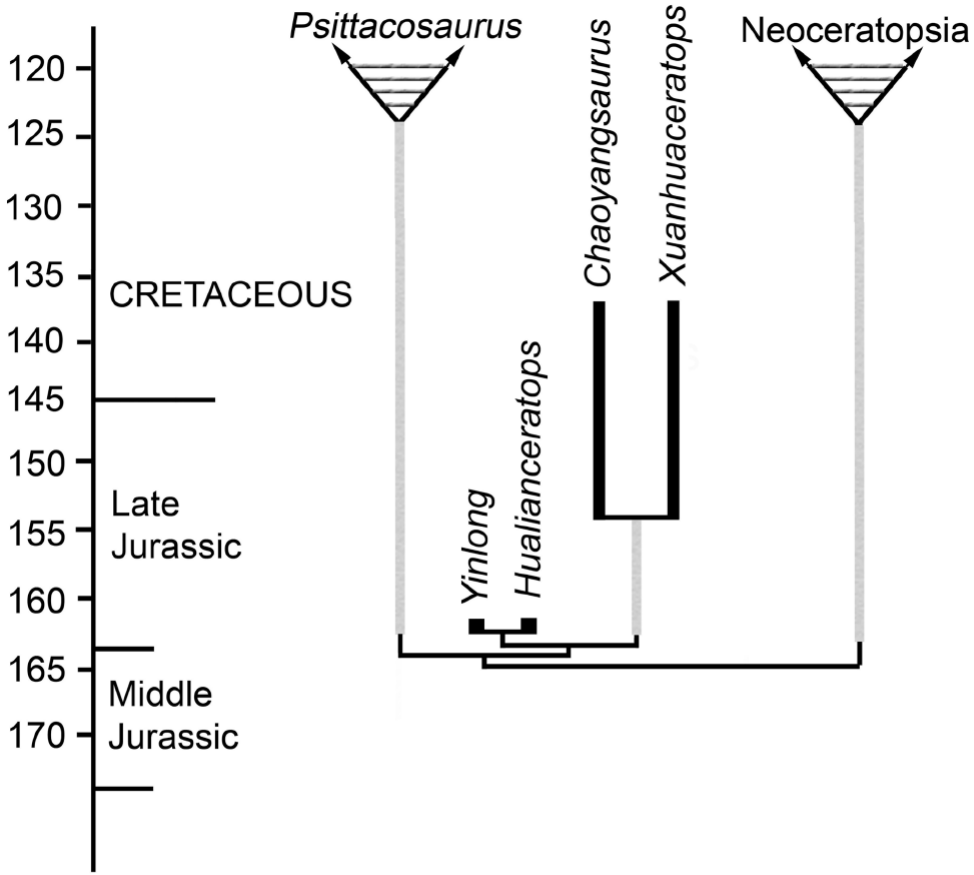

Fig 11. Ghost lineages implied by this phylogenetic analysis. Ghost lineages (gray lines) implied by the stratigraphic distributions of taxa and the most parsimonious trees. Thick black lines indicate single occurrences, their length reflects uncertainty in dating. One of the phylogenies implying the fewest lineages is shown. Geochronology from [41].

doi:10.1371/journal.pone.0143369.g011

Han et al., 2015

Neoceratopsia

Definición: Neoceratopsia es el clado menos inclusivo que contiene al *Triceratops horridus*, pero no al *Psittacosaurus mongolensis.*

Liaoceratops, *Archaeoceratops*. Aún bipedos. Mayor expansión del parietoescamoso

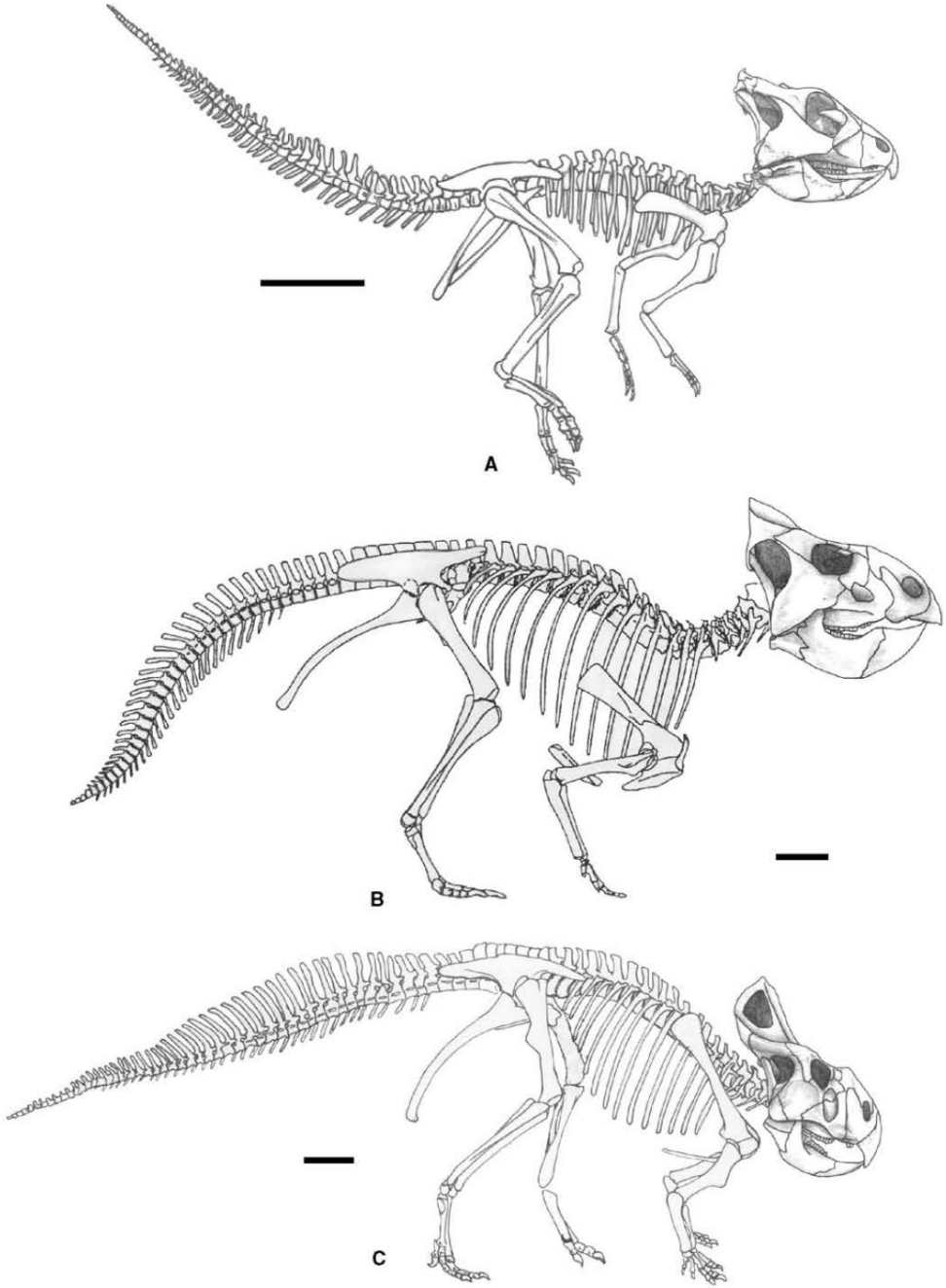

FIGURE 22.2. Skeletons of basal Neoceratopsia in right lateral view: A, *Archaeoceratops oshimai;* B, *Leptoceratops gracilis;* C, *Protoceratops andrewsi.* Scale = 10 cm. (A after Dong and Azuma 1997; B after Russell 1970; C after Granger and Gregory 1923.)

Liaoceratops yanzigouensis

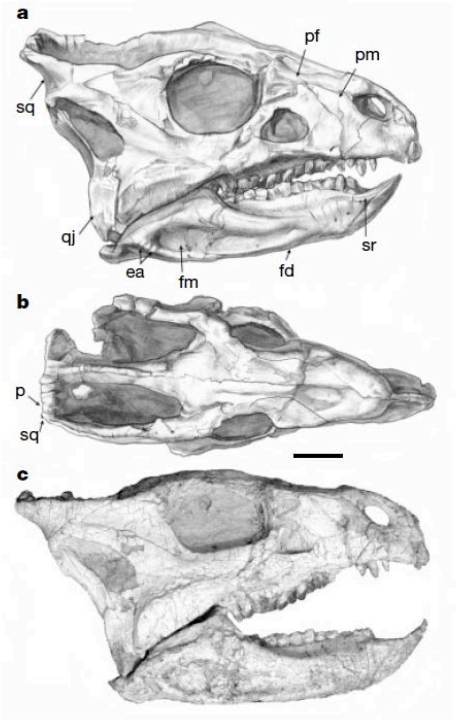

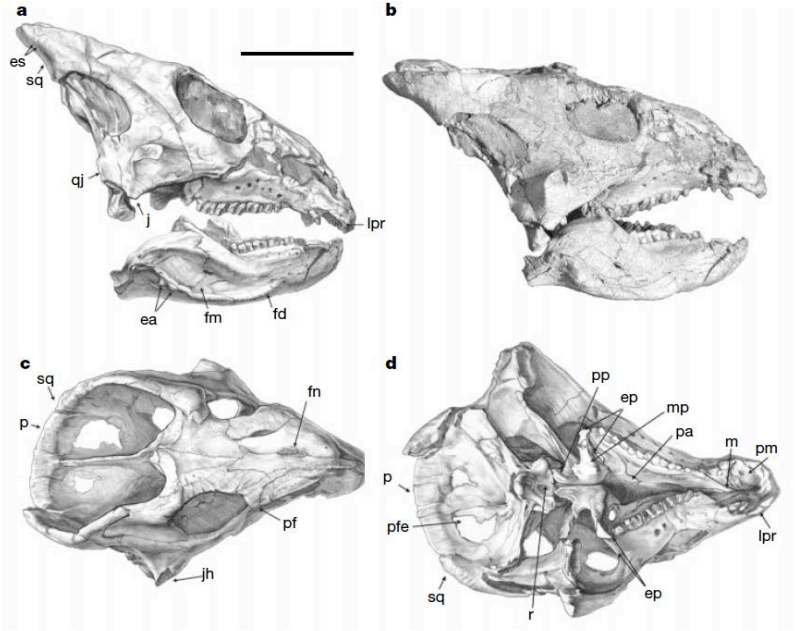

Figure 1 Holotype skull of the ceratopsian *Liaoceratops yanzigouensis* (IVPP V12738) in lateral (**a**, **b**), dorsal (**c**) and ventral (**d**) views. Scale bar, 4.5 cm. Abbreviations: ea, eminences on angular; ep, ectopterygoid; es, eminences on squamosal; fd, flange on dentary; fm, fossa on external surface of the mandible; fn, fossa on nasals; j, jugal; jh, jugal horn; lpr, lateral process of jugal; m, maxilla; mp, mandibular process of pterygoid; p, parietal; pa, palatine; pf, prefrontal; pm, premaxilla; pp, posterior process of pterygoid; r, ridge; pfe, parietal fenestra; qj, quadrojugal; sq, squamosal.

Figure 2 Skull of the juvenile specimen referred to *Liaoceratops yanzigouensis* (IVPP V12633) in lateral (**a**, **c**) and dorsal (**b**) views. Scale bar, 1 cm. Abbreviations as in Fig. 1, except for Sr, sharp ridge.

Aquilops americanus

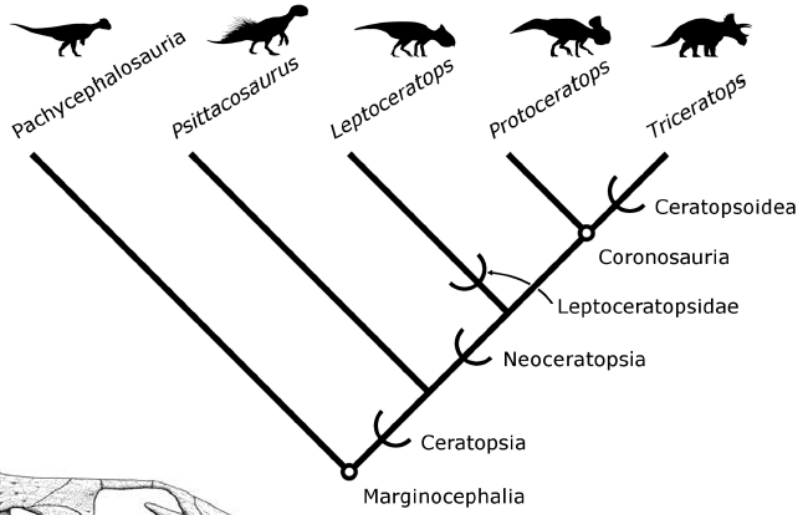

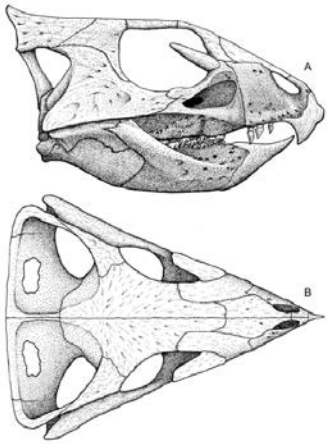

Figure 6. Cranial reconstruction and life restoration of *Aquilops americanus*. Cranium in A) right lateral and B) dorsal views; C) life restoration in right lateral view. The rendering is based on OMNH 34557 (holotype), with missing details patterned after *Liaoceratops yanzigouensis* and *Archaeoceratops oshimai*. Life restoration by Brian Engh.
doi:10.1371/journal.pone.0112055.g006

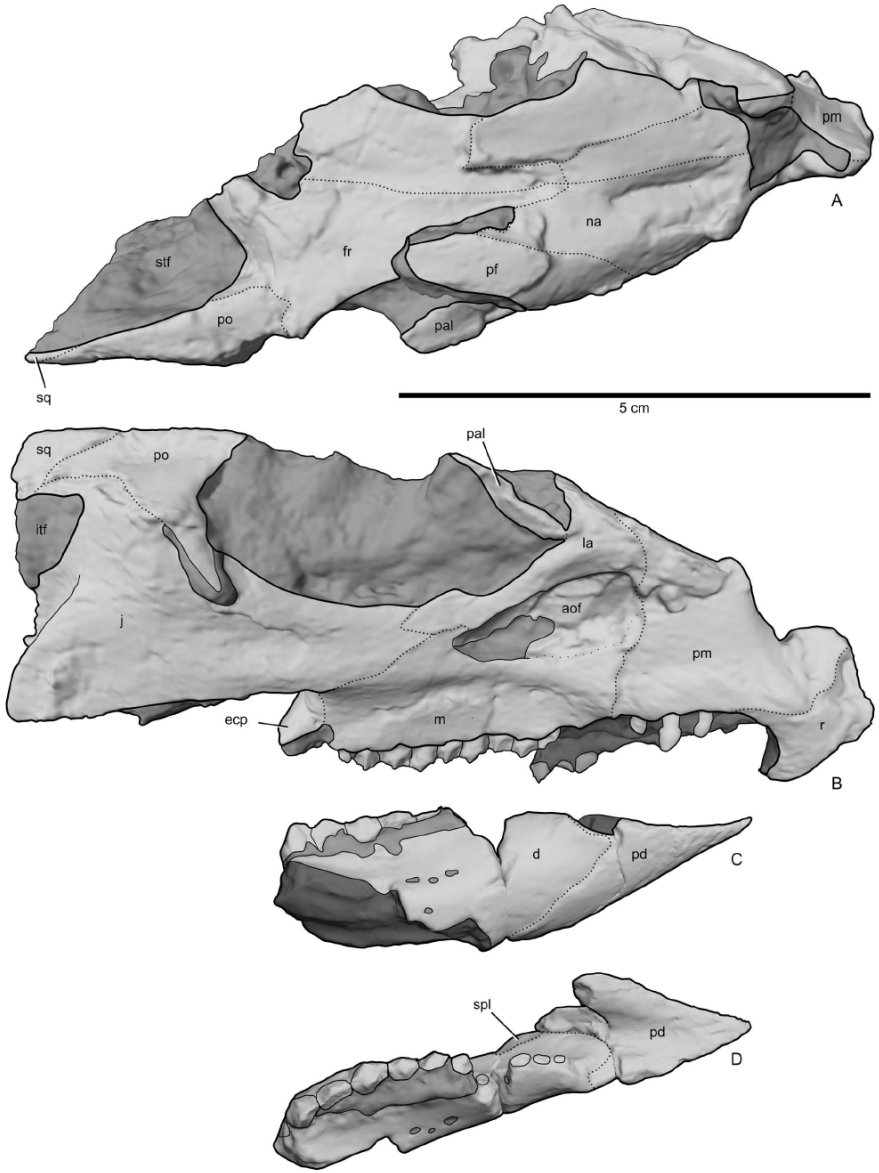

Figure 3. Skull of *Aquilops americanus*, OMNH 34557 (holotype). Partial cranium in A) dorsal and B) right lateral views. Partial lower jaw in C) right lateral and D) dorsal views. This interpretive figure is based on surface scans of the original specimen, with sutures highlighted. The lower jaw is reversed, to facilitate placement with the skull. Abbreviations: aof, antorbital fossa; d, dentary; ecp, ectopterygoid; fr, frontal; itf, infratemporal fenestra; j, jugal; la, lacrimal; m, maxilla; na, nasal; pal, palpebral; pd, predentary; pf, prefrontal; pm, premaxilla; po, postorbital; r, rostral; spl, sutural surface for splenial; sq, squamosal; stf, supratemporal fenestra.
doi:10.1371/journal.pone.0112055.g003

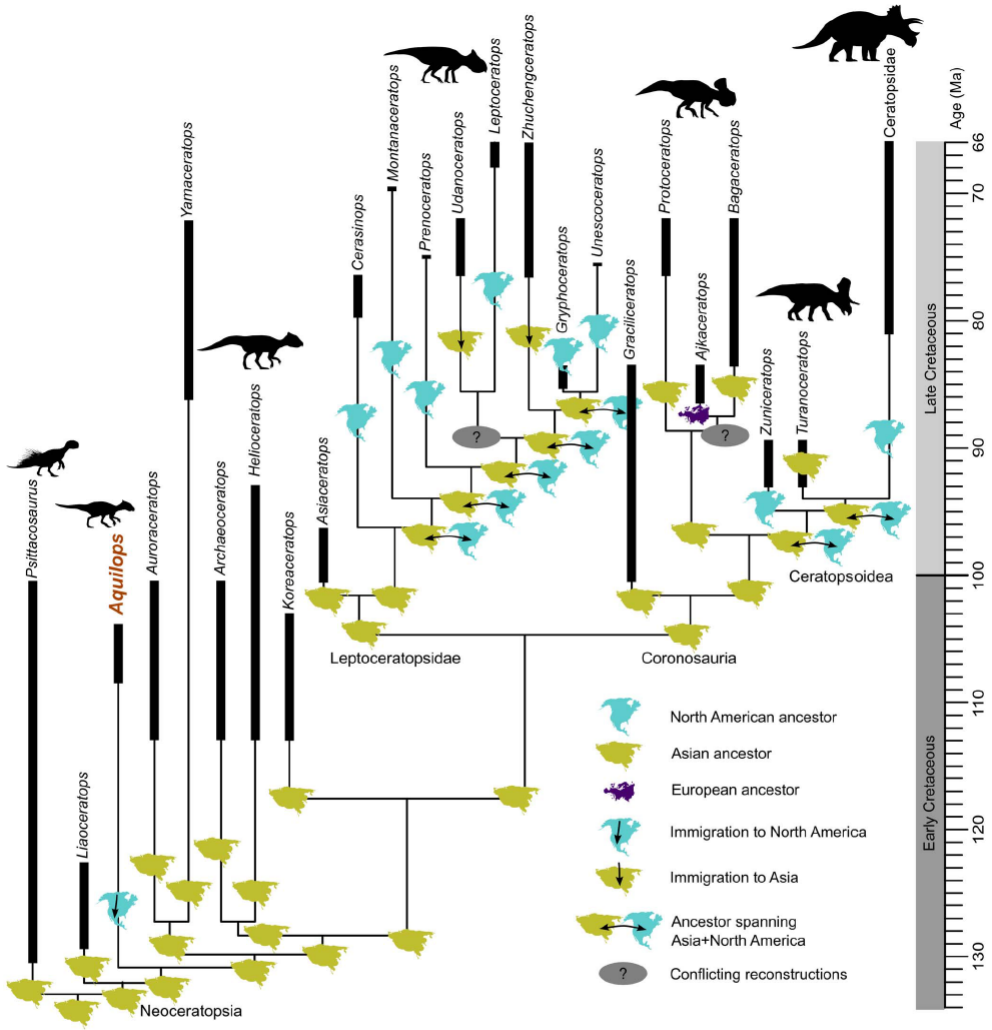

Figure 10. Hypothesis of phylogeny and biogeography for Neoceratopsia. Some terminal taxa have been combined for space considerations, and the range bars for each taxon indicate uncertainty rather than known geological ranges. Continent icons indicate the ancestral areas reconstructed by DEC modeling. Silhouettes depict representative members of major clades and grades (*Psittacosaurus* by J. Headden, *Zuniceratops* by N. Tamura and modified by T. M. Keesey; *Triceratops* by R. Amos; all others by A. Farke; all images are CC-BY and provided via www.phylopic.org). Full results are presented in File S1.
doi:10.1371/journal.pone.0112055.g010

Auroraceratops rugosus

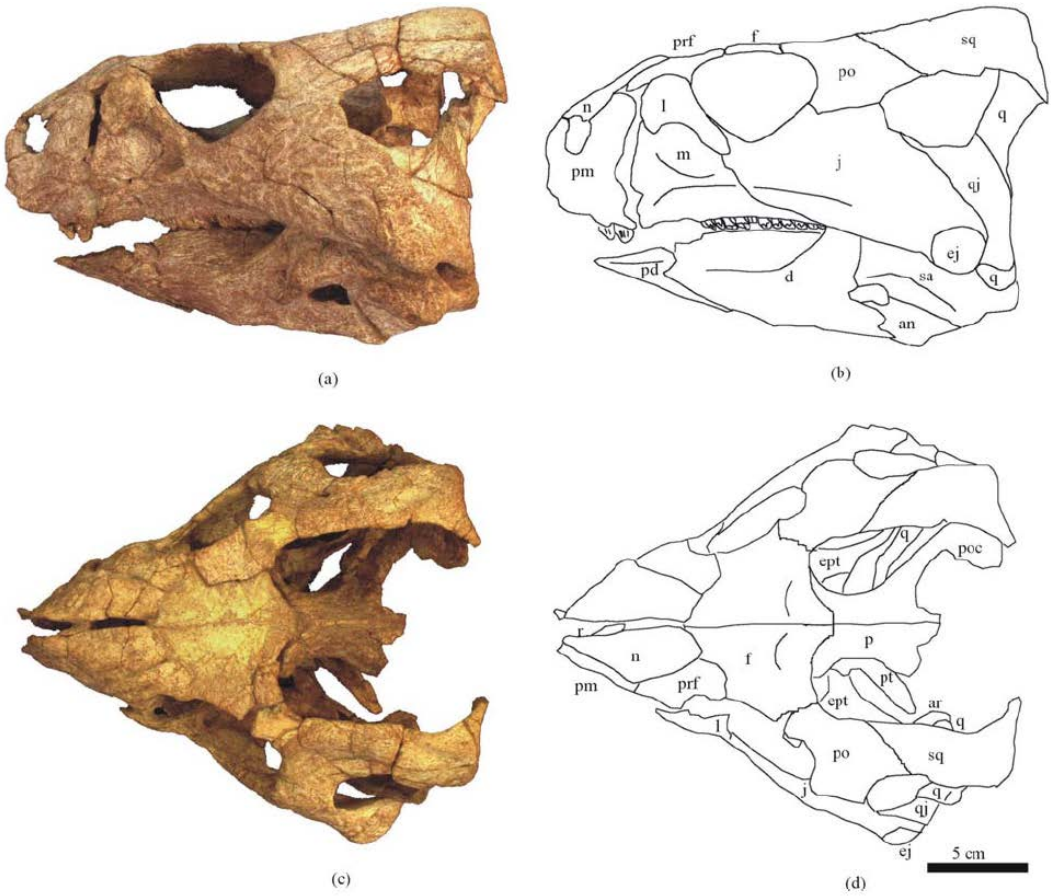

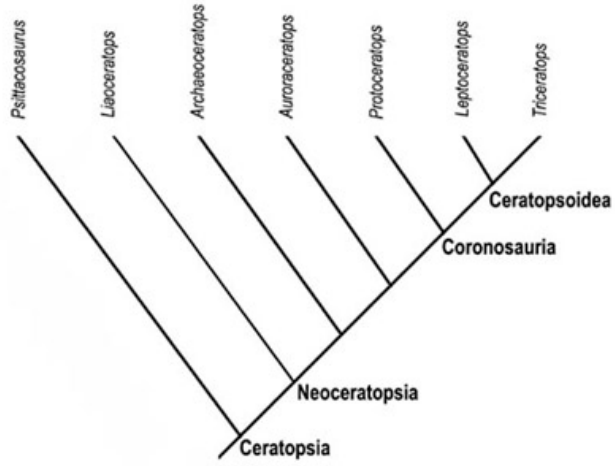

Fig. 1. Left lateral (a, b) and dorsal (c, d) views of the skull of holotype of *Auroraceratops rugosus* gen. et sp. nov. (a) and (c): photographs; (b) and (d): interpretive outlines.

Please notice the gap between the premaxilla rostrally and the maxilla and the lacrimal caudally. Abbreviations: an – angular; ar – articular; d – dentary; ej – epijugal; ept – ectopterygoid; f – frontal; j – jugal; l – lacrimal; m – maxilla; n – nasal; p – parietal; pd – predentary; pm – premaxilla; po – postorbital; poc – paroccipital process; prf – prefrontal; pt – pterygoid; q – quadrate; qj – quadratojugal; r – rostral; sa – surangular; sq – squamosal.

Mosaiceratops azumai

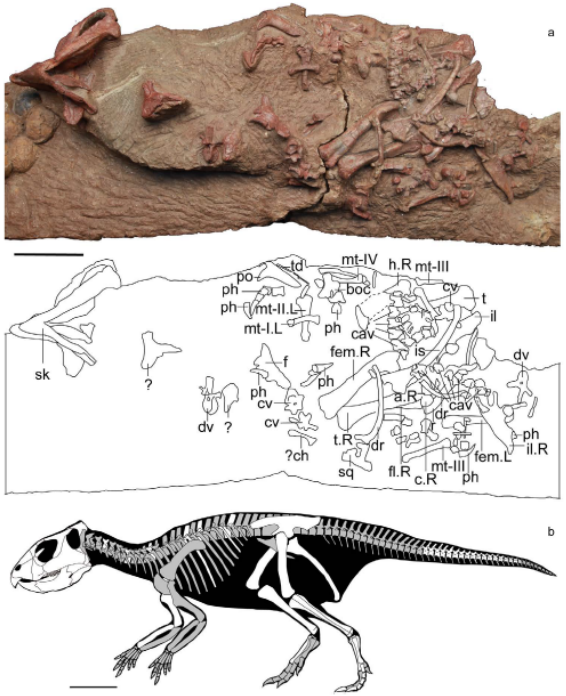

Figure 1. Holotype and skeletal reconstruction of *Mosaiceratops azumai*, gen. et sp. nov (ZMNH M8856). (a) photograph and line drawing of ZMNH M8856; (b) skeletal reconstruction showing preserved elements in white. Scale bar 10 cm. Abbreviations: a, astragalus; boc, basioccipital; c, calcaneum; cav, caudal vertebra; ch, chevron; cv, cervical vertebra; dr, dorsal rib; dv, dorsal vertebra; f, frontal; fem, femur; fl, fibula; h, humerus; il, ilium; is, ischium; L, left; mt, metatarsal; ph, phalanx/phalanges; po, postorbital; R, right; sk, skull; sq, squamosal; t, tibia; td, tendon; ?, undiagnostic remains.

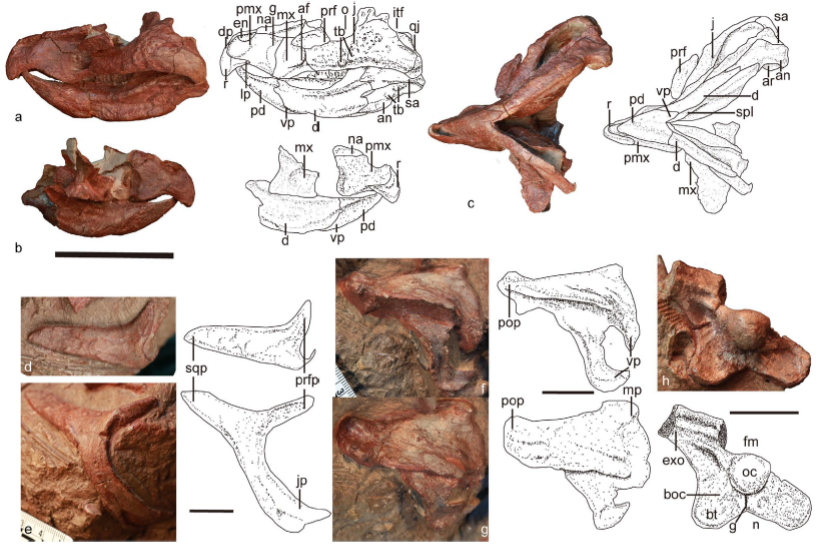

Figure 2. Cranial remains of *Mosaiceratops azumai*, gen. et sp. nov. Photograph and interpretive drawing of skull in left lateral (a), right lateral (b) and ventral (c) views; right postorbital in dorsal (d) and anterolateral (e) views; left squamosal in lateral (f) and laterodorsal (g) views; partial braincase in occipital (h) view. Scale bars in a–c, 5 cm, in d–h, 2 cm. Abbreviations: af, antorbital fossa; an, angular; ar, articular; boc, basioccipital; bt, basioccipital tubera; d, dentary; dp, dorsal process of rostral; en, external naris; exo, exoccipital; fm, foramen magnum; g, groove; itf, infratemporal fenestra; j, jugal; jp, jugal process; lp, lateral process; mp, medial process; mx, maxilla; n, notch; na, nasal; o, orbit; oc, occipital condyle; pd, predentary; pmx, premaxilla; pop, postorbital process; prf, prefrontal; prfp, prefrontal process; qj, quadratojugal; r, rostral bone; sa, surangular; spl, splenial; sqp, squamosal process; tb, tubercle; vp, ventral process.

Coronosauria

Definición: clado más inclusivo que contiene al *Triceratops horridus* y al *Protoceratops andrewsi.*

Presencia de una gola craneal

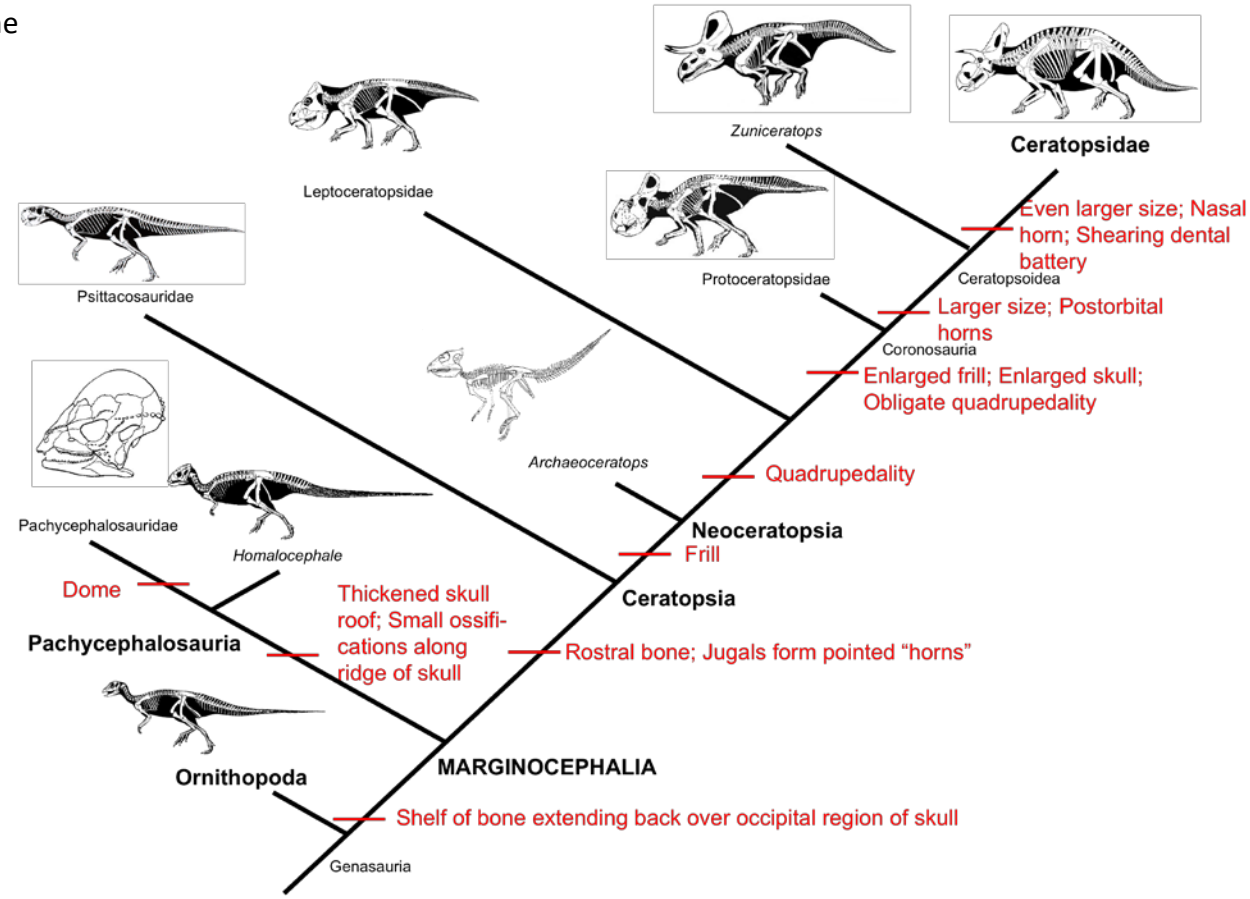

Ceratopsidae

Fig. 3. Synthetic phylogenetic tree with all ceratopsian species considered valid in this study. See text and Tables S4 and S5 in 3008Appendix for details about topology and branch length calibration. Thicker lines indicate the stratigraphic range of taxa. Black bars indicate confident stratigraphic occurrence, whereas white bars indicate less confidence. *Psittacosaurus* image by J. Headden; *Zuniceratops* and *Einiosaurus* images by Nobu Tamura, modified by T. Michael Keesey; *Archaeoceratops*, *Protoceratops*, *Leptoceratops*, *Aquilops*, *Pachyrhinosaurus*, *Centrosaurus*, *Styracosaurus*, *Yinlong*, and *Chasmosaurus* by Andrew A. Farke; *Triceratops* by Raven Amos. All images except *Zuniceratops* (in public domain) are licensed under Creative Commons Attribution 3.0 licence.

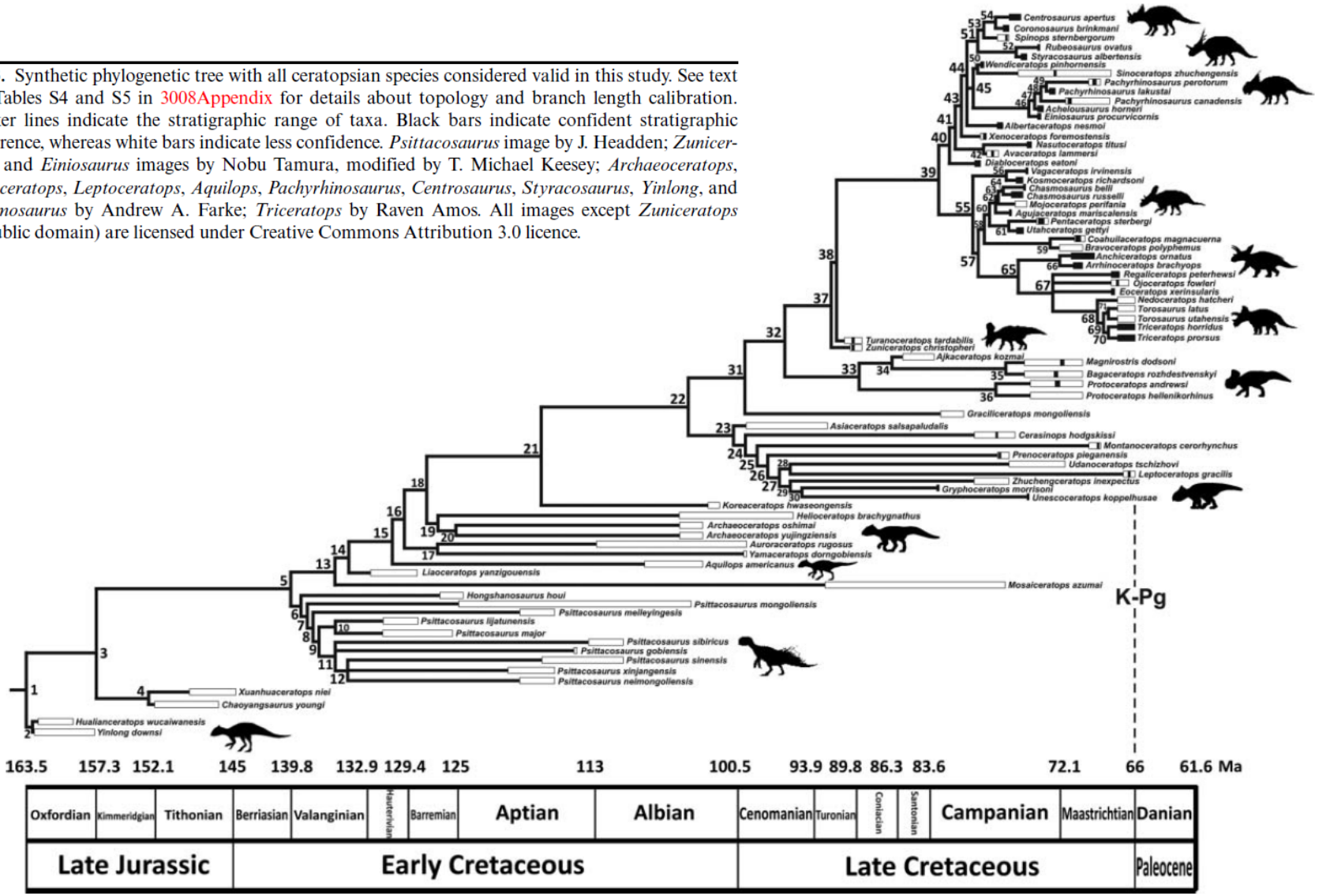

Maiorino et al 2017

Current Biology

A New Horned Dinosaur Reveals Convergent Evolution in Cranial Ornamentation in Ceratopsidae

Graphical Abstract

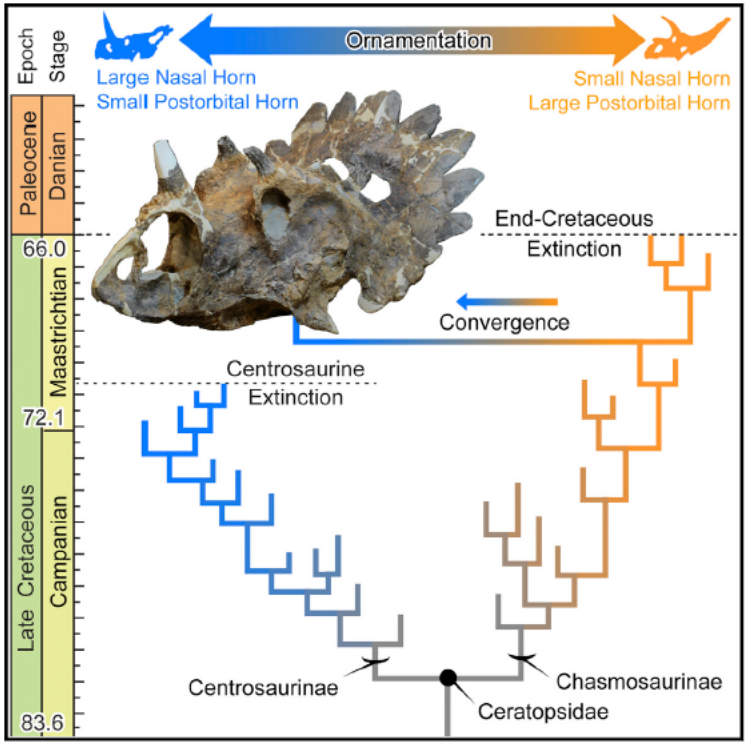

Authors

Caleb M. Brown, Donald M. Henderson

Correspondence

caleb.brown@gov.ab.ca

In Brief

Brown and Henderson describe a new horned dinosaur, *Regaliceratops peterhewsi*, from a nearly complete skull characterized by a large nasal horn, small postorbital horns, and large frill epiossifications. This new chasmosaurine shows display features more similar to centrosaurines and suggests evolutionary convergence in display morphology in horned dinosaurs.

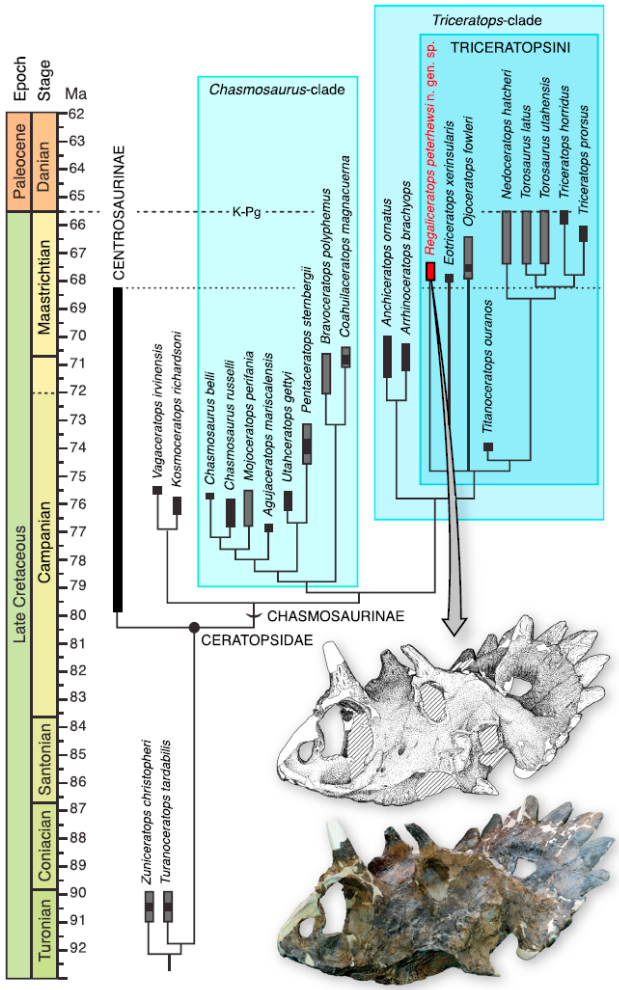

Figure 3. Time-Calibrated Phylogeny of Chasmosaurinae

Time-calibrated strict consensus tree of five most parsimonious trees for Chasmosaurinae utilizing the new episossification homology scheme (for tree details, see Figure S1B). For comparison of results and support indices, see Figure S1. Black bars indicate confident stratigraphic occurrence, whereas gray bars indicate less confidence. Stratigraphic information is derived from [17]. Bottom right: oblique view of the holotype of *Regaliceratops peterhewsi*, TMP 2005.055.0001.

The median epiparietal of *Regaliceratops* is similar, and likely homologous, to the median epiparietal of *Triceratops* spp., previously termed P0 (e.g., [28] and K.E. Clayton et al., 2010, Soc. Vertebrate Paleontol., abstract), in terms of (1) a median position, (2) being of unpaired morphology, and (3) projecting caudal to the parietal margin. Additionally, based on (1) dorsally offset position from the plane of the frill, (2) rostrally offset position from the caudal margin of the frill, and (3) roughly triangular cross-section, the median episossification of *Regaliceratops* is likely also homologous with the laterally curved hooks of *Anchiceratops*, which have previously been termed P1 [15]. To test this homology across Chasmosaurinae, we shifted the identity of the epiparietals of *Anchiceratops*, *Pentaceratops*, and *Utahceratops* one position medially (Figure S3; see Supplemental Experimental Procedures, "Phylogenetic Methods"). The phylogenetic analysis of this revised homology scheme for the episossifications results in a simpler and better-resolved evolutionary history (i.e., a shorter, better-resolved tree), indicating support for the revised homology hypothesis proposed here (Figure S1; see Supplemental Experimental Procedures, "Phylogenetic Methods").

Regaliceratops and Display Evolution in Ceratopsidae

The cladistic analysis of relationships within Chasmosaurinae recovers *Regaliceratops* in a polytomy with *Eotriceratops* and *Ojoceratops*, as sister taxa to the remaining Triceratopsini (*Triceratops*, *Torosaurus*, *Nedoceratops*, *Titanoceratops*) (Figures 3 and S1). This phylogenetic position hypothesized for *Regaliceratops* is consistent with its temporal occurrence, being roughly time equivalent to *Eotriceratops* (Figure 3). This suggests that *Regaliceratops* is part of an evolutionary trend showing both

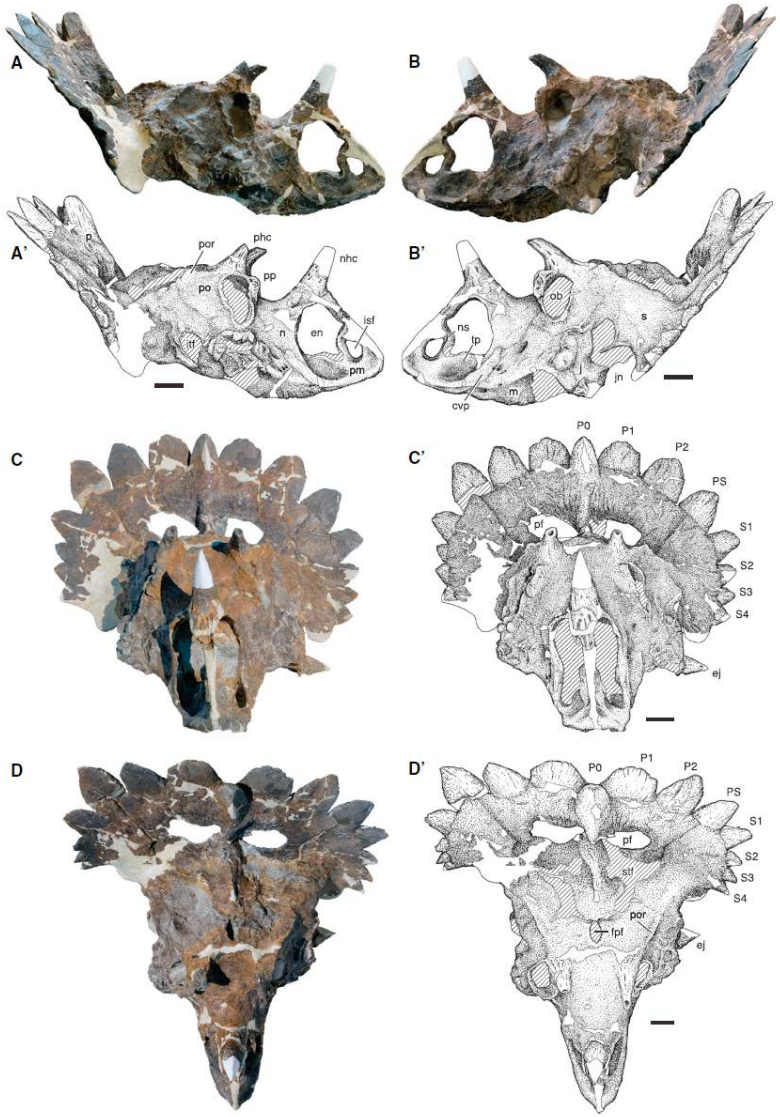

Figure 2. Photographs and Interpretive Line Drawings of the Holotype of *Regaliceratops peterhewsi* gen. et sp. nov.

(A–D) Nearly complete cranium, TMP 2005.055.0001, in right lateral (A), left lateral (B), rostral (C), and dorsal (D) views. (A′–D′) Interpretive drawings of photographed views in (A)–(D).

Pachycephalosauria

Los Pachycephalosauria son estrictamente bípedos, y un techo del cráneo engrosado. El procesamiento de material vegetal era más importante en el tracto digestivo que en la masticación, por lo cual desarrollaron un enorme vientre y un aspecto muy ancho

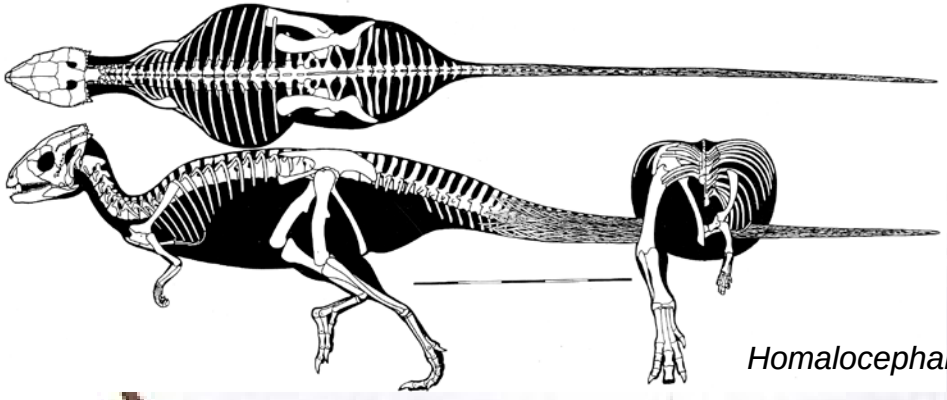

Homalocephale

Hueso palepebral a supraorbital: Coronosauria. Archaeoceratops aun tiene palpebral

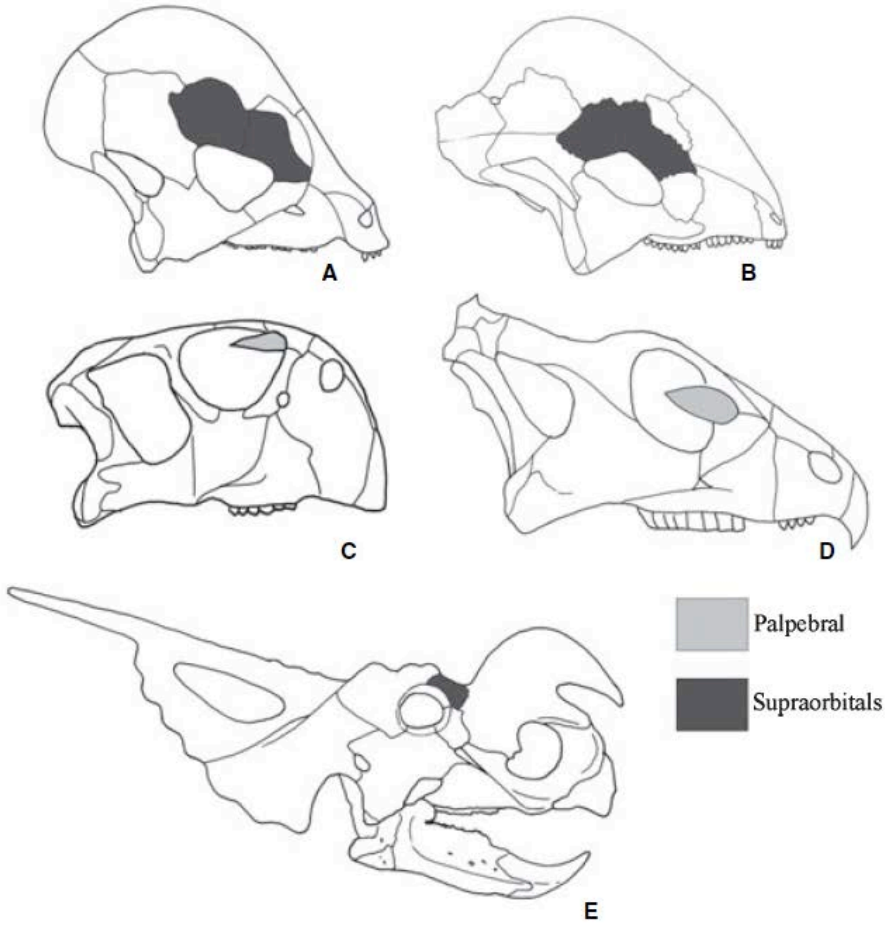

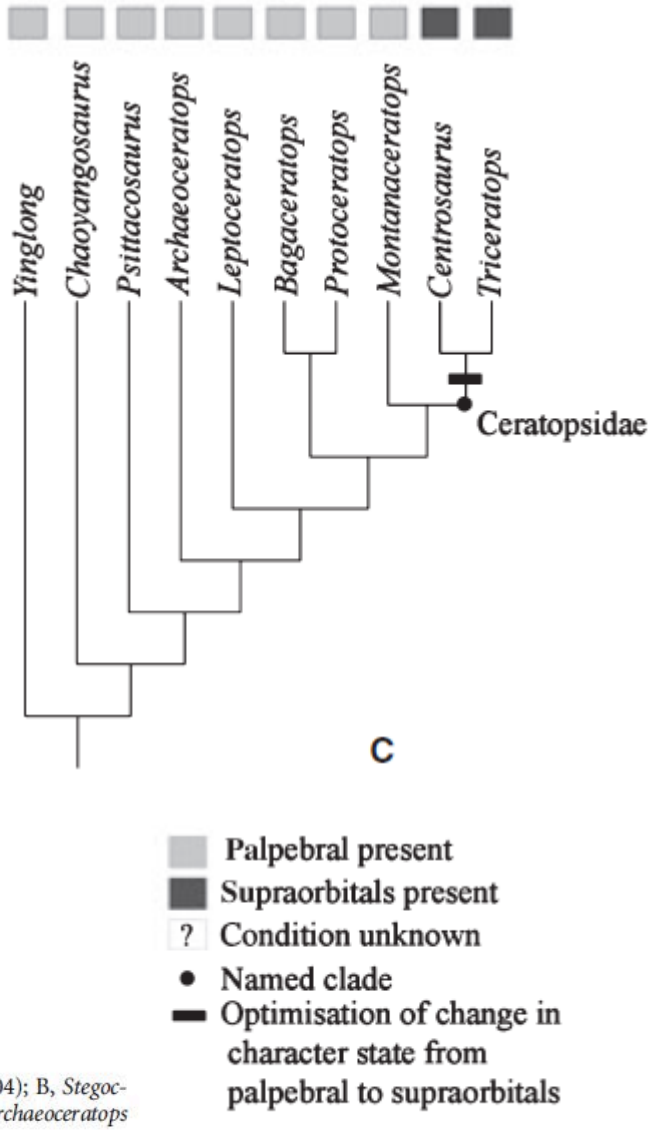

Fig. 8. Skulls of marginocephalians in lateral view. A,B, Pachycephalosauria; A, *Prenocephale prenes* (after Maryanska *et al.* 2004); B, *Stegoceras validum* (after Maryanska *et al.* 2004). C–E, Ceratopsia; C, *Psittacosaurus meileyingensis* (after You & Dodson 2004); D, *Archaeoceratops oshimai* (after You & Dodson 2004); E, *Einiosaurus procurvicornis* (after Sampson 1995). Not to scale.

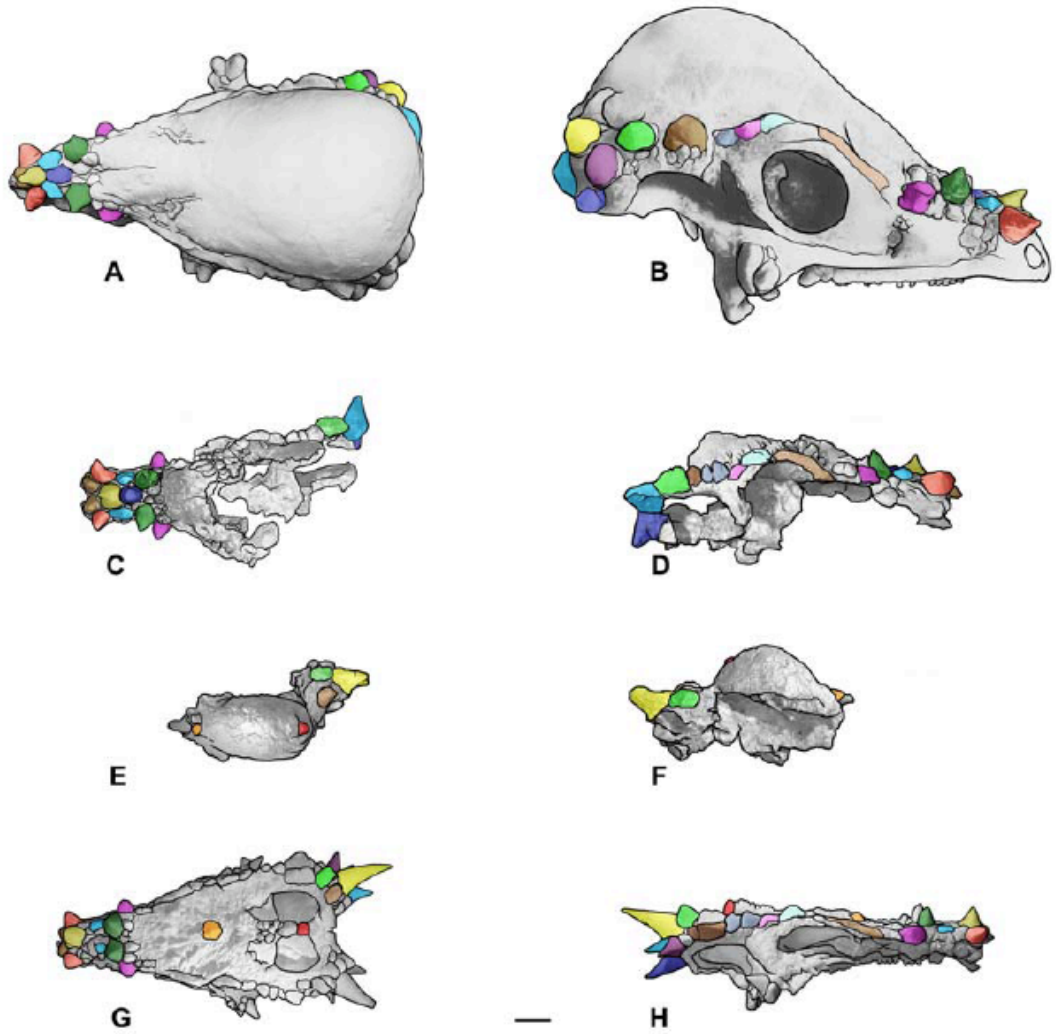

Figure 3. Cranial ontogenetic sequence of *Pachycephalosaurus wyomingensis* with morphological landmarks highlighted in color. The ontogenetically oldest adult, AMNH 1696, in **(A)** dorsal and **(B)** right lateral views. A younger adult, UCMP 556078 (cast) with inflation of the frontoparietal dome+lateral cranial elements and mature nasal and squamosal nodal ornamentation in **(C)** dorsal and **(D)** right lateral views. MPM 8111, a partial skull of "*Stygimoloch*" in **(E)** dorsal and **(F)** left lateral views (reversed) illustrates the high narrow frontoparietal dome, squamosal nodes and horns characteristic of the subadult growth stage. Landmarks on the dorsal skull of MPM 8111 in orange (anterior) and red (posterior) constrain the position of the dome. The youngest growth stage in this cranial ontogenetic series is "*Dracorex*", TCNI 2004.17.1 (cast) in **(G)** dorsal and **(H)** right lateral views. The position of the squamosal horns and nasal nodes are consistent in these four pachycephalosaurid skulls, which increase in overall length and size from youngest **(G,H)** to oldest **(A,B)**. Scale bar is 5 cm.
doi:10.1371/journal.pone.0007626.g003

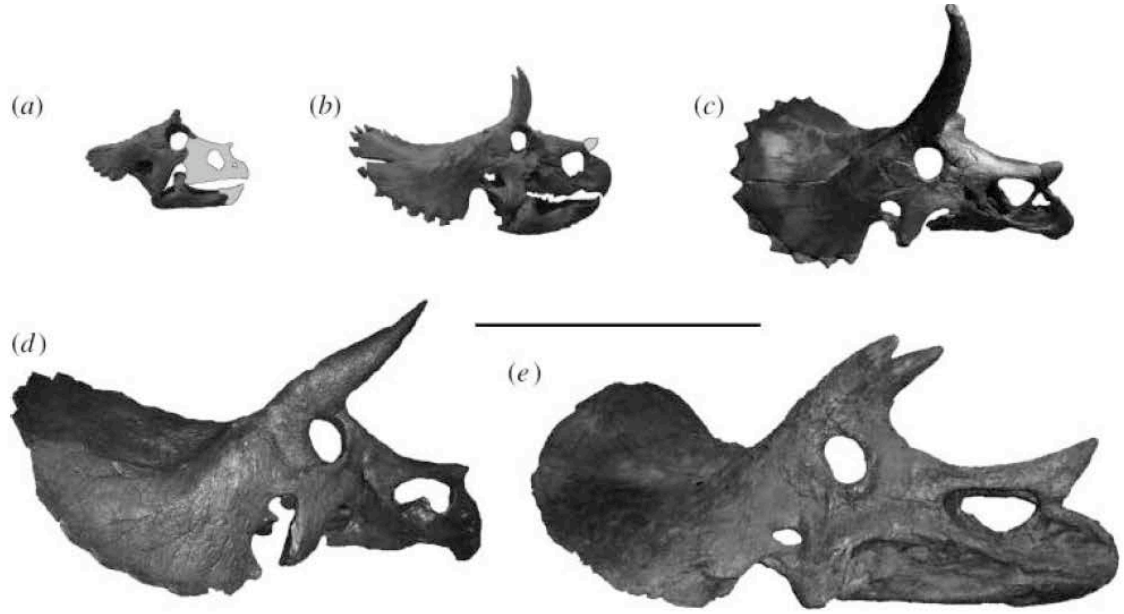

Figure 1. Five examples of the four cranial ontogenetic growth stages in *Triceratops* skulls in right lateral view. Skull length is given in parentheses. (*a*) UCMP 154452, baby skull (38 cm); (*b*) MOR 1199, small juvenile skull (87 cm); (*c*) MOR 1110, large juvenile skull (135 cm); (*d*) MOR 1120, subadult skull (165 cm); and (*e*) MOR 004, adult skull (208 cm). Reconstructed area of (*a*) UCMP 154452 and the epinasal in (*b*) MOR 1199 are drawn in white. Scale bar,1 m.

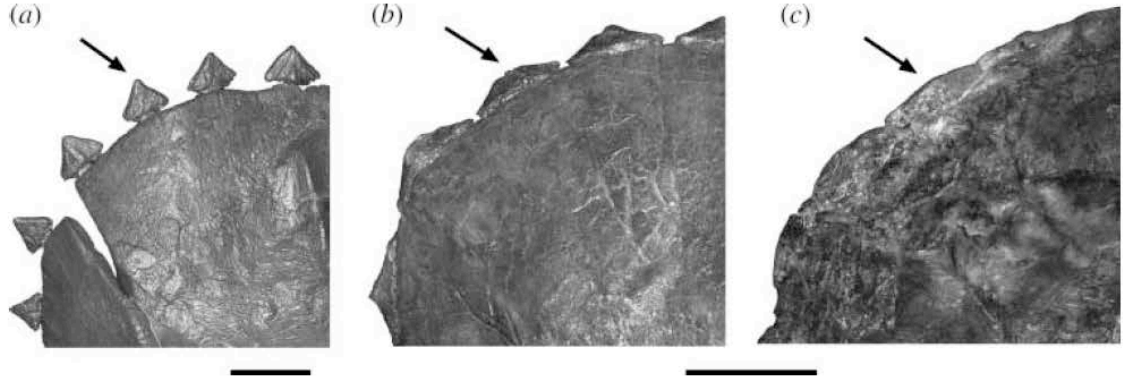

Figure 2. Anteroposterior view of three *Triceratops* parietal–squamosal frills showing the ontogenetic shape change of the epoccipitals. (*a*) MOR 1199, small juvenile; (*b*) MOR 1120, subadult and (*c*) MOR 004, adult skull. The arrow points to the epoccipital in each skull. Scale bar, 8 cm for (*a*) and 20 cm for (*b*) and (*c*).